AN ABSTRACT OF THE DISSERTATION OF

David J. Dickson for the degree of Doctor of Philosophy in Biological & Ecological Engineering presented on February 8, 2011.

Title: Photobiological Hydrogen Production from the Cyanobacterium *Synechocystis* sp. PCC 6803 Encapsulated in Sol-gel Processed Silica.

Abstract approved:

Roger L. Ely

Photobiological hydrogen production from live cells of the cyanobacterium *Synechocystis* sp. PCC 6803 encapsulated in silica gel was investigated. Hydrogen is a dense energy carrier with potential to reduce dependence on fossil fuels, provided a renewable and sustainable means of production can be achieved. Under certain conditions, *Synechocystis* sp. PCC 6803 can produce molecular hydrogen through the activity of a reversible [Ni-Fe] hydrogenase using energy derived from photosynthesis. The current work improved hydrogen production through encapsulation of viable cells in silica gel and through manipulation of the phycobilisomes (PBS), the light harvesting antennae.

First, various formulations of silicon alkoxide-derived gels were screened with a high throughput screening assay to verify the organism could be successfully encapsulated and hydrogen production was comparable to similar cells in liquid culture. It was found that wild-type (*wt*) *Synechocystis* sp. PCC 6803 and a mutant known as M55 are both amenable to encapsulation within gels derived from

tetraethoxysilane (TEOS) precursors of low silica content, and observed hydrogen production was comparable to liquid cultures.

Subsequent investigations explored the effects of encapsulation stress and possible effects of gel additives on the photosynthetic activity and efficiency of this organism. *Synechocystis* sp. PCC 6803 was found to be moderately robust against salt stress, somewhat sensitive to ethanol stress, and very sensitive to osmotic stresses and interference with excitation transfer created by polyethylene glycol and glycerol, respectively.

Finally, three PBS mutants known as ΔcpcAB, ΔapcE, and ΔapcF were evaluated for glycogen accumulation, pigment content, hydrogen production, photosynthetic activity, and suitability for silica sol-gel encapsulation. The ΔcpcAB strain lacks PBS rods, the ΔapcE strain completely lacks a functional PBS, and the ΔapcF strain has a functional PBS with disrupted excitation transfer to the photosystems. Under 200 $\mu Em^{-2}s^{-1}$ light, all strains accumulated similar levels of glycogen, and the ΔapcE and ΔapcF strains produced similar levels of hydrogen while the ΔcpcAB strain produced less hydrogen compared to *wt* cells, although its photosynthetic efficiency was actually improved. Under 400$\mu Em^{-2}s^{-1}$ light, the ΔapcE and ΔapcF mutants both produced approximately 25% more hydrogen than *wt* cells from the same amount of glycogen, accumulating a 1.2% headspace hydrogen concentration. Hydrogen production from cells encapsulated in gels derived from aqueous precursors was approximately 3.5 times higher than similar cells in liquid culture, and more than double that from cells in alkoxide-derived gels. This investigation demonstrates the efficacy of silica sol-gel encapsulation as a tool to enhance photobiological hydrogen production from *Synechocystis* sp. PCC 6803 and that manipulation of photoantennae can lead to improved hydrogen production.

Photobiological Hydrogen Production from the Cyanobacterium *Synechocystis* sp. PCC 6803 Encapsulated in Sol-gel Processed Silica

by

David J. Dickson

A DISSERTATION

submitted to

Oregon State University

in partial fulfillment of

the requirements for the

degree of

Doctor of Philosophy

Presented February 8, 2011

Commencement June 2011

Doctor of Philosophy dissertation of David J. Dickson presented on February 8, 2011.

APPROVED:

Major Professor, representing Biological & Ecological Engineering

---

Head of the Department of Biological & Ecological Engineering

---

Dean of the Graduate School

I understand that my dissertation will become part of the permanent collection of Oregon State University libraries. My signature below authorizes release of my dissertation to any reader upon request.

David J. Dickson, Author

ACKNOWLEDGEMENTS

I would like to thank my advisor, Prof. Roger Ely, for giving me the opportunity to earn a PhD under his guidance. I appreciate the opportunity to craft the research in my own manner, I learned a great deal about my own strengths and weaknesses as a researcher, which I could not have learned otherwise. I also greatly appreciate the time and space granted to maintain balance. It was wonderful to have an advisor who gave excellent counsel, but was not overbearing and understood, even expected, that I have more in my life than graduate school.

My committee members, Professors Alex Yokochi, Catherine Page, Frank Chaplen, and Hong Liu have been very helpful throughout the entire process, always providing thoughtful guidance whenever asked.

I would like to thank agencies that have supported this research, including the Air Force Office of Scientific Research, National Science Foundation, and Chevron Corporation. I also thank organizations and people that have provided me with generous scholarship support, including the University Club of Portland, the Oregon Lottery Scholarship, Myron G. Cropsey, the Chambers Family Foundation, Edward S. Allen, and the Agricultural Engineering Research Foundation.

I would like to thank Dept. Head John Bolte and the Department of Biological & Ecological Engineering staff, who have all been extremely helpful. I especially appreciate the departmental fellowship that supported me when I first arrived.

My lab mates, past and present, including Tyler Radniecki, Paul Schrader, Liz Burrows, Sunhwa Park, Jed Eberly, Mark Luterra, and Hatem Mohamed, have all been wonderful and amazingly helpful. I have been very fortunate to have lab mates who were all so incredibly friendly, supportive, and intelligent. I also had outstanding help from many undergraduate and high school students, including Kelsey Baker, Mark

McGuire, Kelsey Ward, Soleil Rowan-Caneer, Rebecca Miller, Ben Glassy, Bethany Lassatter, Lucas Winiarski, Anne Wynn, Siri Erickson, Phoenix Bruno, Matt Galvin, and Peter Wong.

My fiancée, Dr. Erica McKenzie, has been incredibly supportive and helpful since the moment we met in 2008. Having been through the process already, she has provided much appreciated empathy, encouragement, and constructive guidance. She has given me direction, support, companionship, laughter, and love, not to mention the occasional thrashing in triathlons and marathons.

I would like to thank my friends and housemates, past and present, for keeping me sane, providing stimulating conversation, many laughs, the opportunity to create some music, and necessary, as well as unnecessary distractions. These people include Niels Damman, Matt Schmidt, Andrea Fideler, Ram Ravichandran, Liz Burrows, Biniam Iyob, Noah Stroup, Dannie Jansik, Erik Helzer, Keir Thomas, Erika Gabonay, Jorah Reinstein, Kami Schott, Seth Ring, Amy Burke, Nechamah Wildenah, Duffin McShane, Barbara Burkholder, Sara Dunham, Pete Kozak, Desiree Tullos, Josh Cuperus, Dave Takush, James Bickford, Jordan Golinkoff, and Miriam Seifter. I would also like to include Jim Phelps, Theresa Gibney, and Brandon Trelstad for their "distracting" dedication to sustainability, another extracurricular activity that kept me sane largely because it has been so much fun working with them.

Many thanks to the OSU Triathlon Club and the Men's and Women's Rugby Clubs for providing camaraderie, shared passion for sport, and much needed exercise and distraction over the past five years.

Finally, and most of all, I would like to express my sincere gratitude to my parents, Jim and Anna Dickson. I could not and would not have attempted graduate school without their support and guidance throughout my entire life. Together with my siblings, Matt Dickson, Paul McGreevy, Tracey Cranston, and Joe McGreevy, they laid the groundwork that set me on this path many years ago.

CONTRIBUTION OF AUTHORS

Prof. Catherine Page, a chemist and collaborator at the University of Oregon, provided electron microscopy, assistance with silica sol-gel processing, constructive conversation, and manuscript editing.

Prof. David Kehoe, a microbiologist and collaborator at the University of Indiana, created the ΔcpcAB, ΔapcE, and ΔapcF mutants of *Synechocystis* sp. PCC 6803, and provided helpful discussion on the evaluation of these mutants.

Prof. Roger Ely was the Principal Investigator for this research. He garnered funding support from the Air Force Office of Scientific Research, provided experimental oversight, and manuscript editing.

TABLE OF CONTENTS

TABLE OF CONTENTS (Continued)

Page

TABLE OF CONTENTS (Continued)

Page

TABLE OF CONTENTS (Continued)

Page

LIST OF FIGURES

LIST OF FIGURES (Continued)

Figure Page

LIST OF FIGURES (Continued)

Figure Page

LIST OF FIGURES (Continued)

Figure Page

LIST OF FIGURES (Continued)

Figure Page

LIST OF TABLES

LIST OF ACRONYMS & ABBREVIATIONS

APC	allophycocyanin (PBS core phycobiliprotein)
DCMU	3-(3,4-dichlorophenyl)-1,1-dimethylurea
ETC	electron transport chain
EtOH	ethanol, or ethyl alcohol
FNR	ferredoxin:$NADP^+$ oxidoreductase
F_v/F_m	maximum quantum efficiency of dark adapted PSII
F_v'/F_m'	maximum quantum efficiency of light adapted PSII
GG	glucosylglycerol
GHG	greenhouse gas
M55	mutant deficient in a functional NDH-1 complex
MTES	methyltriethoxysilane
NADPH	nicotinamide adenine dinucleotide phosphate (oxidized form = $NADP^+$)
ORMOSIL	organically modified siloxane
PAR	photosynthetically active radiation
PBS	phycobilisome
PC	phycocyanin (PBS rod phycobiliprotein)
PEG	polyethylene glycol
PQ	plastoquinone
PSI	Photosystem I
PSII	Photosystem II
Q_A	primary quinone electron acceptor, donor side of PSII
q_N	coefficient of nonphotochemical quenching
q_P	coefficient of photochemical quenching
TEOS	tetraethoxysilane
wt	wild-type strain of *Synechocystis* sp. PCC 6803
ΔapcE	mutant lacking the L_{CM} linker peptide (no fully assembled PBS)
ΔapcF	mutant lacking the allophycocyanin-B subunit (disrupted PBS core)
ΔcpcAB	mutant lacking α and β subunits of phycocyanin (PBS rod pigments)
ϕPSII	quantum efficiency of light adapted PSII (actual efficiency)
$\mu Em^{-2}s^{-1}$	micro-Einstein per m^2 per second (Einstein = a mole of photons)

CHAPTER 1 - INTRODUCTION & LITERATURE REVIEW

1.1 - Introduction & Project Overview

The cyanobacterium *Synechocystis* sp. PCC 6803 is a model organism for photosynthesis, being perhaps the simplest organism to contain the full complement of proteins required for oxygenic photosynthesis. The genome of *Synechocystis* sp. PCC 6803 was fully sequenced in 1996 [1] and has since been fully annotated, enabling rapid development in the use of this organism to elucidate phototrophic metabolism. One distinguishing feature of *Synechocystis* sp. PCC 6803 that separates it from many of the higher eukaryotic phototrophs it serves to model is its ability to produce molecular hydrogen under certain conditions via the activity of a reversible bimetallic hydrogenase.

Synechocystis sp. PCC 6803 contains a reversible [Ni-Fe] hydrogenase which is capable of producing molecular hydrogen, H_2, through two pathways: under anaerobic conditions through fermentation, presumably by catabolizing accumulated glycogen; and transiently during the onset of oxygenic photosynthesis. The substrate initially providing the protons and electrons that eventually find their way through the photosynthetic electron transport chain (ETC) to hydrogen is water, and sunlight is the driving force behind the oxidation of water, as in all oxygenic photosynthesis. Therefore, although the wild-type (*wt*) yield is low, this organism offers the possibility of utilizing sunlight and water to produce hydrogen, an extremely energy rich compound with enormous potential as an energy carrier, via a biological and renewable process.

Before this system can provide hydrogen in any practical or economically viable format, many fundamental challenges must be addressed. First, the hydrogenase enzyme is reversibly inhibited by molecular oxygen, meaning hydrogen production ceases upon exposure to oxygen, which naturally occurs through the

action of photosystem II (PSII) during oxygenic photosynthesis. Although direct photobiological hydrogen production is theoretically possible, and even transiently observed in *Synechocystis* sp. PCC 6803 [2], it is the oxygen sensitivity of the hydrogenase that ultimately thwarts this process. As a result, hydrogen production is predominantly through anaerobic fermentation of accumulated glycogen during darkness. Second, the metabolic conditions under which hydrogen production is favored (i.e., highly reduced NADPH/$NADP^+$ pool) are not necessarily compatible with optimal cell growth and viability. Various metabolic manipulations must be undertaken in order to maximize reductant availability to the hydrogenase. Finally, *Synechocystis* sp. PCC 6803 is well adapted to growing under low light conditions. The organism can harvest light so well that under moderately bright light, about 200 $\mu Em^{-2}s^{-1}$, or approximately 10% of full sunlight, its ability to use absorbed light becomes saturated and the organism redirects absorbed energy to nonproductive processes, including losses to heat and fluorescence. Improving light utilization efficiency toward glycogen accumulation in the light may provide a way to improve the efficiency of subsequent hydrogen production in the dark.

Active research is taking place in all three areas of inquiry. The primary foci of the current investigation are directed at the second and third challenges. To address metabolic constraints to hydrogen production, this project explores ways to manipulate the environment and growing conditions of the cells to improve reductant availability. To this end, live cultures were encapsulated within silica sol-gel, a stable and biologically compatible matrix that can potentially enhance activity and improve longevity, in addition to constraining growth, which should positively affect reductant availability.

Silica is abundant, and sol-gel processing is a well-developed science with rigorous investigation dating back to the World War II era [3]. However, applications have historically been completely inorganic in nature, and encapsulation of viable

organisms was not achieved until 1989 [4], rendering this approach relatively new and unexplored. To date, the approach has been used successfully to encapsulate a variety of organisms, most often to produce secondary metabolites of value or for biosensing. This investigation is among the first to encapsulate a phototroph.

To address the issue of light utilization efficiency, three antenna mutants were characterized during the course of this research. By truncating or creating other disruptions in the light harvesting antenna complex, called the phycobilisome (PBS), it is expected that light absorption in any given cell will be reduced, thereby increasing the light intensity at which the organism becomes saturated while reducing unproductive dissipation of excess excitation energy under higher light conditions, improving overall light utilization of the entire culture. Encapsulation within silica sol-gel then allows for layering of various strains to create a system where the most light tolerant cells are on the surface exposed to the brightest light, with strains more accustomed to low light below, where light intensity is attenuated.

The objectives of this research serve to advance basic and applied research in the field of photobiological hydrogen production and biological encapsulation toward a system that is stable, efficient, and economically viable. The three primary objectives are:

1. Successfully demonstrate hydrogen production from cultures of *Synechocystis* sp. PCC 6803 encapsulated in silica gel (Manuscript 1, Chapter 2);
2. Evaluate viability and activity of encapsulated cells over time to improve encapsulation protocols (Manuscript 2, Chapter 3); and
3. Evaluate growth, photosynthetic activity, encapsulation within silica gel, and hydrogen production from antenna mutants of *Synechocystis* sp. PCC 6803 (Manuscript 3, Chapter4).

The above objectives are all intended to better understand the encapsulation process and facilitate improved hydrogen production from encapsulated cultures of *Synechocystis* sp. PCC 6803. The ultimate goal is a system of encapsulated cells that can produce an economically significant amount of hydrogen from reasonably bright light over an extended period of time. Further detail in relevant areas of renewable energy, photobiological hydrogen production, and silica sol-gel processing are provided in the following review of refereed scientific literature.

1.2 - The Challenge of Renewable Energy

Global power demand is projected to reach an estimated 46 TW by the end of this century, representing more than a threefold increase above the current demand of 14 TW [5, 6]. Meeting this demand presents an incredibly daunting challenge. Where will humanity derive such massive amounts of power? This power is absolutely essential to provide everything from basic necessities, like clean water, food, and shelter, to the amenities of a higher standard of living and thriving economy, like personal transportation, health care, and recreation. Fossil and nuclear fuels share the same terminal flaw in that both rely on finite, exhaustible resources. Both have severe environmental consequences associated with their large scale use, including greenhouse gas emissions, impacts from drilling and extraction, mining and processing waste, and disposal of highly hazardous spent nuclear fuel. Furthermore, fossil fuels and uranium ore are not uniformly distributed across the globe, contributing to geopolitical tension as nations posture for access to these increasingly rare and precious resources, sometimes aggressively and belligerently. Continued reliance upon these finite fuels as our primary sources of energy, without devising appropriate alternatives while we have the means, will certainly lead to catastrophic economic and social turmoil, potentially on a global scale. Therefore, developing renewable energy technology is not merely a niche endeavor for environmentally conscious scientists and engineers, it is a critical matter of survival.

There are few challenges facing humanity with more urgency, or more severe consequences should we fail.

Ultimately, the one and only renewable resource capable of meeting such a power demand is the Sun, which provides the Earth's surface with a constant deluge of 89,000 TW. Harnessing a mere 1% of this power at 10% efficiency would provide 89 TW and meet the world's power demand for the foreseeable future. Solar energy is also the most widely distributed energy resource available, and the only one that can meet demand at such a large scale, in perpetuity.

Solar energy is already utilized on a global scale to provide primary input of energy to the biosphere through photosynthesis. Humans can leverage this process by direct utilization of biomass as a fuel or feedstock for the production of higher quality fuels. Exploiting photosynthesis to produce energy is leveraging billions of years of evolution to our advantage, harnessing processes which we cannot yet replicate artificially. Furthermore, solar energy is widely available in nearly every populated place on the planet, a compelling scenario for meeting energy needs locally and regionally, shifting humanity toward independent, distributed generation and reducing reliance on foreign sources of energy.

1.3 - Hydrogen as an Energy Carrier & the Hydrogen Economy

In addition to being used for the production of conventional fuels, solar energy can also be utilized by some phototrophic organisms to produce hydrogen. Hydrogen offers great potential as a versatile energy carrier and viable alternative to conventional carbon based fossil fuels. Development of hydrogen as an alternative fuel has received a great deal of research and popular press [7-13]. On a mass basis, aside from fissile uranium, hydrogen is the most energy dense fuel available, containing nearly 3 times the energy of an equivalent mass of gasoline or diesel and 2.5 times the energy of natural gas [14]. Hydrogen offers flexibility through a variety of production processes and relatively easy exchange with electricity through

electrolysis and electrochemical fuel cells. On an atomic basis, hydrogen is among the most abundant and well distributed elements on the planet, present in water, biomass, and minerals, meaning that viable production is a matter of technological development, not purely economic or political access to resources [9]. On a mass basis, the earth's crust is composed of approximately 0.14% hydrogen, which would appear scarce until compared with carbon, which makes up only 0.03% of the crust, and yet, is the foundational element of all life and the existing fossil fuel economy. Finally, upon combustion or consumption in a fuel cell, the exhaust is water, making a closed loop cycle between source and fuel, with no emissions of carbon dioxide, a greenhouse gas (GHG). A variety of available pathways for renewable hydrogen production are illustrated in Figure 1-1, below.

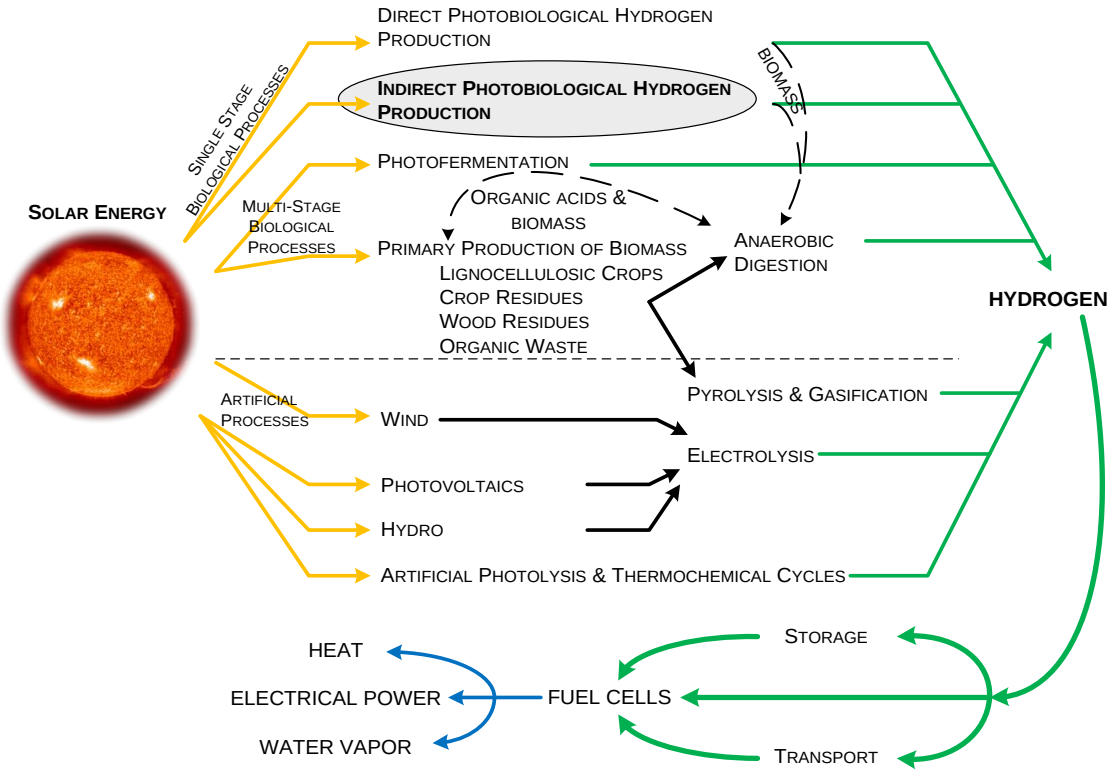

Figure 1-1: A schematic of the numerous pathways for sustainable hydrogen production. Indirect photobiological hydrogen production, the primary focus of the current research, is circled in gray.

Before hydrogen can be utilized as a major energy carrier, numerous technological hurdles must be overcome. Improved and sustainable methods of production are essential, since hydrogen production would need to be dramatically increased to meet any significant portion of future energy needs. This cannot be done relying on reforming conventional fossil fuels into hydrogen. Drastic improvements are also required in storage, transport, and infrastructure as well as in fuel cells. The breadth and scope of the requisite technologies have been reviewed at length elsewhere and are beyond the scope of the current review [8, 10, 15].

Currently, most hydrogen is produced from nonrenewable fossil fuels, predominantly steam reforming of natural gas, and to a much lesser extent, coal gasification [16, 17]. Although steam methane reforming (SMR) can theoretically have a thermal efficiency greater than 70% [17-19], this is difficult to achieve in practice and SMR consumes a great deal of natural gas in the reaction and by combustion, releasing a significant amount of carbon dioxide. Furthermore, natural gas resources, while more abundant than petroleum, are in decline in some regions and are ultimately finite, just like petroleum. Virtually none of this hydrogen is currently used as a fuel, it is generally used on-site in petrochemical refineries or for fertilizer production. If hydrogen from natural gas were to become a significant portion of the energy economy, long term production potential simply does not exist and natural gas supplies would rapidly be depleted. Therefore, alternative sources of hydrogen must be sought.

The next most developed technology for hydrogen production is electrolysis. Under ideal standard conditions, water will dissociate into hydrogen and oxygen at a potential of 1.23 V to yield 1 kg of hydrogen from 8.9 L of water and 39 kWh of electricity [20]. However, under real operational conditions, at least 1.48 V is required to overcome inefficiencies, like overpotential, internal resistance, etc. In practice, the industry average is 66.3% efficiency, requiring 58.8 kWh electricity per

kilogram of hydrogen [11]. Still, this is a modest efficiency penalty considering the simplicity of the technology and the fact that any source of electricity will suffice. Development of more efficient and robust electrolyzers is an active area of research and a high priority area of the Department of Energy Hydrogen Program [8]. This is also a critical technological component of a viable hydrogen energy system because it enables efficient exchange between hydrogen and electricity. However, large scale electrolyzers remain very expensive compared to SMR and account for less than 10% of current hydrogen production in the United States [10, 21].

When used to produce electricity in a fuel cell, water is released in precisely the reverse reaction of electrolysis, illustrating how hydrogen may buffer spatial and temporal variation in electricity demand. For example, off-peak electricity could be used to produce hydrogen through electrolysis. That hydrogen could then be stored and used in a fuel cell to produce electricity during peak demand hours, or during times when intermittent sources of electricity (like wind or solar energy) are unavailable. It is this interplay between hydrogen production from a variety of sources and the production of electricity from hydrogen that lead the electrochemist John Bockris to coin the term “hydrogen economy” in a series of publications in the early 1970’s [22-24]. Since then, more diverse technologies have been discovered and are currently being developed, including biological means of hydrogen production, to bring the hydrogen economy closer to fruition.

1.4 - Photobiological Hydrogen Production

An attractive and intriguing option for renewable hydrogen production is using phototrophic organisms for photobiological production of hydrogen from sunlight and water, perhaps the most abundant and ubiquitous resources available. This process would, most importantly, avoid fossil fuel use and also the inefficiencies of an electricity intermediate during initial production. Depending on the process, it may also avoid intermediate production of carbohydrate or biomass. This takes

advantage of a naturally occurring and completely renewable process that has been evolving for over 3 billion years. This process occurs in a variety of cyanobacteria and algae, although it does not occur in any higher eukaryotic plants. Conversion efficiencies as high as 16%, sunlight to hydrogen, are considered practically achievable [12, 25, 26], warranting a great deal of active research. Fundamental aspects of photosynthesis and how it can lead to hydrogen production are summarized in subsequent sections.

1.4.1 - Overview of Photosynthesis

Photosynthesis is a means to capture incoming solar radiation biologically, through the activity of photoautotrophs, the primary producers. Although this process has very limited efficiency in terms of converting solar energy into biomass, typically on the order of 1% or less [6], photosynthesis is remarkably efficient at the initial absorption of solar energy to achieve charge separation and oxidize water. Under ideal conditions, the light harvesting apparatus of algae and cyanobacteria may harvest as much as 98% of photosynthetically active radiation, or PAR [25, 26], radiation in the wavelength range of 400 nm to 700 nm for oxygenic phototrophs.

The first step of photosynthesis is the absorption of PAR by the photoantennae and photosystem chlorophylls. This process is described in further detail in §1.4.2. Once absorbed, the energy of four photons are used simultaneously by photosystem two (PSII) to oxidize water, splitting it into electrons and protons while releasing molecular oxygen, the very oxygen aerobic organisms rely upon to breathe. The free protons are released into the lumen, the space within the thylakoid membrane, creating a trans-membrane pH gradient used for the production of ATP by the trans-membrane enzyme ATP-synthase. This pH gradient is also augmented by other steps in the electron transport chain which pump protons against the gradient during the transfer of energetic electrons. In contrast to protons, electrons do not exist unbound. Instead, they are carried by protein electron carriers, first the primary

acceptor plastoquinone Q_A then on through the remainder of the photosynthetic ETC. Plastoquinone (PQ) is a hydrophobic protein that resides within the thylakoid membrane. Once reduced by primary acceptors, reduced PQ transfers electrons to the cytochrome b_6f complex, which reduces plastocyanin, a hydrophilic protein in the lumen. With the absorption of light energy, PSI then oxidizes plastocyanin to reduce ferredoxin on the cytoplasmic side of the thylakoid. Reduced ferredoxin can then be used by ferredoxin-$NADP^+$ oxidoreductase (FNR) to reduce $NADP^+$ to NADPH, a primary source of reductant utilized heavily in the Calvin Cycle to reduce atmospheric carbon dioxide (2 moles of NADPH per mole of carbon fixed). Figure 1-2 illustrates the basic processes of the photosynthetic ETC as they occur in *Synechocystis* sp. PCC 6803.

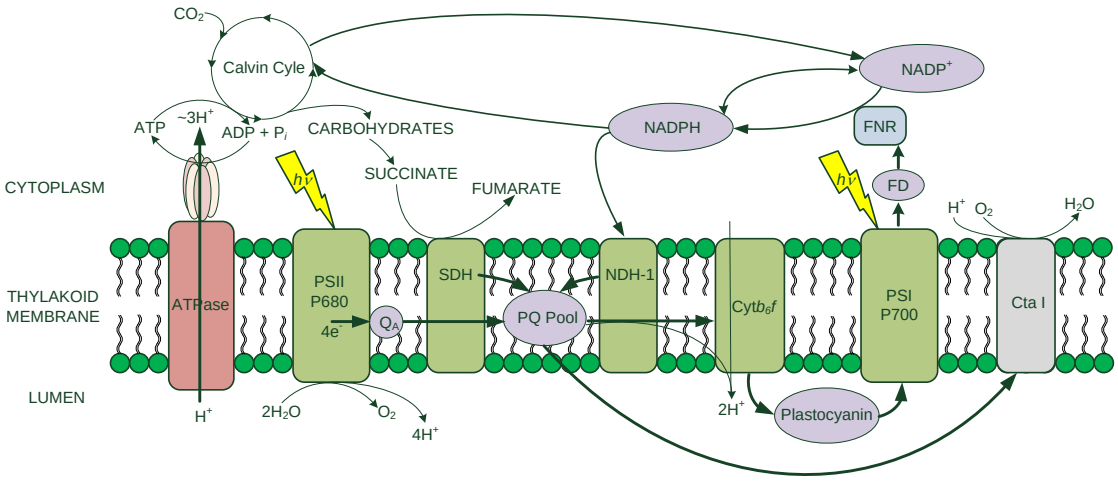

Figure 1-2: Primary electron transport pathway during oxygenic photosynthesis. PSI = photosystem one; PSII = photosystem two; SDH = succinate dehydrogenase; NDH-1 = NADPH dehydrogenase; Cyt b_6f = cytochrome b_6f; Q_A = primary quinone electron acceptor; PQ = plastoquinone pool; FD = ferredoxin; FNR = ferredoxin:$NADP^+$ oxidoreductase; ATPase = ATP synthase; NADP+/NADPH = nicotinamide adenine dinucleotide phosphate (oxidized/reduced); and CtaI = a terminal oxidase.

Losses are incurred along each and every step of the ETC, from initial absorption, through the point of carbon fixation in the Calvin Cycle, and including subsequent biomass accumulation. In many cases, these inefficiencies are obligatory, thermodynamically speaking, in order to drive each reaction to proceed irreversibly. Shown in Figure 1-3 is a standard Z-scheme for photosynthesis, which shows the transfer of energetic electrons through the electron transport chain. Small drops in redox potential, which are effectively losses in energy, occur at each transfer of electrons between carriers, with the exception of the two large boosts achieved by the excitation of the two photosystems (PSII = P680 and PSI = P700).

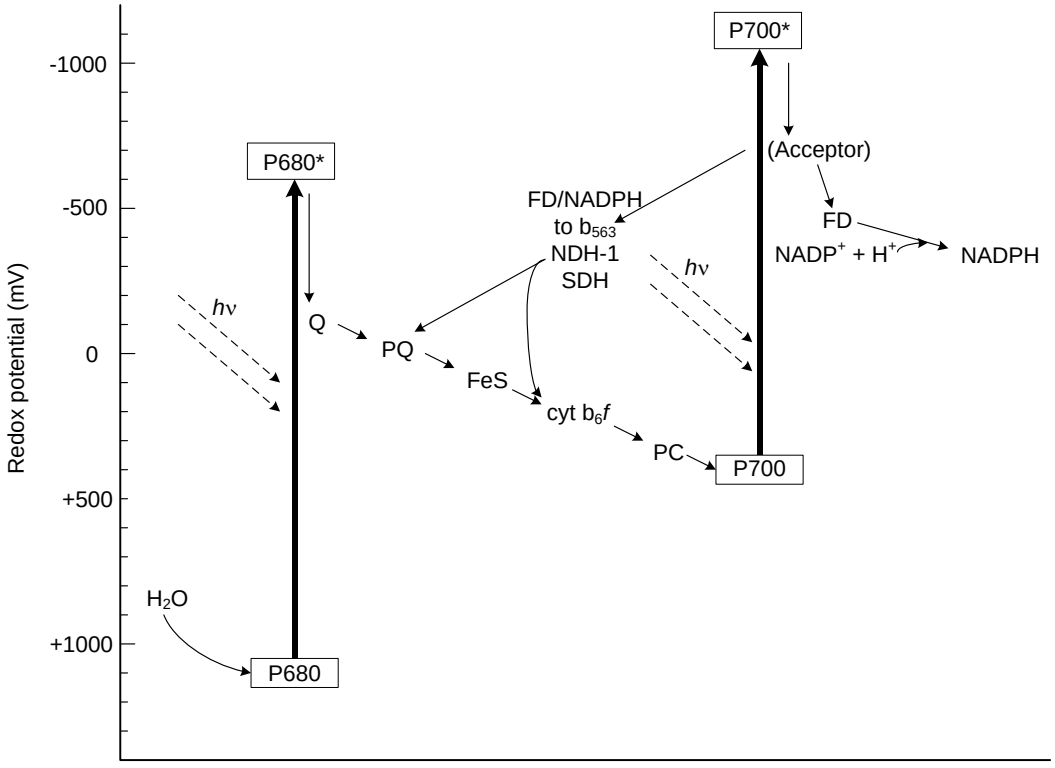

Figure 1-3: "Z-scheme" of excitation energy transfer through the electron transport chain. Excitation is provided by the photosystems, beginning with the oxidation of water and concluding with the reduction of $NADP^+$.

In *Synechocystis* sp. PCC 6803, the reversible [Ni-Fe] hydrogenase enzyme can then use NADPH generated at the end of the photosynthetic ETC to produce molecular hydrogen under certain conditions. When the hydrogenase uses NADPH regenerated as a direct result of PSI activity, this is referred to as direct photobiological hydrogen production. When that NADPH is directed toward carbon fixation, and regenerated later through glycolytic and fermentative metabolic pathways, that is called indirect photobiological hydrogen production. Both processes are discussed in further detail below.

Understanding and improving hydrogen production is the goal of this and many other research efforts. Altering light absorption characteristics and energy availability to the hydrogenase enzyme are the two parallel lines of inquiry pursued in the current work toward understanding and improving hydrogen production from this organism. *Synechocystis* sp. PCC 6803 has been an incredibly productive platform for these investigations because the genome is sequenced and annotated, the organism is readily transformable, and it grows autotrophically, mixotrophically, and heterotrophically.

1.4.2 - Light Absorption in Cyanobacteria

Synechocystis sp. PCC 6803 contains large protein complexes called phycobilisomes (PBS), responsible for light absorption and excitation distribution to the photosystems. In contrast to higher plants, where light harvesting complexes dominated by chlorophyll *a* reside within the thylakoid membranes to affect light absorption and excitation energy transfer, the PBS is a hydrophilic protein complex that attaches to the cytoplasmic side of the thylakoid membrane. From there, it associates with the photosystems, predominantly PSII, to achieve energy transfer from absorbed photons. Furthermore, rather than chlorophyll, the pigments of the PBS are phycocyanin (PC) and allophycocyanin (APC), which both have different absorption spectra compared to chlorophyll. Absorption peaks occur around 617 nm

for PC and 650 nm for APC [27], which are at longer wavelengths than the Soret band of chlorophyll but shorter than the strong red absorption peak, meaning excitation energy flows “downhill,” energetically speaking, to efficiently transfer from the PBS to the reaction center chlorophylls of the photosystems. Chlorophyll pigments in the reaction centers of PSI and PSII have excitation energies corresponding to photon wavelengths of 700 nm and 680 nm, respectively.

The common characteristic of all photosynthetic pigments that allows for the absorption of light energy is molecular electron orbitals with many π-bonds. Whether in a tetrapyrrole structure like chlorophyll, or more linear structures of linked pyrrole rings, like in PC and APC, both have multiple π-bonds that have many excitation levels. In these molecular orbitals, a resonant interaction between photon and electron can excite the electron to a higher energy level, provided the photon has an energy corresponding to an available energy level, creating an excited electron – hole pair, commonly called an exciton [28]. This exciton then moves through the pigment structure by a process called resonance, a coupling of energy levels of adjacent electrons. The net effect is that although electrons do not physically move through the antennae, excitation energy certainly does, and its tendency is toward slightly lower energy levels with each transfer (resulting in nonradiative decay), effectively channeling the energy toward the reaction center chlorophylls.

Once in the reaction center, the excitation energy causes charge separation within terminal chlorophyll pigments. In the oxygen evolving complex of PSII, four photons are used to oxidize two water molecules into protons, electrons, and molecular oxygen. The charge separation created from those four photons is stabilized simultaneously on manganese clusters within the reaction center, a process that is critical in preventing the formation of reactive oxygen species [29, 30]. Literature devoted specifically to PSII, water oxidation, and the oxygen evolution complex is expansive, and reviews have been published recently [31-33].

The PBS is the primary antennae complex of most cyanobacteria, and is composed of numerous proteins and chromophores. The complete structure has been recently elucidated at a resolution of 13 Å [34]. To summarize, the overall structure is hemidiscoidal, composed of three stacked cylinders at the core, where it interacts with the thylakoid and photosystems, and six rods radiating from this core, as shown in Figure 1-4.

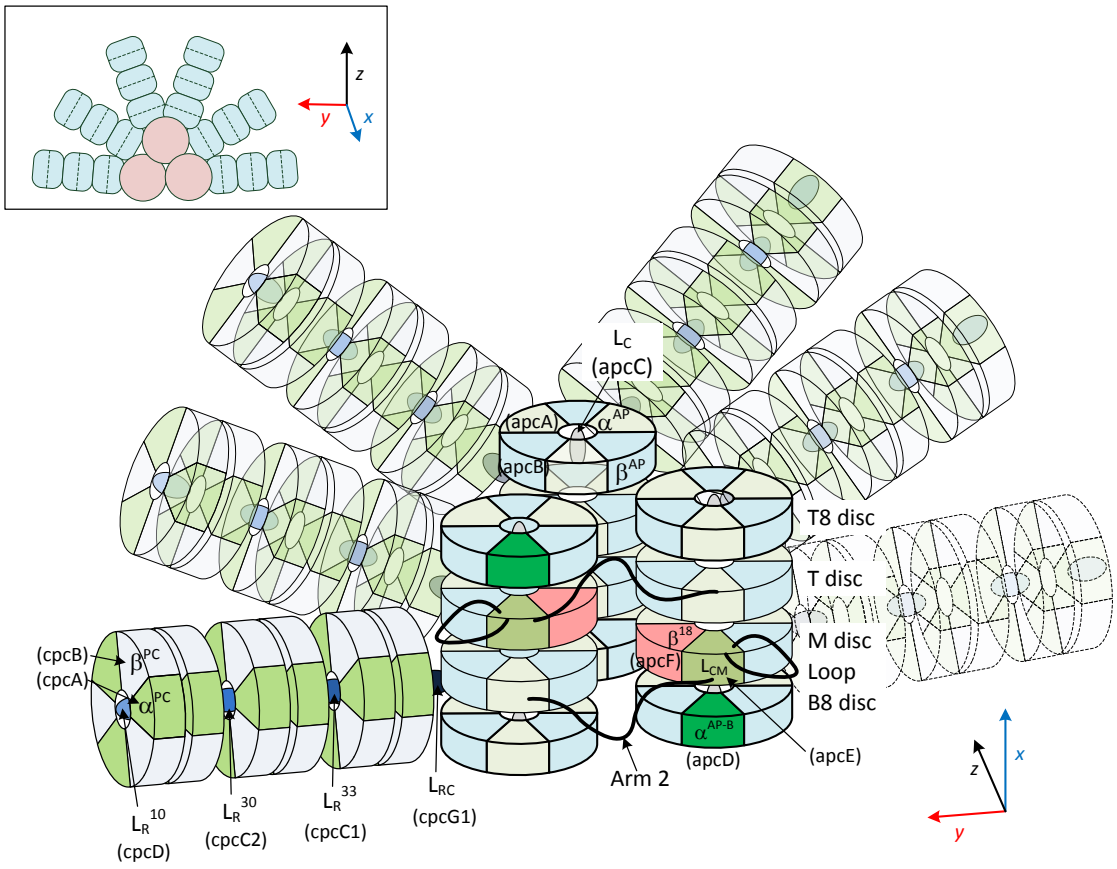

Figure 1-4: A detailed illustration of the PBS structure, adapted from Arteni et al. [34], including all known subunits and linker peptides (thylakoid parallel to page). A 2D profile is shown in the inset (thylakoid orthogonal to page). Primary labels are protein names, while labels in brackets are corresponding genes.

In *Synechocystis* sp. PCC 6803, each rod is thought to be identical, composed of three discs of hexameric α and β PC dimers. Other cyanobacteria may have other chromophores in the PBS rods, including phycoerythrin or phycoerythrocyanin, but these are not present in *Synechocystis* sp. PCC 6803 [34]. The hexameric discs have a central channel where linker polypeptides bind the rod together. At the base, a linker peptide attaches the rod to the core, in a somewhat flexible manner that is easily disturbed. Each of the three cylinders of the core is composed of four discs. In the upper cylinder, which is spatially separated from PSII, two discs have an identical composition of APC trimers $(\alpha\beta)_3$, denoted T discs, and two other discs that are similar but with the addition of a L_C linker peptide, denoted T8 discs (the linker peptide is 8 kDa). The bottom discs, adjacent to each other and to PSII, are identical, oriented 180° to each other. They each contain one T disc and one T8 disc, as well as a B8 disc where one α subunit of APC is replaced by a different isoform called allophycocyanin-B (AP-B) in a T8 disc, and a M disc where one $\alpha\beta$ dimer is replaced by a domain of the L_{CM} peptide and the β^{18} isoform of APC [34, 35].

The PBS is capable of distributing excitation energy to either photosystem, in a controlled process known as a state transition which is regulated by the redox state of the PQ pool [36]. In the dark, the PQ pool generally tends to be reduced. This causes a reorganization of the PBS to distribute more excitation energy toward PSI, which is known as State 2 (even though there is no excitation energy being absorbed in the dark). Increased PSI activity with exposure to actinic light would act to oxidize the PQ pool. If the PQ pool becomes predominantly oxidized, as may occur in light when PSII activity cannot keep pace with PSI activity, a transition to State 1 is induced where more excitation energy is directed toward PSII [36, 37]. This state transition allows the organism to adapt to light conditions and metabolic demands in order to efficiently allocate excitation energy between the photosystems. Although the exact mechanisms of the state transition and excitation distribution in *Synechocystis* sp.

PCC 6803 are not fully understood [38], it is suspected that both direct transfer of excitation energy from PBS to PSI and spillover, a transfer of energy from PSII to PSI, are likely occurring [39, 40]. It is also known that multiple subunits in the PBS play a role in the state transition, including proteins encoded by the genes apcD, apcF, and rpaC [41, 42]. As a result, alterations to the PBS structure not only directly affect light absorption, but also create secondary effects by disrupting the state transition in ways that are difficult to predict.

A detailed understanding of light harvesting in this organism is critical in order to rationally attempt to improve the efficiency of light utilization. The PBS is extremely efficient at light absorption and excitation energy transfer to the photosystems. Indeed, under ideal conditions, PBS may direct more than 90% of absorbed energy to photochemistry [43]. However, under relatively moderate light intensity, typically around 200 $\mu Em^{-2}s^{-1}$, down-stream reactions are saturated and mechanisms for dissipating excess excitation energy increase in activity. *Synechocystis* sp. PCC 6803 has evolved to grow well under low light, so when available light exceeds the organism's ability to effectively use that light, wasteful absorption occurs which does not yield photochemistry. While it may seem counter intuitive, reducing the efficiency of light absorption has been proposed as a means to improve the overall efficiency of light utilization (reviewed recently by Melis [44]). This approach has been demonstrated successfully in algae [45, 46] and cyanobacteria [47] and may be further leveraged for increased hydrogen production in *Synechocystis* sp. PCC 6803, verified for the first time in the current research. Changes to light absorption efficiency were explored through the creation of three antennae mutants, which are described in more detail in Chapter 4 with implications for light absorption, excitation distribution, and hydrogen production.

1.4.3 - Hydrogenase Enzymes

A hydrogenase enzyme is an enzyme that can catalyze the following reversible reaction:

$$2H^+ + 2e^- \leftrightarrow H_2$$

The direction of the reaction is largely governed by the redox potential of the substrates that are interacting with the enzyme and the concentration of those substrates. While free protons are often readily available under physiological conditions, free electrons are not, they are provided by some other reduced energy carrier, such as NAD(P)H or reduced ferredoxin. Hydrogen is a highly energetic compound, so much of the time, hydrogenase enzymes function to scavenge this energy in uptake rather than production. In *Synechocystis* sp. PCC 6803, hydrogen can be oxidized to reduce $NADP^+$. In other organisms and environments, hydrogen uptake can lead to the reduction of other electron acceptors, including carbon dioxide, sulfate, ferric iron, nitrate, or even oxygen [48]. Uptake hydrogenase activity is also very common in nitrogen fixing organisms to recover hydrogen produced through the activity of the nitrogenase enzyme.

In nature, biological hydrogen production through hydrogenase activity typically occurs during anaerobic degradation of organic matter under conditions of highly negative redox potential. That hydrogen is then readily consumed and oxidized by a variety of organisms to reduce the compounds mentioned above. In a stratified system, hydrogen is present only in trace amounts by the time the system becomes aerobic and redox potential turns positive. This rapid consumption of hydrogen upon its production is one reason why hydrogen does not constitute a significant portion of the atmosphere [48].

Hydrogenase enzymes are widespread in nature, occurring in a variety of bacteria, cyanobacteria, algae, archaea, and some fungi, but no higher plants [48].

There are three known types of hydrogenase enzymes, characterized by the metal cluster at the core of their active sites:

1. [Fe-Fe] hydrogenases, common in bacteria, algae, and some fungi;
2. [Ni-Fe] hydrogenases, widespread through bacteria, cyanobacteria, and archaea; and
3. [Fe] hydrogenases, known only to occur in methanogenic archaea (synonymous with methylene-tetrahydromethanopterin dehydrogenases, or simply the group of Hmd enzymes [48, 49]).

Photobiological hydrogen production is known to occur in algae through the activity of [Fe-Fe] hydrogenases using reduced ferredoxin as substrate, and in cyanobacteria through the activity of [Ni-Fe] hydrogenases using NAD(P)H as substrate. These processes are discussed in further detail below. The [Fe] hydrogenase occurs only in methanogenic archaea and is thought to function exclusively in uptake, serving an intermediate role in the reduction of carbon dioxide to methane [48].

A comprehensive review of the structure and catalytic mechanisms of hydrogenase enzymes is beyond the scope of the current review, although there is an expansive body of literature devoted to this topic. High resolution crystal structures are available for multiple [Ni-Fe] hydrogenases [50-54], and a number of excellent reviews on the phylogeny, diversity, and function of hydrogenase enzymes have been recently published [48, 49, 55-57].

1.4.4 - Direct Photobiological Hydrogen Production

Direct photobiological hydrogen production means the production of hydrogen directly from the activity of the hydrogenase enzyme and photosynthetic processes *without* the intermediate storage of carbohydrate. That is, there is no spatial or temporal separation between the two processes (photosynthetic light absorption and hydrogen production). For this to take place, electrons enter the

photosynthetic ETC after the oxidation of water at PSII, and move directly through PSI to reduce ferredoxin. In algae, which possess a [Fe-Fe] hydrogenase, reduced ferredoxin can then be oxidized to reduce protons and yield hydrogen. In cyanobacteria, with a [Ni-Fe] hydrogenase, the additional step of reducing $NADP^+$ to NADPH by the activity of FNR is required prior to oxidizing NADPH to reduce protons and yield hydrogen. Both processes represent a direct linear transfer of excitation energy from sunlight and electrons from water to molecular hydrogen.

The primary hurdle to achieving significant hydrogen production from this pathway is its inherent transience due to the oxygen sensitivity of hydrogenase enzymes. [Fe-Fe] hydrogenases are irreversibly inhibited by molecular oxygen, and [Ni-Fe] hydrogenases are reversibly inhibited [50, 58]. Oxygen production is inevitably occurring through the activity of PSII, usually at a faster rate than aerobic respiration can consume it, so it will quickly accumulate and arrest the activity of the hydrogenase. From an evolutionary standpoint, this is a predictable adaptation, intended to prevent the loss of biochemical energy that would otherwise be directed toward growth.

The obvious solution would be to utilize a system with an oxygen tolerant hydrogenase. However, although some hydrogenases with limited oxygen tolerance have been discovered [58, 59], no reversible hydrogenases are truly tolerant to atmospheric levels of oxygen, nor do they occur in oxygenic phototrophs. The mechanism of oxygen tolerance is also not clearly understood, although it is likely related to the number and placement of ligands coordinating the bi-metallic active site [60] and the gas channel which presumably controls access of both hydrogen and oxygen to the active site [61]. To date, expression of oxygen tolerant hydrogenase subunits in oxygenic phototrophs has met with little success, likely due to missing accessory proteins in the host organism required for correct folding and assembly of a functional enzyme [60]. Since no oxygenic phototroph has been discovered with an

oxygen tolerant hydrogenase, oxygen sensitivity remains a recalcitrant challenge [62].

Some researchers have achieved improved hydrogen production in algae through the direct pathway by using sulfur stress to reduce the rate of oxygen evolution at PSII within chloroplasts so that it matches the rate of respiratory oxygen consumption in the mitochondria [63-66]. This creates a micro-aerobic environment within the cell allowing hydrogenase activity to continue. Although this approach allows for hydrogen production during autotrophic or mixotrophic growth, it also constrains the organism energetically, possibly constraining potential hydrogen production. This approach is also not feasible in cyanobacteria because respiratory and photosynthetic electron transport overlap, they are not well segregated in chloroplasts and mitochondria as they are in algae. Ultimately, direct photobiological hydrogen production is the most efficient option and the end goal, but until an oxygen tolerant hydrogenase can be found or engineered into an oxygenic phototroph, it will remain limited and a model platform for various forms of engineered in vitro systems. Alternatively, much progress has been made with in vivo systems designed at indirect photobiological production.

1.4.5 - Indirect Photobiological Hydrogen Production

Indirect photobiological hydrogen production refers to the production of hydrogen after the intermediate storage of biomass, typically a carbohydrate, such as starch or glycogen, or possibly as polyhydroxyalkanoates, like poly-β-hydroxybutyrate (PHB). The process begins with the same photosynthetic processes, and concludes with the hydrogenase producing hydrogen from excess reductant. However, the reductant is made available only through the anaerobic fermentative breakdown of stored organic carbon, after energy had been directed toward biomass accumulation during the light. This creates a temporal separation between light harvesting and hydrogen production, and avoids oxygen inhibition of the hydrogenase. Although

hydrogen can be reliably and consistently produced by this pathway, the extra steps incur losses in efficiency. This is the primary pathway of hydrogen production in *Synechocystis* sp. PCC 6803, explained in more detail in §1.4.7.

1.4.6 - Nitrogenase-Mediated Hydrogen Production

Some cyanobacteria have the ability to reduce, or "fix" atmospheric nitrogen into ammonia through the action of a nitrogenase enzyme. ATP is used to catalyze this reaction and hydrogen is released as a byproduct, as illustrated by the reaction:

$$\mathrm{N_2} + 8\mathrm{e^-} + 8\mathrm{H^+} + 16\mathrm{ATP} \rightarrow 2\mathrm{NH_3} + \mathrm{H_2} + 16\mathrm{ADP} + 16\mathrm{P}_i$$

Nitrogenase enzymes are extremely sensitive to oxygen, which forces cyanobacteria to create temporal or spatial separation between the activity of PSII and the nitrogenase. Some species form heterocyst cells which are fundamentally different from vegetative cells. Heterocysts contain no PSII, so produce no oxygen. They contain a robust cell wall which is impermeable to oxygen, creating a nearly anaerobic environment within the cell. Adjacent vegetative cells provide some energy to these cells through active transport of organic carbon, while the heterocysts become singularly devoted to fixing nitrogen. Although there is no PSII activity, PSI is present and remains active, as cyclic electron flow around PSI is an effective way to rapidly regenerate the ATP required for this reaction. There is some evidence that phycobilisome rods may specifically associate with PSI to facilitate increased energy transfer [67], increasing nitrogen fixation rates.

Despite oxygen sensitivity, the most significant limitation illustrated in the reaction above is the incredible demand for ATP: 8 moles per mole of N_2 fixed and 16 moles per mole of H_2 produced. Theoretically, this can be improved by a factor of 4 by removing nitrogen from the atmosphere of the nitrogenase, effectively transforming the nitrogenase into an ATP-driven hydrogenase, as illustrated in the following reaction [12, 68]:

$$2e^- + 2H^+ + 4ATP \rightarrow H_2 + 4ADP + 4P_i$$

One advantage to this approach over hydrogenase mediated systems is that the hydrogen production activity of the nitrogenase is irreversible. There is no evidence of uptake activity in any known nitrogenase. Many nitrogen fixing organisms contain uptake hydrogenases to recover the hydrogen produced by the nitrogenase, but these can and have been easily knocked out through mutation to allow for hydrogen evolution [68, 69].

The fundamental limitation of hydrogen production by nitrogenase enzymes is the energetic requirement of ATP. Hydrogen that is not scavenged by an uptake hydrogenase comes at an enormous expense to these organisms. By some estimates, this constrains the maximum achievable overall efficiency, light to hydrogen, at approximately 6% [12], and hydrogen production documented in the literature is approaching this threshold (3.7%) [69]. This leaves little remaining potential with this system. Some have even suggested that further investigation into nitrogenase-based systems is not warranted due to the low inherent efficiency [70], although this seems extreme. Nevertheless, investigation of the nitrogenase active site continues, and is warranted, to determine features that make hydrogen production irreversible.

1.4.7 - Hydrogen Production in Synechocystis sp. PCC 6803

The cyanobacterium *Synechocystis* sp. PCC 6803, the species used exclusively in this investigation, possesses one reversible [Ni-Fe] hydrogenase which can utilize NADPH or NADH and a cytoplasmic proton as substrates to produce molecular hydrogen. The enzyme has similar affinity for each substrate [2], perhaps with slight preferences for NADH, although NADPH is present in *Synechocystis* sp. PCC 6803 at a concentration approximately one order of magnitude higher than that of NADH [71], so it is expected to be the primary substrate. The physiological role of this reversible hydrogenase is not exactly known, although it has been suggested as a mechanism for redox balance [72, 73] or playing a role in anaerobic fermentation [74]. NADPH is

typically used for anabolic reactions, including the fixation of atmospheric carbon dioxide in the Calvin cycle. When excess NADPH is available, the cells may be able to effectively "vent" excess energy through the production of molecular hydrogen, producing $NADP^+$ in the process. This helps draw electrons through the electron transport chain. This is believed to serve as a venting mechanism to allow the organism to maintain redox balance through the oxidation of NADPH back to $NADP^+$ with concomitant consumption of a proton, although this hypothesis remains to be decisively proven experimentally.

Like all hydrogenases, the [Ni-Fe] hydrogenase in *Synechocystis* sp. PCC 6803 is oxygen sensitive, so any consistent amount of hydrogen production from this organism will generally occur in the dark under anaerobic conditions through the fermentation of accumulated glycogen, an indirect pathway. Direct production has been observed in a mutant known as the M55, deficient in a functional NDH-1 protein complex (integral to cyclic electron flow around PSI), but even after an initial burst of hydrogen production with the onset of photosynthesis, hydrogenase activity is still arrested by oxygen inhibition [2, 75]. The initial burst has been attributed to a delayed onset of PSII activity because the PQ pool and other down stream acceptors are more reduced than they would generally be in the *wt*.

In order to increase indirect hydrogen production from *Synechocystis* sp. PCC 6803, metabolic engineering to direct more electron flux and reductant to the hydrogenase has proven among the most effective strategies [74, 76-79]. At physiologic conditions, the redox potential of the $NAD(P)^+$/NAD(P)H couple is approximately 320 mV, while that of the H^+/H_2 couple is 420 mV, meaning the reductant pool must be approximately 99.9% reduced for hydrogen evolution to take place [2]. The implication is that other reactions which draw on NADPH, like carbon fixation or protein synthesis and repair, will come at the expense of hydrogen production. Furthermore, constraints in energy sources, like glycogen, which help

regenerate NADPH, also reduce hydrogen production. Therefore, in theory, decreasing other electron fluxes draining NADPH, coupled with increased glycogen accumulation (i.e., that occurs in the light as a result of carbon fixation) should yield increased hydrogen production. This has been successfully demonstrated through the M55 mutant of *Synechocystis* sp. PCC 6803, deficient in a functional NDH-1 complex linking respiratory and photosynthetic electron transport [2, 75-77], through sulfur, nitrogen, and pH optimization to enhance glycogen storage during the light to improve fermentative hydrogen production in the dark [74, 78, 80], and rational use of specific inhibitors to manipulate electron flux [79].

Both encapsulation and manipulation of photoantennae can be viewed as metabolic manipulations as well. By restricting growth, energy flux that would be used for biomass production and cell division may be redirected toward hydrogen production. Furthermore, a restriction in photoantennae size is intended to make more excitation energy available for glycogen accumulation under higher light intensities. Applied together, it is expected that antennae mutants encapsulated in silica gel would yield a higher conversion efficiency, light to hydrogen, over a complete light-dark cycle.

Complicating such efforts to enhance hydrogen production from *Synechocystis* sp. PCC 6803 is our poor understanding of the precise physiological function of the hydrogenase [73]. One especially puzzling observation is that the hydrogenase affected photosynthesis even when it was supposed to be inactive, that is, in the presence of oxygen [73]. The hypothetical role for the hydrogenase under these conditions may be the dissipation of excess excitation from PSI, as shown by increased sensitivity to photoinhibition in a ΔhoxEF mutant, but this is difficult to reconcile with well documented oxygen inhibition. Furthermore, redox regulation of transcript levels is not clearly understood, having been shown to be independent of the redox state of the PQ pool [81]. The enzyme is known to be under the regulation

of transcriptional regulator LexA, which is itself redox sensitive, as well as the activity of the Calvin Cycle. Inhibition of the Calvin Cycle leads to down regulation of the *hox* operon, which is counterintuitive [81, 82]. Transcript levels have also been observed to be lower in the dark as compared to the light, yet higher under anoxia compared to aerobic conditions, which again appear to be contradictory observations [81]. Clearly, there is still much to learn about this deceptively simply yet incredibly adaptable organism.

1.5 - Sol-Gel Processed Silica

1.5.1 - Overview of Sol-Gel Processing

Sol-gel processing is a well developed area of materials science for the fabrication of metal oxide gels. These gels can be formed into virtually any geometry, and then further processed into lenses, membranes, coatings, powders, and monoliths, with a variety of applications in fields ranging from optical and electrical devices to separation technologies to adsorption to biosensing. The term “sol-gel” is generic and quite broad, referring to a variety of liquid chemistry routes for material synthesis rather than melt extraction. This approach offers a great deal of flexibility in terms of available process space and materials. Many metals, transition metals, and metalloids are amenable to sol-gel processing, the most common being silicon, copper, zinc, titanium, aluminum, boron, and nickel, among many others. The two primary advantages of sol-gel processing are that it can be carried out at room temperature under mild conditions, and that it allows for the synthesis of some materials that are not possible through conventional melts because of phase separation, crystallization, or other complications [83].

The name “sol-gel” is short hand for the two steps of sol-gel processing, which may or may not be separated temporally. The first is the preparation of a solution, or “sol,” of hydrolyzed metal monomers, small oligomers, and colloidal particles. This can be done numerous ways, described more below in the specific case of silicon, but

the end goal is a stable or metastable solution of metal atoms covalently bound to active hydroxyl groups. For example, in the case of silicon, the sol will be a solution of silicic acid, $Si(OH)_4$. These hydroxyl groups then condense, forming an oxygen bridge between adjacent metal atoms with the release of water. Polymers and small particles form, and once they have bridged the geometry of the solution, gelation has occurred, and a “gel” has formed, hence the name sol-gel.

While simple in concept, the chemistry of sol-gel processing is actually quite complex. Indeed, a complete theoretical description from first principles has not yet been developed. The fundamental reason is the underlying complexity of the hydrolysis and condensation reactions. Each reaction can be described by its own rate constant, but those rate constants will vary depending on the chemistry of adjacent bonds on the central metal ion. The result is that on any given silicon atom, at the next nearest neighbor, there are 1,365 distinct chemical environments requiring 199,290 rate constants for an accurate quantitative description [84]! Obviously, the full description of any useful number of metal atoms quickly becomes untenable. Nevertheless, sol-gel chemistry has been the subject of countless peer-reviewed publications and a great deal of progress has been made toward understanding this complex chemistry, resulting in at least some reliable qualitative predictions.

In the current research, silicon was used exclusively due to its ease of processing and biocompatibility when compared to other inorganic matrices. Silicon is likely the most extensively studied sol-gel system; publications on silica sol-gel chemistry include a treatise by Iler [3], large sections of a seminal text by Brinker [85], many reviews [86-90], and innumerable peer reviewed articles. All gels used in the current project were prepared by a two step process; acid catalyzed hydrolysis followed by base catalyzed condensation. Two different sol preparation methods were also used, and each are explained separately below.

1.5.2 - Precursors

Two general types of precursors were used for sol preparation in this research, each offering different advantages and challenges in regards to biological encapsulation. The first was a silicon alkoxide precursor, in which a silicon atom is coordinated by ester linkages to four alkyl groups. This is exemplified by tetraethoxysilane (TEOS), a central silicon atom bound to four ethyl groups via an oxygen bridge with a chemical formula of $Si(OC_2H_5)_4$. TEOS and other alkoxide precursors are synthesized by the alcoholysis of silicon tetrachloride [85]. Tetramethoxysilane (TMOS) was also used in the current research, as well as methyltriethoxysilane (MTES), an alkoxide precursor where one ethoxy group is substituted with a methyl group, introducing a silicon – carbon bond which does not hydrolyze. There are a wide variety of such substitutions available in alkoxide precursors, which are addressed separately in §1.5.7.

In aqueous solution, alkoxide precursors can be hydrolyzed by either acid or base catalysis, although acid catalysis was used exclusively during the current investigation. Alcohol is released during hydrolysis, and TEOS was selected after initial screening in no small part because ethanol proved less cytotoxic than methanol generated by similar hydrolysis of TMOS precursors. Nevertheless, alcohol evolved during hydrolysis (which remains present through gelation) presents a real challenge to long term viability of encapsulated biological components.

The other type of silicon precursor is a solution of sodium silicate, Na_2SiO_3, often called “water glass,” or a solution of sodium oxide, Na_2O, and silica, SiO_2, in equilibrium. In a 40% aqueous solution, the substance forms a strongly alkaline but stable solution. Acid or base catalysis can also be used with this precursor to accelerate hydrolysis. However, without additional treatment, the resulting sol can have a very high concentration of sodium ions which may place osmotic stress on encapsulated components.

1.5.3 - Hydrolysis of Alkoxide Precursors

During the hydrolysis of silicon alkoxide precursors, an alkoxide group is replaced with a hydroxyl group by the consumption of water and concomitant release of alcohol. The reaction for a generic alkoxide precursor is illustrated below (R represents an alkyl side group, such as an ethyl group in the case of TEOS):

$$\equiv \mathrm{Si} - \mathrm{O} - \mathrm{R} + \mathrm{H_2O} \rightarrow \equiv \mathrm{Si} - \mathrm{OH} + \mathrm{ROH}$$

The reaction above is shown as proceeding in one direction, but is truly reversible, the forward reaction being hydrolysis and the reverse reaction being esterification, which is expected to be minimal in silicon alkoxide systems [85]. Furthermore, once precursors have begun to hydrolyze to silicic acid, condensation will begin to occur in competition with hydrolysis, although at low pH with acid catalysis, hydrolysis is strongly favored.

The hydrolysis reaction is expected to proceed via a nucleophilic attack of a electronegative water oxygen upon a weakly electropositive silicon atom [85, 91, 92]. The kinetics occurs rather slowly in a silicon system compared with other metals because other metals are more strongly electropositive [3]. However, this offers the advantage of allowing a temporal separation between the competing hydrolysis and condensation reactions.

Without an acid catalyst, the pH of an alkoxide sol may be as high as 5. Although hydrolysis still occurs, the kinetics are extremely slow and full hydrolysis may take thousands of hours [93]. The use of a strong acid catalyst, such as hydrochloric or nitric acid, will drop the pH of the sol below the isoelectric point of silicic acid, pH 2, and greatly accelerate the hydrolysis reaction. Under these conditions, the rate of each subsequent hydrolysis on any given silicon atom accelerates after the first, meaning the last hydrolysis reaction occurs at a rate approximately 144 times faster than the first [94]. This also means that in the

presence of excess water, hydrolysis proceeds nearly to completion, leaving very few unhydrolyzed alkoxide monomers in solution [92, 95]. Furthermore, prior to catalyzing gelation, condensation is minimal, resulting in the formation of some small cyclic and/or short linear polymers rather than larger colloidal particles [95, 96].

The characteristics of the sol prior to catalyzing condensation are important in determining the overall structure of the final gel. Acid catalysis of hydrolysis, in contrast to base catalysis, has been demonstrated to be superior for achieving mesoporous structure and high porosity [97, 98]. Under the conditions of base catalysis, the sol typically has highly condensed silica particles in solution with unhydrolyzed monomers. In the context of biological encapsulation, this is undesirable because hydrolysis after gelation can lead to the production of cytotoxic alcohol. Finally, the distinct separation between hydrolysis and condensation that can be achieved with acid catalysis allows for at least partial removal of the alcohol generated during the hydrolysis reaction.

1.5.4 - Hydrolysis of Aqueous Precursors

Aqueous precursors are usually used in systems with basic catalysis of hydrolysis because the precursor itself is already extremely alkaline. However, acid catalysis can also be used for aqueous precursors, as shown by the general reaction:

$$\mathrm{Na_2SiO_3 + H_2O + 2HCl \rightarrow Si(OH)_4 + 2Na^+ + 2Cl^-}$$

It should be noted, however, that the above reaction usually results in a highly unstable supersaturated solution of silicic acid, often bringing the solution toward neutral pH where gelation occurs [3]. In the presence of a strongly acidic ion exchange resin, this reaction will proceed to the formation of a stable sol at an acidic pH below the isoelectric point of silicic acid. At such a pH, the reaction mechanism of hydrolysis remains the same, and hydrolysis should similarly proceed virtually to completion.

The ion exchange resin serves two functions. First and foremost, it brings the sol from alkaline to acidic pH while avoiding gelation and stabilizes the sol by adsorbing sodium ions and releasing protons. Secondly, and very importantly in the case of biological encapsulation, the adsorption of sodium ions reduces ionic and osmotic stress upon biological components in the gel after encapsulation. Left as a salt, sodium ions would remain in solution after gelation. However, with ion exchange followed by base catalysis of gelation, protons and hydroxide ions will combine to form water, leaving a much lower final salt concentration (e.g., potassium chloride will remain in solution if potassium hydroxide was the neutralizing base used to catalyze condensation).

All other factors being equal, alkoxide and aqueous precursors undergoing acid catalysis should theoretically yield nearly identical acidic sols. However, it is unknown if this has been confirmed experimentally and is difficult to achieve in practice. Complicating factors such as alcohol evolution and its effect as a solvent, the presence of the ion exchange resin and sodium ions, and differences in condensation resulting from these factors all may influence the evolution of the sol and the resulting gel structure, warranting the investigation of both as candidates for biological encapsulation.

1.5.5 - Base Catalyzed Condensation & Gelation

Condensation is the reaction whereby two adjacent hydroxyl groups condense to form an oxygen bridge between silicon atoms with the release of a water molecule, as shown in the general reaction below:

$$\equiv \mathrm{Si} - \mathrm{OH} + \mathrm{HO} - \mathrm{Si} \equiv \rightarrow \equiv \mathrm{Si} - \mathrm{O} - \mathrm{Si} \equiv \ + \mathrm{H_2O}$$

The reaction illustrates proper stoichiometry, but does not accurately reflect the reaction mechanism. The reaction is expected to take place by the nucleophilic attack of a deprotonated silanol upon a protonated silanol [85]. The first pK_a of silicic acid is

9.8, so at acidic pH, silicic acid is fully protonated and therefore condensation is strongly suppressed. By bringing the pH into the range of 7 to 8, the concentration of deprotonated silanol groups becomes appreciable. Furthermore, the acidity of silanol groups is influenced by the chemical environment of the central silicon [85]. Any degree of condensation will result in a modest increase in acidity of adjacent silanol groups, meaning that in this pH range, the concentration of protonated and deprotonated groups should be comparable. This situation strongly accelerates the condensation reaction. It should also be noted that the pH range for the ideal conditions of condensation also correspond to a biologically compatible physiologic pH, and this is the step in the process where biological components should be added.

Once condensation has proceeded to the point where the solid phase bridges the entire geometry of the solution, gelation has occurred. However, this does not mean hydrolysis and condensation are complete. The gel continues to age and evolve until equilibrium is reached.

1.5.6 - Aging

After gelation, hydrolysis and condensation are by no means arrested, the gel continues to undergo structural changes until monomers and particles in solution are consumed and equilibrium is achieved. There are a variety of processes taking place that can cause changes to occur after gelation, including Ostwald ripening, coarsening, and syneresis. Each is caused by slightly different forces, and each affects the final structure of the gel in a different manner.

Ostwald ripening (Figure 1-5a) is a process taking place among uncondensed monomers and particles remaining in solution, prior to and after gelation. At the surface of small particles, solubility is increased due to the tight positive curvature of the particle. This is turn creates a concentration gradient driving diffusion of free monomers away from the dissolving small particle toward larger particles. These monomers then condense upon the surface of larger particles, where the large radius

of curvature decreases solubility. In effect, small particles dissolve and large particles grow, until the particle size distribution is more uniform and stable. The amount of ripening that has taken place prior to gelation can influence how coarse or fine the gel structure becomes. In an acidic system, such as the one used in this investigation, silica particles are expected to be stable in the sol at a diameter of approximately 2 nm. In contrast, with a base catalyzed system at pH 7 or greater, particles may be 10 nm in diameter or larger [85].

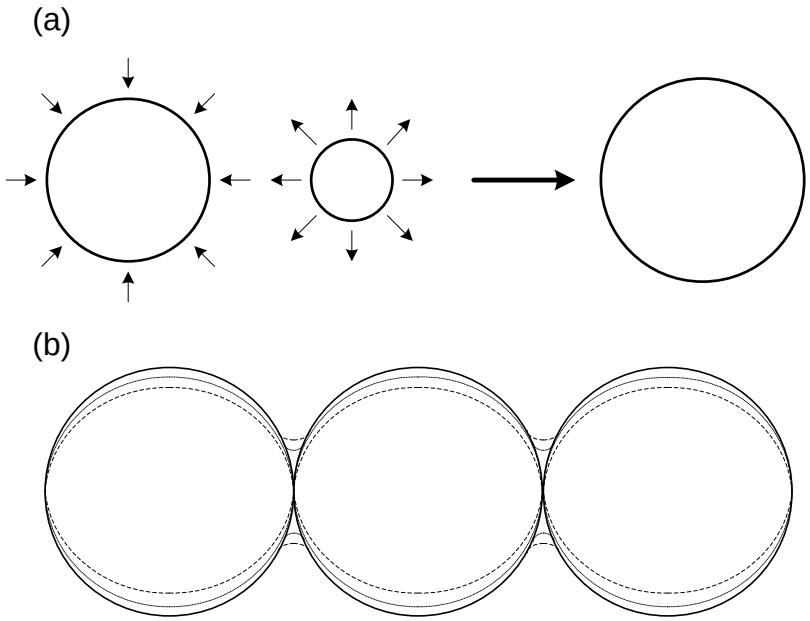

Figure 1-5: (a) Ostwald ripening and (b) coarsening. Ripening occurs during sol preparation and continues after gelation, while coarsening occurs only after gelation.

Coarsening is similar to Ostwald ripening in that it is driven by surface energy and results from dissolution in one area with condensation in another (Figure 1-5b). While Ostwald ripening occurs with mobile particle in solution, coarsening occurs with particles once they are fixed in space within the gel structure. When two particles come into contact, they create an area of tight negative curvature between the two. Silica tends to deposit and condense at this surface, at the expense of silica

that has dissolved from areas of broad positive curvature. This does not result in shrinkage, as the center of mass of each particle does not move, but it does result in necking, which is a thickening of connections between adjacent particles. This can serve to strengthen and stabilize the gel, but it can also decrease surface area and hinder diffusion by obstructing or separating pore spaces.

Syneresis is a process that causes the gel to contract to varying degrees under the forces of on-going condensation and internal capillary pressures, which can be incredibly high within a gel with pores on the scale of nanometers [85]. Immediately upon gelation, the gel remains soft and flexible, and on-going condensation under relatively minor capillary forces can cause the gel to contract. Contraction will continue until an equilibrium is achieved between coarsening, which strengthens the gel and causes an increase in bulk modulus, and capillary forces [99]. In wet gels, meaning gels that are never subjected to heat treatments and complete drying, capillary forces are never fully realized and syneresis, while observable, is often minimal (shrinkage observed during this investigation was generally ≤5%). Severe syneresis, as would be expected as the gels are dried, would obviously be detrimental to encapsulated biological components.

1.5.7 - Organically Modified Siloxanes

Organically modified siloxanes, commonly called ORMOSILs, are any alkoxide precursor with a silicon – carbon bond, tethering an organic functional group to the sol precursor. The silicon – carbon bond is unreactive to hydrolysis, meaning this side group remains through hydrolysis and condensation and is present in the final gel matrix. This can have profound effects throughout the entire process. Among the most commonly used ORMSOLs is singly substituted methyltriethoxysilane (MTES), with a chemical formula of $SiCH_3(OC_2H_5)_3$, which was used in the current research.

First, covalently bound side groups create steric and inductive effects on the hydrolysis reaction. The steric effects are reasonably easy to predict, at least

qualitatively. The larger the side group, the more impeded hydrolysis becomes as this may prevent access for the initial nucleophilic attack. Methyl and even ethyl groups are expected to cause minimal steric interference as they are both smaller than an ethoxy side group [85]. Although not used in this investigation, numerous other ORMOSILs with larger side groups, that will have significant steric effects, are available.

Inductive effects manifest through alterations to the electron density on the silicon – carbon bond as compared to a silicon – oxygen bond. Specifically, oxygen is more electronegative, and therefore more electron withdrawing as compared to carbon. As a result, the bond to carbon stabilizes charge distribution of reaction intermediates and actually accelerates the hydrolysis reaction for the other three ethoxy side groups [85]. In acid catalyzed systems with excess water, hydrolysis is expected to proceed nearly to completion, so while this may influence the rate, it is not expected to alter the final equilibrium.

Once the gel is formed, the ORMOSIL creates two competing effects. First, the organic side groups tend to present at the surface of the gel, as they are hydrophobic and sterically obstructed from being turned within a hydrophilic and condensed gel. This alters the surface chemistry of the gel, making the surface more hydrophobic. This will reduce the interfacial energy between the solid and liquid phases, reducing capillary forces and syneresis as a result. The second effect is a result of the organic side group occupying potential bridging sites and sterically hindering condensation in their immediate vicinity. This can improve porosity and also make the gels more flexible, which in turn facilitates more complete reaction toward condensation. It has been observed that brittle gels of pure TEOS are only 87% reacted while flexible gels with varying amounts of ORMOSIL can achieve 98% completion of condensation reactions [100].

The two effects of increasing flexibility (i.e. decreasing bulk modulus) while also decreasing capillary forces need to be managed appropriately to tune the structure of the gel. Too much ORMOSIL and the gel loses pore structure and becomes viscous, unable to maintain any structure at all. Not enough, and the benefit is lost as the gel resembles a brittle gel of pure TEOS. It has been shown that the optimal composition of a blend of TEOS and MTES, in terms of maximizing porosity and minimizing syneresis, is 20% MTES with 80% TEOS [101].

The single substitution of a methyl group is obviously the simplest form of ORMOSIL. Increasing complexity and chemical functionality can be achieved by multiple substitutions on a single silicon or by substitution of larger groups, including longer alkanes as well as branched and cyclic side groups. Hundreds of ORMOSILs are readily available, allowing for quite a broad spectrum of gel properties.

1.5.8 - Additives

Another advantage of sol-gel chemistry is the flexibility to use countless additives during the gelation process. Additives of a variety of chemical characteristics have been used to improve biocompatibility of the encapsulation process by either improving the surface interaction between the gel matrix and the biological component or through protecting the component from stress created during encapsulation. The gel structure itself may also be altered. Some additives can increase porosity or pore size, and some, particularly organic polymers and surfactants, have been used as templates to provide a scaffold upon which the silica gel condenses, creating a more ordered structure. The most commonly used additives include: glycerol [102, 103], polyethylene glycol (PEG) [104, 105], surfactants [106], crown ethers [107], gelatin [108-110], alginate [111], collagen [112-114], formamide [89], and organic acids [115]. Glycerol and PEG were the only two additives used in the current investigation because of their potential to improve the biocompatibility of the gels. Glycerol has previously been used to protect

encapsulated components from osmotic stress [103]. PEG is known to act as a surfactant [3], reducing the interfacial energy between liquid and gel, which can result in increased porosity through reduced syneresis and possibly an improved interaction with the encapsulated biological component. A comprehensive review of the use of additives in sol-gel chemistry is beyond the scope of this dissertation.

1.6 - Silica Sol-gel Encapsulation of Biological Components

The encapsulation of biological components within silica gel has received a great deal of recent research attention. The attraction is that silica gel can be processed in a biocompatible manner and the material provides an inert, robust, and stable platform when compared to organic polymers that are more vulnerable to biological degradation. Applications of sol-gel encapsulation are quite broad, including the stabilization of purified enzymes [116], such as hydrogenases [117] and photosystems [118], and prolonging activity from whole viable cells [119]. Many recent reviews on silica encapsulation of biological components are available [102, 120-129].

1.6.1 - Encapsulation of Viable Cells

The encapsulation of viable cells within silica gel was first demonstrated in 1989 by Carturan et al. using the yeast *Saccharomyces* cerevisiae and a TEOS-derived alkoxide gel [4]. The organism was selected for its tolerance of ethanol, generated during hydrolysis of the TEOS precursor. In the 22 years since, researchers have encapsulated a variety of proteins and enzymes [116, 118, 124, 130], bacterial cells [103, 119, 131], cyanobacteria [132, 133], diatoms [134], algae [135-137], plant cells [138, 139], and mammalian cells [140, 141]. The silica gel provides a stable and inert matrix that physically confines the encapsulated cells, keeping them contained while excluding contaminant cells, and remaining porous enough to facilitate diffusion and transport of metabolites and waste products. The illustration in Figure 1-6 shows schematically how an encapsulated cell might appear within the gel. The surface of

the gel is mostly condensed with some hydrophilic hydroxyl groups remaining, while the internal bulk of the gel is condensed silica, also reasonably hydrophilic. The structure is highly porous, with pores usually on the order of tens of nanometers in size, in contrast to the encapsulated cells which are approximately 1-2 μm in diameter, a difference of two orders of magnitude.

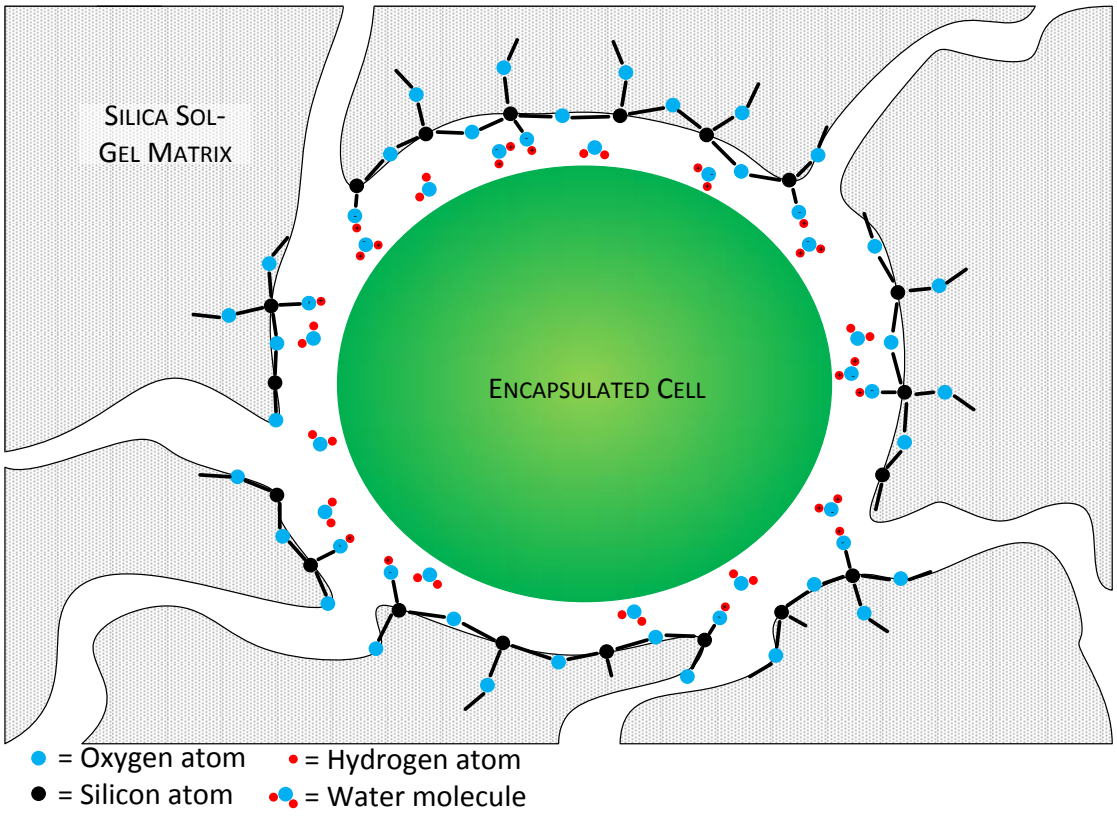

Figure 1-6: A schematic illustration (not to scale) of a cyanobacterial cell encapsulated in silica gel. The gel structure is porous on the scale of tens of nanometers, with larger channels throughout.

The pore structure is often bimodal, containing fine micropores through the bulk and larger mesopores that persist in dilute hydrated gels commonly used for encapsulation of biological components (Figure 1-7). This pore structure allows for

diffusion rates of small ionic species of approximately 25% as large as diffusion rates in unconfined aqueous solution [142]. This suggests that, provided the geometry of the gel monolith is not too large, transport of metabolites, gases, and waste products will not be limited sufficiently to hinder cell activity and viability [119].

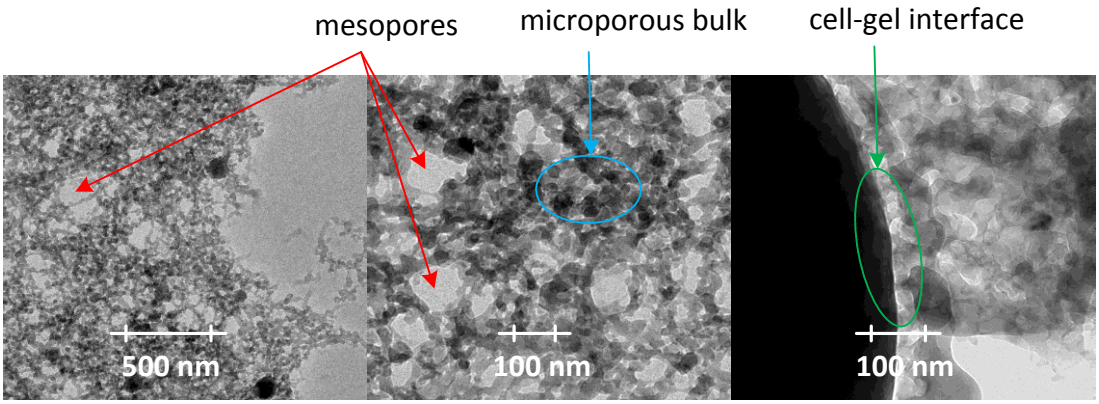

Figure 1-7: TEM images showing the structure of an alkoxide gel (left and center), and the interface between an encapsulated cell of *Synechocystis* sp. PCC 6803 and the gel (right)(TEM provided by Prof. Catherine Page of University of Oregon).

The rationale behind encapsulating whole cells is two-fold. First, whole cells contain all the enzymes, proteins, cofactors, and transport mechanisms to carry out many valuable reactions that are difficult and/or costly to replicate in vitro or artificially. Secondly, by confining growth, it is expected that cells will direct more energy toward the production of secondary metabolites. Although the mechanisms for this phenomenon are not well understood and are the focus of recent investigations, this approach has been validated with cells of the plant *Ajuga reptans* [138] and the current work demonstrates this is also an effective technique for enhancing hydrogen production from *Synechocystis* sp. PCC 6803. The material is also suitable for phototrophs, like *Synechocystis* sp. PCC 6803, because despite its

amorphous character, its optical properties vary little from the crystalline silica, α-quartz, making the material highly transparent to visible light [143-145].

Finally, although there is a great deal of empirical development in the field of biological encapsulation, the process is still not fully understood from first principles, due both to the complexity of sol-gel chemistry and the variety of biological components. As a result, refinement of encapsulation protocol for each new component(s) requires numerous iterations. The encapsulation process can place a variety of stresses on the cells, and researchers have attempted different approaches to reduce the impact of these stresses, depending on the vulnerabilities of the cell of interest. *Synechocystis* sp. PCC 6803 is actually quite a robust organism, moderately halo-tolerant [146, 147] and able to tolerate reasonable levels of ethanol (shown within the current investigation). High concentrations of sodium may be present during the preparation of gels from aqueous precursors, and ethanol is evolved during the hydrolysis of alkoxide gels, so both present potential risks to *Synechocystis* sp. PCC 6803. While low levels of each may not be lethal, any energy devoted to stress response is energy that cannot be used for hydrogen production, reducing overall efficiency. As a result, glycerol and PEG were both explored in the current investigation as candidates to improve the biocompatibility of the encapsulation process, as demonstrated in other studies [103-105]. There are numerous other possible protocols, including different precursors or additives, which may be explored in future work.

1.7 - Evaluation of Post-Encapsulation Cellular Activity

In order to improve cell viability and longevity after encapsulation, numerous techniques were used to examine cellular activity over time after encapsulation. Two techniques, chlorophyll fluorescence and confocal microscopy, provided a noninvasive look at encapsulated cells and are summarized below.

1.7.1 - Chlorophyll Fluorescence

When a phototroph absorbs light energy, there are three possible fates of that absorbed energy: photochemistry, dissipation as heat, and dissipation as fluorescence. Photochemistry is the productive use of absorbed radiation that leads to the fixation of carbon, accumulation of biomass, and growth. The other two processes are nonproductive, wasteful uses of absorbed energy, but since conditions are almost never optimal for photochemistry, both alternatives are critical in protecting the organism from photodamage.

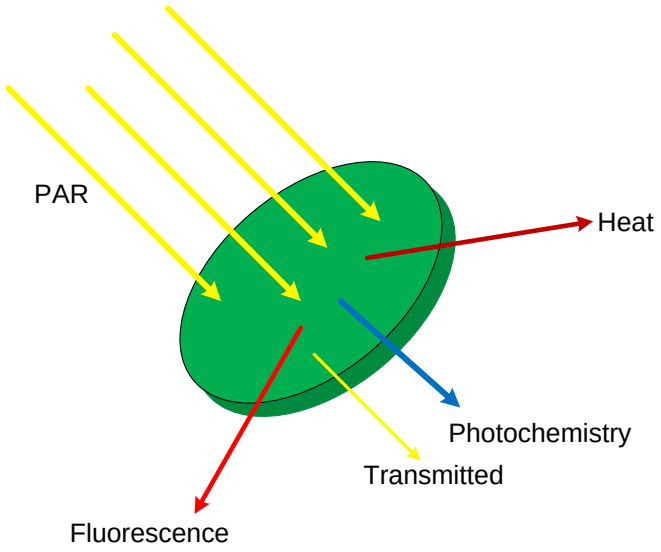

Figure 1-8: The fate of incident light upon a phototrophic culture. Absorbed light has three fates: photochemistry, fluorescence, or nonphotochemical quenching (heat). Unabsorbed light may also be transmitted. PAR = photosynthetically active radiation.

Fluorescence is re-emission of absorbed, but ultimately unusable photons, predominantly from chlorophyll *a* pigments within the reaction centers, and it occurs for a variety of reasons. First, many phototrophs and especially cyanobacteria have evolved to optimally utilize low intensity light. Through sophisticated light harvesting antennae, these organisms can create a large effective cross sectional absorption

profile and channel excitation energy toward the reaction centers of PSII and PSI. In cyanobacteria, which thrive under low light conditions, photochemistry can account for as much as 90% of absorbed photons, while fluorescence will typically amount to 0.3 to 3% [43]. However, under relatively moderate intensity light, well below full sunlight, the ability of these organisms to utilize absorbed light becomes saturated. It is this monitoring of fluorescence quenching that provides information about the relative health and of the phototroph through its photosynthetic activity.

First described in the 19th Century, it was not until the pioneering work of Kautsky and Hirsch in the 1930's that a rigorous description of fluorescence phenomena began to emerge [148]. Since then, the use of fluorescence as a non invasive tool to evaluate the activity and health of photosynthetic organisms has become common place. However, although there has been much theoretical development in describing fluorescence, the phenomenon is still not completely understood and results are subject to interpretation.

Fluorescence primarily occurs when excitation energy encounters a "closed" reaction center, which is a reaction center that is currently using excitation energy it has already received to carry out a reaction and therefore cannot utilize additional energy. An "open" reaction center, in contrast, is able to receive excitation energy and "quench" fluorescence as a result. If the plastoquinone pool is heavily reduced, due to excess PSII activity and/or relatively low PSI activity, the tendency for PSII reaction centers to be closed will be increased, creating a corresponding increase in fluorescence signal. If the PQ pool is more oxidized, more PSII centers will be open, reducing fluorescence.

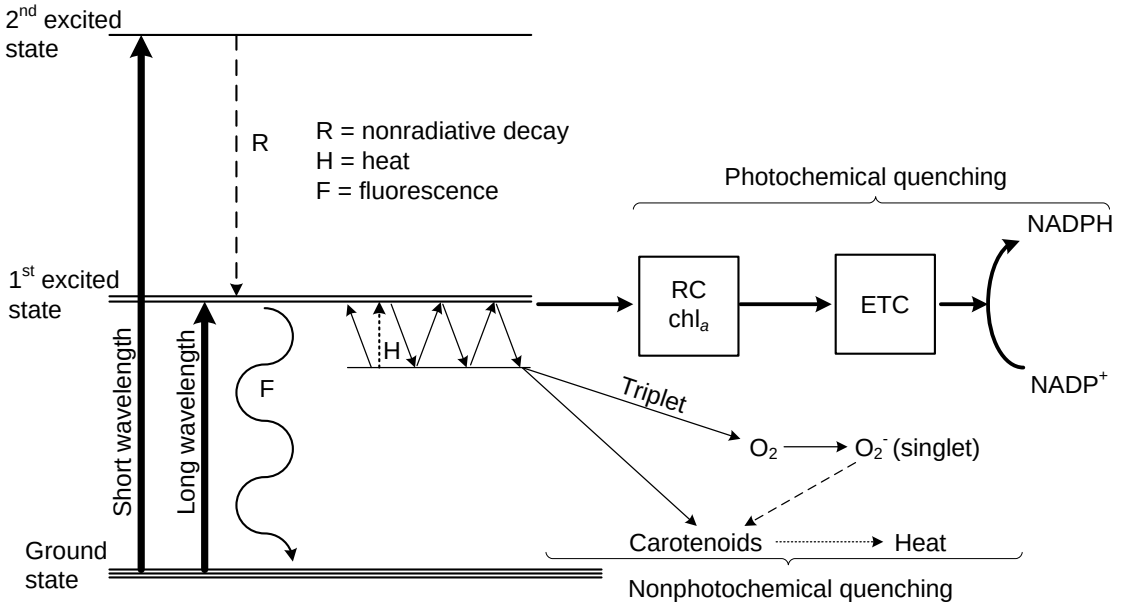

Figure 1-9: Electron excitation through the absorption of photons. Higher excitation levels are achieved by more energetic, shorter wavelength light, absorbed by chlorophyll in the Soret band or by distal PC in the PBS ("2nd excited state"). Nonradiative decay occurs as the exciton moves via resonance toward the reaction center (RC) chlorophylls ("1st excited state," RC chl$_a$). Excitation energy may then be directed to photochemistry ("photochemical quenching"), fluorescence ("F"), or heat (nonphotochemical quenching). *Synechocystis* sp. PCC 6803 has one known orange carotenoid protein (OCP) with known nonphotochemical quenching activity [149].

The most useful parameters as indicators of cell health include the maximum quantum efficiency of PSII (F_v/F_m), the quantum efficiency of light adapted PSII (ϕPSII), the coefficient of photochemical quenching (q_P), and the coefficient of nonphotochemical quenching (q_N). All of the above parameters can be measured with a pulse amplitude-modulated (PAM) fluorometer. As a baseline, the PAM fluorometer can measure fluorescence yield in the absence of actinic light, a parameter called F_o. In a dark acclimated sample, F_o is the minimal fluorescence yield

of the sample. F_v/F_m, defined as $(F_m-F_o)/F_m$, is measured by exposing a dark acclimated sample with a short, but bright and saturating pulse of actinic light. In this state, all PSII reaction centers are presumably open, so upon exposure to a saturating pulse of light, all reaction centers will become closed (i.e. all Q_A acceptors become reduced), providing a maximum fluorescence yield, F_m, without immediately inducing down stream photochemistry or nonphotochemical quenching mechanisms. In plants, this approach reliably yields a true F_m. However, in cyanobacteria, the regulation of energy transfer between the photosystems is managed in such a way that a true F_m often cannot be measured without 3-(3,4-dichlorophenyl)-1,1-dimethylurea (DCMU), an inhibitor that blocks electron transfer from PSII to Q_A. As a result, F_m measurements are often taken with a separate sample of the same culture, or at the end of an experimental procedure if photoinhibition has not been induced in the sample during the analysis. In the absence of a true F_m, F_m' can still serve as basis for relative comparison [150].

F_v is variable fluorescence, or the difference between F_m and F_o, providing a relative and internally consistent estimate of PSII quantum efficiency. In the presence of actinic light, baseline fluorescence yield will increase from F_o to F_s, or "steady-state" fluorescence yield. F_m will also change to a light acclimated maximum fluorescence yield, or F_m'. Under actinic light, these measurements can then be used to calculate ϕPSII as $(F_m' - F_s)/F_m'$, illustrating that F_v/F_m is really a special case of ϕPSII. F_o' is analogous to F_o, only measured in a light adapted sample. To measure F_o', the actinic light is turned off for 5 seconds and a red LED is turned on to selectively stimulate PSI activity. Changes in F_o' compared to F_o indicate changes in excitation distribution between the photosystems and accounts for possible nonphotochemical losses occurring in the PBS. While ϕPSII gives the *actual* quantum efficiency of PSII, a slightly different parameter, F_v'/F_m', defined as $(F_m' - F_o')/F_m'$, gives an estimate of *maximum* quantum efficiency of PSII in the light adapted state. Since F_s will always be

larger than F_o', likewise, F_v'/F_m' will always be larger than ϕPSII. This has lead to the interpretation of F_v'/F_m' as an indication of the quantum efficiency of the photoantennae. Since ϕPSII is smaller, the difference between the two parameters indicates efficiency losses in the PBS or in excitation transfer between PBS and photosystems. Theoretically, should F_v'/F_m' equal ϕPSII, that would suggest that energy transfer from PBS to photosystems is 100% efficient, a physical impossibility.

The coefficient of photochemical quenching, q_P (= $(F_m'-F_s)/(F_m'-F_o')$ [150]), provides a relative estimate of the efficiency of photochemistry toward quenching fluorescence, while q_N (= $1 – (F_m' – F_o')/(F_m – F_o)$ [151]) provides a relative estimate of how much excitation energy is being dissipated in nonphotochemical quenching of fluorescence. It should be noted that the absolute value of all the above mentioned parameters should not be subject to over interpretation. In cyanobacteria especially, these parameters are best interpreted as indications of relative health and photosynthetic activity as they change in the same samples over time or under varying conditions with experimental treatments [150, 151].

The peer reviewed literature on chlorophyll fluorescence is expansive. Additional details pertinent to this investigation are provided in Chapters 3 and 4. Reviews of fluorescence in general [152-154], and specific to cyanobacteria [37, 150, 155], have been published recently.

1.7.2 - Live/Dead Staining & Confocal Microscopy

Encapsulation within a solid matrix can stress viable cells. While the objective is to enhance stability and improve hydrogen production, this cannot be rationally achieved without examining how well cells survive the encapsulation process. One approach to provide some insight in this area is live/dead staining coupled with confocal microscopy. The approach is to treat cultures with two dyes, one that stains *all* cells, and one that stains only dead cells, which presumably have compromised cell membranes. The dyes must have different absorption and emission peaks in

order to be resolved by the confocal microscope, which will excite each with laser light at very specific wavelengths.

Syto 9™ (Molecular Probes, Eugene, OR) is a very common “live” stain, a stain that emits green light at 500 nm only when bound with double stranded DNA. This dye can penetrate all cells in the silica matrix, providing an indication of total cell count. As with the “live” stains, there are numerous “dead” stains to choose from, but the dye must emit at a wavelength where emission from the organism, the live stain, or the matrix will not interfere. In the case of *Synechocystis*, Sytox orange™ is appropriate because its emission peak is at 570 nm, below the onset of chlorophyll fluorescence and therefore resolvable by the confocal microscope.

Chlorophyll fluorescence above 650 nm also provided a third look at cells contained within the gel matrix. This provided a duplicate look at “live” cells to verify the penetration of the Syto 9™ dye. It also allowed for a comparison of cells stained as “dead” with Sytox orange™ to see if active chlorophyll fluorescence was coming from cells otherwise identified as dead. Finally, it allowed for the location of cells without dyes present to observe negative controls, verifying that fluorescence within the filter ranges specified for the dyes was not occurring in their absence. Autofluorescence as seen with confocal microscopy has been used elsewhere to examine cyanobacteria encapsulated in silica gel [132]. Taken together, this technique allowed for a semi-quantitative count of live, dead, and active cells.

1.8 - Summary

General aspects of hydrogen as a renewable fuel, photobiological hydrogen production, silica sol-gel processing, and encapsulation of biological components within silica gel have been reviewed. Developing renewable and sustainable alternatives to carbon-based fossil fuels is a matter of incredible urgency, and hydrogen offers a viable solution. Photobiological hydrogen production is potentially the most efficient means of renewable hydrogen production available, and the

cyanobacterium *Synechocystis* sp. PCC 6803 is among the most well-studied organisms capable of this process. Various metabolic and genetic manipulations have been successfully demonstrated to enhance hydrogen production from this organism. Truncation of photoantennae is a related approach that theoretically has promise, but is yet to be fully explored. Encapsulation in silica gel provides a way to stabilize biological components and enhance production of secondary metabolites. Combined, these approaches may significantly improve photobiological hydrogen production from *Synechocystis* sp. PCC 6803, taking a step closer toward a technically feasible and commercially viable system. This effort will also contribute fundamental knowledge toward our understanding of the underlying mechanisms of both photobiological hydrogen production and encapsulation of viable cells within silica sol-gel.

Chapter 1 References

1 Kaneko T, et al. Sequence Analysis of the Genome of the Unicellular Cyanobacterium *Synechocystis* sp. PCC 6803. Sequence Determination of the Entire Genome and Assignment of Potential Protein-coding Regions. DNA Research 1996; 3: 109 - 136.

2 Cournac L, Guedeney Gv, Peltier G, Vignais PM. Sustained Photoevolution of Molecular Hydrogen in a Mutant of Synechocystis sp. Strain PCC 6803 Deficient in the Type 1 NADPH-Dehydrogenase Complex. J Bacteriol 2004; 186(6): 1737-1746.

3 Iler RK. The Chemistry of Silica. New York: Wiley, 1979.

4 Carturan G, Campostrini R, Dire S, Scardi V, Alteriis ED. Inorganic Gels for Immobilization of Biocatalysts: Inclusion of Invertase-Active Whole Cells of Yeast (Saccharomyces cerevisiae) into thin Layers of SiO_2 Gel Deposited on Glass Sheets. J Mol Catal 1989; 57: L13 - L16.

5 Hoffert MI, Caldeira K, Jain AK, Haites EF, Harvey LDD, Potter SD, et al. Energy implications of future stabilization of atmospheric CO_2 content. Nature 1998; 395(6705): 881-884.

6 Barber J. Photosynthetic energy conversion: natural and artificial. Chem Soc Rev 2009; 38(1): 185-196.

7 Rifkin J. The Hydrogen Economy. New York: J.T. Tarcher/Putnam, 2002.

8 National Hydrogen Energy Roadmap. United States Department of Energy, 2002.

9 Crabtree GW, Dresselhaus MS, Buchanan MV. The Hydrogen Economy. Physics Today 2004; December 2004: 39-44.

10 Marban G, Valdes-Solis T. Towards the hydrogen economy? Int J Hydrogen Energy 2007; 32(12): 1625-1637.

11 Milbrandt A, Mann M. Potential for Hydrogen Production from Key Renewable Resources in the United States. NREL 2007.

12 Ghirardi ML, Dubini A, Yu J, Maness P-C. Photobiological hydrogen-producing systems. Chem Soc Rev 2009; 38(1): 52-61.

13 Züttel A, Remhof A, Borgschulte A, Friedrichs O. Hydrogen: the future energy carrier. Philosophical Transactions of the Royal Society A: Mathematical, Physical and Engineering Sciences 2010; 368(1923): 3329-3342.

14 McGowan TF, ed. Biomass and Alternate Fuel Systems: An Engineering and Economic Guide. John Wiley & Sons, Inc., Hoboken, NJ, 2009.

15 NAS. The Hydrogen Economy: Opportunities, Costs, Barriers, and R&D Needs. Washington, DC: The National Academies Press, 2004.

16 Hankamer B, Lehr F, Rupprecht J, Mussgnug JH, Posten C, Kruse O. Photosynthetic biomass and H_2 production by green algae: from bioengineering to bioreactor scale-up. Physiol Plant 2007; 131(1): 10-21.

17 Simpson AP, Lutz AE. Exergy analysis of hydrogen production via steam methane reforming. Int J Hydrogen Energy 2007; 32: 4811-4820.

18 Lutz AE, Bradshaw RW, Keller JO, Witmer D. Thermodynamic analysis of hydrogn production by steam reforming. Int J Hydrogen Energy 2003; 28: 159-167.

19 Bargigli S, Raugei M, Ulgiati S. Comparison of thermodynamic and environmental indexes of natural gas, syngas and hydrogen production processes. Energy 2004; 29: 2145-2159.

20 Turner J, Sverdrup G, Mann MK, Maness P-C, Kroposki B, Ghirardi M, et al. Renewable hydrogen production. International Journal of Energy Research 2008; 32(5): 379-407.

21 McKinlay JB, Harwood CS. Photobiological production of hydrogen gas as a biofuel. Curr Opin Biotechnol 2010; 21(3): 244-251.

22 Bockris JOM. Environment 1971; 1: 13-51.

23 Bockris JOM, Appleby AJ. Environment This Month 1972: 1-29.

24 Bockris JOM. The origin of ideas on a Hydrogen Economy and its solution to the decay of the environment. Int J Hydrogen Energy 2002; 27: 731-740.

25 Prince R. The Photobiological Production of Hydrogen: Potential Efficiency and Effectiveness as a Renewable Fuel. Critical Reviews in Microbiology 2005; 31: 19-31.

26 Kruse O, Rupprecht J, Mussgnug JH, Dismukes GC, Hankamer B. Photosynthesis: a blueprint for solar energy capture and biohydrogen production technologies. Photochemical & Photobiological Sciences 2005b; 4(12): 957-970.

27 Toole CM, Plank TL, Grossman AR, Anderson LK. Bilin deletions and subunit stability in cyanobacterial light-harvesting proteins. Mol Microbiol 1998; 30(3): 475-486.

28 McIntosh L, ed. Photosynthesis: Molecular Biology of Energy Capture. Methods Enzymol, 297. Academic Press, San Diego, CA, 1998.

29 Bryant D, ed. The Molecular Biology of Cyanobacteria. Advances in Photosynthesis, Kluwer Academic Publishers, Dordrecht, 1994.

30 Falkowski PG, Raven JA. Aquatic Photosynthesis. Princeton, NJ: Princeton University Press, 2007.

31 Clausen J, et al. Time-resolved Oxygen Production by PSII: Chasing Chemical Intermediates. Biochim Biophys Acta 2004; 1655: 184-194.

32 Dau H, Haumann M. The manganese complex of photosystem II in its reaction cycle--Basic framework and possible realization at the atomic level. Coord Chem Rev 2008; 252(3-4): 273-295.

33 Raymond J, Blankenship RE. The origin of the oxygen-evolving complex. Coord Chem Rev 2008; 252(3-4): 377-383.

34 Arteni AA, Ajlani G, Boekema EJ. Structural organisation of phycobilisomes from Synechocystis sp. strain PCC6803 and their interaction with the membrane. Biochimica et Biophysica Acta (BBA) - Bioenergetics 2009; 1787(4): 272-279.

35 Liu H, Grot S, Logan BE. Electrochemically Assisted Microbial Production of Hydrogen from Acetate. Environmental Science & Technology 2005; 39(11): 4317-4320.

36 Mullineaux C, Allen JF. State 1-State 2 transitions in the cyanobacterium *Synechococcus* 6301 are controlled by the redox state of the electron carriers between Photosystems I and II. Photosynthesis Research 1990; 23: 297-311.

37 Bailey S, Grossman A. Photoprotection in Cyanobacteria: Regulation of Light Harvesting. Photochem Photobiol 2008; 84(6): 1410-1420.

38 Dominy P, Mullineaux C. State transitions in cyanobacteria. In: M. Yunus, U. Pathre and P. Mohanty, editor. Probing Photosynthesis. New York: Taylor & Francis, 2000. p. 310-323.

39 McConnell M. Regulation of the Distribution of Chlorophyll and Phycobilin-Absorbed Excitation Energy in Cyanobacteria. A Structure-Based Model for the Light State Transition. Plant Physiol 2002; 130: 1201-1212.

40 Mullineaux CW. Phycobilisome-reaction centre interaction in cyanobacteria. Photosynthesis Research 2008; 95(2): 175-182.

41 Ashby MK, Mullineaux CW. The role of ApcD and ApcF in energy transfer from phycobilisomes to PS I and PS II in a cyanobacterium. Photosynthesis Research 1999; 61: 169-179.

42 Emlyn-Jones D, Ashby MK, Mullineaux CW. A gene required for the regulation of photosynthetic light harvesting in the cyanobacterium *Synechocystis* 6803. Mol Microbiol 1999; 33(5): 1050-1058.

43 El Bissati K, Delphin E, Murata N, Etienne A-L, Kirilovsky D. Photosystem II fluorescence quenching in the cyanobacterium Synechocystis PCC 6803: involvement of two different mechanisms. Biochimica et Biophysica Acta (BBA) - Bioenergetics 2000; 1457(3): 229-242.

44 Melis A. Solar energy conversion efficiencies in photosynthesis: Minimizing the chlorophyll antennae to maximize efficiency. Plant Science 2009; 177(4): 272-280.

45 Polle JEW, Kanakagiri S-D, Melis A. tla1, a DNA insertional transformant of the green alga Chlamydomonas reinhardtii with a truncated light-harvesting chlorophyll antenna size. Planta 2003; 217(1): 49-59.

46 Berberoglu H, Pilon L, Melis A. Radiation characteristics of Chlamydomonas reinhardtii CC125 and its truncated chlorophyll antenna transformants tla1, tlaX and tla1-CW+. Int J Hydrogen Energy 2008; 33(22): 6467-6483.

47 Nakajima Y, Ueda R. Improvement of microalgal photosynthetic productivity by reducing the content of light harvesting pigment. Journal of Applied Phycology 1999; 11: 195-201.

48 Vignais PM, Billoud B. Occurrence, Classification, and Biological Function of Hydrogenases: An Overview. Chemical Reviews 2007; 107(10): 4206-4272.

49 Heinekey DM. Hydrogenase enzymes: Recent structural studies and active site models. J Organomet Chem 2009; In Press, Corrected Proof.

50 Volbeda A, Charon M, Piras C, Hatchikian E, Frey M, Fontecilla-Camps J. Crystal structure of the nickel-iron hydrogenase from *Desulfovibrio gigas*. Nature 1995; 373: 580-587.

51 Volbeda A, Garcin E, Piras C, De Lacey A, Fernandez V, Hatchikian E, et al. Structure of the [NiFe] hydrogenase active site: evidence for biologically uncommon Fe ligands. J Am Chem Soc 1996; 118: 12989-12996.

52 Higuchi Y, Ogata H, Miki K, Yasuoka N, Yagi T. Removal of the bridging ligand atom at the Ni–Fe active site of [NiFe] hydrogenase upon reduction with H2, as revealed by X-ray structure analysis at 1:4 Å resolution. Structure 1999; 7: 549-556.

53 Matias P, Soares C, Saraiva L, Coelho R, Morais J, Le Gall J, et al. [NiFe] hydrogenase from *Desulfovibrio desulfuricans* ATCC 27774: gene sequencing, three-dimensional structure determination and refinement at 1.8 Å and modelling studies of its interaction with the tetraheme cytochrome c3. Journal of Biological and Inorganic Chemistry 2001; 6(1): 63-81.

54 Volbeda A, Montet Y, Vernede X, Hatchikian EC, Fontecilla-Camps JC. High-resolution crystallographic analysis of Desulfovibrio fructosovorans [NiFe] hydrogenase. Int J Hydrogen Energy 2002; 27(11-12): 1449-1461.

55 Tamagnini P, Costa J-Ls, Almeida Lg, Oliveira M-J, Salema R, Lindblad P. Diversity of Cyanobacterial Hydrogenases, a Molecular Approach. Curr Microbiol 2000; 40(6): 356-361.

56 Tamagnini P, Axelsson R, Lindberg P, Oxelfelt F, Wunschiers R, Lindblad P. Hydrogenases and hydrogen metabolism of cyanobacteria. Microbiol Mol Biol Rev 2002; 66: 1 - 20.

57 Vignais PM, Colbeau A. Molecular biology of microbial hydrogenases. Current Issues in Molecular Biology 2004; 6: 159-188.

58 Maness P, Smolinski S, Dillon A, Heben M, Weaver P. Characterization of the oxygen tolerance of a hydrogenase linked to a carbon monoxide oxidation pathway in *Rubrivivax gelatinosus*. Appl Environ Microbiol 2002; 68: 2633-2636.

59 Bleijlevens B, Buhrke T, van der Linden E, Friedrich B, Albracht SPJ. The Auxiliary Protein HypX Provides Oxygen Tolerance to the Soluble [NiFe]-Hydrogenase of *Ralstonia eutropha* H16 by Way of a Cyanide Ligand to Nickel. J Biol Chem 2004; 279(45): 46686-46691.

60 Ghirardi ML, Posewitz MC, Maness P-C, Dubini A, Yu J, Seibert M. Hydrogenases and Hydrogen Photoproduction in Oxygenic Photosynthetic Organisms. Annual Review of Plant Biology 2007; 58(1): 71-91.

61 Montet Y, Amara P, Volbeda A, Vernede X, Hatchikian E, Field M, et al. Gas access to the active site of Ni–Fe hydrogenases probed by X-ray crystallography and molecular dynamics. Nature Structural and Molecular Biology 1997; 4(7): 523-526.

62 Hallenbeck PC, Benemann JR. Biological hydrogen production; fundamentals and limiting processes. Int J Hydrogen Energy 2002; 27(11-12): 1185-1193.

63 Melis A, Zhang L, Forestier M, Ghirardi ML, Seibert M. Sustained Photobiological Hydrogen Gas Production upon Reversible Inactivation of Oxygen Evolution in the Green Alga Chlamydomonas reinhardtii. Plant Physiol 2000; 122(1): 127-136.

64 Laurinavichene T, Tolstygina I, Tsygankov A. The effect of light intensity on hydrogen production by sulfur-deprived Chlamydomonas reinhardtii. J Biotechnol 2004; 114(1-2): 143-151.

65 Jo JH, Lee DS, Park JM. Modeling and Optimization of Photosynthetic Hydrogen Gas Production by Green Alga *Chlamydomonas reinhardtii* in Sulfur-Deprived Circumstance. Biotechnology Progress 2006; 22(2): 431-437.

66 Kosourov S, Patrusheva E, Ghirardi ML, Seibert M, Tsygankov A. A comparison of hydrogen photoproduction by sulfur-deprived Chlamydomonas reinhardtii under different growth conditions. J Biotechnol 2007; 128(4): 776-787.

67 Kondo K, Mullineaux CW, Ikeuchi M. Distinct roles of CpcG1-phycobilisome and CpcG2-phycobilisome in state transitions in a cyanobacterium Synechocystis sp. PCC 6803. Photosynthesis Research 2009; 99: 217-225.

68 Liu J, Bukatin VE, Tsygankov AA. Light energy conversion into H2 by Anabaena variabilis mutant PK84 dense cultures exposed to nitrogen limitations. Int J Hydrogen Energy 2006; 31(11): 1591-1596.

69 Yoshino F, Ikeda H, Masukawa H, Sakurai H. High Photobiological Hydrogen Production Activity of a Nostoc sp. PCC 7422 Uptake Hydrogenase-Deficient Mutant with High Nitrogenase Activity. Marine Biotechnology 2007; 9(1): 101-112.

70 Benemann JR. Hydrogen production by microalgae. Journal of Applied Phycology 2000; 12(3): 291-300.

71 Cooley Jw, et al. Succinate Dehydrogenase and Other Respiratory Pathways in Thylakoid Membranes of Synechocystis sp. PCC 6803: Capacity Comparisons and Physiological Function. J Bacteriol 2001; 183(14): 4251-4258.

72 Appel J, Phunpruch S, Steinmüller K, Schulz R. The Bidirectional Hydrogenase of Synechocystis sp. PCC 6803 Works as an Electron Valve during Photosynthesis. Arch Microbiol. 2000; 173: 333-338.

73 Antal TK, Oliveira P, Lindblad P. The bidirectional hydrogenase in the cyanobacterium Synechocystis sp. strain PCC 6803. Int J Hydrogen Energy 2006; 31(11): 1439-1444.

74 Antal TK, Lindblad P. Production of H_2 by sulphur-deprived cells of the unicellular cyanobacteria Gloeocapsa alpicola and Synechocystis sp. PCC 6803 during dark incubation with methane or at various extracellular pH. J Appl Microbiol 2005; 98(1): 114-120.

75 Cournac L, Mus F, Bernard L, Guedeney G, Vignais P, Peltier G. Limiting Steps of Hydrogen Production in Chlamydomonas reinhartii and Synechocystis sp. PCC 6803 as Analysed by Light Induced Gas-Exchange Transients. Int J Hydrogen Energy 2002; 27: 1229-1237.

76 Vignais PM, Willison JC. Increasing Biohydrogen Production by Metabolic Engineering. 2005.

77 Vignais PM, Magnin JP, Willison JC. Increasing biohydrogen production by metabolic engineering. Int J Hydrogen Energy 2006; 31: 1478 - 1483.

78 Burrows EH, Chaplen FWR, Ely RL. Optimization of media nutrient composition for increased photofermentative hydrogen production by Synechocystis sp. PCC 6803. Int J Hydrogen Energy 2008; 33(21): 6092-6099.

79 Burrows EH, Chaplen FWR, Ely RL. Effects of selected electron transport chain inhibitors on 24-h hydrogen production by Synechocystis sp. PCC 6803. Bioresour Technol 2010; 102: 3062-3070.

80 Burrows EH, Wong W-K, Fern X, Chaplen FWR, Ely RL. Optimization of pH and nitrogen for enhanced hydrogen production by *Synechocystis* sp. PCC 6803 via statistical and machine learning methods. Biotechnology Progress 2009; 25(4): 1009-1017.

81 Kiss É, Kósa PB, Vass I. Transcriptional regulation of the bidirectional hydrogenase in the cyanobacterium *Synechocystis* 6803 J Biotechnol 2009; 142(1): 31-37.

82 Oliveira P, Lindblad P. LexA, a transcription regulator binding in the promoter region of the bidirectional hydrogenase in the cyanobacterium Synechocystis sp. PCC 6803. FEMS Microbiol Lett 2005; 251(1): 59-66.

83 Yoldas BE. Monolithic glass formation by chemical polymerization. J Mater Sci 1979; 14(8): 1843-1849.

84 Kay BD, Assink RA. Sol-gel kinetics: II. Chemical speciation modeling. J Non-Cryst Solids 1988; 104(1): 112-122.

85 Brinker CJ, & G. W. Scherer. Sol-Gel Science. San Diego, CA: Academic Press, Inc., 1990.

86 Klein LC. Sol-Gel Processing of Silicates. Annual Reviews in Materials Science 1985; 15: 227-248.

87 Brinker CJ. Sol-Gel Processing of Silica. In: H. E. Bergna, editor. The Colloid Chemistry of Silica. Washington, D.C.: American Chemical Society, 1994. p. 361-402.

88 Brinker CJ. Sol-Gel Processing of Silica. Advances in Chemistry Series 1994; 234: 41.

89 Hench LL. Sol-Gel Silica: Properties, Processing and Technology Transfer. Westwood, NJ: Noyes Publications, 1998.

90 McCormick A. Recent Progress in the Study of the Kinetics of Sol-Gel SiO_2 Synthesis Reactions. In: Y. A. Attia, editor. Sol-Gel Processing and Applications. New York: Plenum Press, 1994. p. 3-16.

91 Bechtold MF, Vest RD, Louis Plambeck J. Silicic Acid from Tetraethyl Silicate Hydrolysis. Polymerization and Properties. J Am Chem Soc 1968; 90(17): 4590-4598.

92 Brinker CJ, Keefer KD, Schaefer DW, Ashley CS. Sol-Gel Transition in Simple Silicates. J Non-Cryst Solids 1982; 48: 47-64.

93 Pope EJA, Mackenzie JD. Sol-gel Processing of Silica II: The role of the catalyst. J Non-Cryst Solids 1986; 87: 185-198.

94 Assink RA, Kay BD. Study of Sol-Gel Chemical Reaction Kinetics by NMR. Annual Reviews in Materials Science 1991; 21: 491-513.

95 Pouxviel JC, Boilot JP, Beloeil JC, Lallemand JY. NMR Study of the Sol-Gel Polymerization. J Non-Cryst Solids 1987; 89: 345-360.

96 Kelts LW, Armstrong NJ. A silicon-29 NMR study of the structural intermediates in low pH sol-gel reactions. J Mater Res 1989; 4(2): 423-433.

97 Brinker CJ, Keefer KD, Schaefer DW, Assink RA, Kay BD, Ashley CS. Sol-Gel Transition in Simple Silicates II. J Non-Cryst Solids 1984; 63: 45-59.

98 Nair BN, Elferink WJ, Keizer K, Verweij H. Sol-Gel Synthesis and Characterization of Microporous Silica Membranes I: SAXS Study on the Growth of Polymeric Structures. J Colloid Interface Sci 1996; 178(2): 565-570.

99 Raman NK, Wallace S, Brinker CJ. Shrinkage and Microstructural Development During Drying of Organically Modified Silica Xerogels. Materials Research Society Symposium Proceedings 1996; 435: 6.

100 Glaser RH, Wilkes GL. Solid-State ^{29}Si NMR of TEOS-Based Multifunctional Sol-Gel Materials. J Non-Cryst Solids 1989; 113: 73-87.

101 Fahrenholtz WG, D. M. Smith, & D. Hua. Formation of microporous silica gels from a modified silicon alkoxide. I. Base-catalyzed gels. J Non-Cryst Solids 1992; 144: 45 - 52.

102 Avnir D, Coradin T, Lev O, Livage J. Recent Bio-applications of Sol-gel Materials. J Mater Chem 2006; 16: 1013 - 1030.

103 Nassif N, Roux Cc, Coradin T, Rager M-N, Bouvet OMM, Livage J. A Sol-gel Matrix to Preserve the Viability of Encapsulated Bacteria. J Mater Chem 2003; 13: 203-208.

104 Conroy J, Power ME, Martin J, Earp B, Hosticka B, Daitch CE, et al. Cells in Sol-Gels I: A Cytocompatible Route for the Production of Macroporous Silica Gels. J Sol Gel Sci Technol 2000; 18: 269-283.

105 Ferrer ML, Yuste L, Rojo F, Monte Fd. Biocompatible Sol-gel Route for Encapsulation of Living Bacteria in Organically Modified Silica Matrices. Chem Mater 2003; 15(19): 3614-3618.

106 Bagshaw SA, E. Prouzet, T. J. Pinnavaia. Templating of Mesoporous Molecular Sieves by Nonionic Polyethylene Oxide Surfactants. Science 1995; 269(5228): 1242-1244.

107 Reetz MT, Patrick Tielmann, Wolfgang Wiesenhofer, Werner Konen, & Albin Zonta. Second Generation Sol-Gel Encapsulated Lipases: Robust Heterogeneous Biocatalysts. Advanced Synthesis and Catalysis 2003; 345: 717 - 728.

108 Coradin T, Saliou Bah, & Jacques Livage. Gelatine/Silicate Interactions: From Nanoparticles to Composite Gels. Colloids and Surfaces B: Biointerfaces 2004; 35: 53 - 58.

109 Ren L, Kanji Tsuru, Satoshi Hayakawa, & Akiyoshi Osaka. Synthesis and Characterization of Gelatin-Siloxane Hybrids Derived through Sol-Gel Procedure. J Sol Gel Sci Technol 2001; 21: 115 - 121.

110 Chernev GE, Borisova BV, Kabaivanova LV, Salvado IM. Silica hybrid biomaterials containing gelatin synthesized by sol-gel method. Central European Journal of Chemistry 2010; 8(4): 870-876.

111 Coradin T, & Jacques Livage. Synthesis and Characterization of Alginate/Silica Biocomposites. J Sol Gel Sci Technol 2003; 26: 1165 - 1168.

112 Armanini L, G. Carturan, S. Boninsegna, R. dal Monte, & M. Muraca. SiO2 Entrapment of Animal Cells. Part 2: Protein Diffusion through Collagen Membranes Coated with SiO2. J Mater Chem 1999; 9: 3057 - 3060.

113 Brasack I, & Horst Bottcher. Biocompatibility of Modified Silica-Protein Composite Layers. J Sol Gel Sci Technol 2000; 19: 479 - 482.

114 Eglin D, Mosser G, Giraud-Guille M-M, Livage J, Coradin T. Type I collagen, a versatile liquid crystal biological template for silica structuration from nano- to microscopic scales. Soft Matter 2005; 1(129-131).

115 Pang JB, Qiu KY, Wei Y. Preparation of mesoporous silica materials with non-surfactant hydroxy-carboxylic acid compounds as templates via sol-gel process. J Non-Cryst Solids 2001; 283(2-3): 101-108.

116 Frenkel-Mullerad H, Avnir D. Sol-Gel Materials as Efficient Enzyme Protectors: Preserving the Activity of Phosphatases Under Extreme pH Conditions. J Am Chem Soc 2005; 127: 8077 - 8081.

117 Zadvorny OA, Barrows AM, Zorin NA, Peters JW, Elgren TE. High level of hydrogen production activity achieved for hydrogenase encapsulated in sol–gel material doped with carbon nanotubes. J Mater Chem 2010; 20: 1065-1067.

118 Kriegl JM, Forster FK, Nienhaus GU. Charge Recombination and Protein Dynamics in Bacterial Photosynthetic Reaction Centers Entrapped in a Sol-Gel Matrix. Biophys J 2003; 85: 1851 - 1870.

119 Taylor A, Finnie KS, Bartlett JR, Holden PJ. Encapsulation of Viable Aerobic Microorganisms in Silica Gels. J Sol Gel Sci Technol 2004; 32: 223-228.

120 Jin W, & John D. Brennan. Properties and Applications of Proteins Encapsulated within Sol-Gel Derived Materials. Anal Chim Acta 2002; 461: 1 - 36.

121 Armon R. Sol-Gel as Reaction Matrix for Bacterial Enzymatic Activity. J Sol Gel Sci Technol 2000; 19: 289-292.

122 Bergogne L, Souad Fennouh, Stephanie Guyon, Cecile Roux, & Jacques Livage. Sol-Gel Entrapment of Enzymes. Materials Research Society Symposium Proceedings 2000; 628: 10.12.11 - 10.12.16.

123 Bhatia RB, & C. Jeffrey Brinker. Aqueous Sol-Gel Process for Protein Encapsulation. Chem Mater 2000; 12(8): 2434 - 2441.

124 Pierre AC. The Sol-Gel Encapsulation of Enzymes. Biocatalysis and Biotransformation 2004; 22(3): 145 - 170.

125 Bottcher H, Soltmann U, Mertig M, Pompe W. Biocers: Ceramics with Incorporated Microorganisms for Biocatalytic, Biosorptive and Functional Materials Development. J Mater Chem 2004; 14: 2176 - 2188.

126 Livage J, Coradin T, Roux C. Encapsulation of Biomolecules in Silica Gels. J Phys: Condens Matter 2001; 13: R673 - R691.

127 Gadre SY, Gouma PI. Biodoped Ceramics: Synthesis, Properties, and Applications. J Am Ceram Soc 2006; 89(10): 2987-3002.

128 Gupta R, Chaudhury NK. Entrapment of biomolecules in sol-gel matrix for applications in biosensors: Problems and future prospects. Biosensors and Bioelectronics 2007; 22(11): 2387-2399.

129 Meunier CF, Dandoy P, Su B-L. Encapsulation of cells within silica matrixes: Towards a new advance in the conception of living hybrid materials. J Colloid Interface Sci 2010; 342: 211-224.

130 Ellerby LM, Nashida CR, Nashida F, Yamanaka SA, Dunn B, Valentine JS, et al. Encapsulation of Proteins in Transparent Porous Silicate Glasses Prepared by the Sol-Gel Method. Science 1992; 255(5048): 1113 - 1115.

131 Kuncova G, Podrazky O. Monitoring of the Viability of Cells Immobilized by Sol-Gel Process. J Sol Gel Sci Technol 2004; 31: 335 - 342.

132 Rooke JC, Alexander L, Su B-L. Targeting photobioreactors: Immobilisation of cyanobacteria within porous silica gel using biocompatible methods. Journal of Materials Chemistry 2008; 18: 9.

133 Dickson DJ, Page CJ, Ely RL. Photobiological hydrogen production from Synechocystis sp. PCC 6803 encapsulated in silica sol-gel. Int J Hydrogen Energy 2009; 34(1): 204-215.

134 Gautier C, Livage J, Coradin T, Lopez PJ. Sol-gel encapsulation extends diatom viability and reveals their silica dissolution capability. Chemical Communications 2006; (44): 4611-4613.

135 Fiedler D, Hager U, Franke H, Soltmann U, Bottcher H. Algae biocers: astaxanthin formation in sol-gel immobilised living microalgae. J Mater Chem 2007; 17(3): 261-266.

136 Nguyen-Ngoc H, Tran-Minh C. Sol-gel process for vegetal cell encapsulation. Materials Science and Engineering: C 2007a; 27(4): 607-611.

137 Nguyen-Ngoc H, Tran-Minh C. Fluorescent biosensor using whole cells in an inorganic translucent matrix. Anal Chim Acta 2007b; 583(1): 161-165.

138 Pressi G, Toso RD, Monte RD. Production of Enzymes by Plant Cells Immobilized by Sol-Gel Silica. J Sol Gel Sci Technol 2003; 26: 1189 - 1193.

139 Carturan G, Monte RD, Pressi G, Secondin S, Verza P. Production of Valuable Drugs from Plant Cells Immobilized by Hybrid Sol-Gel SiO_2. J Sol Gel Sci Technol 1998; 13: 273 - 276.

140 Pope EJA, Karen Braun, & Charles M. Peterson. Bioartificial Organs I: Silica Gel Encapsulated Pancreatic Islets for the Treatment of Diabetes Mellitus. J Sol Gel Sci Technol 1997; 8: 635 - 639.

141 Boninsegna S, Bosetti P, Carturan G, Dellagiacoma G, Monte RD, Rossi M. Encapsulation of Individual Pancreatic Islets by Sol-Gel SiO_2: A Novel Procedure for Perspective Cellular Grafts. J Biotechnol 2003; 100: 277 - 286.

142 Dickson DJ. Influence of Processing Parameters on Diffusion of Divalent Nickel in Wet Silica Sol-Gel Monoliths. Oregon State University, 2010.

143 Laughlin RB, J. D. Joannopoulos, & D. J. Chadi. Bulk electronic structure of SiO_2. Physical Review B 1979; 20(12): 5228 - 5237.

144 Gupta RP. Electronic structure of crystalline and amorphous silicon dioxide. Physical Review B 1985; 32(12): 8278 - 8292.

145 Koslowski T, W. Kob, & K. Vollmayr. Numerical study of the electronic structure of amorphous silica. Physical Review B 1997; 56(15): 9469 - 9476.

146 Ferjani A, Mustardy L, Sulpice R, Marin K, Suzuki I, Hagemann M, et al. Glucosylglycerol, a Compatible Solute, Sustains Cell Division under Salt Stress. Plant Physiol 2003; 131(4): 1628-1637.

147 Hagemann M, Jeanjean R, Fulda S, Havaux M, Joset F, Erdmann N. Flavodoxin accumulation contributes to enhanced cyclic electron flow around photosystem I in salt-stressed cells of Synechocystis sp. strain PCC 6803. Physiol Plant 1999; 105(4): 670-678.

148 Kautsky H, Hirsch A. Neue Versuche Zur Kohlensaureassimilation. Naturwissenschaften 1931; 19(48): 964-989.

149 Rakhimberdieva MG, Elanskaya IV, Vermaas WFJ, Karapetyan NV. Carotenoid-triggered energy dissipation in phycobilisomes of Synechocystis sp. PCC 6803 diverts excitation away from reaction centers of both photosystems. Biochimica et Biophysica Acta (BBA) - Bioenergetics 2010; 1797(2): 241-249.

150 Campbell D, Hurry V, Clarke AK, Gustafsson P, Oquist G. Chlorophyll Fluorescence Analysis of Cyanobacterial Photosynthesis and Acclimation. Microbiol. Mol. Biol. Rev. 1998; 62(3): 667-683.

151 Campbell D, Oquist G. Predicting Light Acclimation in Cyanobacteria from Nonphotochemical Quenching of Photosystem II Fluorescence, Which Reflects State Transitions in These Organisms. Plant Physiol 1996; 111(4): 1293-1298.

152 Maxwell K, Johnson GN. Chlorophyll fluorescence--a practical guide. J Exp Bot 2000; 51(345): 659-668.

153 Papageorgiou GC, Govindjee, ed. Chlorophyll a Fluorescence. Advances in Photosynthesis and Respiration, 19. Springer, Dordrecht, The Netherlands, 2004.

154 Baker NR. Chlorophyll Fluorescence: A Probe of Photosynthesis In Vivo. Annual Review of Plant Biology 2008; 59: 89-113.

155 Karapetyan NV. Non-photochemical quenching of fluorescence in cyanobacteria. Biochemistry 2007; 72(10): 1127-1135.

CHAPTER 2 - PHOTOBIOLOGICAL HYDROGEN PRODUCTION FROM SYNECHOCYSTIS SP. PCC 6803 ENCAPSULATED IN SILICA SOL–GEL

David J. Dickson, Catherine J. Page, Roger L. Ely

International Journal of Hydrogen Energy

Elsevier Press

3251 Riverport Lane

Maryland Heights, MO 63043, USA

International Association of Hydrogen Energy

5794 SW 40 St. #303

Miami, FL 33155, USA

Issue 34 (2009), pages 204 – 215

2.1 - Abstract

Hydrogen production was measured from viable wild-type and M55 mutant cells of *Synechocystis* sp. PCC 6803 encapsulated in silica sol-gel derived from tetraethoxysilane, tetramethoxysilane, and a mixture of tetraethoxysilane with methyltriethoxysilane. Glycerol and polyethylene glycol were used as additives in concentrations up to 14%wt. to increase porosity and pore connectivity and to reduce stress on the encapsulated cells. Mixtures were evaluated for hydrogen production in a high-throughput screening assay, and samples were imaged with environmental scanning electron microscopy. Compositions showing improved H_2 production were selected for further study via quantitative analysis of H_2 production in GC vial assays. H_2 production activity was monitored for up to 5 days and H_2 production from encapsulated cells was observed at levels comparable to or exceeding cells suspended in liquid media.

Keywords: tetraethoxysilane, tetramethoxysilane, polyethylene glycol, glycerol, biosolar, biophotolysis, hydrogenase, cyanobacteria

2.2 - Introduction

Synechocystis sp. PCC 6803 has been extensively studied since it was first isolated in 1968 and is a well characterized model organism for photosynthesis. The genome is fully sequenced and annotated and the organism is highly transformable. PCC 6803 has been of particular interest recently because, in addition to possessing a full complement of photosynthetic capabilities, it contains a bidirectional [Ni-Fe] hydrogenase enzyme capable of producing molecular hydrogen (H_2) from the reduction of protons under certain metabolic conditions [1-5]. A photobiological means of producing H_2 from water offers an attractive option as a sustainable source of this increasingly valuable fuel [6]. However, many issues must be resolved before this process can become a practical, widespread, and economically feasible source of H_2.

One approach to achieving increased and sustained levels of biosolar H_2 production from phototrophic microorganisms may be to encapsulate viable cells in a solid silica matrix. Encapsulation within silica sol-gel is a relatively new technique for encapsulating viable cells, first shown in 1989 with *Saccharomyces cerevisiae* cells by Carturan et al. [7], and has been successfully demonstrated with a variety of biological components including enzymes and proteins [8-11], bacteria [12-14], yeast [7, 15, 16], plant cells [17, 18], mammalian cells [19], and phototrophic cyanobacteria [20]. The matrix creates a solid framework that provides structural, thermal and chemical stability to the encapsulated cultures. Under the right conditions, this can prolong cell life for many months [21], protect cells from contamination, prevent out-growth, and increase the production of secondary metabolites such as H_2. The matrix is also transparent, allowing for the encapsulation of phototrophs, making this approach useful for biosensors that employ fluorescence or, in this case, for photobiological production of H_2.

2.2.1 - H_2 Production in Synechocystis sp. PCC 6803

H_2 production in this species generally has been reported to occur in two situations: at a low, steady rate in the dark as the cells break down accumulated glycogen anaerobically; and during a transient burst of H_2 production activity at the initial on-set of photosynthesis with light exposure [2]. The predicted photobiological pathway of H_2 production is illustrated in Figure 2-1 and can be summarized as follows: Oxygenic photosynthesis is initiated at photosystem II (PSII) where water is split into protons and electrons with the release of molecular oxygen. The protons are used to create a potential gradient across the thylakoid membrane enabling the production of ATP from ADP and phosphate. The electrons enter the electron transport chain where they proceed through a series of transport molecules and proteins, including plastoquinone, cytochrome b_6f, and plastocyanin, to photosystem I (PSI). The excited electrons are finally used to produce reducing equivalents in the form of NADPH, which are used in the Calvin Cycle for carbon fixation and other metabolic reactions. Excess reducing equivalents can also be used by the hydrogenase enzyme to produce gaseous H_2. The enzyme reportedly is sensitive to oxygen, with activity being drastically reduced or completely halted during oxygenic photosynthesis. Under any conditions, reductant availability also can limit H_2 production. The reported substrates for the hydrogenase are a molecule of NADPH, which is oxidized to $NADP^+$, and a proton, which is reduced to produce one molecule of H_2 [2]. NADPH supplies reductant to numerous metabolic pathways, however, which compete with the hydrogenase. These two challenges have been considered to be the primary obstacles to improved H_2 production in this species.

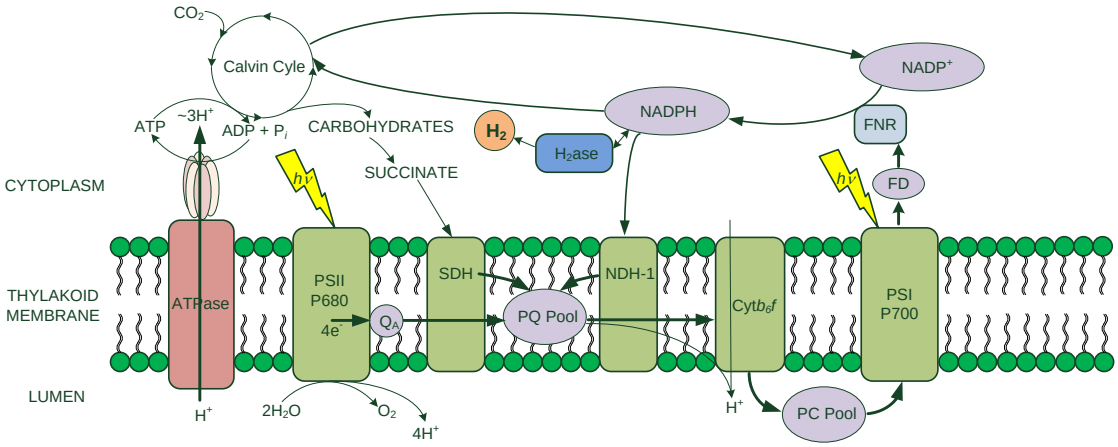

Figure 2-1: A schematic of the predicted photobiological pathway of hydrogen production in Synechocystis, adapted from Cournac et al. [2]. Dominant electron transport pathways are illustrated with bold arrows and boxes indicate enzyme complexes. ATPase – ATP synthase; PSI – photosystem I; PSII – photosystem II; SDH – succinate dehydrogenase; NDH-1 – NADPH dehydrogenase; Cytb6f – cytochrome b6f complex; PQ Pool – plastoquinone pool; PC Pool – plastocyanin pool; FD – ferredoxin; FNR – ferredoxin-NADP+ reductase; H_2ase – hydrogenase. The M55 mutant lacks a functional NDH-1 complex, hindering cyclic electron flow around PSI.

Researchers have taken various approaches to overcome these two challenges. Two general approaches include genetic manipulation, such as altering the hydrogenase enzyme to confer some degree of added oxygen tolerance or other enhanced activity, or metabolic approaches [22], which manipulate the environment of the cells in order to enhance H_2 production through improved reductant availability. For example, Antal and Lindblad showed that sulfur deprivation can be used to promote a more than four-fold increase in H_2 production from *Synechocystis* in a methane atmosphere [23]. Burrows has shown that optimizing nutrient concentrations can yield nearly a 150-fold increase in H_2 production compared to

sulfur deprived cells, after conditioning the cells in media optimized for H_2 production [24]. Encapsulation may also be regarded as a metabolic manipulation since it will alter cell metabolism and potentially increase reductant availability for H_2 production.

2.2.2 - Silica Sol-gel for Encapsulating Whole Cells

Sol-gel processing is an empirically well characterized materials science technique used for fabricating metal oxide thin films, optoelectrical devices, monoliths for separations, and other specialty applications. The process is generic and can be used with numerous transition metals and semi-metal elements to make amorphous or crystalline metal oxides after heat treatment. The fundamentals of sol-gel processing are described in the seminal text of Brinker & Scherer [25]. A common two step sol-gel process employs metal alkoxide precursors, such as tetraethoxysilane (TEOS), $Si(OC_2H_5)_4$, which is hydrolyzed in the presence of an acid catalyst and alcohol solvent. Subsequent condensation and hydrolysis reactions then reach an equilibrium, forming a sol, or colloidal suspension, of metal oxide clusters. With subsequent basic catalysis, condensation reactions accelerate and the clusters aggregate into a randomly cross-linked, polymeric gel. With aging, the gel becomes increasingly dense and cross-linked as solvent is expelled from the pore volume. Finally, a heat treatment can be used to remove the solvent and fully condense the gel into a microstructure suited for the application. The literature on sol-gel processing in the context of fabricating optoelectrical devices is expansive.

Recently, this process was borrowed from materials science to demonstrate encapsulation of biological components, first with viable yeast cells [7]. Silica sol-gel was selected for its biocompatibility, and *S. cerevisiae* for its tolerance to ethanol, which is evolved from the hydrolysis of TEOS to silicic acid, $Si(OH)_4$. Immobilization of biological components was not new, but using a purely inorganic solid matrix was a

novel approach. Unlike most other commonly used organic encapsulation matrices, which can swell and are vulnerable to biological degradation, silica sol-gel creates an inert matrix that restricts cell growth. As a result, cells may enter an altered steady-state metabolism that yields increased production of secondary metabolites. The rigidity also prevents cell outgrowth, maintains the mechanical integrity of the matrix, and prevents contamination by other organisms. This allows for applications in biosensors and bioreactors where fluid streams with analytes of interest or fresh substrate can pass over porous matrices containing immobilized biological components. Several recent reviews are available [10, 26-29].

Despite the variety of biological components that have been successfully encapsulated in silica sol-gel, the use of this technique for biosolar H_2 production by viable phototrophs has not been investigated previously. The matrix is transparent and therefore suitable for phototrophs and photoactive proteins, as was demonstrated with photoactive proteins in 1992 by Ellerby [8]. More recently, sol-gel encapsulation has been used for the development of a biosensor based on immobilized algal cells [30, 31] and an alternate method using colloidal precursors has also been used to encapsulate multiple strains of *Synechococcus* [32]. Our evaluations indicate that approximately 12% of incident light is absorbed by the gels described in this report, which is consistent across all gel compositions and remains stable after 24 hours for the duration of the study (data not shown), illustrating that most of the incident radiation can be available for photosynthesis. Therefore, this approach may be well suited for immobilizing *Synechocystis* sp. PCC 6803 and potentially for improving H_2 production. Cyanobacteria use most of the energy collected during photosynthesis for the production of biomass. It has been suggested that cells may direct no more than 15% of their available energy toward H_2 production [33]. However, if growth is restricted, that percentage could potentially

increase. In a different format, Laurinavichene et al. demonstrated that cells of Chlamydomonas reinhardtii immobilized on glass fibers produced approximately 2.5 times more H_2 than cultures under otherwise identical conditions in liquid suspension [34].

2.3 - Materials and Methods

2.3.1 - Cell Culturing

Synechocystis sp. PCC 6803 wild-type (*wt*) cells and a mutant strain deficient in the NDH-1 complex (M55) [2] were grown photoautotrophically, with constant illumination of approximately 50 $\mu E/m^2s^{-1}$, on BG-11 media supplemented with 35 mM HEPES buffer and 80 mM sodium bicarbonate in 250 mL of media in 500 mL flasks maintained at 30°C on orbital shaker tables. For encapsulation studies, cells were harvested during log-growth phase and conditioned in optimized media [24] at 30°C for 40 hours under the same illumination.

2.3.2 - Encapsulation

For initial screening experiments, sol-gel precursors, including TEOS, tetramethoxysilane (TMOS), and methyltriethoxysilane (MTES) were mixed in molar hydration ratios varying from 20:1 to 40:1 (water to precursor) and adjusted with a strong acid, either hydrochloric or nitric acid, to a pH of approximately 1.0 (TEOS, TMOS, and TMES; Alfa Aesar, Ward Hill, MA). Precursor solutions were allowed to mix in Erlenmeyer flasks up to 24 hours exposed to ambient air in a fume hood to allow evaporation of evolved methanol or ethanol. When initially mixed, the solution was clear but phase-separated. The solution became homogeneous typically within an hour, but phase separation occurred if stirring stopped too soon. A minimum of approximately four hours was required under these conditions for hydrolysis to proceed until a homogeneous sol was produced.

Encapsulation was performed by re-suspending conditioned cells in fresh optimized media containing 35 mM phosphate buffer at a pH of 8.0. Synechocystis sp. PCC 6803 cells can tolerate elevated pH levels, so the strong base, NaOH or KOH, was added to the media prior to resuspension in a molar equivalent to the strong acid present in the volume of sol to be used for encapsulation, typically approximately 50 μL of 1.0 M base solution per mL of cell suspension, depending on the composition of the sol. This resulted in a pH of approximately 9 - 10. The cell suspension was then directly mixed with the sol solution in a volume ratio of 1 part sol to 3 parts cell suspension, which induced gelation within 5 minutes. Final cell concentration in the gels was $1.0x10^{10}$ cells/mL. Final pH was estimated to be approximately 8.

2.3.3 - Initial Formulation Screening

For initial screening studies, various compositions were compared in a high-throughput screening assay [35] to determine more favorable encapsulation protocols for H_2 production. A total volume of 500 μL of sol and cell suspension was mixed in each 1 mL well of 96-well microtiter plates, 125 μL sol with 375 μL of cell suspension. The plates were degassed in a nitrogen atmosphere for approximately 3 hours, sealed, and placed in an incubator at 30°C under cycled light/dark exposure, 2 minutes on/18 minutes off, at approximately 70 $\mu E/m^2s^{-1}$. Each 96-well plate had a 96-well membrane-bottom plate sealed above it, with each well containing a catalyst (sulfonated Wilkinson's catalyst; Acros, Morris Plains, NJ) and water soluble tetrazoleum color indicator (WST-3; Dojindo, Gaithersburg, MD) that changed color when exposed to H_2. See Schrader et al. for a detailed explanation of the screening assay [35]. The color indicator in each well was scanned at 450 nm in a spectrophotometric microplate reader (Biorad, Hercules, CA) to assess net H_2 production over the course of the assay.

2.3.4 - Evaluations of H_2 Production

Subsequent encapsulation studies with formulations showing the most H_2 production were carried out similarly in 2 mL GC vials. Vials were prepared in a sterile laminar hood, allowed to fully gel, and then transferred to a nitrogen atmosphere to degas for approximately 3 hours. Vials were capped, placed in an incubator at 30°C, and cycled under light/dark exposure, 2 minutes on/18 minutes off, at approximately 70 $\mu E/m^2s^{-1}$. Headspace H_2 and CO_2 concentrations were measured after 16, 40 and 80 hours with an Agilent 6890N gas chromatograph (Agilent Technologies, Santa Clara, CA). After 80 hours, the vials were opened within a nitrogen atmosphere, allowed to degas, re-sealed and placed back in the incubator.

Formulation screening experiments included all combinations of hydrochloric acid, nitric acid, potassium hydroxide, and sodium hydroxide, as well as a range of molar ratios of alkoxide precursor to water, mixtures of precursors, and a range of glycerol and polyethylene glycol (PEG) 400 concentrations as additives. Later studies to evaluate H_2 production used only nitric acid and potassium hydroxide, TEOS and a blend of 90% TEOS and 10% MTES, by weight, and 10% wt. PEG. Formulations and results from screening assay and subsequent H_2 production evaluations are summarized in Tables 2-1 and 2-2.

2.3.5 - Environmental Scanning Electron Microscopy

Environmental scanning electron microscopy (ESEM) was performed at the Center for Advanced Materials Characterization (CAMCOR)(FEI Quanta 200 ESEM/UPSEM Microscope. FEI Company, Hillsboro, OR) at the University of Oregon in Eugene, OR. Samples were flash frozen in liquid nitrogen and placed on a cold stage for imaging. This approach avoids extensive fixing and mounting typically required for

biological samples prepared for SEM because the system can image at pressures above the partial pressure of water at reduced temperatures.

2.4 - Results

2.4.1 - Encapsulation and Initial Screening

Currently, optimal encapsulation formulations cannot be designed from first principles because a complete theoretical description of silica sol-gel processing and encapsulation does not exist. Hence, an optimal formulation for each new type of encapsulated cell must be explored empirically through iterative experiments. Similarities exist across a broad range of cell types and the literature provides a reasonable starting point, but optimizing the process for any given cell type depends on the characteristics of that particular cell and the gel within which it is encapsulated. In this study, common precursors, TEOS, TMOS, and MTES, were selected and both *wt* and M55 strains were compared to determine if they differ in their responses to encapsulation.

Many variables in the initial gel formulation and its processing can affect the final properties of the gel. In this investigation, we examined precursor type, molar ratio of water to precursor, type of acid and base used for catalysis, and a blend of precursors with and without additives. In initial formulation screening studies comparing TEOS- and TMOS-derived gels, cells in TMOS, which evolves methanol during hydrolysis, showed less activity, producing less H_2 than cells in TEOS, which evolves ethanol (Figure 2-2). The growth of *Synechocystis* sp. PCC 6803 was not significantly inhibited by low concentrations of ethanol (up to 100 mM, data not shown), indicating that the cells can tolerate some residual ethanol present in TEOS-derived gels. These results suggest methanol is more cytotoxic to *Synechocystis* than ethanol, which presumably caused reduced activity in cells immobilized in TMOS

derived gels. In fact, cells encapsulated in TMOS gels displayed activity only slightly above cell-free controls (data not shown). However, although the alkoxide type is the only variable, the type of alcohol present after hydrolysis is not the only difference between the gels. The type of alkoxide can influence both the hydrolysis and condensation reactions, which will alter the final structure of the gel. Other cell types have shown some tolerance to low levels of methanol [36], which suggests other factors may be hindering the H_2 production from *Synechocystis* cells encapsulated in TMOS and merits further investigation.

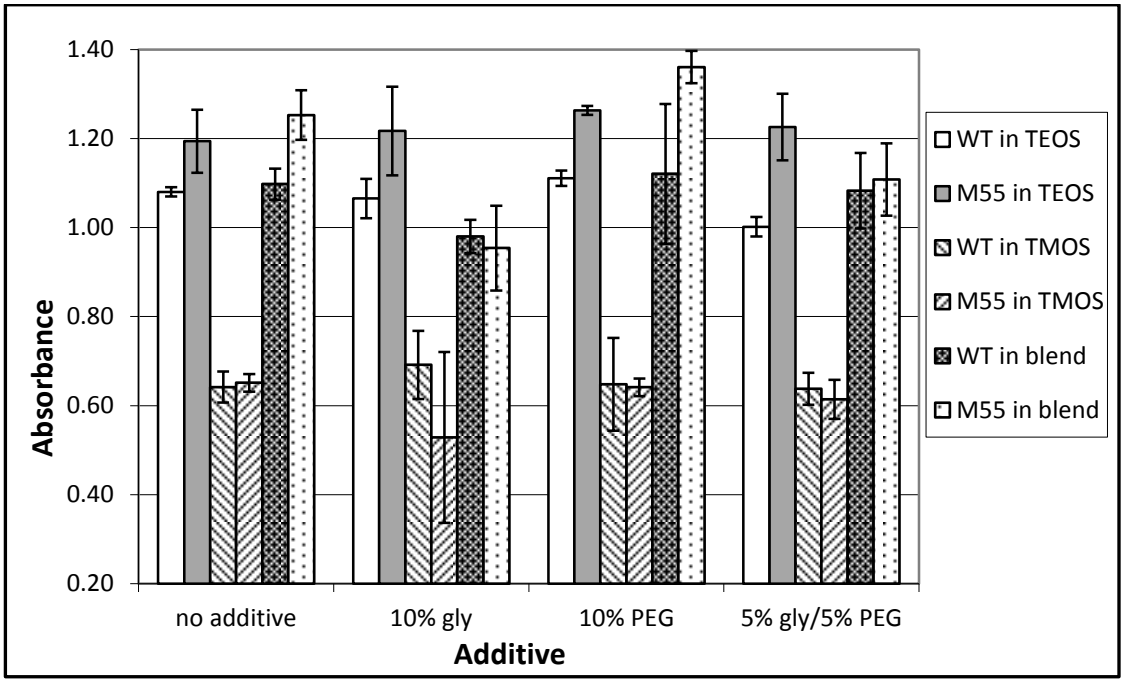

Figure 2-2: Comparison of hydrogen production over 5 days of wild type (*wt*) and M55 cells encapsulated in three different gel compositions, as detected through a high throughput screening assay. All gels were hydrolyzed by nitric acid and neutralized with potassium hydroxide. The blend contains 10% MTES in TEOS. As shown, both types of cells evolve considerably less H_2 when encapsulated in TMOS derived gels. The absorbance of cell-free controls (not shown) are typically on the

order of approximately 0.55. Samples were analyzed in triplicate and error bars indicate one standard deviation. All gels contain 10^{10} cells/mL.

MTES was also explored as a precursor to determine if some degree of hydrophobicity contributed by unhydrolyzed methyl groups present in the final matrix would promote a more favorable interaction with the encapsulated cells. Pure MTES cannot be used because the gels are too viscous and opaque. However, MTES is fully miscible in TEOS, which allows for a controlled introduction of hydrophobic methyl groups with negligible loss in light transmittance. Blends consisting of 5%, 10% and 15% MTES in TEOS were compared, with and without PEG, to determine the most favorable composition for H_2 production. In the absence of PEG, the blend composition did not have a statistically significant effect on H_2 production in either cell type (Table 2-2). In the presence of 10% PEG, the 10% blend was slightly beneficial to both cell types and was selected for subsequent H_2 production evaluation studies.

Table 2-1: Summary of initial screening assay conditions and results. TMOS was compared with other formulations of TEOS and a TEOS/MTES blend. All values indicate absorbance as measured by a spectrophotometric plate reader at 450 nm and are indicative of net H_2 production over the 5 ½ day assay. The ratios indicate hydration ratio, precursor to water, on a molar basis, and for the blend, the fraction represents the weight fraction of MTES (TEOS/MTES, by mass). Cell-free controls were included in all assays (data not shown).

		Wild-Type		M55	
Precursor	Formulation	HCl/NaOH	HNO_3/KOH	HCl/NaOH	HNO_3/KOH
TMOS	pure 1:20	0.595	0.642	0.637	0.651
	1:20 + 10% glycerol	0.627	0.692	0.656	0.529
	1:20 + 10% PEG	0.584	0.648	0.671	0.641
	1:20 + 5% gly. + 5% PEG	0.632	0.638	0.593	0.614
TEOS	pure 1:30	0.848	0.862	1.118	0.9980
	1:30 + 10% glycerol	0.768	0.826	0.707	0.8350
	1:30 + 10% PEG	-	0.892	-	1.1287
	1:30 + 5% gly.+ 5% PEG	-	0.928	-	0.8620
	pure 1:20	0.993	1.080	1.048	1.194
	1:20 + 10% glycerol	0.879	1.065	1.048	1.217
	1:20 + 10% PEG	0.945	1.111	1.167	1.264
	1:20 + 5% gly.+ 5% PEG	0.949	1.002	1.079	1.226
Blend	pure 1:20 (90/10)	0.924	1.098	1.181	1.253
	90/10 + 10% glycerol	0.802	0.980	1.015	0.954
	90/10 + 10% PEG	0.973	1.121	1.274	1.361
	90/10 + 5% gly. + 5% PEG	0.907	1.083	0.961	1.108

Table 2-2: Summary of results from a series of assays comparing PEG concentrations and blend compositions as well as all salt combinations. All values indicate absorbance as measured by a spectrophotometric plate reader at 450 nm and are indicative of net H_2 production over the 5 ½ day assay. Cell-free controls were included in all assays (data not shown).

		Wild-Type				M55			
Precursor	Formulation	HCl + NaOH	HNO_3 + KOH	HCl + KOH	HNO_3 + NaOH	HCl + NaOH	HNO_3 + KOH	HCl + KOH	HNO_3 + NaOH
TEOS	pure 1:20	-	0.897	0.882	0.971	-	0.810	0.639	0.874
	1:20 + 6% PEG	-	0.834	-	-	-	0.818	-	-
	1:20 + 8% PEG	-	0.777	-	-	-	0.673	-	-
	1:20 + 10% PEG	-	0.877	0.866	0.855	-	0.819	0.822	0.691
	1:20 + 12% PEG	-	0.794	-	-	-	0.697	-	-
	1:20 + 14% PEG	-	0.918	-	-	-	0.712	-	-
Blend	pure 95/5	-	0.979	-	-	-	0.993	-	-
	95/5 + 10% PEG	-	0.839	-	-	-	0.886	-	-
	pure 90/10	-	0.959	-	-	-	0.971	-	-
	90/10 + 10% PEG	-	1.035	-	-	-	1.055	-	-
	pure 85/15	-	1.032	-	-	-	0.970	-	-
	85/15 + 10% PEG	-	0.881	-	-	-	1.057	-	-

The ratio of water to precursor is also an important parameter because it influences the initial hydrolysis reactions, subsequent condensation reactions, and the final structure of the gel. More water favors more complete hydrolysis and also stabilizes the sol in the presence of minimal solvent [37]. A molar ratio of 4:1, water to precursor, is the minimum theoretically required for complete hydrolysis of silicon alkoxides, but excess water promotes more complete hydrolysis and also prevents gelation in the absence of excess alcohol solvent. Ratios varying from 20:1 to 40:1, water to precursor, were prepared and examined in varying proportions with cell suspension, which induced gelation upon mixing due to the basic catalyst present in the suspension. The more dilute sols could not accommodate a significant proportion of cell suspension and did not gel adequately at desired cell concentrations (data not shown). A ratio of 20:1 diluted by 3 parts cell suspension (375 μL) per 1 part (125 μL) sol was more favorable for H_2 production than other formulations (Table 2-1) and was selected for subsequent GC studies.

Because residual salts in the gel may influence activity of encapsulated cells, the type of strong acid used to hydrolyze the alkoxide precursor and promote the formation of a stable sol and the strong base required to induce gelation were also considered. Hydrochloric acid, nitric acid, potassium hydroxide, and sodium hydroxide were evaluated as the strong acids and neutralizing bases, respectively. These particular acids and bases have been used extensively for sol-gel processing and are commonly used to adjust pH in biological systems. A factorial experimental design was used to examine combinations of acid and base and it was determined that nitric acid neutralized by potassium hydroxide produced the most favorable environment for H_2 production (Tables 2-1 and 2-2, and Figure 2-3), perhaps because potassium nitrate provides both nitrogen and potassium to the encapsulated cells. The other salts, potassium chloride, sodium chloride, and sodium nitrate, may be less

useful or less available to the cells and the lingering concentration of each, particularly excess sodium, may contribute to increased osmotic stress on the encapsulated cells. Pairing hydrochloric acid with potassium hydroxide and nitric acid with sodium hydroxide produced nearly identical results as hydrochloric acid paired with sodium hydroxide, suggesting the effects of osmotic stresses are similarly small but not insignificant (Table 2-2). Salts may also influence the gelation process and the resulting gel structure, so the effects of salts in this application merit further investigation.

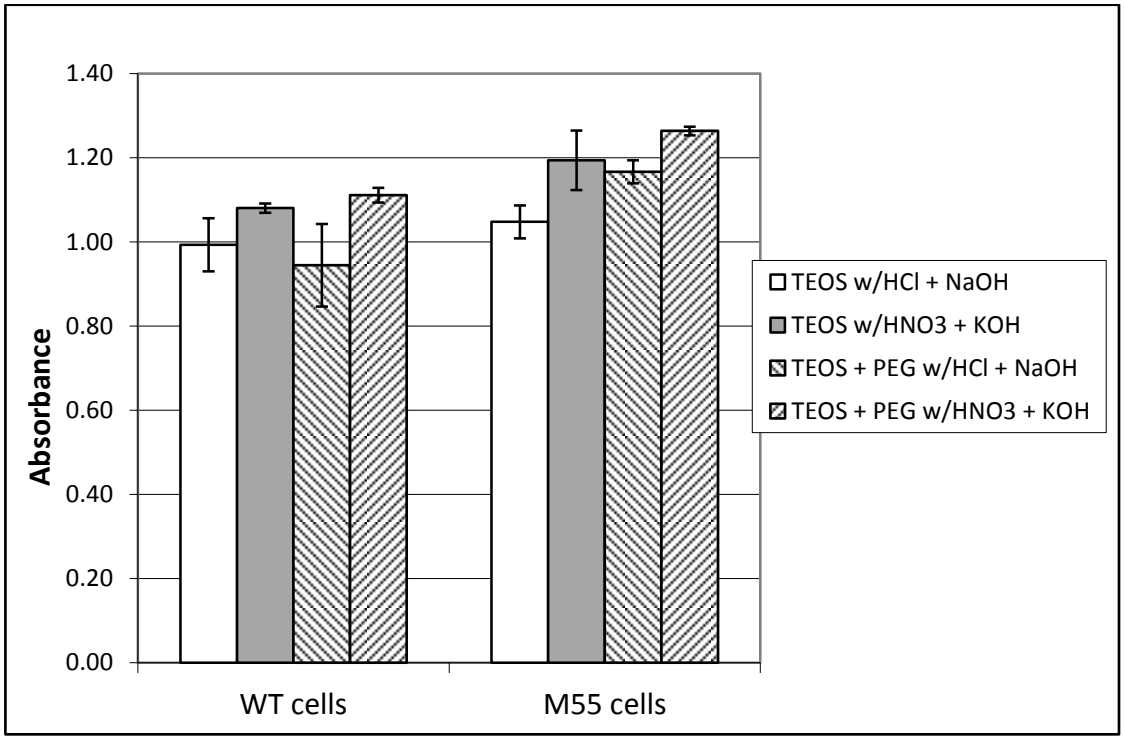

Figure 2-3: Hydrogen production in screening assays comparing the effects of the acid and base used. Pairing hydrochloric acid with potassium hydroxide and nitric acid with sodium hydroxide produced nearly identical results as hydrochloric acid with sodium hydroxide and are not shown. The only clear combination that was slightly beneficial in terms of hydrogen production was nitric acid with potassium

hydroxide. Samples were analyzed in triplicate and error bars indicate one standard deviation. All gels contain 10^{10} cells/mL.

To assess the structure of the gels and the arrangement of the cells within them, TEOS gels with 10% wt. glycerol in the initial sol and containing $5x10^{9}$ cells/mL were imaged by ESEM (Figure 2-4). Of particular concern was verifying that the gels were adequately porous and that the cells were intact and dispersed, not aggregated into flocs. The formation of such aggregates would cause shading effects and limitations in diffusion of nutrients to cells within flocs, which could tend to reduce activity. Both *wt* and M55 cells were seen to be individually encapsulated and the gel structures were quite porous. However, ESEM images showed different gel structures, suggesting the two strains may have interacted differently with the gel matrix. Shown in Figure 2-4a, the matrix around *wt* cells appeared to form larger pockets, whereas the matrix around M55 cells, shown in Figure 2-4b, appeared to more closely adhere to the surfaces of the cells.

(a)

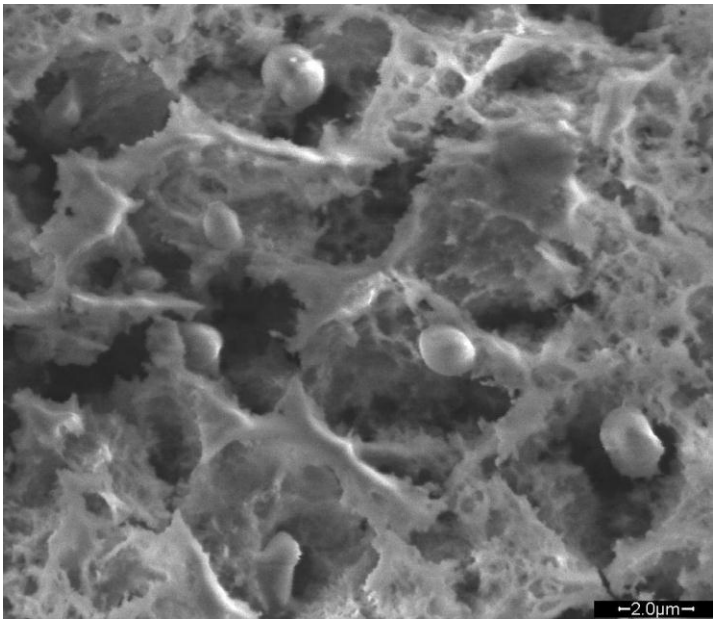

(b)

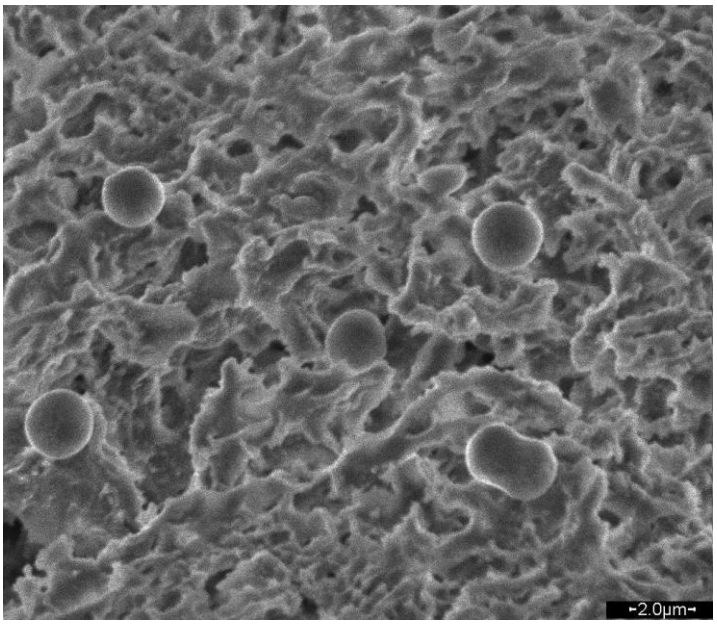

Figure 2-4: ESEM images showing wild-type cells (a), and M55 cells (b), encapsulated in a TEOS gel containing 10% wt. glycerol in the precursor sol. Both gels contain $5x10^9$ cells/mL.

2.4.2 - Cell Activity and H_2 Production Studies

Four representative gel compositions, in addition to controls in liquid media, were selected for quantitative analysis of H_2 production: gels of pure TEOS; TEOS with 10% wt. PEG 400; a composite blend of TEOS containing 10% wt. MTES; and the same blend with 10% wt. PEG. All gels were prepared in a hydrolysis ratio of 20:1 with nitric acid and potassium hydroxide as catalysts. Gels were prepared in 500 μL volumes within 2 mL GC vials, allowed to gel within a sterile laminar hood, and then degassed before being sealed and placed in the light cycling incubator as described.

H_2 content in the headspace was analyzed by GC at intervals of 16, 40 and 80 hours. The light cycle regime of 2 minutes on/18 minutes off was selected based on preliminary data (not shown) which allowed both detectable H_2 production, minimal production of oxygen, and enough time in the dark to consume that oxygen. The light regime was held constant for this study to avoid complex effects on efficiency through alterations to cell metabolism and the distribution between photofermentative (dark) and direct photobiological (light) H_2 production. After 40 hours of light cycling in the first round of the assay, M55 cells in pure TEOS produced a headspace concentration of approximately 0.29 mM H_2. This amount of H_2 produced over that time interval at that light intensity gives an efficiency of H_2 production from incident photons of approximately 1%, in line with the highest values previously reported for photobiological hydrogen production [38]. This efficiency estimate only considers the measured H_2 retained in the GC vial; no allowance for H_2 uptake by the reversible hydrogenase enzyme was included. Also, it is possible that some H_2 may have been lost from the vials by diffusion through the septum cap. At 80 hours, the vials were removed from the incubator, opened in a nitrogen atmosphere to completely degas again, and then placed back in the incubator and sampled again at 16, 40, and 80 hours. This was done to evaluate if,

after approximately 5 days, the encapsulated cells would remain active within the gel and continue to produce H_2. Figure 2-5 illustrates results from this assay, including 40 and 80 hours from the first cycle and 40 hours from the second cycle. Under the conditions of this assay, by 80 hours on the second cycle, one week after initial encapsulation, all cells of both types, in media and gel, had senesced and H_2 production was no longer detectable (data not shown). The cause for the loss in activity is not known, but since this was observed for all samples, including cells in gel as well as cells in media, it may be due to nutrient depletion in the small volume of media included in each GC vial or some other factor associated with this format and the small geometry, such as limitations in gas exchange.

Figure 2-5 (a)

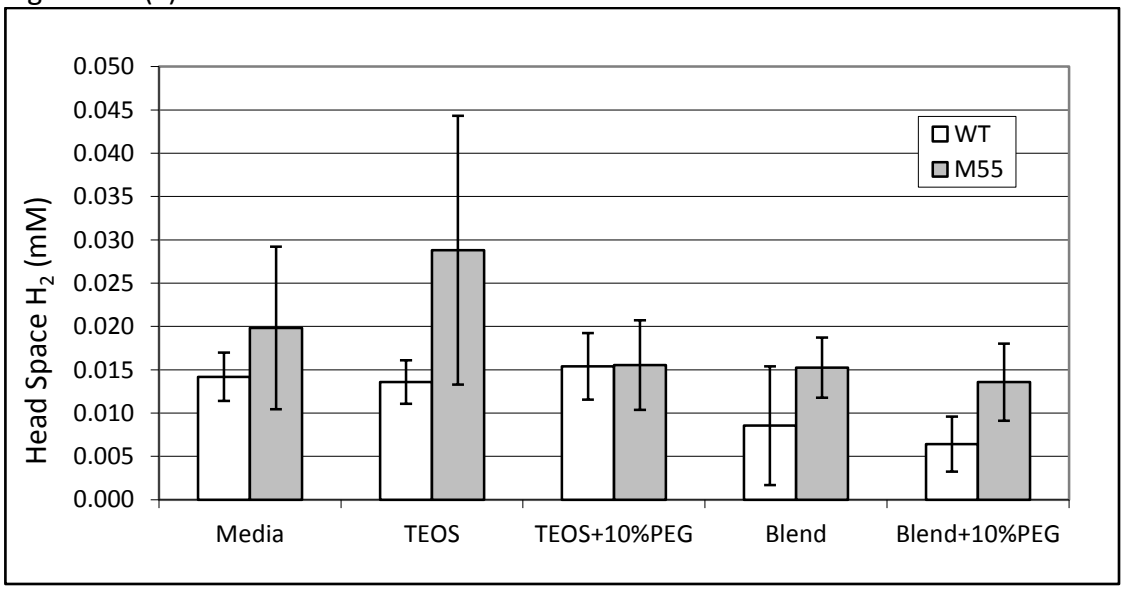

Figure 2-5 (b)

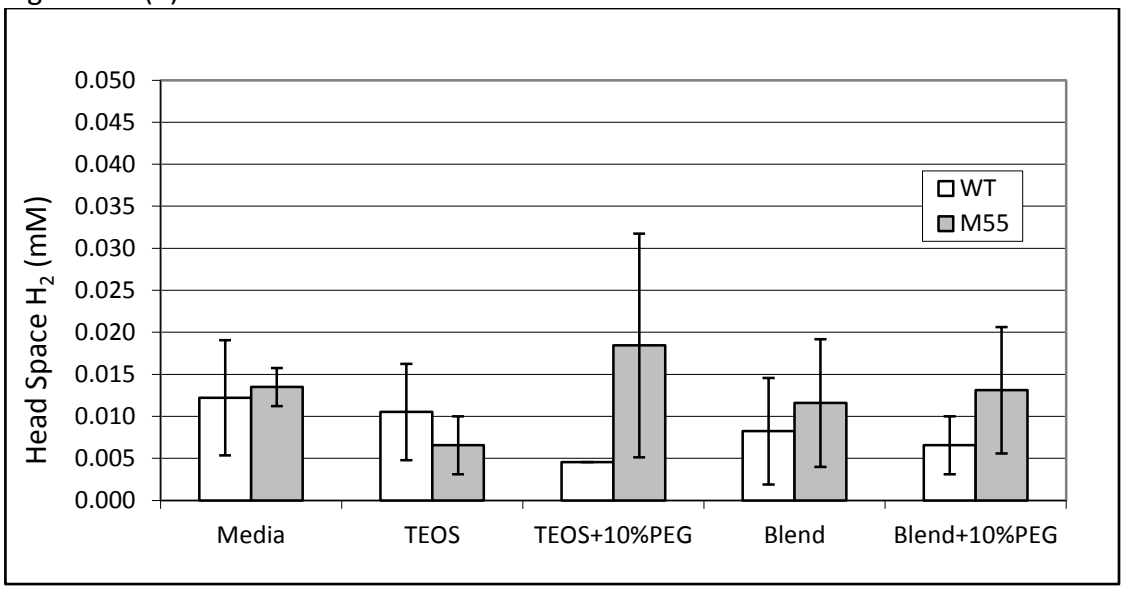

Figure 2-5 (c)

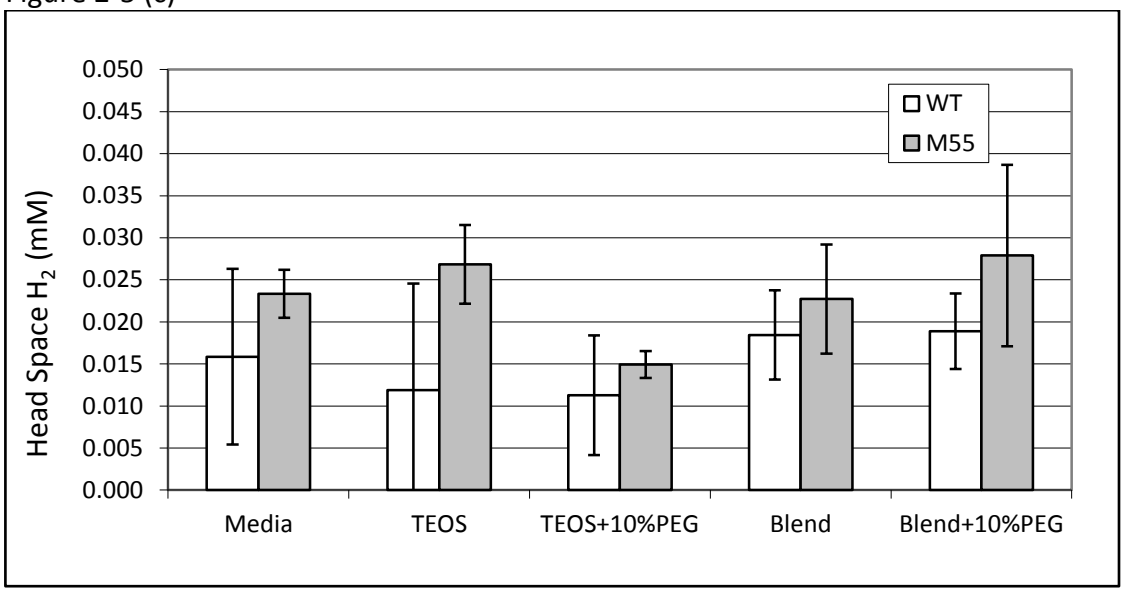

Figure 2-5: GC vial test results, showing initial incubation at 40 hours (a), initial incubation at 80 hours (b), and secondary incubation at 40 hours (c), which includes the same samples degassed in nitrogen atmosphere for 4 hours and returned to the incubator. Hydrogen production in encapsulated cultures was initially comparable to

similar cultures in media, and showed relative improvement in hydrogen production as time increased as compared to cells in media. All samples include 0.5 mL of media or gel in a 2 mL GC vial with a cell concentration of 10^{10} cells/mL. All gels were prepared with nitric acid and potassium hydroxide as catalysts. Samples were analyzed in triplicate and error bars represent one standard deviation.

H_2 production, over the time intervals examined, was consistently comparable between suspended and encapsulated cells (Figure 2-5). Encapsulated cells and suspended cells had similar capacities to produce H_2 under the conditions of this study, but vials with suspended cells contained substantially more CO_2 in the head space than vials with encapsulated cells (Figure 2-6). The optimized media contained bicarbonate, which contributed CO_2 to the headspace after the vials were sealed. However, the vials with gel contained 25% less bicarbonate (375 μL of media plus 125 μL of sol as compared to 500 μL of media), yet typically had less than half as much CO_2 in the headspace, suggesting possible differences in metabolic activity between encapsulated cells and those suspended in nutrient media.

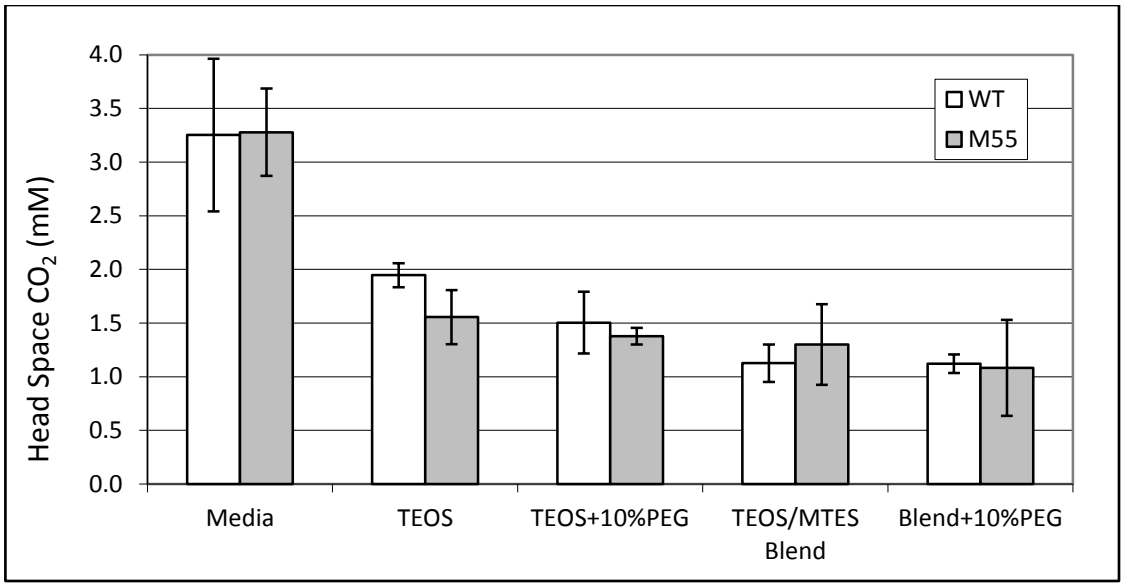

Figure 2-6: Carbon dioxide concentrations in the head space after 40 hours in the second cycle, corresponding to Figure 2-5(c). All samples include 0.5 mL of media or gel in a 2 mL GC vial with a cell concentration of 10^{10} cells/mL. All gels were prepared with nitric acid and potassium hydroxide as catalysts. Samples were analyzed in triplicate and error bars represent one standard deviation.

The silica sol-gel matrix offers a biocompatible environment that provides mechanical and chemical stability, and the rigidity of the matrix physically restricts growth. The ESEM images (Figure 2-4) show cells that appear to be in the process of dividing, but we cannot know whether cell division was initiated before or after encapsulation. The ability of sol-gel to restrict growth has been cited as both a liability and an asset, depending on the type of cell and the application. Long-term viability of encapsulated cells is a significant challenge [39], but the growth of cells within the gel, even at a reduced rate, could help overcome that challenge. Studies

are ongoing to examine how encapsulation affects growth and long term viability of the cells.

2.4.3 - Additives

Glycerol and PEG 400 were used as additives in this study because of their previously demonstrated utility. Glycerol has been used, in concentrations as high as 20% [40], by numerous investigators for its ability to increase the biocompatibility of silica sol-gel matrices by reducing osmotic stress and improving the interaction between the pore surfaces of the gel and the immobilized cells [26, 30, 41, 42]. PEG may also provide some osmotic protection to encapsulated cells but is generally used more for its ability to stabilize sols in the absence of an alcohol solvent [37, 43]. Both additives can act to increase pore size by reducing capillary forces that develop during gelation, thereby reducing pore collapse as the matrix forms and ages. High surface tension produces high capillary forces, but both additives serve as surfactants to differing degrees which can reduce surface tension and yield larger pores [44].

Figures 2-2 and 2-7 illustrate screening assay results comparing glycerol, PEG, and a mixture of PEG and glycerol against additive-free controls. Contrary to expectations, glycerol tended to have negligible effect on *wt* cells and actually hindered H_2 production in M55 cells. The effects of PEG were modest, but gels with 10% PEG generally performed better than other formulations in this format. In other assays, PEG concentrations varying from 6 to 14% were compared and showed minimal differences (Table 2-2). *Synechocystis* sp. PCC 6803 is a relatively robust cell, so beneficial effects of additives may result more from structural changes in the gel rather than from osmotic protection and reduction of stress. The effects of additives on gel structure, beyond these observations for improved H_2 production, merit further evaluation.

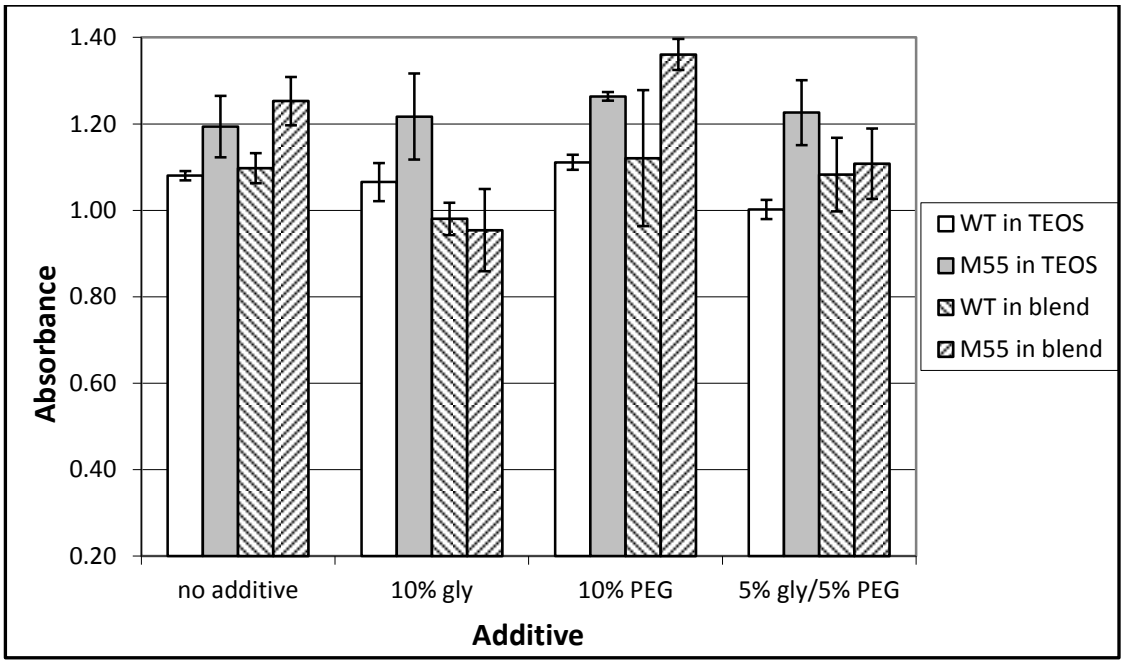

Figure 2-7: A screening assay comparison of gel formulations of pure TEOS and the 10% MTES/TEOS blend with different additives. All additive compositions are as a weight percent of the initial sol. Samples were analyzed in triplicate and error bars indicate one standard deviation. All gels contain 10^{10} cells/mL.

2.5 - Discussion

The activity of encapsulated cells was confirmed through the production of H_2 gas detected by the high-throughput screening assay and GC analyses. Activity varied significantly depending on the composition of the gel matrix. Cells encapsulated in TEOS-derived gels performed comparably to cells in liquid media and better than cells encapsulated in TMOS, presumably due to the presence of methanol generated by the hydrolysis of TMOS. However, the hydrolysis of both compounds produces silicic acid, $Si(OH)_4$, which should behave similarly upon gelation if the alcohol solvent is removed prior to encapsulation. If the solvent is not removed, its presence can

influence the kinetics between condensation and hydrolysis during gelation and aging, producing gels of different structures. Since PCC 6803 can tolerate low levels of ethanol, TEOS is the preferred precursor for this application. Complete removal of alcohol prior to encapsulation is possible, but the stability of the sol may be reduced.

The use of MTES represents initial efforts to explore the use of organically modified silanes (ORMOSIL's) for encapsulating PCC 6803. The presence of a covalently tethered functional group, in this case a methyl group, can alter the structure of the matrix by occupying one of four bonds on a given silicon atom, thereby preventing hydrolysis at that site and reducing subsequent cross linking. The presence of the group can also alter hydrolysis and condensation reactions on the other three bond sites through electrostatic interactions and steric hindrance. In addition to effecting the gel structure directly, these groups can also have electrostatic effects that can alter the interaction between the matrix and both the pore fluid and the encapsulated cells. Predicting the exact effect of a given ORMOSIL on the gel structure is not possible from first principles. Therefore, exploring their use for a given application must be iterative. MTES was selected because it is the simplest ORMOSIL, it is fully miscible in TEOS, it also produces ethanol upon hydrolysis, and it allows for the controlled introduction of hydrophobic methyl groups into a matrix that is generally hydrophilic.

Phenotypic differences between *wt* and M55 suggested they would respond to encapsulation differently. When the cells are harvested, *wt* cells tend to adhere to each other after centrifugation and are relatively difficult to resuspend, perhaps due to extracellular polysaccharides. In contrast, M55 cells resuspend much more easily, indicating different surface features in the two types of cells. The tendency of *wt* cells to aggregate suggests that they have more hydrophobic surface moieties relative to the M55, the surface chemistry of which is likely more hydrophilic. The gel matrix

itself is hydrophilic, containing residual hydroxyl groups on pore surfaces. In initial investigations, the ESEM images suggest that the gel matrix may form tighter pockets around M55 cells, whereas *wt* cells may have a stronger repulsive interaction with the gel matrix, causing larger pore features around each individual cell. These observations, which are being more fully explored in ongoing studies, lend credence to the suggestion that gels should be formulated to achieve beneficial interactions with each specific type of cell. Figure 2-4 illustrates how the same formulation appeared to act differently with the two strains of the same microbial species.

M55 cells responded well to the TEOS/MTES blend compared to pure TEOS gels, whereas *wt* cells seem to show negligible difference between these two types of gels. The effect appears to be further enhanced by the presence of PEG, as shown in Figures 2-2 and 2-7. This evidence that a more hydrophobic matrix has a favorable interaction with relatively hydrophilic M55 cells suggests that a larger pocket in the matrix surrounding the cell is more advantageous for H_2 production. However, the GC time series data in Figure 2-5 do not consistently support this hypothesis. These data were collected at different time intervals, but the screening assay data were produced after the same consistent time interval of 5 ½ days. Cellular activity and hydrogen production will vary over these time intervals and the apparatus for each method also detects H_2 differently. In the screening assay, H_2 leaves the headspace and reacts with a catalyst and dye in a separate plate, providing a qualitative indication of H_2 production. With GC analyses, H_2 is accumulated in the headspace of the vial, allowing for both uptake and diffusion of H_2 through the vial septum cap. These differences make comparisons between the two methods difficult. Also, ESEM imaging has not yet been performed on a full series of gel compositions, with and without PEG for a comparison of gel structure and with both cell types. Further

investigation is merited to better describe the effects of matrix composition with encapsulating pocket size and resulting cellular activity.

Differences in H_2 production and CO_2 concentrations between suspended and encapsulated cells suggest differences in cellular metabolism between the two environments. As Figure 2-5 shows, H_2 production is generally comparable across all environments (within error bars). However, as shown in Figure 2-6, CO_2 concentrations are significantly lower for all encapsulated cultures, consistently approximately half or less than the concentrations observed with cultures in media. The gel samples contained 25% less media and therefore 25% less carbonate, yet there is roughly a 50% drop in CO_2 concentration, more than would be expected from differences in equilibrium (data not shown). Because the light cycling regime included 18 minutes of dark followed by 2 minutes of light exposure, this observation could suggest that the suspended cells may have had a higher respiration rate than encapsulated cells. Taken together, comparable hydrogen production with reduced respiration would support our hypothesis that a larger percentage of net metabolism in encapsulated cells is directed toward hydrogen production. However, very little is known about the genomic, proteomic, or overall metabolic response of these cells to encapsulation and additional work is required to elucidate these changes.

2.6 - Conclusion

Successful encapsulation of viable cells of *Synechocystis* sp. PCC 6803 in silica sol-gel was demonstrated, and H_2 production quantities from *wt* and M55 cells were comparable to those from cultures in optimized media for at least 5 days. The encapsulation process was evaluated iteratively by initially comparing multiple formulations through a high-throughput screening assay for H_2 production. A smaller range of formulations was then defined for analysis of activity through H_2 production as measured by GC. This research provides a proof of concept demonstrating the

ability to achieve measurable H_2 production from sol-gel encapsulated cells, but the process is currently far from optimized. For example, the possibility of composite matrices containing other organically modified silicates (ORMOSIL's) besides MTES or some proportion of organic polymers, such as alginate or gelatin, among others, has not yet been explored. Longevity of encapsulated cultures has also not yet been fully studied. Additional studies are underway to analyze H_2 production more precisely to determine the effects of encapsulation on H_2 production rates over shorter time scales. On-going research is also seeking to characterize in more detail the interactions between the gel matrix and the encapsulated cells and the specific responses of those cells to encapsulation. An improved understanding of these interactions will foster more favorable encapsulation and improved a priori design of these biocomposite materials, enhancing performance and longevity from encapsulated cultures.

Acknowledgements

The authors would like to thank Elizabeth Burrows, Dr. Hatem Mohamed, Jed Eberly, Dr. Sunhwa Park, and Dr. Paul Schrader for laboratory assistance; John Donovan and Lucas Winiarski of University of Oregon for assistance in ESEM and helpful discussion on sol-gel processing; and Chris Dandeneau of Oregon State University for helpful discussion on sol-gel processing. This research was supported by a graduate student fellowship provided by the Department of Biological & Ecological Engineering, Oregon State University, and by a grant from the Air Force Office of Scientific Research, Proposal No. 08NL208.

Chapter 2 References

1 Appel J, Phunpruch S, Steinmüller K, Schulz R. The Bidirectional Hydrogenase of Synechocystis sp. PCC 6803 Works as an Electron Valve during Photosynthesis. Arch Microbiol. 2000; 173: 333-338.

2 Cournac L, Mus F, Bernard L, Guedeney G, Vignais P, Peltier G. Limiting Steps of Hydrogen Production in Chlamydomonas reinhartii and Synechocystis sp. PCC 6803 as Analysed by Light Induced Gas-Exchange Transients. Int J Hydrogen Energy 2002; 27: 1229-1237.

3 Cournac L, Guedeney Gv, Peltier G, Vignais PM. Sustained Photoevolution of Molecular Hydrogen in a Mutant of Synechocystis sp. Strain PCC 6803 Deficient in the Type 1 NADPH-Dehydrogenase Complex. J Bacteriol 2004; 186(6): 1737-1746.

4 Lindblad P. The Potential of Using Cyanobacteria as Producers of Molecular Hydrogen. In: J. Miyake, editor. Biohydrogen III. Elsevier, 2004. p. 75 - 82.

5 Antal TK, Oliveira P, Lindblad P. The bidirectional hydrogenase in the cyanobacterium Synechocystis sp. strain PCC 6803. Int J Hydrogen Energy 2006; 31(11): 1439-1444.

6 Kotay SM, Das D. Biohydrogen as a renewable energy resource--Prospects and potentials. Int J Hydrogen Energy 2008; 33(1): 258-263.

7 Carturan G, Campostrini R, Dire S, Scardi V, Alteriis ED. Inorganic Gels for Immobilization of Biocatalysts: Inclusion of Invertase-Active Whole Cells of Yeast (Saccharomyces cerevisiae) into thin Layers of SiO_2 Gel Deposited on Glass Sheets. J Mol Catal 1989; 57: L13 - L16.

8 Ellerby LM, Nashida CR, Nashida F, Yamanaka SA, Dunn B, Valentine JS, et al. Encapsulation of Proteins in Transparent Porous Silicate Glasses Prepared by the Sol-Gel Method. Science 1992; 255(5048): 1113 - 1115.

9 Kriegl JM, Forster FK, Nienhaus GU. Charge Recombination and Protein Dynamics in Bacterial Photosynthetic Reaction Centers Entrapped in a Sol-Gel Matrix. Biophys J 2003; 85: 1851 - 1870.

10 Pierre AC. The Sol-Gel Encapsulation of Enzymes. Biocatalysis and Biotransformation 2004; 22(3): 145 - 170.

11 Frenkel-Mullerad H, Avnir D. Sol-Gel Materials as Efficient Enzyme Protectors: Preserving the Activity of Phosphatases Under Extreme pH Conditions. J Am Chem Soc 2005; 127: 8077 - 8081.

12 Taylor A, Finnie KS, Bartlett JR, Holden PJ. Encapsulation of Viable Aerobic Microorganisms in Silica Gels. J Sol Gel Sci Technol 2004; 32: 223-228.

13 Kuncova G, Podrazky O. Monitoring of the Viability of Cells Immobilized by Sol-Gel Process. J Sol Gel Sci Technol 2004; 31: 335 - 342.

14 Nassif N, Roux Cc, Coradin T, Rager M-N, Bouvet OMM, Livage J. A Sol-gel Matrix to Preserve the Viability of Encapsulated Bacteria. J Mater Chem 2003; 13: 203-208.

15 Szilva J, Kuncova G, Patzak M, Dostalek P. The Application of a Sol-Gel Technique to Preparation of a Heavy Metal Biosorbent from Yeast Cells. J Sol Gel Sci Technol 1998; 13: 289 - 294.

16 Desimone MF, Degrossi J, D'Aquino M, Diaz LE. Ethanol tolerance in free and sol-gel immobilised Saccharomyces cerevisiae. Biotechnol Lett 2002; 24(19): 1557-1559.

17 Pressi G, Toso RD, Monte RD. Production of Enzymes by Plant Cells Immobilized by Sol-Gel Silica. J Sol Gel Sci Technol 2003; 26: 1189 - 1193.

18 Carturan G, Monte RD, Pressi G, Secondin S, Verza P. Production of Valuable Drugs from Plant Cells Immobilized by Hybrid Sol-Gel SiO_2. J Sol Gel Sci Technol 1998; 13: 273 - 276.

19 Boninsegna S, Bosetti P, Carturan G, Dellagiacoma G, Monte RD, Rossi M. Encapsulation of Individual Pancreatic Islets by Sol-Gel SiO_2: A Novel Procedure for Perspective Cellular Grafts. J Biotechnol 2003; 100: 277 - 286.

20 Rooke JC, Alexander L, Su B-L. Targeting photobioreactors: Immobilisation of cyanobacteria within porous silica gel using biocompatible methods. J Mater Chem 2008; 18: 9.

21 Campostrini R, Carturan G, Caniato R, Piovan A, Filippini R, Innocenti G, et al. Immobilization of plant cells in hybrid sol-gel materials. J Sol Gel Sci Technol 1996; 7(1): 87-97.

22 Vignais PM, Magnin JP, Willison JC. Increasing biohydrogen production by metabolic engineering. Int J Hydrogen Energy 2006; 31: 1478 - 1483.

23 Antal TK, Lindblad P. Production of H_2 by sulphur-deprived cells of the unicellular cyanobacteria Gloeocapsa alpicola and Synechocystis sp. PCC 6803 during dark incubation with methane or at various extracellular pH. J Appl Microbiol 2005; 98(1): 114-120.

24 Burrows EH, Chaplen FWR, Ely RL. Optimization of media nutrient composition for increased photofermentative hydrogen production by Synechocystis sp. PCC 6803. Int J Hydrogen Energy 2008; 33(21): 6092-6099.

25 Brinker CJ, & G. W. Scherer. Sol-Gel Science. San Diego, CA: Academic Press, Inc., 1990.

26 Avnir D, Coradin T, Lev O, Livage J. Recent Bio-applications of Sol-gel Materials. J Mater Chem 2006; 16: 1013 - 1030.

27 Bottcher H, Soltmann U, Mertig M, Pompe W. Biocers: Ceramics with Incorporated Microorganisms for Biocatalytic, Biosorptive and Functional Materials Development. J Mater Chem 2004; 14: 2176 - 2188.

28 Livage J, Coradin T. Living Cells in Oxide Glasses. Reviews in Mineralogy and Geochemistry 2006; 64(1): 315-332.

29 Carturan G, Toso RD, Boninsegna S, Monte RD. Encapsulation of Functional Cells by Sol-Gel Silica: Actual Progress and Perpective for Cell Therapy. J Mater Chem 2004; 14: 2087 - 2098.

30 Nguyen-Ngoc H, Tran-Minh C. Sol-gel process for vegetal cell encapsulation. Materials Science and Engineering: C 2007a; 27(4): 607-611.

31 Nguyen-Ngoc H, Tran-Minh C. Fluorescent biosensor using whole cells in an inorganic translucent matrix. Anal Chim Acta 2007b; 583(1): 161-165.

32 Rooke JC, Leonard A, Su B-L. Targeting photobioreactors: Immobilisation of cyanobacteria within porous silica gel using biocompatible methods. J Mater Chem 2008; 18: 1333-1341.

33 Tsygankov AA. Hydrogen Production by Suspension and Immobilized Cultures of Phototrophic Microorganisms. Technological Aspects. In: J. Miyake, editor. Biohydrogen III. Elsevier, 2004. p. 57 - 71.

34 Laurinavichene TV, Fedorov AS, Ghirardi ML, Seibert M, Tsygankov AA. Demonstration of sustained hydrogen photoproduction by immobilized, sulfur-deprived Chlamydomonas reinhardtii cells. Int J Hydrogen Energy 2006; 31(5): 659-667.

35 Schrader PS, Burrows EH, Ely RL. High-Throughput Screening Assay for Biological Hydrogen Production. Anal Chem 2008; 80(11): 4014 - 4019.

36 Coiffier A, Coradin T, Roux C, Bouvet OMM, Livage J. Sol-Gel Encapsulation of Bacteria: a Comparison between Alkoxide and Aqueous Routes. J Mater Chem 2001; 11: 6.

37 Conroy J, Power ME, Martin J, Earp B, Hosticka B, Daitch CE, et al. Cells in Sol-Gels I: A Cytocompatible Route for the Production of Macroporous Silica Gels. J Sol Gel Sci Technol 2000; 18: 269-283.

38 Hankamer B, Lehr F, Rupprecht J, Mussgnug JH, Posten C, Kruse O. Photosynthetic biomass and H_2 production by green algae: from bioengineering to bioreactor scale-up. Physiol Plant 2007; 131(1): 10-21.

39 Nassif N, Roux C, Coradin T, Bouvet OMM, Livage J. Bacteria Quorum Sensing in Silica Matrices. J Mater Chem 2004; 14: 2264 - 2268.

40 Desimone MF, De Marzi M, Copello G, Fernandez M, Malchiodi E, Diaz L. Efficient preservation in a silicon oxide matrix of Escherichia coli, producer of recombinant proteins. Appl Microbiol Biotechnol 2005; 68(6): 747-752.

41 Gadre SY, Gouma PI. Biodoped Ceramics: Synthesis, Properties, and Applications. J Am Ceram Soc 2006; 89(10): 2987-3002.

42 Ferrer ML, Garcia-Carvajal ZY, Yuste L, Rojo F, Monte Fd. Bacteria Viability in Sol-Gel Materials Revisited: Cryo-SEM as a Suitable Tool to Study the Structural Integrity of Encapsulated Bacteria. Chem Mater 2006; 18: 1458 - 1463.

43 Ferrer ML, Yuste L, Rojo F, Monte Fd. Biocompatible Sol-gel Route for Encapsulation of Living Bacteria in Organically Modified Silica Matrices. Chem Mater 2003; 15(19): 3614-3618.

44 Deshpande R, Hua D, Smith DM, Brinker CJ. Pore structure evolution in silica gel during aging/drying. III. Effects of surface tension. J Non-Cryst Solids 1992; 144: 32 - 44.

CHAPTER 3 - EVALUATION OF ENCAPSULATION STRESS AND THE EFFECT OF ADDITIVES ON VIABILITY AND PHOTOSYNTHETIC ACTIVITY OF *SYNECHOCYSTIS* SP. PCC 6803 ENCAPSULATED IN SILICA GEL

David J. Dickson, Roger L. Ely

Applied Microbiology and Biotechnology

Springer

233 Spring Street

New York, NY 10013

(manuscript to be submitted)

3.1 - Abstract

Stresses imposed on the cyanobacterium *Synechocystis* sp. PCC 6803 by various compounds present during silica sol-gel encapsulation, including salt (NaCl), ethanol (EtOH), glycerol, and polyethylene glycol formula weight 200 (PEG), were investigated. Viability of encapsulated cells and photosynthetic activity of cells stressed by immediate (2 minute) and 24-hour exposure to the four stress-inducing compounds were monitored by confocal microscopy and chlorophyll *a* fluorescence, respectively. Cells of *Synechocystis* sp. PCC 6803 readily survive encapsulation in both alkoxide-derived gels and in gels from aqueous precursors, and can remain active at least six weeks with slight degradation in PSII efficiency. Post-encapsulation survival was also improved in gels containing no additive when compared to gels containing PEG or glycerol. Glycerol was shown to have a detrimental effect on *Synechocystis* sp. PCC 6803 through its disruption of excitation transfer between the phycobilisomes and photosystems, reducing ϕPSII and F_v'/F_m' by as much as 75%. PEG was similarly deleterious, dramatically reducing the ability to carry out a state transition and adequately manage excitation energy distribution. EtOH stress also hindered state transitions, although less severely than PEG, and the cells were able to recover nearly all photosynthetic efficiency within 24 hours after an initial drop. Finally, *Synechocystis* sp. PCC 6803 was shown to recover well from salt stress.

Keywords: Silica sol-gel encapsulation, osmotic stress, salt stress, fluorescence, *Synechocystis* sp. PCC 6803, glycerol, polyethylene glycol, ethanol stress

3.2 - Introduction

The cyanobacterium *Synechocystis* sp. PCC 6803 has been extensively studied as a model organism for photosynthesis and more recently for photobiological hydrogen production [1-8]. Hydrogen is a compelling option as an alternative to carbon-based fossil fuels, if a cost effective and environmentally responsible means of production can be achieved. *Synechocystis* sp. PCC 6803 contains a reversible [Ni-Fe] hydrogenase which, under certain conditions, can produce molecular hydrogen through energy derived from light absorption and photolysis originating in the activity of photosystem II (PSII).

However, substantial and sustained hydrogen production rates at high efficiency remain elusive. One of the underlying limitations to hydrogen production in this organism, aside from oxygen sensitivity of the hydrogenase, is reductant availability to the enzyme. In *Synechocystis* sp. PCC 6803, electrons for hydrogen production are provided by NADPH [3, 9], which is required in the light by the Calvin Cycle to fix atmospheric carbon, and in the dark for cellular maintenance and repair. Metabolic engineering has successfully been applied to increase glycogen accumulation in the light through nutrient deprivation, resulting in increased fermentative hydrogen production in the dark [4, 6]. Electron transport can also be manipulated to direct more NADPH flux toward the hydrogenase through the selective use of inhibitors [10]. Ultimately, though, many general metabolic activities, including biomass production and maintenance, are in competition with hydrogen production. Ideally, cells could be stabilized in an environment where growth would be minimal and the energy devoted to maintenance could be minimized, maximizing reductant availability for hydrogen production.

Encapsulation of viable cells within an inorganic silica matrix may help to direct increased reductant flux toward the production of secondary metabolites, like hydrogen, by restricting cell growth and forcing cells into an altered, steady-state

metabolism. Successful encapsulation of a variety of organisms has been demonstrated, including yeast [11], bacteria [12-16], cyanobacteria [7, 17], algae [18-20], plant cells [21-23], and mammalian cells [24-26]. Improved stability compared to liquid cultures over the course of many weeks to months has been observed [14], as has enhanced production of secondary metabolites [22]. Many researchers believe the technique holds great potential, although means for achieving long term viability and activity of encapsulated cells have not been adequately studied.

Silica sol-gel is attractive for encapsulation because it involves mild, biocompatible conditions. The sol can be pre-hydrolyzed under acidic conditions, before the addition of biological components, and gelation can be catalyzed at near-neutral, physiologic pH. Compared to organic polymers, silica is inert and robust against biological attack. It can also provide mechanical stability, preventing swelling and degradation. The material is highly porous, allowing adequate diffusion of substrates, metabolites and waste products, while confining the encapsulated cells and keeping contaminant cells out. Finally, it is highly transparent and thus suitable for encapsulating phototrophs. Many excellent reviews of biological encapsulation using silica sol-gel are available [27-34].

Nearly any bacterial cells that can be readily cultured are likely amenable to silica sol-gel encapsulation [29]. Yet the conditions for optimal activity and viability within the gel are not identical for all types of cells, therefore the gel should be tailored to best suit the cell of interest. Different species have different metabolic requirements and vary in their sensitivity and vulnerability to stresses inflicted during encapsulation. However, an optimal encapsulation protocol and gel environment cannot be designed *a priori*; adequate predictive power for this application is simply not available. As a result, gels are often iteratively evaluated with different preparation protocols to determine the best formulations and methods. Changes in formulations and methods, as well as the use of additives or organically modified

siloxanes (ORMOSILs), can change the physical and chemical properties of the gel, with profound effects on encapsulated cells. These effects must be evaluated by monitoring the metabolic activity of encapsulated cells.

In a previous investigation, successful encapsulation of *Synechocystis* sp. PCC 6803 was demonstrated and hydrogen production from encapsulated cells was confirmed [7]. Glycerol and polyethylene glycol (PEG) were used as additives to improve biocompatibility, as monitored through hydrogen production, but their effects were not explored in depth. Glycerol was chosen as an additive because of its well documented use as an osmotic protectant for cells encapsulated within silica gel [12, 18, 35-37]. In one study, improved production of astaxanthin from encapsulated cultures of the microalgae *Haematococcus pluvialis* was observed in gels containing glycerol compared with gels lacking the additive [18]. However, in the case of cyanobacteria, it is also known that glycerol can have a significant impact on photosynthetic processes. Specifically, it has been shown that glycerol can disrupt excitation transfer between the phycobilisomes (PBS) and photosystems by decoupling the PBS [38-40], although the effect is reported to be minimal at low glycerol concentrations. It remains to be determined if the benefits of adding glycerol outweigh its negative effects on *Synechocystis* sp. PCC 6803.

PEG also provides potentially beneficial and detrimental effects to encapsulated cyanobacteria. PEG has been shown to increase gel pore size while decreasing overall pore volume and surface area, which serves to improve stability of the gel and to facilitate diffusion [41]. However, PEG can also create osmotic stress, causing cytoplasmic water to be expelled from encapsulated cells. Indeed, PEG has been used to induce osmotic stress in other cyanobacteria with effects similar to those of other common osmolytes, like sorbitol, sucrose, and mannitol [42, 43]. Very specific responses to osmotic stress have evolved in cyanobacteria, although the mechanisms and signaling pathways for induction are not fully understood. In one

investigation, a transmembrane protein called Tic22, whose function has not yet been identified, was up-regulated in *Synechocystis* sp. PCC 6803 under osmotic stress [44], and a dehydrin-like protein induced under osmotic stress has also been identified in *Anabaena* 7120 [42]. While heterotrophic bacteria generally show an identical response to ionic and osmotic stress, cyanobacteria have differentiated responses [43, 45], complicating the encapsulation process.

In *Synechocystis* sp. PCC 6803, osmotic stress can adversely impact the photosystems and excitation transfer. For example, it has been shown that osmotic stress induced by sorbitol is more detrimental than ionic stress induced by NaCl and causes a specific decrease in D1 expression (*psbA*), a critical protein for PSII function [46]. Hyper-osmotic stress has also been shown to reduce the amplitude of fluorescence in *Synechocystis* sp. PCC 6803, although the mechanism remains unclear [47]. One possible explanation is a redistribution of excitation as the PBS direct more energy to PSI under hyper-osmotic conditions [48]. Although PEG may prove beneficial in altering the gel structure, it is unclear whether these benefits outweigh the detrimental effects potentially inflicted upon photosynthetic processes. Any interference with excitation transfer from the PBS to the photosystems will have profound effects on the organism's ability to manage excitation energy and adapt to changes in the light environment and metabolic demands.

Glycerol may also help to protect encapsulated cells from ionic and alcohol stresses. Ionic stress may occur after encapsulation procedures using aqueous precursors of sodium silicate and can detrimentally effect photosynthetic activity. Specifically, salt stress has been shown to slow protein synthesis globally, including the *psbA* gene encoding the D1 subunit of PSII. This renders PSII vulnerable to irreversible photodamage since D1 cannot be repaired, it must be synthesized de novo [49]. However, *Synechocystis* sp. PCC 6803 is moderately halotolerant, able to survive under salt concentrations up to 1.2M [50]. The organism contains a

constitutively expressed gene, *ggpS*, under posttranslational control, which is responsible for the synthesis of glucosylglycerol (GG), an osmotic protectant that is synthesized during salt stress [50-52]. The organism also increases cyclic electron flow around PSI in response to salt stress [53-56]. An increase in PSI activity has been observed with a corresponding decrease in PSII activity, which also suggests a response from the PBS affecting excitation transfer to the photosystems. This has significant implications for the health and long term viability of encapsulated cells.

Ethanol (EtOH), which can be present in gels created by hydrolysis of ethoxysilane precursors, can also pose a stress to encapsulated cultures. EtOH is not produced by *Synechocystis* sp. PCC 6803 and is rarely encountered in its natural environment. Therefore, the organism is expected to be vulnerable to EtOH stress through attacks on membranes and soluble chromophores, like chlorophyll. While EtOH stress is not well explored in *Synechocystis* sp. PCC 6803, and there is even some evidence the organism can utilize limited amounts of EtOH as a carbon source [57], it is expected that EtOH will generally be detrimental. Improved removal of EtOH prior to encapsulation should only serve to improve long term viability. However, sol stability decreases with the loss of the EtOH co-solvent, so it is worth exploring how tolerant *Synechocystis* sp. PCC 6803 may be to EtOH stress and how resilient its photosynthetic activity remains in alkoxide-derived gels.

In an effort to understand the various effects of encapsulation and the effects of specific compounds used in or resulting from the encapsulation process, including glycerol, PEG, NaCl, and EtOH, the current study examined the viability of encapsulated cells by confocal microscopy and photosynthetic activity through chlorophyll fluorescence. Gels prepared from alkoxide and aqueous precursors were compared, and activity was monitored with fluorescence over the course of six weeks. Cells in liquid culture were also acutely and chronically exposed to these stress compounds and chlorophyll fluorescence was used to probe cellular responses

in terms of photosynthetic efficiency. A long term goal is to design encapsulation protocols that minimize stresses inflicted upon encapsulated cells, enabling prolonged viability and activity, and ultimately to provide a platform for improved photobiological hydrogen production.

3.3 - Materials & Methods

3.3.1 - Cell Culturing

All cells of wild-type (*wt*) *Synechocystis* sp. PCC 6803 were grown in 125 mL Erlenmeyer flasks containing 50 mL of cell culture. All cells were grown in BG-11 media at a pH of 7.8, buffered with 35 mM of HEPES organic buffer. Flasks were placed on an orbital shaker table in a constant temperature room held at 30°C, under constant illumination of approximately 70 $\mu Em^{-2}s^{-1}$. Laboratory grade sodium chloride was used as received (Sigma Aldrich, St. Louis, MO) to prepare a 5.0 M stock solution, which was autoclaved. Sterile 100% glycerol and PEG200 were used as provided from the manufacturer (Alfa Aesar, Ward Hill, MA). Prior to encapsulation, cells were harvested at late log growth phase, concentrated via centrifugation, and resuspended in fresh BG-11 media. Cells were concentrated by varying amounts, depending on experiment, generally two to five fold, from approximately $2x10^8$ to $5x10^8$ cells/mL, by resuspending in a reduced volume of media.

3.3.2 - Sol-Gel Preparation & Encapsulation

Silicon alkoxide sol precursors were prepared with tetraethoxysilane (TEOS)(Alfa Aesar, Ward Hill, MA), used as received. Sols were prepared by mixing deionized water, alkoxide precursor, and 1.0 M nitric acid in a molar ratio of 20:1:0.005, respectively. No supplemental ethanol or other alcohol was added as a mutual solvent. As a result, this mixture was initially phase separated due to the immiscibility of the alkoxide compound in water. The mixture was vigorously stirred on a heated magnetic stir-plate in an open Erlenmeyer flask at a temperature of

approximately 60°C for 90 minutes. This procedure promoted hydrolysis and the evaporation of EtOH as the hydrolysis reaction proceeded. The solution became homogeneous after approximately 30 minutes. Stirring was continued for another hour with the heat off to allow the solution to return to room temperature prior to encapsulation. The sol was sterile filtered through a 0.22 μm membrane prior to being used for encapsulation.

The aqueous sol was prepared by acid hydrolysis of a 6.3 M (40°-42°Bé) solution of sodium silicate (Fisher Scientific, Fair Lawn, NJ). In an Erlenmeyer flask, deionized water, sodium silicate solution, and 1.0 M HCl acid were combined in a molar ratio of 63:1:0.037, respectively. Amberlite™ IR-120 H ion exchange resin (Sigma Aldrich, St. Louis, MO) was also used, 0.40 g/mL of water, during hydrolysis to exchange protons for Na^+ ions. The solution was mixed for 2 hours at room temperature and then vacuum filtered through a 0.22 μm membrane filter.

To encapsulate, the sol precursor and buffered cell suspension were combined in a volumetric ratio of 4:1, suspension to sol, respectively, for alkoxide prepared gels, and 2.5:1.5 for gels from aqueous precursors. Gels from aqueous precursors also contained 50 mM NaCl, added to the cell suspension prior to encapsulation. This amount of salt helped catalyze gelation in this system and has been observed not to have a significant effect on the growth of *Synechocystis* sp. PCC 6803 (data not shown).

3.3.3 - Live/Dead Staining

Live/dead staining was performed with dyes from Molecular Probes (Eugene, OR). The “live” stain was SYTO 9™, a nucleic acid stain which penetrates *all* cells and fluoresces at 498 nm once bound with double stranded DNA. The “dead” stain is SYTOX orange™, also a nucleic acid stain, but one that can only penetrate cells with a compromised cell membrane. Presumably, cells with such a compromised membrane are dead or about to die, although some internal components, including proteins and

enzymes, may remain intact and active for some period of time after the cell is labeled as “dead.” Upon binding to DNA, SYTOX orange™ fluoresces at 570 nm. The normal Live/Dead kit contains propidium iodide as the “dead” stain, but this compound fluoresces at 617 nm, which begins to overlap with phycobilin and chlorophyll autofluorescence. Therefore, SYTOX orange™, an orange “dead” stain, was selected to replace propidium iodide. A Zeiss LSM510 META confocal microscope (Carl Zeiss MicroImaging, LLC, Thornwood, NY) was used to examine cell viability, and chlorophyll fluorescence was also examined by using a 650 nm filter in order to provide a second check on cell staining and activity. It should also be noted that for clarity, in all images shown, software manipulation was used to make Sytox orange™ appear red and chlorophyll fluorescence appear blue even though it was actually red.

3.3.4 - Chlorophyll Fluorescence

Chlorophyll fluorescence was monitored by a FMS-1 pulse modulated fluorometer (Hansatech Instruments Ltd., Norfolk, England). A chamber (DW2/2, Hansatech Instruments Ltd.) with four optical ports and water bath temperature control was used to examine liquid samples. Gel samples in 35 mm Petri dishes were held inside a closed polystyrene box with the fluorescence light source and detector incident upon the sample from above. Samples were dark acclimated for 3 minutes prior to all experimental trials. The fluorescence parameters used in this investigation include (calculated according to Campbell et al. [58, 59]):

- F_v/F_m = Maximum efficiency of PSII in a dark acclimated state;
- F_v'/F_m' = Maximum efficiency of PSII in a light acclimated state (i.e., antennae efficiency);
- ϕPSII = Actual efficiency of PSII in a light acclimated state;
- q_P = Coefficient of photochemical quenching; and
- q_N = Coefficient of nonphotochemical quenching.

Finally, in some fluorescence trials, DCMU, an inhibitor of the donor side of PSII, was used at a concentration of approximately 10 μM to measure maximum fluorescence, F_m, because cyanobacteria are generally very difficult to completely saturate with a 0.7 second pulse of bright actinic light [60].

3.4 - Results

3.4.1 - Confocal Microscopy

Confocal microscopy provided a semi-quantitative glimpse of cell survival after encapsulation. Fluorescence from chlorophyll and the phycobilins provided some interference in certain regions of the visible spectrum but this was accounted for by using dye-free controls to adjust filters and detector gains accordingly. In unstained controls, chlorophyll fluorescence was readily visible while cells killed by exposure to formaldehyde were clearly stained by SYTOX orange™, verifying the validity of this technique (data not shown).

Figure 3-1 shows confocal images for cells in a TEOS alkoxide gel (a), an identical gel with 10% glycerol (b), and an identical gel with 10% PEG (formula weight 200) (c). Cell survival immediately following encapsulation in the additive-free gel and the gel containing glycerol appeared high. However, PEG had a dramatic effect on cell survival, and also appeared to alter gel structure. Unlike the other two samples, cells appeared to be clustered, although it is unclear if this is because the PEG created larger pores in the gel within which the cells collected, or the PEG caused the cells to clump prior to and during gelation. Also readily apparent is the dramatic increase in Sytox orange™ signal. Despite the presence of chlorophyll fluorescence from cells that are also stained by Sytox orange™, these cells are likely becoming senescent.

Figure 3-1(a)

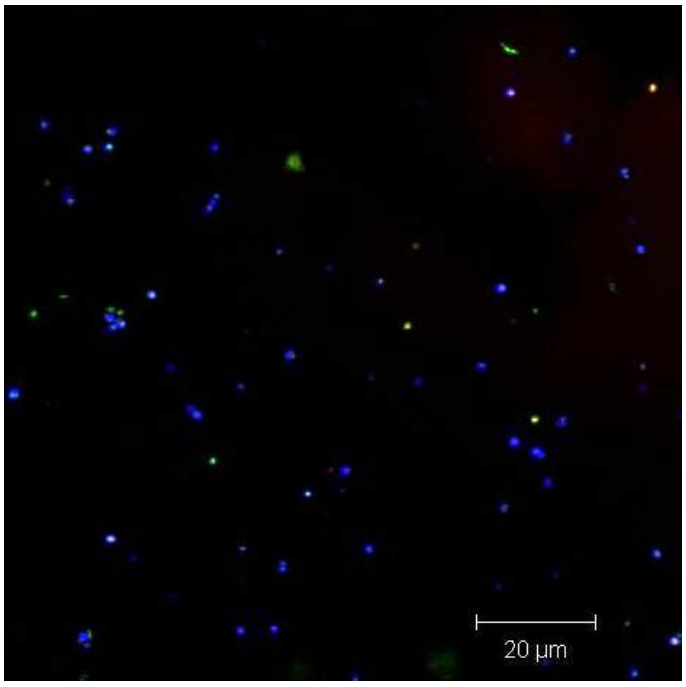

Figure 3-1(b)

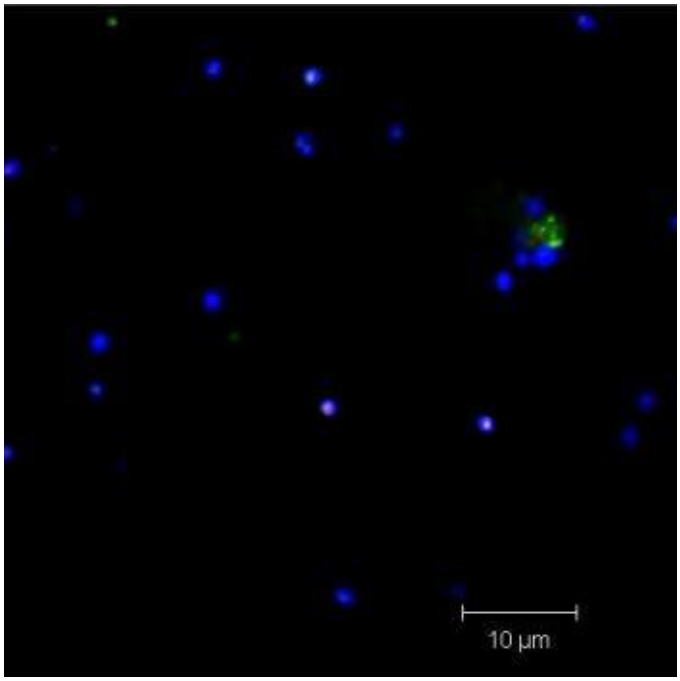

Figure 3-1(c)

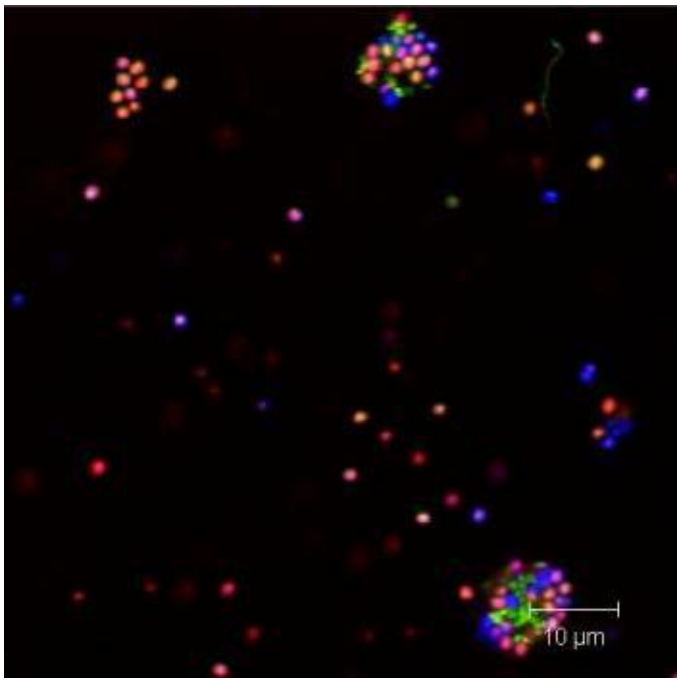

Figure 3-1: WT cells encapsulated in a pure TEOS alkoxide gel (a), a similar gel with 10% glycerol (b), and with 10% PEG200 (c).

Figure 3-2 is similar to Figure 3-1 except that gels were derived from aqueous precursors. No cells in the pure gel from aqueous precursors had a strong red signal, indicating a high encapsulation survival rate. There is some slight evidence of increased Sytox orange™ signal in the gel containing glycerol as shown by a pair of cells near the center of the image with a strong red signal and another cell at left with a similar coloration. The clumping that occurred in the presence of PEG in the alkoxide gel did not occur with the gel from aqueous precursors, suggesting that PEG influenced the gelation of the alkoxide precursor and not aggregation of the cells. There is also much less Sytox orange™ signal as compared with the alkoxide gel containing PEG, indicating there may be a synergistic negative impact on survival resulting from the presence of both PEG and EtOH.

Figure 3-2(a)

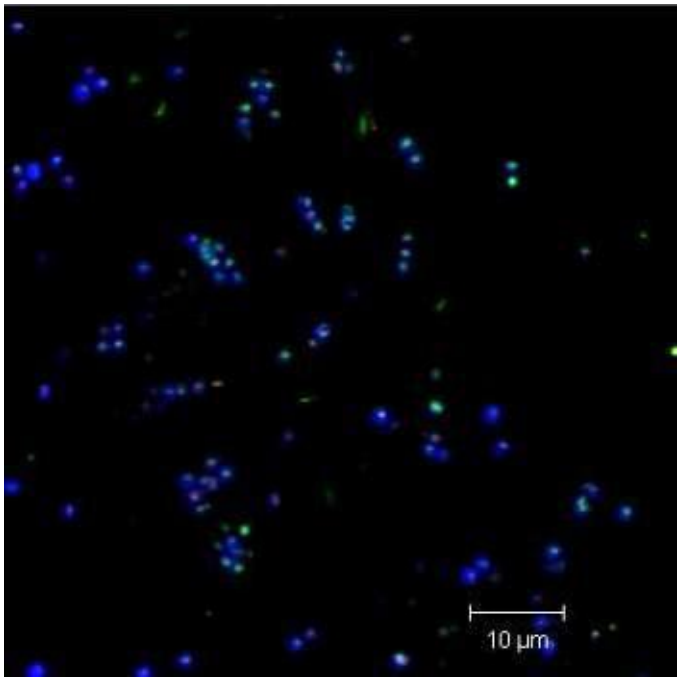

Figure 3-2(b)

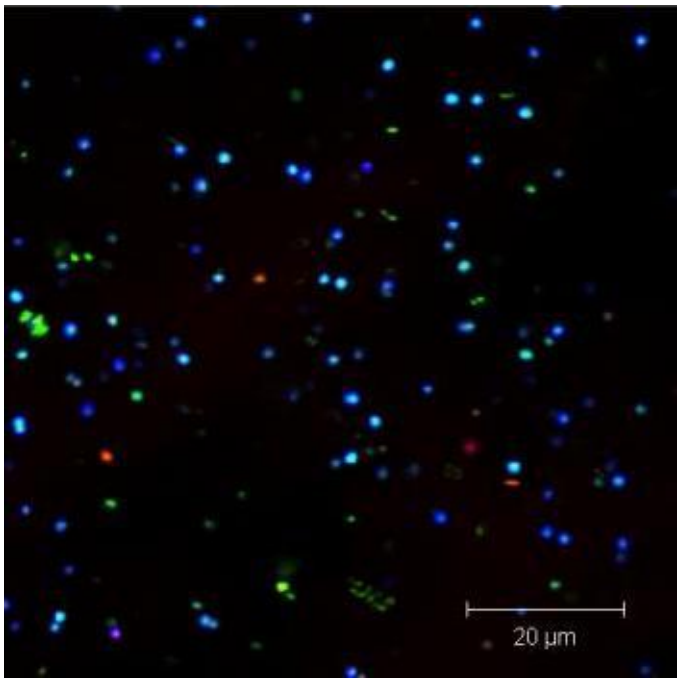

Figure 3-2(c)

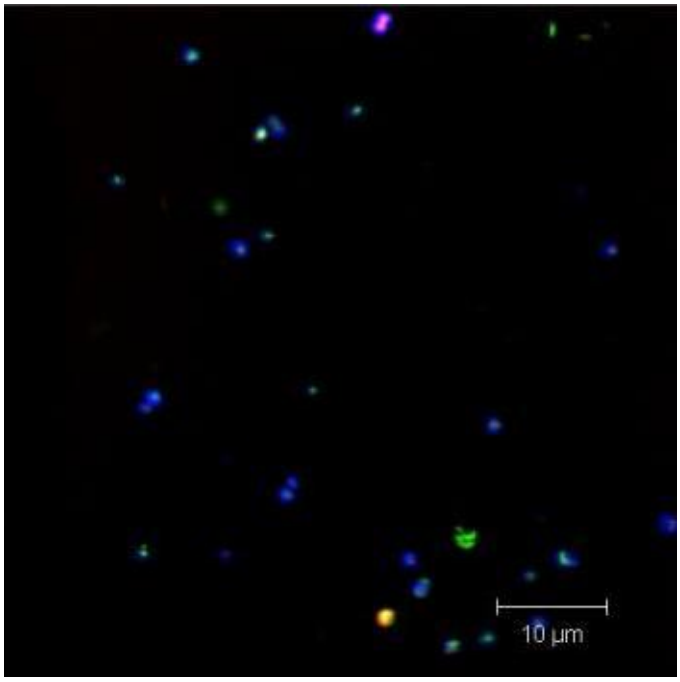

Figure 3-2: WT cells encapsulated in a pure aqueous gel (a), a similar gel with 10% glycerol (b), and with 10% PEG200 (c).

3.4.2 - Fluorescence & Photosynthetic Activity

To discern whether additives protect encapsulated cells from certain stresses inherent to encapsulation (or contribute to those stresses), cells were conditioned with selected stress-inducing compounds in liquid culture and chlorophyll fluorescence was used to monitor the responses of photosynthetic processes. Cells were exposed to EtOH, NaCl, glycerol, and PEG in concentrations comparable to what might be the highest reasonably anticipated through standard encapsulation protocols. First, cells were exposed to 500 mM (2.9%) EtOH, 500 mM NaCl, 5% glycerol, and 5% PEG. Cultures were adjusted to an OD_{730} of approximately 0.8 and incubated under constant 70 $\mu Em^{-2}s^{-1}$ actinic light for 24 hours prior to chlorophyll fluorescence analysis. The efficiency of PSII (F_v/F_m for dark acclimated samples, ϕPSII

for light acclimated samples), maximum efficiency of light adapted PSII (F_v'/F_m'), and coefficients of photochemical and nonphotochemical quenching, q_P and q_N, respectively, were calculated for all samples at increasing light intensity up to 200 $\mu Em^{-2}s^{-1}$. These results are shown in Figures 3-3a through 3-3d.

Figure 3-3(a)

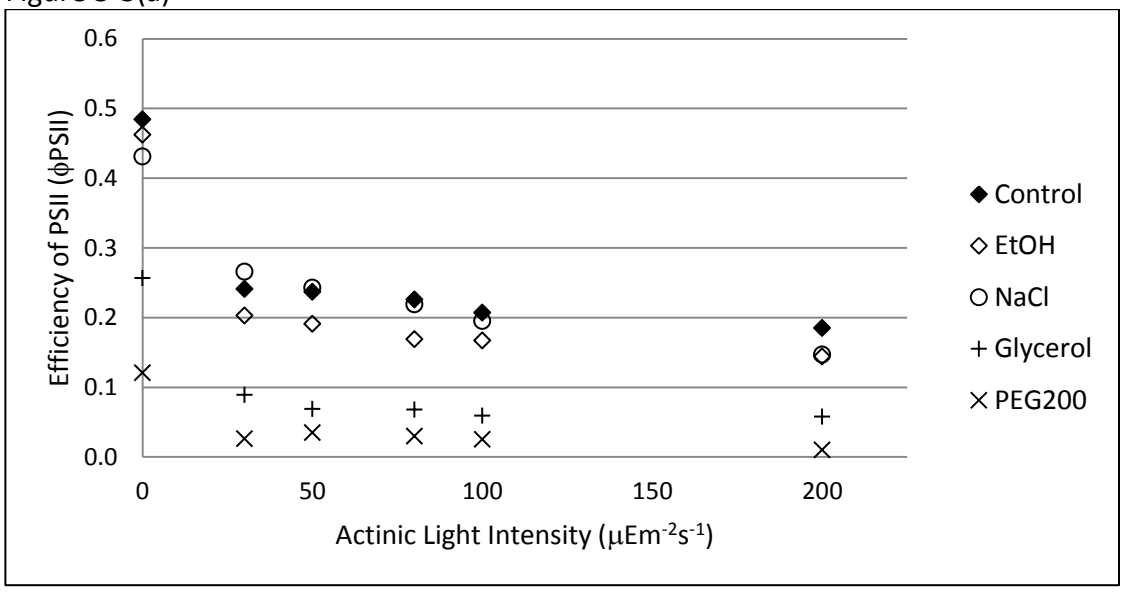

Figure 3-3(b)

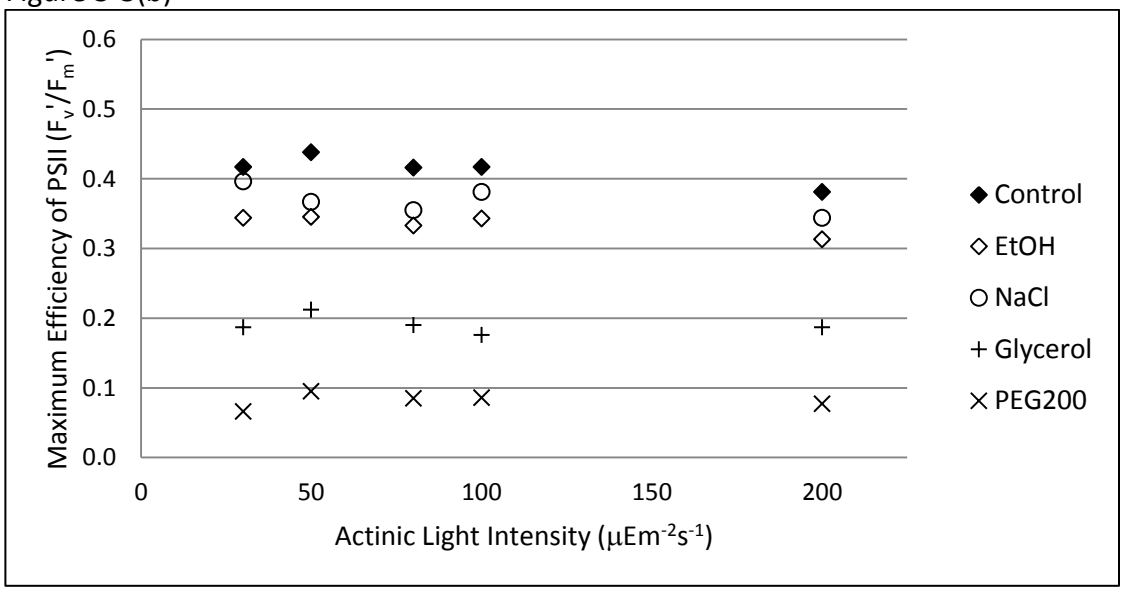

Figure 3-3(c)

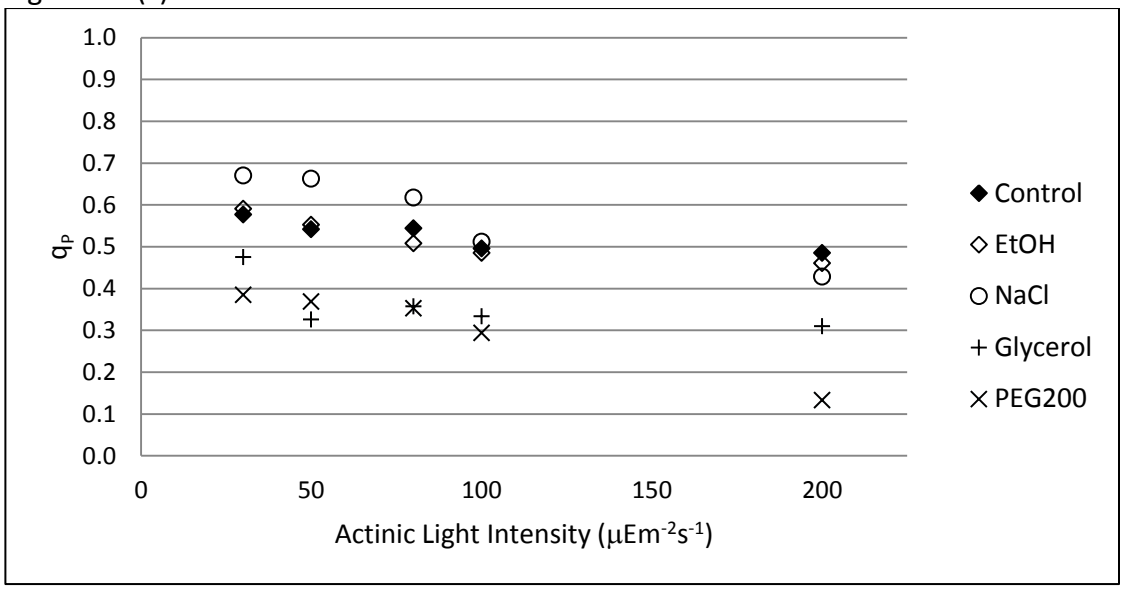

Figure 3-3(d)

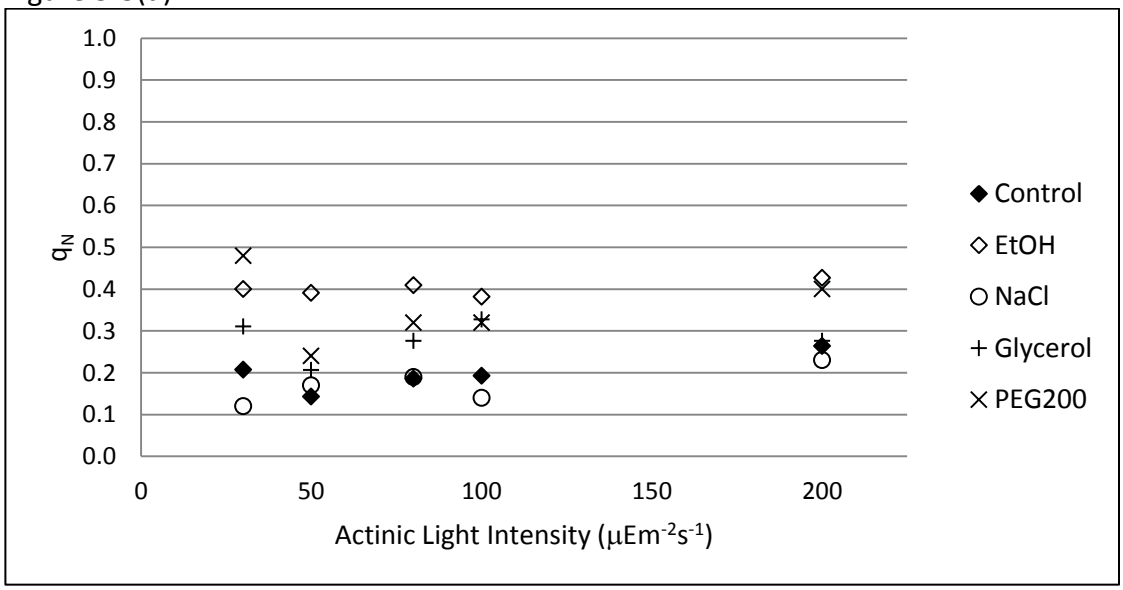

Figure 3-3: Fluorescence parameters for cells in liquid culture, exposed to indicated stress compound for 24 hours in constant light of approximately 70 μEm^{-2}s^{-1}. In (a), points at actinic light = 0 are F_v/F_m, a special case of ϕPSII.

Figures 3-3a and 3-3b clearly show that the efficiency of PSII is dramatically reduced in the presence of PEG and glycerol, yet was minimally affected by NaCl and EtOH stress. ϕPSII ranged from 0.20 to 0.26 at the lowest actinic light intensity of 30 $\mu Em^{-2}s^{-1}$ and slowly declined to the range of 0.14 to 0.18 for control cells and cells exposed to NaCl and EtOH. For cells exposed to PEG or glycerol, ϕPSII was less than 0.10 at all light intensities, and as low as 0.01 for cells exposed to PEG under 200 $\mu Em^{-2}s^{-1}$ light. The effects of PEG and glycerol were also pronounced on F_v'/F_m', with values <0.10 for cells exposed to PEG, around 0.20 for cells exposed to glycerol, and >0.30 for NaCl and EtOH treated cells and controls. Figure 3-3c shows a similar trend in q_P with lower values for PEG and glycerol treated cells while NaCl and EtOH treated cells generally agreed with the control. In some instances at lower light intensity, q_P for NaCl treated cells actually exceeded the untreated controls. The effects were less pronounced on q_N, shown in Figure 3-3d, which was increased most dramatically in cells exposed to EtOH, less so with cells exposed to glycerol and PEG, and basically unaltered by NaCl. Cumulatively, these results demonstrate that at the levels used in this study, *Synechocystis* sp. PCC 6803 is more sensitive to stress inflicted by PEG or glycerol than by NaCl or EtOH.

Figure 3-4 shows the same parameters as Figure 3-3 but immediately after two minutes of exposure to the stress-inducing compounds. The same source flask was used for all trials shown in Figure 3-4. Samples were dark acclimated and fluorescence was measured at increasing light intensity without the presence of a stress-inducing compound (providing multiple replicates of the same control sample). Then a stress compound was added (500 mM EtOH, 500 mM NaCl, 10% glycerol, or 10% PEG), the sample was allowed to incubate in the dark for 2 minutes, and the fluorescence analysis was repeated. Shown most dramatically in Figures 3-4a and 3-4c, all stress-inducing compounds had a similarly strong effect on reducing

photosynthetic efficiency. ϕPSII was consistently reduced approximately 70% below the control, while q_P was reduced approximately 50 to 75%.

Figure 3-4(a)

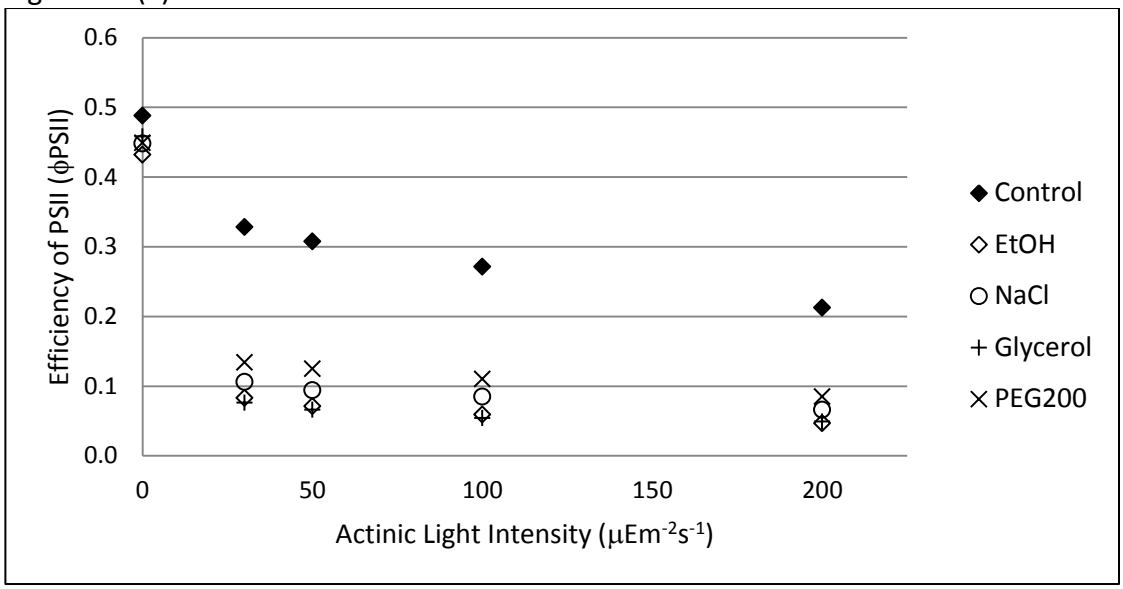

Figure 3-4(b)

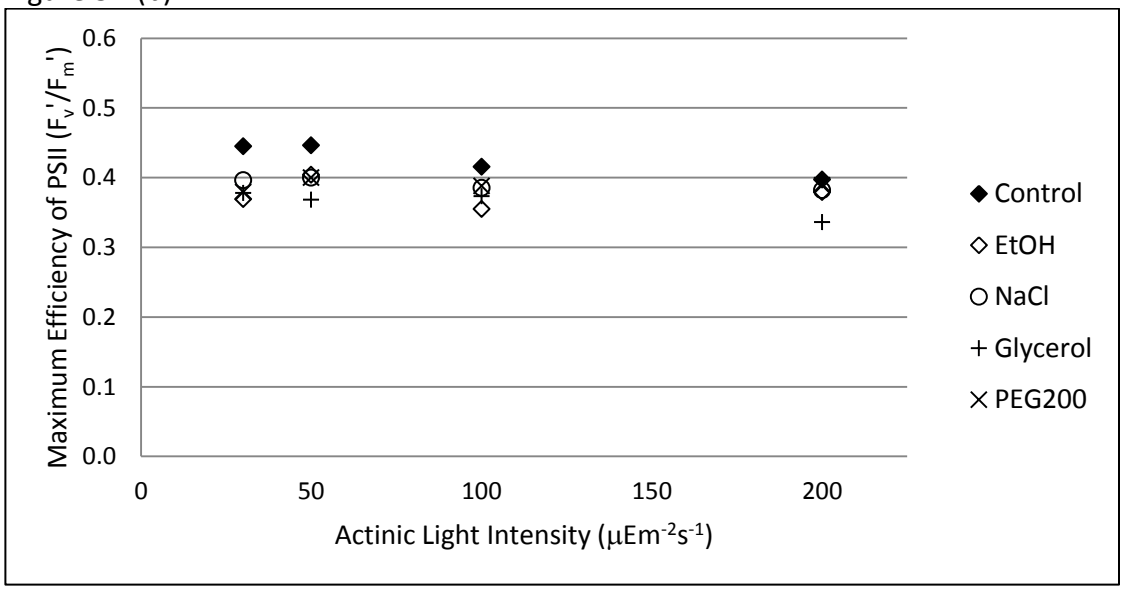

Figure 3-4(c)

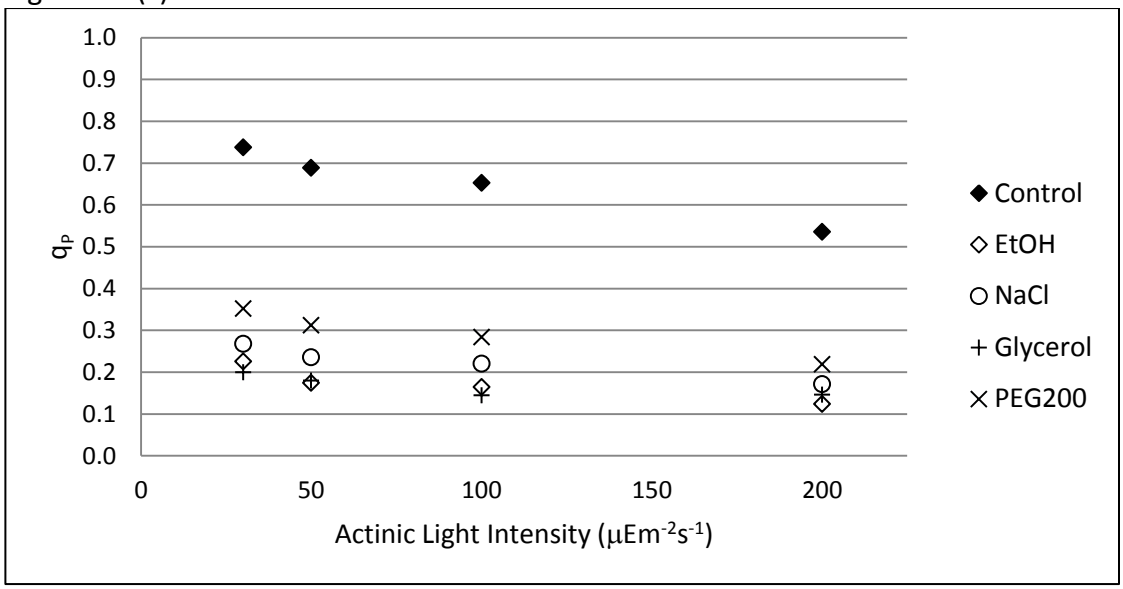

Figure 3-4(d)

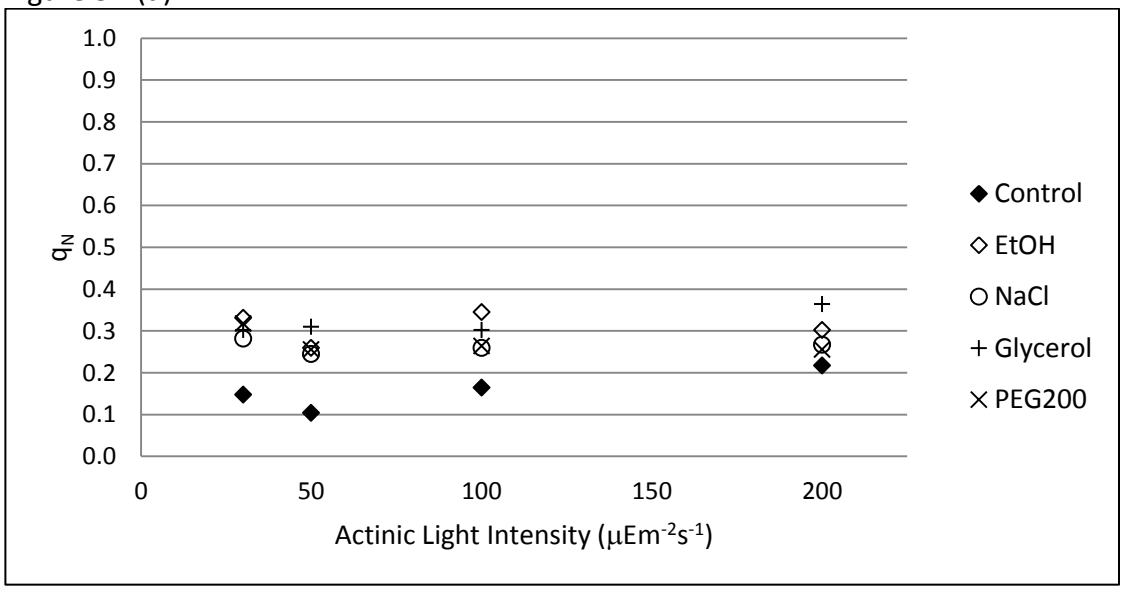

Figure 3-4: Fluorescence parameters for cells acutely exposed to the given stress factor for 2 minutes prior to analysis. In (a), points at actinic light = 0 are F_v/F_m, a special case of ϕPSII.

Encapsulation creates an initial shock on encapsulated cells, but they may recover from the shock and regain activity. However, this had not yet been clearly observed in encapsulated cultures of *Synechocystis* sp. PCC 6803 prior to the current investigation. To explore recovery and longevity of encapsulated cells, samples of alkoxide (TEOS) gels and gels from aqueous precursors, at a cell density of approximately $5x10^8$ cells/mL, were prepared in 35 mm Petri dishes and incubated under diurnal light cycling (12 hours on, 12 hours off) at a light intensity of approximately 80 $\mu Em^{-2}s^{-1}$ for six weeks. Fluorescence measurements to assess photosynthetic activity were taken initially upon encapsulation, daily for three days, and weekly thereafter. These results are shown in Figure 3-5. Samples of alkoxide and aqueous-derived gels containing either 5% PEG or 5% glycerol were prepared simultaneously. However, the samples containing PEG bleached out and died within the first week, and although some samples containing glycerol survived for six weeks, cellular health and activity as indicated through fluorescence deteriorated dramatically and significant chlorosis occurred (data not shown).

Figure 3-5(a)

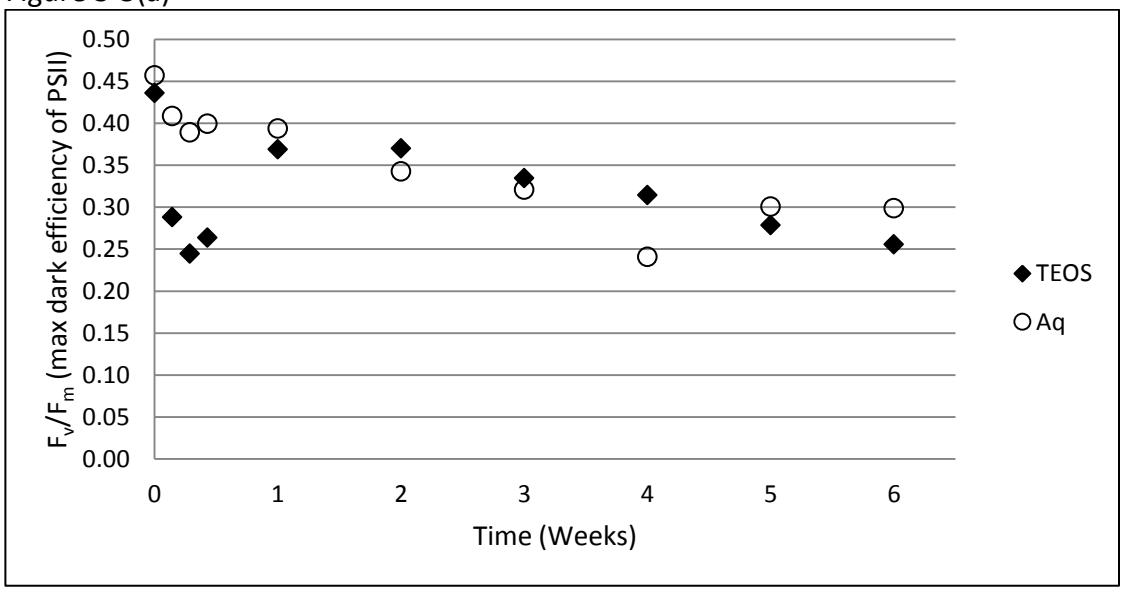

Figure 3-5(b)

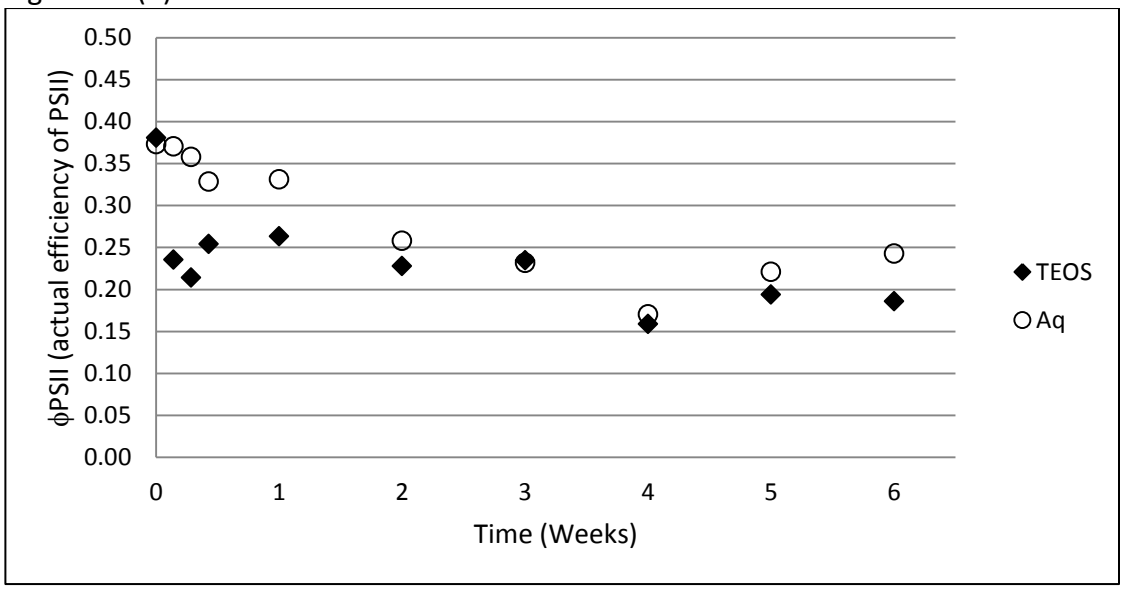

Figure 3-5(c)

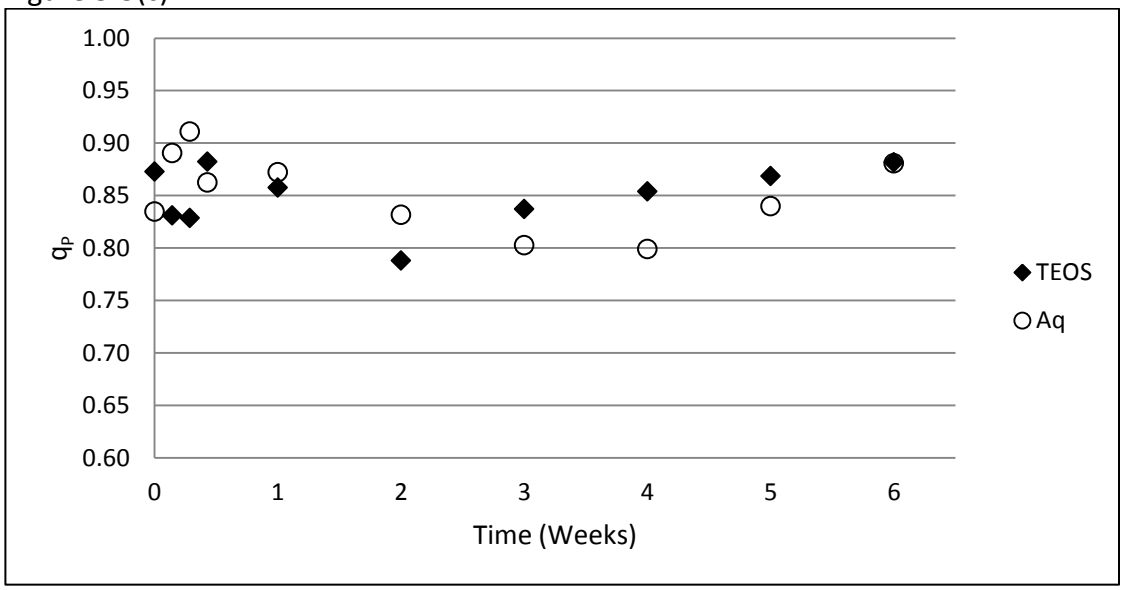

Figure 3-5(d)

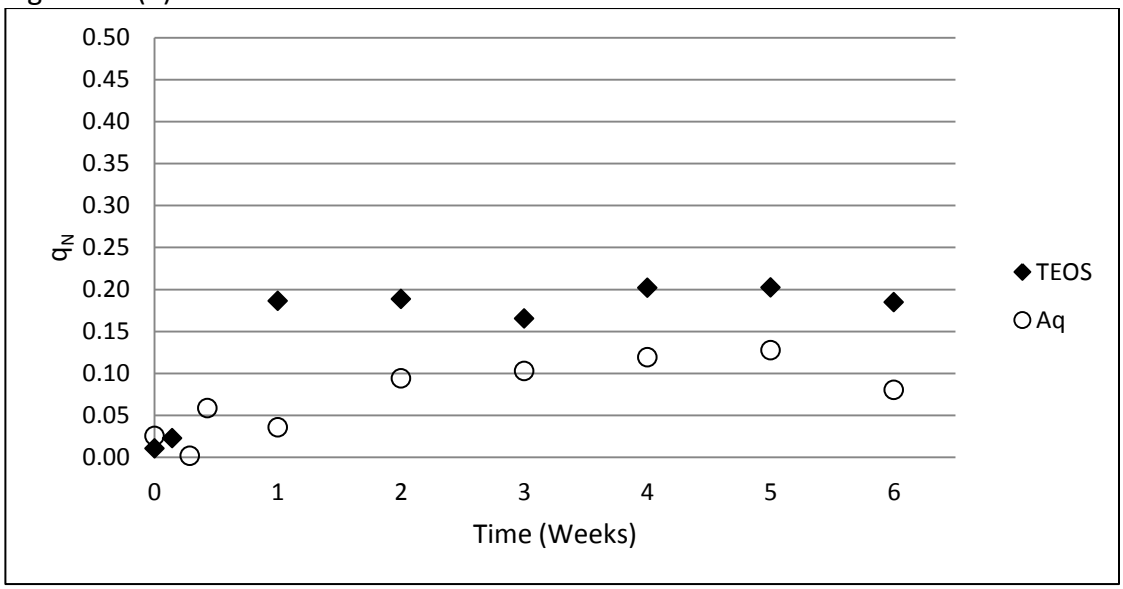

Figure 3-5: Fluorescence parameters for cells in alkoxide gels and gels from aqueous precursors monitored over six weeks. Parameters in (b), (c), and (d), ϕPSII, q_P, and q_N, respectively, were measured at an actinic light intensity of 50 $\mu Em^{-2}s^{-1}$.

Maximum quantum efficiency of PSII in dark acclimated cells, F_v/F_m (Figure 3-5a), shows an initial peak for cells in the gels from aqueous precursors at 0.46, followed by a mostly consistent, steady decline to a value of 0.30 at 6 weeks. Cells in the alkoxide gels started at 0.44, declined to 0.25 by day 2, and then recovered to a peak of 0.37 at 2 weeks before a steady decline to 0.26 at 6 weeks, suggesting that cells in both gel environments slowly deteriorate over time. Although the magnitudes of ϕPSII varied slightly compared to F_v/F_m, the overall trend was similar, shown in Figure 3-5b, measured with 50 $\mu Em^{-2}s^{-1}$ actinic light. Figure 3-5c shows a slight drop in q_P in the first two weeks after encapsulation followed by four weeks of steady recovery by cells in alkoxide gels and a slower but similar recovery by cells in aqueous-derived gels, each returning to values of nearly 0.90, similar to that immediately following encapsulation. Values of q_N, shown in Figure 3-5d, measured

under 50 $\mu Em^{-2}s^{-1}$, increased over the first week for both gels, reaching a value of 0.19 for cells in alkoxide gels and 0.04 for cells in aqueous-derived gels. Thereafter, q_N more or less plateaued in both samples, at approximately 0.20 for alkoxide gel samples and 0.10 for aqueous-derived gels.

Figure 3-6 shows fluorescence traces for control cells and cells exposed to the four stress-inducing compounds for 24 hours under continuous 70 $\mu Em^{-2}s^{-1}$ light. It appeared that both glycerol and PEG interfered with excitation transfer from PBS to photosystems and may have also interfered with state transitions. The traces for cells exposed to PEG and glycerol show limited response to increased actinic light intensity, in contrast to the control trace. Cells exposed to PEG in particular showed very little ability to effectively implement a state transition, as would be indicated by a gradual increase in the magnitude of F_m' with increasing light intensity [61]. As light intensity increased, the fluorescence trace was basically flat, and saturating pulses generated F_m' values decreasing in magnitude, suggesting limited ability to adjust to light intensity, and possibly even photoinhibition. In an unstressed cell, the PBS would be expected to be in State 2 upon dark acclimation (reduced PQ pool, increased proportion of excitation directed to PSI). Upon illumination, the PQ pool becomes increasingly oxidized and induces a transition to State 1, with more excitation energy directed toward PSII [58, 62]. This transition to State 2 should generate an increase in variable fluorescence originating from PSII chlorophylls, visible in an increased F_m', which was observed in control cells and cells exposed to NaCl, but not with cells exposed to PEG.

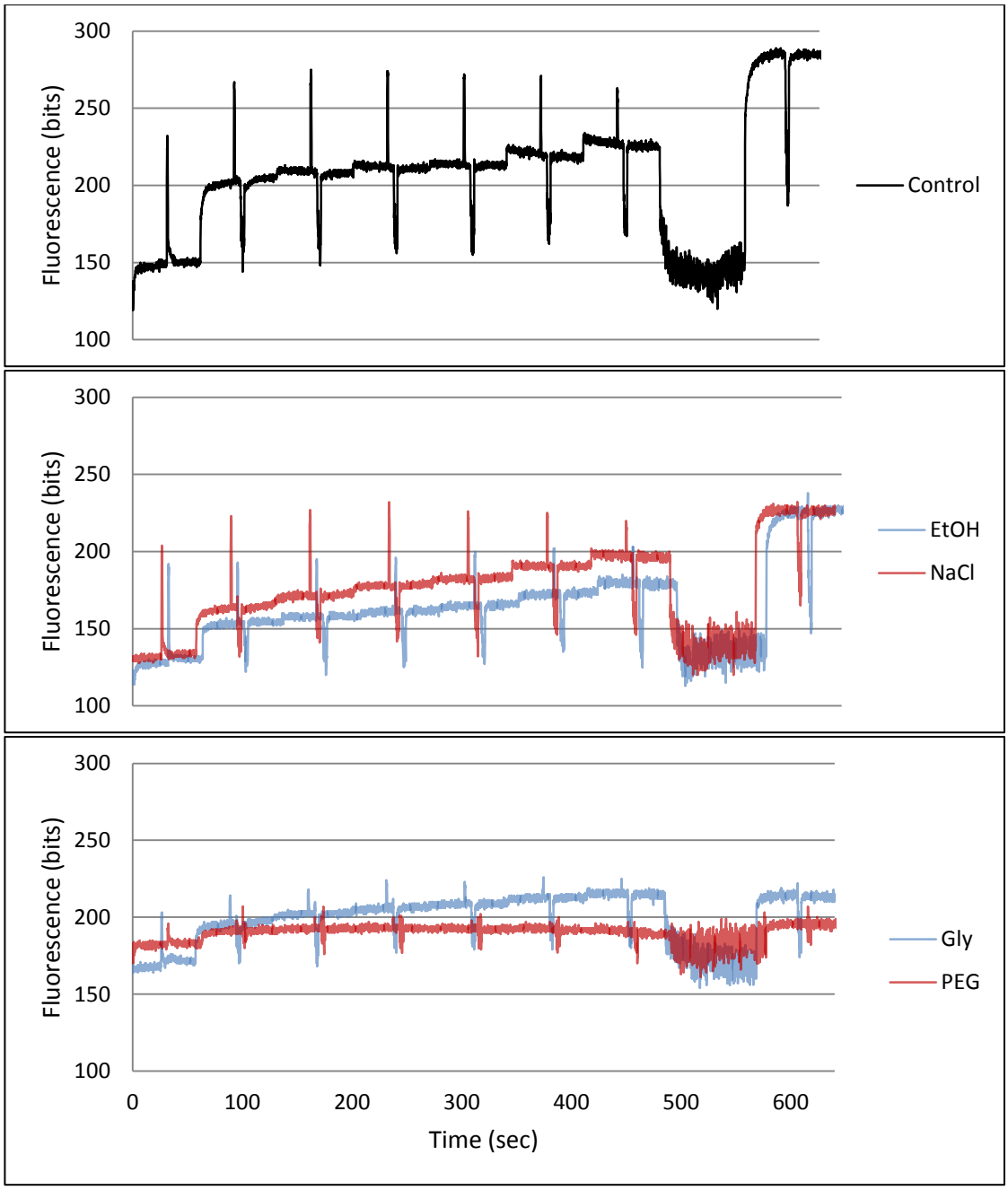

Figure 3-6: Fluorescence traces for *wt* cells exposed to 500 mM EtOH, 500 mM NaCl, 5% glycerol, or 5% PEG for 24 hours under constant illumination of approximately 70 $\mu Em^{-2}s^{-1}$ (All trials concluded with 10 µM DCMU to measure F_m).

The trace for cells exposed to glycerol was qualitatively more similar to the control, although, again, evidence of a state transition was limited, illustrated by only a slight increase in the magnitude of F_m' with increasing actinic light intensity. Furthermore, exposure to DCMU did not yield a significant increase in F_m', as it did in the control and cells exposed to NaCl and EtOH, indicating that cells exposed to PEG or glycerol cannot adequately manage excitation distribution between the photosystems and, as a result, become saturated, a situation that potentially leads to photoinhibition and photodamage.

3.5 - Discussion

Glycerol has demonstrated utility in protecting many kinds of cells encapsulated in silica gel [12, 18, 35-37], yet these results clearly show that glycerol is actually detrimental to *Synechocystis* sp. PCC 6803 when compared to similar gels without the additive. The decrease in the efficiency of PSII upon exposure to glycerol is dramatic (Figure 3-4a), and efficiency does not recover over 24 hours (Figure 3-3a). A similar trend was shown for cells exposed to PEG. In contrast, EtOH and NaCl stress created a similar initial shock with a correlating decrease in ϕPSII (Figure 3-4a), yet under the conditions of this study, ϕPSII nearly completely recovered after 24 hours (Figure 3-3a). Confocal microscopy images confirmed the deleterious effects of these additives, the effects of PEG being most apparent in an alkoxide gel while the effects of glycerol were somewhat visible in a gel from aqueous precursors.

A comparison of changes in F_v'/F_m', q_P and q_N with initial exposure and over 24 hours also corroborates the conclusion that *Synechocystis* sp. PCC 6803 is robust to salt stress, moderately sensitive to EtOH stress, and highly sensitive to both glycerol and PEG at the concentrations used in this investigation. A dramatic drop in q_P was observed with all additives upon initial exposure (Figure 3-4c), although there was not a corresponding drop in F_v'/F_m' (Figure 3-4b). This suggests the photoantennae, at least initially, are intact and still absorbing light effectively. Since

the low values of q_P suggest that excitation energy is not going to photochemistry, and considering the negligible rise in q_N (Figure 3-4d), it is possible these cells are experiencing photoinhibition and photodamage under these conditions.

After 24 hours, q_N increased for cells in the presence of EtOH and, to a lesser extent, in the presence of PEG, but very little in the presence of NaCl or glycerol (Figure 3-3d). q_P continued to be depressed for cells exposed to glycerol and PEG, although there was some recovery over 24 hours (Figure 3-3c). What has changed dramatically is the pattern in F_v'/F_m' (Figure 3-3b). While consistently high for acutely exposed samples (Figure 3-4b), it decreased dramatically over 24 hours in cells exposed to PEG and glycerol. Changes in q_P indicate these stressed cells remain able to use excitation energy once it reaches PSII, yet they are effectively directing less excitation energy through the antennae to PSII reaction centers, possibly due to decoupling of the PBS from PSII. Again, considering the weak response in q_N, this may suggest these cells are suffering the effects of photoinhibition and photodamage.

Synechocystis sp. PCC 6803 is resilient to salt stress, a documented response achieved through the production of GG, an endogenous osmotic protectant [50-52]. While the cells are sensitive to an initial shock, indicated by a drop in ϕPSII and q_P (Figures 3-4a and 3-4c), the cells readily recovered within 24 hours (Figures 3-3a and c). As shown in Figure 3-6, after 24 hours exposure to 500 mM NaCl, the fluorescence trace is qualitatively very similar to the control trace. An increase in the magnitude of F_m' with increasing light intensity indicates a state transition [61]. Furthermore, the magnitude of F_m, measured with DCMU, increased above F_m' recorded at higher actinic light intensity, indicating an intact ability to manage excitation transfer between the PBS and photosystems. However, the overall magnitude of fluorescence was lower than the control, even though these samples were prepared from the same source culture at similar cell density. It is possible that the salt stress may have caused the degradation of some photosystems, particularly PSII reaction centers

through photodamage to D1 proteins, leading to the decrease in overall fluorescence.

EtOH stress had an effect that was qualitatively similar to PEG stress, although it was not as strong and cells appeared more resilient to EtOH. Recovery in ϕPSII and q_P was observed after 24 hours exposure to EtOH (Figures 3-3a and 3-3c), despite a dramatic drop in both parameters upon acute exposure, similar to the other stress-inducing compounds (Figures 3-4a and 3-4c). The fluorescence trace in Figure 3-6 also indicates that EtOH stressed cells are unable to carry out a state transition as well as the control cells. The value of F_m' is nearly identical at all actinic light intensities, including dark-acclimated cells. Also, F_m, measured in the presence of DCMU, is significantly higher than all measured values of F_m'. This indicates the cells are fixed in State 2, directing an increased proportion of excitation energy to PSI. PSII cannot be saturated in this state without the addition of DCMU. At lower light intensities, this will reduce the efficiency of light utilization in these cells, and at higher light intensities, this will hinder their ability to manage excitation transfer, leading to increased nonphotochemical quenching (Figure 3-3d), and possibly photoinhibition. Although the impact of EtOH is less severe than PEG, it is still detrimental and to be avoided.

Shown in Figure 3-5, cells encapsulated in both types of gel formulations considered, alkoxide and aqueous-derived, survived over the course of six weeks. F_v/F_m and ϕPSII remained reasonably high and deteriorated slowly over time (Figures 3-5a and 3-5b). The initial drop in both parameters in the TEOS gels is presumably the result of EtOH stress. Considering q_N did increase initially (Figure 3-5d), these cells were likely suffering photodamage, yet were able to recover. There was no similar drop and recovery in the aqueous-derived gel samples likely because there was not enough salt present in the gel formulation to induce significant stress. The fact that q_P remained consistently high, above 0.80 in most instances, also indicates the cells

remained photosynthetically active over the course of the six week experimental trial. Finally, similar samples were prepared with PEG and glycerol. However, cells exposed to PEG died and bleached within the first week of the trial, supporting the conclusion of sever photodamage and photoinhibition suggested by the stress tests discussed above. Cells exposed to glycerol survived the six week trial, but were visibly stressed, showing signs of chlorosis and very low values of F_v/F_m, ϕPSII, and q_P, and very high values of q_N (data not shown).

Together, these results suggest that *Synechocystis* sp. PCC 6803 is robust against moderate salt stress, moderately sensitive to EtOH stress, and quite sensitive to stress induced by glycerol and PEG. While osmotic protection is still a concern while encapsulating cells, it is advantageous that *Synechocystis* sp. PCC 6803 is capable of producing GG as a protectant. It is feasible that preconditioning cells in salt to stimulate the production of GG prior to encapsulation may improve long term survival of encapsulated cultures. Further investigation is required to determine the efficacy of this approach.

3.6 - Conclusion

While glycerol and PEG are routinely and successfully used to enhance the viability and activity of cells encapsulated in silica gel, *Synechocystis* sp. PCC 6803 is surprisingly vulnerable to stress induced by both compounds. Both stress photosynthetic processes, either through general osmotic stress (in the case of PEG), or interfering with PBS-photosystem excitation transfer (in the case of glycerol). Cells were better able to survive encapsulation long term in gels derived from alkoxide or aqueous precursors when PEG and/or glycerol were not used, which is contradictory to other investigations of sol-gel encapsulation using non-photosynthetic organisms. However, this is likely due to the specific sensitivity of *Synechocystis* sp. PCC 6803 and perhaps other cyanobacteria to PEG and glycerol. It has also been shown that over a period of six weeks, cells recover photosynthetic efficiency approximately

equally well in gels from aqueous precursors and in alkoxide gels. As an alternative to adding supplemental protective agents, cells may be conditioned in liquid culture containing a moderate level of salt to induce the production of GG, an osmotic protectant, although this approach is yet to be explored thoroughly. Continuing research on the responses of *Synechocystis* sp. PCC 6803 to encapsulation within silica gel will improve our understanding of stresses imposed by encapsulation and ultimately allow further improvement of encapsulation protocols. These results further support the idea that while encapsulation within silica gel is an effective means to maintain activity, there are no universally effective protocols; each must be optimized for the species of interest.

Acknowledgements

The authors wish to thank the Air Force Office of Scientific Research, Grant # RF0260, for supporting this research, and Chevron Energy Corp., Grant # V02640, for providing funding for the purchase of the FMS-1 fluorometer. This publication was made possible in part by the Confocal Microscopy Facility of the Center for Genome Research and Biocomputing and the Environmental and Health Sciences Center at Oregon State University, supported by Grant # 1S10RR107903-01 from the National Institutes of Health. The authors also acknowledge Dr. Jed Eberly, Markael Luterra, and Dr. Elizabeth Burrows for helpful comments, as well as Soleil Rowan-Caneer and Rebecca Miller for valuable laboratory assistance.

Chapter 3 References

1 Appel J, Phunpruch S, Steinmüller K, Schulz R. The Bidirectional Hydrogenase of Synechocystis sp. PCC 6803 Works as an Electron Valve during Photosynthesis. Arch Microbiol. 2000; 173: 333-338.

2 Cournac L, Mus F, Bernard L, Guedeney G, Vignais P, Peltier G. Limiting Steps of Hydrogen Production in Chlamydomonas reinhartii and Synechocystis sp. PCC 6803 as Analysed by Light Induced Gas-Exchange Transients. Int J Hydrogen Energy 2002; 27: 1229-1237.

3 Cournac L, Guedeney Gv, Peltier G, Vignais PM. Sustained Photoevolution of Molecular Hydrogen in a Mutant of Synechocystis sp. Strain PCC 6803 Deficient in the Type 1 NADPH-Dehydrogenase Complex. J Bacteriol 2004; 186(6): 1737-1746.

4 Antal TK, Lindblad P. Production of H_2 by sulphur-deprived cells of the unicellular cyanobacteria Gloeocapsa alpicola and Synechocystis sp. PCC 6803 during dark incubation with methane or at various extracellular pH. J Appl Microbiol 2005; 98(1): 114-120.

5 Antal TK, Oliveira P, Lindblad P. The bidirectional hydrogenase in the cyanobacterium Synechocystis sp. strain PCC 6803. Int J Hydrogen Energy 2006; 31(11): 1439-1444.

6 Burrows EH, Chaplen FWR, Ely RL. Optimization of media nutrient composition for increased photofermentative hydrogen production by Synechocystis sp. PCC 6803. Int J Hydrogen Energy 2008; 33(21): 6092-6099.

7 Dickson DJ, Page CJ, Ely RL. Photobiological hydrogen production from Synechocystis sp. PCC 6803 encapsulated in silica sol-gel. Int J Hydrogen Energy 2009; 34(1): 204-215.

8 Bernát G, Waschewski N, Rögner M. Towards efficient hydrogen production: the impact of antenna size and external factors on electron transport dynamics in Synechocystis PCC 6803. Photosynthesis Research 2009; 99(3): 205-216.

9 Navarro E, Montagud A, Córdoba PFd, Urchueguía JF. Metabolic flux analysis of the hydrogen production potential in Synechocystis sp. PCC6803. Int J Hydrogen Energy 2009; 34(21): 8828-8838.

10 Burrows EH, Chaplen FWR, Ely RL. Effects of selected electron transport chain inhibitors on 24-h hydrogen production by Synechocystis sp. PCC 6803. Bioresour Technol 2010; 102: 3062-3070.

11 Carturan G, Campostrini R, Dire S, Scardi V, Alteriis ED. Inorganic Gels for Immobilization of Biocatalysts: Inclusion of Invertase-Active Whole Cells of Yeast (Saccharomyces cerevisiae) into thin Layers of SiO_2 Gel Deposited on Glass Sheets. J Mol Catal 1989; 57: L13 - L16.

12 Nassif N, Roux Cc, Coradin T, Rager M-N, Bouvet OMM, Livage J. A Sol-gel Matrix to Preserve the Viability of Encapsulated Bacteria. J Mater Chem 2003; 13: 203-208.

13 Taylor A, Finnie KS, Bartlett JR, Holden PJ. Encapsulation of Viable Aerobic Microorganisms in Silica Gels. J Sol Gel Sci Technol 2004; 32: 223-228.

14 Yu D, Joanne Volponi, Swapnil Chhabra, C. Jeffrey Brinker, Ashok Mulchandani, & Anup K. Singh. Aqueous sol-gel encapsulation of genetically engineered Moraxella spp. cells for the detection of organophosphates. Biosensors and Bioelectronics 2005; 20(7): 1433-1437.

15 Desimone MF, De Marzi MC, Copello GJ, Fernandez MM, Pieckenstain FL, Malchiodi EL, et al. Production of recombinant proteins by sol-gel immobilized Escherichia coli. Enzyme Microb Technol 2006; 40(1): 168-171.

16 Chen J, Y. Xu, J. Xin, S. Li, C. Xia, & J. Cui. Efficient immobilization of whole cells of *Methylomonas* sp. strain GYJ3 by sol-gel entrapment. J Mol Catal 2004; 30: 167 - 172.

17 Rooke JC, Leonard A, Su B-L. Targeting photobioreactors: Immobilisation of cyanobacteria within porous silica gel using biocompatible methods. J Mater Chem 2008; 18: 1333-1341.

18 Fiedler D, Hager U, Franke H, Soltmann U, Bottcher H. Algae biocers: astaxanthin formation in sol-gel immobilised living microalgae. J Mater Chem 2007; 17(3): 261-266.

19 Nguyen-Ngoc H, Tran-Minh C. Sol-gel process for vegetal cell encapsulation. Materials Science and Engineering: C 2007a; 27(4): 607-611.

20 Nguyen-Ngoc H, Tran-Minh C. Fluorescent biosensor using whole cells in an inorganic translucent matrix. Anal Chim Acta 2007b; 583(1): 161-165.

21 Carturan G, Monte RD, Pressi G, Secondin S, Verza P. Production of Valuable Drugs from Plant Cells Immobilized by Hybrid Sol-Gel SiO_2. J Sol Gel Sci Technol 1998; 13: 273 - 276.

22 Pressi G, Toso RD, Monte RD. Production of Enzymes by Plant Cells Immobilized by Sol-Gel Silica. J Sol Gel Sci Technol 2003; 26: 1189 - 1193.

23 Perullini M, Rivero MM, Jobbágy M, Mentaberry A, Bilmes SA. Plant cell proliferation inside an inorganic host. J Biotechnol 2007; 127(3): 542-548.

24 Pope EJA, Karen Braun, & Charles M. Peterson. Bioartificial Organs I: Silica Gel Encapsulated Pancreatic Islets for the Treatment of Diabetes Mellitus. J Sol Gel Sci Technol 1997; 8: 635 - 639.

25 Boninsegna S, Bosetti P, Carturan G, Dellagiacoma G, Monte RD, Rossi M. Encapsulation of Individual Pancreatic Islets by Sol-Gel SiO_2: A Novel Procedure for Perspective Cellular Grafts. J Biotechnol 2003; 100: 277 - 286.

26 Nieto A, Areva S, Wilson T, Viitala R, Vallet-Regi M. Cell viability in a wet silica gel. Acta Biomaterialia 2009; 5(9): 3478-3487.

27 Armon R. Sol-Gel as Reaction Matrix for Bacterial Enzymatic Activity. J Sol Gel Sci Technol 2000; 19: 289-292.

28 Livage J, Coradin T, Roux C. Encapsulation of Biomolecules in Silica Gels. J Phys: Condens Matter 2001; 13: R673 - R691.

29 Bottcher H, Soltmann U, Mertig M, Pompe W. Biocers: Ceramics with Incorporated Microorganisms for Biocatalytic, Biosorptive and Functional Materials Development. J Mater Chem 2004; 14: 2176 - 2188.

30 Avnir D, Coradin T, Lev O, Livage J. Recent Bio-applications of Sol-gel Materials. J Mater Chem 2006; 16: 1013 - 1030.

31 Gadre SY, Gouma PI. Biodoped Ceramics: Synthesis, Properties, and Applications. J Am Ceram Soc 2006; 89(10): 2987-3002.

32 Kandimalla V, Tripathi V, Ju H. Immobilization of Biomolecules in Sol-Gels: Biological and Analytical Applications. Crit Rev Anal Chem 2006; 36(2): 73-106.

33 Gupta R, Chaudhury NK. Entrapment of biomolecules in sol-gel matrix for applications in biosensors: Problems and future prospects. Biosensors and Bioelectronics 2007; 22(11): 2387-2399.

34 Meunier CF, Dandoy P, Su B-L. Encapsulation of cells within silica matrixes: Towards a new advance in the conception of living hybrid materials. J Colloid Interface Sci 2010; 342: 211-224.

35 Nassif N. Living Bacteria in Silica Gels. Nature Materials 2002; 1: 42-44.

36 Nassif N, Roux C, Coradin T, Bouvet OMM, Livage J. Bacteria Quorum Sensing in Silica Matrices. J Mater Chem 2004; 14: 2264 - 2268.

37 Desimone MF, De Marzi M, Copello G, Fernandez M, Malchiodi E, Diaz L. Efficient preservation in a silicon oxide matrix of Escherichia coli, producer of recombinant proteins. Appl Microbiol Biotechnol 2005; 68(6): 747-752.

38 Shen G. Synechocystis sp. PCC 6803 Strains lacking Photosystem I and Phycobilisome Function. The Plant Cell 1993; 5: 1853-1863.

39 Mao H-B, Li G-F, Li D-H, Wu Q-Y, Gong Y-D, Zhang X-F, et al. Eɨects of glycerol and high temperatures on structure and function of phycobilisomes in *Synechocystis* sp. PCC 6803. FEBS Lett 2003; 553: 68-72.

40 Rakhimberdieva MG, Vavilin DV, Vermaas WFJ, Elanskaya IV, Karapetyan NV. Phycobilin/chlorophyll excitation equilibration upon carotenoid-induced non-photochemical fluorescence quenching in phycobilisomes of the cyanobacterium Synechocystis sp. PCC 6803. Biochimica et Biophysica Acta (BBA) - Bioenergetics 2007a; 1767(6): 757-765.

41 Conroy J, Power ME, Martin J, Earp B, Hosticka B, Daitch CE, et al. Cells in Sol-Gels I: A Cytocompatible Route for the Production of Macroporous Silica Gels. J Sol Gel Sci Technol 2000; 18: 269-283.

42 Close TJ, Lammers PJ. An Osmotic Stress Protein of Cyanobacteria is lmmunologically Related to Plant Dehydrins. Plant Physiol 1993; 101(773-779).

43 Fernandes TA, Apte SK. Differential regulation of nitrogenase activity by ionic and osmotic stresses and permeable sugars in the Cyanobacterium *Anabaena* sp. strain L-31. Plant Science 2000; 150: 181-189.

44 Sergeyenko TV, Los DA. The Effect of Various Stresses on the Expression of Genes Encoding the Secreted Proteins of the Cyanobacterium *Synechocystis* sp. PCC 6803. Russion Journal of Plant Physiology 2002; 49(5): 650-656.

45 Kanesaki Y, Suzuki I, Allakhverdiev SI, Mikami K, Murata N. Salt Stress and Hyperosmotic Stress Regulate the Expression of Different Sets of Genes in Synechocystis sp. PCC 6803. Biochem Biophys Res Commun 2002; 290(1): 339-348.

46 Jantaro S, Mulo P, Jansen T, Incharoensakdi A, Mäenpää P. Effect of long-term ionic and osmotic stress conditions on photosynthesis in the cyanobacterium *Synechocystis* sp. PCC 6803. Functional Plan Biology 2005; 32: 807-815.

47 Papageorgiou GC, Alygizaki-Zorba A. A sensitive method for the estimation of the cytoplasmic osmolality of cyanobacterial cells using chlorophyll fluorescence. Biochim Biophys Acta 1997; 1335: 1-4.

48 Stamatakis K, Papageorgiou GC. The osmolality of the cell suspension regulates phycobilisome-to-photosystem I excitation transfers in cyanobacteria. Biochim Biophys Acta 2001: 172-181.

49 Allakhverdiev SI, Nishiyama Y, Miyairi S, Yamamoto H, Inagaki N, Kanesaki Y, et al. Salt Stress Inhibits the Repair of Photodamaged Photosystem II by Suppressing the Transcription and Translation of psbA Genes in Synechocystis. Plant Physiol 2002; 130(3): 1443-1453.

50 Ferjani A, Mustardy L, Sulpice R, Marin K, Suzuki I, Hagemann M, et al. Glucosylglycerol, a Compatible Solute, Sustains Cell Division under Salt Stress. Plant Physiol 2003; 131(4): 1628-1637.

51 Engelbrecht F, Marin K, Hagemann M. Expression of the ggpS Gene, Involved in Osmolyte Synthesis in the Marine Cyanobacterium Synechococcus sp. Strain PCC 7002, Revealed Regulatory Differences between This Strain and the Freshwater Strain Synechocystis sp. Strain PCC 6803. Appl Environ Microbiol 1999; 65(11): 4822-4829.

52 Marin K, Huckauf J, Fulda S, Hagemann M. Salt-Dependent Expression of Glucosylglycerol-Phosphate Synthase, Involved in Osmolyte Synthesis in the Cyanobacterium Synechocystis sp. Strain PCC 6803. J Bacteriol 2002; 184(11): 2870-2877.

53 Jeanjean R, Matthijs HCP, Onana B, Havaux M, Joset F. Exposure of the Cyanobacterium Synechocystis PCC6803 to Salt Stress Induces Concerted Changes in Respiration and Photosynthesis. Plant Cell Physiol 1993; 34(7): 1073-1079.

54 Tanaka Y, Katada S, Ishikawa H, Ogawa T, Takabe T. Electron Flow from NAD(P)H Dehydrogenase to Photosystem I is Required for Adaptation to Salt Shock in the Cyanobacterium Synechocystis sp. PCC 6803. Plant Cell Physiol 1997; 38(12): 1311-1318.

55 Jeanjean R, Bédu S, Havaux M, Matthijs HCP, Joset F. Salt-induced photosystem I cyclic electron transfer restores growth on low inorganic carbon in a type 1 NAD(P)H dehydrogenase deficient mutant of *Synechocystis* PCC6803. FEMS Microbiol Lett 1998; 167(2): 131-137.

56 Ryu J-Y, Suh K-H, Chung Y-H, Park Y-M, Chow WS, Park Y-I. Cytochrome c Oxidase of the Cyanobacterium Synechocystis sp. PCC 6803 Photosynthesis from Salt Stress. Molecules & Cells 2003; 16(1): 74-77.

57 Panda B, Jain P, Sharma L, Mallick N. Optimization of cultural and nutritional conditions for accumulation of poly-β-hydroxybutyrate in Synechocystis sp. PCC 6803. Bioresour Technol 2006; 97(11): 1296-1301.

58 Campbell D, Oquist G. Predicting Light Acclimation in Cyanobacteria from Nonphotochemical Quenching of Photosystem II Fluorescence, Which Reflects State Transitions in These Organisms. Plant Physiol 1996; 111(4): 1293-1298.

59 Campbell D, Hurry V, Clarke AK, Gustafsson P, Oquist G. Chlorophyll Fluorescence Analysis of Cyanobacterial Photosynthesis and Acclimation. Microbiol. Mol. Biol. Rev. 1998; 62(3): 667-683.

60 El Bissati K, Delphin E, Murata N, Etienne A-L, Kirilovsky D. Photosystem II fluorescence quenching in the cyanobacterium Synechocystis PCC 6803: involvement of two different mechanisms. Biochimica et Biophysica Acta (BBA) - Bioenergetics 2000; 1457(3): 229-242.

61 Bailey S, Grossman A. Photoprotection in Cyanobacteria: Regulation of Light Harvesting. Photochem Photobiol 2008; 84(6): 1410-1420.

62 Mullineaux C, Allen JF. State 1-State 2 transitions in the cyanobacterium *Synechococcus* 6301 are controlled by the redox state of the electron carriers between Photosystems I and II. Photosynthesis Research 1990; 23: 297-311.

CHAPTER 4 - PHOTOSYNTHETIC ACTIVITY AND HYDROGEN PRODUCTION FROM THREE PHYCOBILISOME-DEFECT MUTANTS OF *SYNECHOCYSTIS* SP. PCC 6803 ENCAPSULATED IN SILICA GEL

David J. Dickson, David Kehoe, Roger L. Ely

International Journal of Hydrogen Energy

Elsevier Press

3251 Riverport Lane

Maryland Heights, MO 63043, USA

International Association of Hydrogen Energy

5794 SW 40 St. #303

Miami, FL 33155, USA

(manuscript to be submitted)

4.1 - Abstract

Three phycobilisome (PBS) mutants of the cyanobacterium *Synechocystis* sp. PCC 6803 were examined for photosynthetic activity under varying light intensities and hydrogen production after encapsulation in silica gel. The mutants included: ΔcpcAB, a deletion of α and β subunits of phycocyanin; ΔapcF, a deletion of the β^{18} allophycocyanin subunit; and ΔapcE, a deletion of the L_{CM} linker peptide. Cultures were conditioned for two days in nutrient-replete BG-11 media prior to being transferred to EHB-1 media, optimized for fermentative hydrogen production, and conditioned for an additional two days under the same constant light. Chlorophyll fluorescence, pigment content, and glycogen contents were measured before and after conditioning in EHB-1 media. After conditioning, cells were encapsulated in silica gel and incubated anaerobically in the dark for fermentative hydrogen production. Increased light intensity yielded increased glycogen accumulation, varying little between the ΔapcE, ΔapcF, and wild-type (*wt*) *Synechocystis* sp. PCC 6803 strains, while the ΔcpcAB strain accumulated approximately 25% less glycogen. The ΔapcE and ΔapcF strains both produced more hydrogen than *wt* cells when conditioned under 400 $\mu Em^{-2}s^{-1}$ light and encapsulated in silica gel derived from aqueous precursors, although increased hydrogen production was not correlated with increased glycogen accumulation. Hydrogen production from all strains encapsulated in gels derived from aqueous precursors was approximately 2.5 to 3.5 times higher than liquid controls. These results illustrate that PBS mutants of *Synechocystis* sp. PCC 6803 and encapsulation in silica gel can be used effectively to enhance photobiological hydrogen production.

Keywords: phycobilisome, *Synechocystis* sp. PCC 6803, photobiological hydrogen production, silica sol-gel encapsulation

4.2 - Introduction

Photobiological hydrogen production has received much attention as a means of renewably producing hydrogen, an energy carrier with great potential to reduce dependence on carbon-based fossil fuels. The cyanobacterium *Synechocystis* sp. PCC 6803, a model organism for the investigation of oxygenic photosynthesis, has also been studied recently for its ability to produce hydrogen through the activity of a bimetallic [Ni-Fe] hydrogenase [1-7]. Deriving energy directly or indirectly from activity of photosynthetic processes, the hydrogenase enzyme can catalyze the reduction of protons under certain conditions, using NADPH and protons as substrates [3, 8], to yield molecular hydrogen.

However, for two main reasons, photobiological hydrogen production from this and many other oxygenic phototrophs is not yet technically feasible or commercially viable at large scale. First, hydrogenase enzymes are very sensitive to oxygen. [Fe-Fe] hydrogenases, typical of green algae, are irreversibly inhibited by molecular oxygen, while [Ni-Fe] hydrogenases, typical of cyanobacteria, are reversibly inhibited (reviewed in [9-14]). As a result, until a robust oxygen-tolerant hydrogenase can be found or engineered, many are investigating hydrogen production through an indirect pathway, separated temporally from oxygenic photosynthesis by intermediate production of storage compounds, such as glycogen.

Second, hydrogen production is energetically and metabolically expensive. In *Synechocystis* sp. PCC 6803, the electrons required to produce hydrogen are provided by NADPH, a critical electron carrier for anabolic reactions, including carbon fixation and cell maintenance. In order for the reversible [Ni-Fe] hydrogenase to produce hydrogen, the NADPH/NADP+ pool must be extremely reduced [3]. Numerous investigations have sought to enhance hydrogen production in *Synechocystis* sp. PCC 6803 by improving reductant availability to the hydrogenase through various manipulations, including sulfur deprivation [4], deletion of the NDH-1 protein

complex (which plays a role in cyclic electron transport) [2, 3], nutrient optimization for glycogen accumulation [6], encapsulation in inorganic matrices [7], and selective use of electron transport chain inhibitors [15]. These investigations have yielded both dramatic improvements in hydrogen production and an improved understanding of the underlying mechanisms, although many questions remain.

The efficiency at which light is utilized by cyanobacteria and other oxygenic phototrophs to produce biomass is ultimately very low, typically less than 2% [16]. There are two fundamental reasons for this. The first is due to the thermodynamics of charge separation, electron transport, and downstream biochemical reactions. The overall process must be irreversible, with energy flowing through a series of electron carriers, incurring an unavoidable energy loss at each step. The only option for improving efficiency from this standpoint is extracting an energetic product as close to initial light absorption as possible, which could be hydrogen produced through direct photobiological activity [17]. The second is because cyanobacteria have evolved to grow optimally under relatively low light conditions. This means their ability to utilize excitation energy effectively becomes saturated at moderate light intensity, resulting in increased losses to heat, fluorescence, and even photodamage as light intensity increases. This second cause of inefficiency is not necessarily inherent and can be addressed through alterations of the light-harvesting proteins, which is of primary interest in the current investigation. This approach has been validated in *Synechocystis* PCC 6714 [18] and algae [17, 19, 20]. An efficiency in the range of 10-16%, sunlight to hydrogen, is considered achievable with photobiological hydrogen production [16, 21, 22]. In fact, the process is expected to become economically feasible at an efficiency of 10% [23, 24]. Rational manipulation of the light harvesting antennae provides one approach toward reaching this efficiency.

In *Synechocystis* sp. PCC 6803, like most cyanobacteria, the primary means of light absorption is by the phycobilisome (PBS), a large protein complex containing

numerous chromophores that absorb photons and channel excitation energy toward both photosystems (Figures 4-1 and 4-2). The PBS is a large complex containing approximately 85% chromophores and 15% colorless structural proteins, by mass [25]. There are many PBS per cell, representing perhaps as much as 50% of soluble protein under certain conditions [26].

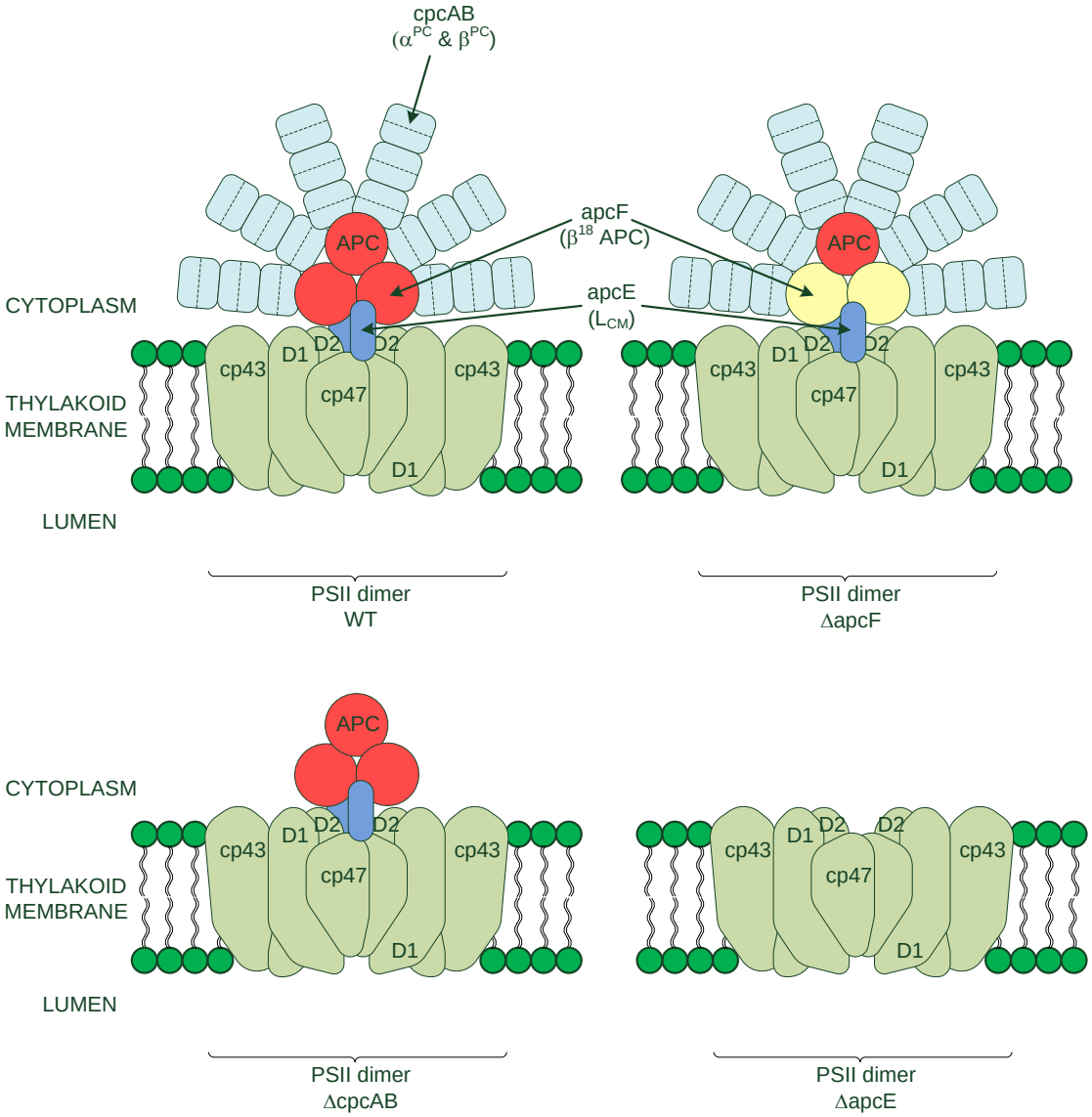

Figure 4-1: A schematic illustration of the PBS, its interaction with PSII, and structural changes expected in each of the three mutants investigated in this study.

The PBS of *Synechocystis* sp. PCC 6803 is hemidiscoidal, containing three cylinders in a core composed predominantly of allophycocyanin (APC) with six peripheral rods attached, containing phycocyanin (PC)(Figure 4-2). The rods are constructed of three hexameric discs, each composed of two trimeric discs of α and β PC heterodimers oriented face to face and linked together by small linker peptides in the central cavity of the discs [27]. From distal end to core attachment, the discs are connected by linker peptides named L_R^{10}, L_R^{30}, L_R^{33}, and L_{RC}, encoded by the genes cpcD, cpcC2, cpcC1, and cpcG1, respectively [28]. Deletion mutants have been characterized to determine the structural role of each of the rod linker peptides [26] and the rod-core linker peptide [29, 30]. A mutant lacking the cpcA and cpcB genes (i.e., ΔcpcAB), coding for the α and β subunits of PC, for example, is unable to synthesis PBS rods, and is therefore expected to produce a functional PBS core without rods [31], which should harvest less light per PBS.

Each of the three core cylinders contains four discs. The top cylinder, separated from the thylakoid, contains two identical discs, each of a simple APC trimer, $(\alpha\beta)_3$, called T discs, and two other discs similar to a T disc plus an additional L_C linker peptide, called T8 discs. The two basal cylinders, adjacent to the thylakoid, contain one T disc, one T8 disc, one B8 disc (a T8 disc with one α-subunit of APC replaced with a $\alpha^{AP\text{-}B}$) and one M disc (a T disc with one $\alpha\beta$ dimer replaced with a β^{18} for β-APC and L_{CM} for α-APC). The structural organization of the PBS has recently been resolved to 13 Å [28]. Of particular interest to the current study are apcE and apcF deletion mutants, genes which code for the β^{18} subunit variant of APC and the L_{CM} linker peptide, respectively.

Investigations with various forms of a ΔapcF mutant have revealed two key features. First, in the absence of a functional apcF gene product, a functional PBS is still assembled. Excitation transfer to both photosystems still occurs, although with slightly diminished efficiency, particularly to PSI [32, 33]. A related protein, apcD,

coding for α-APC-B in the B8 disc, can also be deleted without the loss of PBS function, but this mutation showed a smaller, more subtle decrease in excitation transfer to the photosystems compared to a ΔapcF mutant [32]. Second, the apcF gene appears to play an important role in the state transition. The ΔapcF mutant is effectively fixed in State 1, with PBS excitation energy being primarily directed toward PSII, resulting in an increased PSI/PSII ratio [32]. It is uncertain what effects this mutation may have on light utilization efficiency toward glycogen accumulation or hydrogen production.

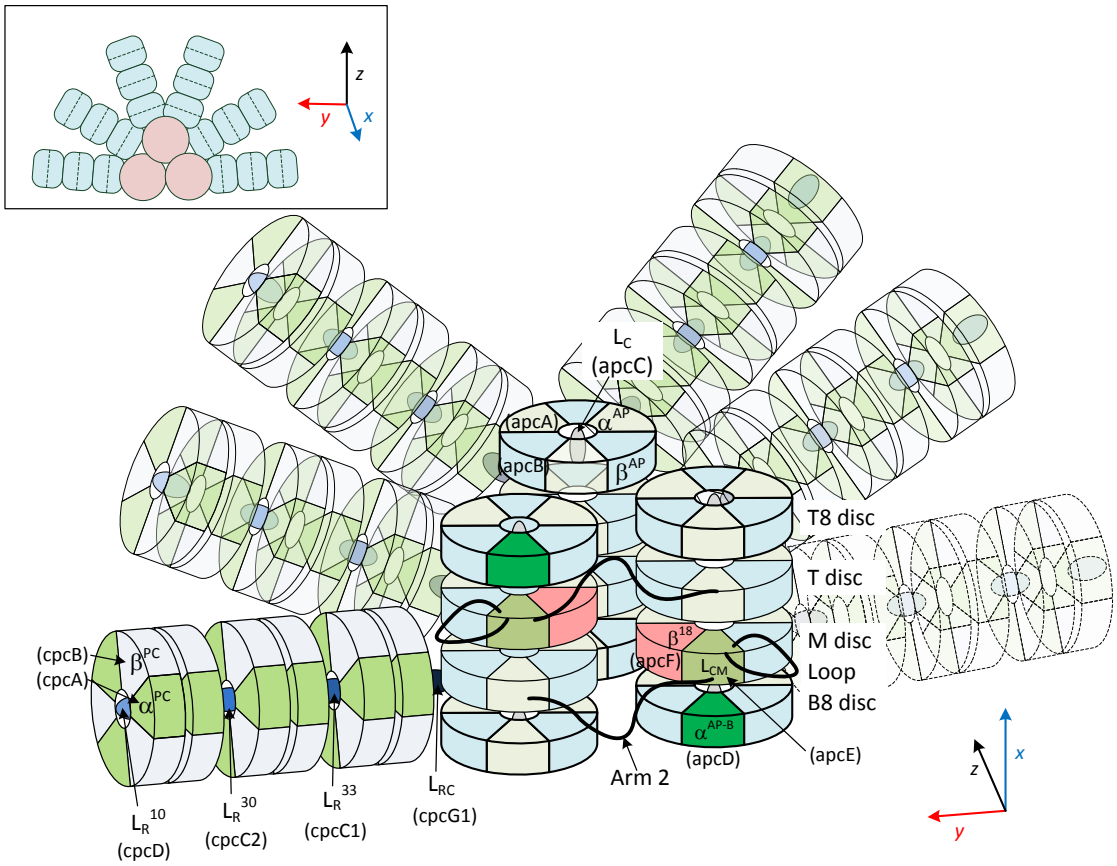

Figure 4-2: A detailed illustration of the PBS structure, adapted from Arteni et al. [28], including all known subunits and linker peptides (thylakoid parallel to page). A 2D profile is shown in the inset (thylakoid orthogonal to page). Primary labels are protein names, while labels in brackets are corresponding genes.

The L_{CM} peptide may be the most thoroughly investigated protein in the PBS complex. This peptide is the largest in the PBS [27], and contains four domains: the phycobiliprotein (PB) domain, similar to an α-APC subunit and part of the M disc; a repeating domain in the C-terminus similar to the linker peptide L_R, expected to be required for assembly of discs into cylinders; the PB loop in the middle of the PB domain which protrudes from the side of the core (the core can assemble and function without the PB loop, although its altered interaction with the thylakoid is unclear); and a domain called "Arm 2," likely responsible for connecting the PBS to the thylakoid membrane [28]. The L_{CM} peptide is critical for PBS assembly and function, so ΔapcE mutants lack a functional PBS, significantly altering light utilization [33, 34].

Although the ΔapcE mutant does not have a functional PBS core, it still produces PC rods, which likely associate with a different linker peptide, encoded by cpcG2, to form PSI-specific rod antennae, directing a disproportionate amount of excitation energy toward PSI [29-31, 33]. There is also evidence of nonphotochemical quenching mechanisms mediated by an orange carotenoid protein (OCP) that associates with the PBS core [35-38] and a chlorophyll-containing protein called IsiA that may associate with uncoupled PBS [35, 39-41]. Both of these processes may be disrupted by the apcE deletion, potentially making the mutant more vulnerable to photodamage under high light intensity. Deletion of the apcE gene clearly has profound and cascading effects throughout the photosynthetic processes, making it challenging to predict photosynthetic activity at varying light intensities.

One goal of this research is to improve the efficiency of light harvest toward glycogen accumulation and, ultimately, hydrogen production. With improved light utilization efficiency, an increase in accumulated biomass, including glycogen, would be expected. In the format used in the current investigation, hydrogen production results from anaerobic fermentation of accumulated glycogen, meaning improved

glycogen accumulation could lead to improved hydrogen production, as has been observed with the *wt* strain [6], and recently predicted with antennae mutants [42]. The three mutants examined in this study represent a range of severity in alteration of the PBS, the ΔapcF being relatively minor, the ΔcpcAB moderate, and the ΔapcE profound.

Pursued further in the current investigation is encapsulation of viable cells within silica gel, which is a relatively new approach to stabilize cultures and potentially to enhance the production of secondary metabolites, including hydrogen. This application has been successfully demonstrated with numerous bacteria [43-46], algae [47-49], plant cells [50-52], and mammalian cells [53, 54], as well as cyanobacteria [7, 55]. In the current investigation, encapsulation was explored to verify that the antennae mutants are amenable to the process, light utilization efficiency is improved, and hydrogen production is increased.

4.3 - Materials & Methods

4.3.1 - Cell Culturing

Cells were grown photoautotrophically in BG-11 media with 35 mM HEPES buffer. Light intensity ranged from approximately 50 $\mu Em^{-2}s^{-1}$ to 400 $\mu Em^{-2}s^{-1}$. Lower intensity light was provided by full spectrum compact fluorescent light bulbs and higher intensity light was provided by a combination of a metal halide halogen and high pressure sodium bulb, which contributed complementing intensity in the blue and red regions of the visible spectrum, respectively, for full spectrum light. Photosynthetically active radiation (PAR) was measured by a LI-188B integrating quantum photometer (Li-Cor Biosciences, Inc., Lincoln, NE).

Prior to hydrogen production assays, cells were conditioned for 48 hours in EHB-1 media [6] under constant light to promote the accumulation of glycogen. EHB-

1 is similar to BG-11 but with limited amounts of nitrogen and sulfur and more bicarbonate.

4.3.2 - Construction of Antennae Mutants

The three mutants of *Synechocystis* sp. PCC 6803 used in this investigation are all clean deletion mutants of genes encoding parts of the phycobilisome structure. The ΔcpcAB is a deletion of cpcA and cpcB, encoding the α- and β- subunits of phycocyanin, respectively, the primary phycobiliproteins of the PBS rods. The ΔapcE mutant is a deletion of apcE, coding for the linker peptide, L_{CM}, a critical structural peptide of the PBS core and responsible for connecting the PBS to the thylakoid membrane. The ΔapcF is a deletion of apcF, the β-18 subunit of the PBS core whose deletion is expected to disrupt excitation energy transfer to the photosystem reaction centers yet still allow the assembly of functional PBS (Figures 4-1 and 4-2).

4.3.3 - Silica Sol-Gel Encapsulation

Cells were encapsulated in silica gel of two different compositions. The first was derived from a mix of 80 mol.% tetraethoxysilane (TEOS)(Alfa Aesar, Ward Hill, MA), an alkoxide precursor, and 20 mol.% methyltriethoxysilane (MTES)(Sigma Aldrich, St. Louis, MO), an organically modified siloxane (ORMOSIL). The sol precursors were combined in a 50 mL Erlenmeyer flask in a molar ratio of 20:1:0.005, distilled water to silicon to nitric acid catalyst, respectively. Initially phase separated, the sol was stirred vigorously with a magnetic stir bar over mild heat of 60°C until homogeneous, approximately 90 minutes. The heat was then turned off and the precursor was allowed to continue stirring for another 60 minutes until cooled to room temperature. This also allowed for the evaporation of some ethanol as it was produced during hydrolysis.

Cells were encapsulated in gels at a final composition of 100:1, molar ratio of water to silica. This was achieved by mixing 200 μL sol precursor with 800 μL of cell

suspension in EHB-1 media buffered with 35 mM HEPES at pH 7.8. An amount of 1.0 M potassium hydroxide in a molar equivalent of the acid catalyst contained in the sol precursor was added to the cell suspension prior to mixing with the sol in order to neutralize the acid catalyst, as described previously [7].

The second gel formulation was derived from an aqueous precursor of sodium silicate solution (Fisher Scientific, Pittsburgh, PA). In an Erlenmeyer flask, 28.8 mL deionized water was combined with 460 mL 1.0 M hydrochloric acid, 5.8 g Amberlite IR-120H ion exchange resin (Sigma Aldrich, St. Louis, MO), and 2.0 mL sodium silicate solution. This was stirred vigorously with a magnetic stir bar at room temperature for approximately 60 minutes. The solution was then vacuum filtered through a 0.2 micron filter to remove the exchange resin and recover pure aqueous precursor. The final pH of the solution was approximately 2.

For encapsulation, cell suspension in EHB-1 media buffered with 35 mM HEPES was mixed in equal parts with the aqueous precursor. Prior to mixing the two components, an amount of 1.0 M potassium hydroxide in molar equivalent to the amount of acid contained in the sol precursor was added to the cell suspension. A small amount of sodium chloride salt was also added to assist gelation, 10 μL per mL of cell suspension of 5.0 M NaCl for a final NaCl concentration in the gel of 50 mM. This salt concentration does not significantly alter growth or hydrogen production from *Synechocystis* sp. PCC 6803 which is moderately salt-tolerant (data not shown).

All gel samples were prepared in a 1.0 mL volume within 5.2 mL borosilicate vials. Samples were transferred to an anaerobic chamber with a nitrogen atmosphere and incubated for 2 hours to allow the samples to become anaerobic. 500 μL of degassed media was added to all gel samples, the vials were capped with septa caps, each containing a PTFE-lined rubber septum. Samples were inverted (the 500 μL of media against the septa reduced hydrogen losses due to diffusion) and incubated in

the dark prior to headspace gas analysis by an Agilent 6890N gas chromatograph (Agilent Technologies, Santa Clara, CA).

4.3.4 - Chlorophyll Fluorescence

Chlorophyll fluorescence was monitored by a pulse modulated fluorometer (FMS-1, Hansatech Instruments Ltd., Norfolk, England). A chamber (DW2/2, Hansatech Instruments Ltd.) with four optical ports and water bath temperature control was used to examine 2.0 mL samples at multiple points during growth and conditioning. Samples were maintained at 30°C and dark acclimated for 3 minutes prior to all experimental trials. Table 4-1 lists the fluorescence parameters used in this investigation.

Table 4-1: Summary of selected fluorescence parameters used in this investigation.

Parameter	Formula	Description
F_o	-	Minimum fluorescence yield of a dark acclimated sample, all reaction centers open
F_m	-	Maximum fluorescence, reaction centers closed*
F_v	$F_m - F_o$	Variable fluorescence
F_v/F_m	$(F_m - F_o)/F_m$	Maximum quantum efficiency of PSII (dark acclimated sample)*
F_m'	-	Maximum fluorescence from a light acclimated sample (*some* reaction centers closed)
F_s	-	Steady state fluorescence yield, light acclimated
F_o'	-	Minimum fluorescence yield, light acclimated
F_v'	$F_m' - F_o'$	Variable fluorescence in light-acclimated sample
ϕPSII	$(F_m' - F_s)/F_m'$	Functional quantum efficiency of PSII in light acclimated sample (actinic light is present)
F_v'/F_m'	$(F_m' - F_o')/F_m'$	Quantum efficiency of photoantennae (or, maximum efficiency of light-acclimated PSII)[56]
q_P	$(F_m'-F_s)/(F_m'-F_o')$	Coefficient of photochemical quenching [57]
q_N	$1 - (F_m' - F_o')/(F_m - F_o)$	Coefficient of non-photochemical quenching [58]

* Cyanobacteria are extremely difficult to fully saturate with a single pulse when dark acclimated [59]. As a result, F_m is usually measured independently with the use of

DCMU, which inhibits the donor side of PSII, ensuring all reaction centers are rapidly closed during a saturating pulse of actinic light.

4.3.5 - Pigment & Glycogen Analysis

Chlorophyll content was measured by standard methanol extraction. Pigment was extracted from a 1.0 mL sample of cell culture, samples were centrifuged, resuspended in 100% methanol, incubated for approximately 30 minutes in the dark at 4°C, and absorbance of the supernatant was measured at 665 nm using a Spectronic Genesys 10 Bio UV-Vis spectrophotometer (Thermo Scientific, Waltham, MA). Chlorophyll concentration was given as: $\mu g\ Chl_a/mL = OD_{665}/0.07143$.

Phycocyanin (PC) and allophycocyanin (APC) were measured spectrophotometrically by collecting a 1.0 mL cell culture sample, resuspending in 50 mM TRIS-HCl buffer at pH 7.0, freezing and thawing, and then bead beating (three x 30 seconds with 30 seconds of cooling between) prior to centrifugation and analysis of the supernatant. Absorbance was measured at 652 nm and 615 nm, and the concentration of PC and APC were calculated by the expressions given by Bennett and Bogorad [60].

Glycogen analysis was performed by first collecting 1.0 mL samples at various points throughout the experimental procedure and freezing at -20°C. Samples were then thawed and concentrated to a volume of 50 μL before being resuspended in 200 μL of 30% KOH solution and incubated for 90 minutes at 100°C. Samples were then cooled, 600 μL of ethanol was added, and samples were stored on ice for 2 hours to precipitate glycogen. The pellet was washed with ethanol twice, resuspended in 300 μL of 100 mM acetate buffer at pH 4.75, 10 μL each of amyloglucosidase (1 U/μL) and amylase (2 U/μL) were added and samples were incubated for 1 hour at room temperature to hydrolyze glycogen to glucose. Glucose content was then analyzed

spectrophotometrically with Sigma GAGO-20 kits (Sigma Aldrich, St. Louis, MO). Samples, after conditioning in BG-11, were analyzed undiluted, yielding concentrations below the standard concentration of the assay kit. Samples after conditioning in EHB-1 were typically diluted two to four fold in order to bring absorbance measurements into the vicinity of the standard.

4.4 - Results

4.4.1 - H_2 & CO_2 Production

After conditioning in EHB-1 for 48 hours to accumulate glycogen at 50, 200, or 400 $\mu Em^{-2}s^{-1}$, culture samples were concentrated to a cell density of approximately $1x10^9$ cells/mL and encapsulated in 1.0 mL silica gels in 5.2 mL borosilicate GC vials. Samples were then incubated in the dark for 40 hours prior to hydrogen and carbon dioxide analyses via GC. Hydrogen accumulations in the headspace are shown in Figure 4-3.

Figure 4-3(a)

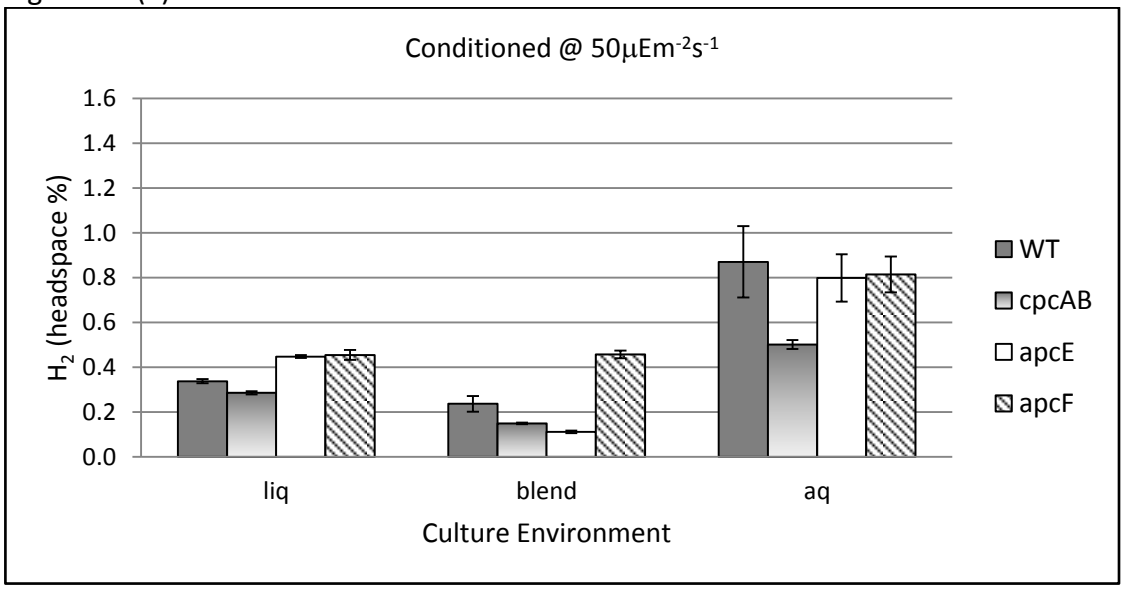

Figure 4-3(b)

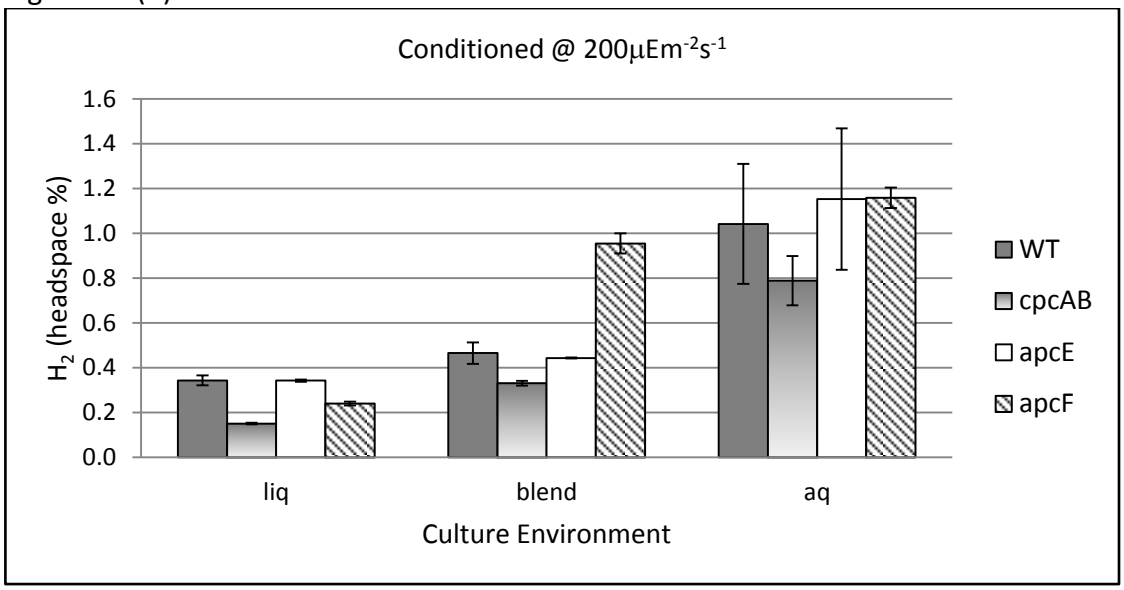

Figure 4-3(c)

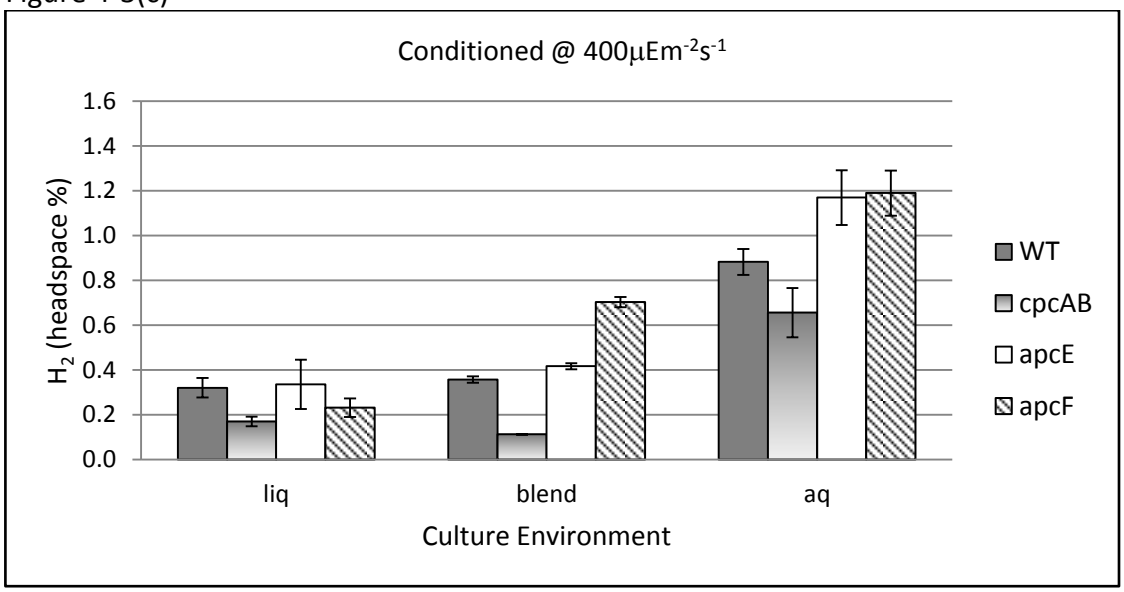

Figure 4-3: Hydrogen production from all four strains, encapsulated in two types of silica gels and liquid controls, conditioned under (a) 50 $\mu Em^{-2}s^{-1}$ light, (b) 200 $\mu Em^{-2}s^{-1}$, and (c) 400 $\mu Em^{-2}s^{-1}$. "Liq" = liquid culture; "blend" = an ORMOSIL alkoxide gel composed of 80% TEOS and 20% MTES; "aq" = a gel derived from aqueous precursors. Error bars represent one standard deviation among triplicate samples.

Hydrogen production remained relatively flat in liquid samples, increased with encapsulated samples when light intensity during glycogen accumulation increased from 50 to 200 $\mu Em^{-2}s^{-1}$, and then increased little from 200 to 400 $\mu Em^{-2}s^{-1}$. Cells encapsulated in aqueous-derived gels produced 2.5 to 3.5 times more hydrogen than liquid controls, and significantly more than cells in alkoxide-derived gels. Cells in alkoxide gels produced less hydrogen compared to liquid controls when incubated under 50 $\mu Em^{-2}s^{-1}$ light, and similar amounts when incubated under 200 and 400 $\mu Em^{-2}s^{-1}$ light. The exception is the ΔapcF strain which accumulated approximately three times the hydrogen as compared to its liquid control when incubated under the two higher light intensities. Conditioned under 200 $\mu Em^{-2}s^{-1}$ light, ΔapcE and ΔapcF cells accumulated nearly 1.2% hydrogen in the headspace, which was slightly more than *wt* cells that accumulated approximately 1.0%, although the difference was not significant (Figure 4-3b). Conditioned under 400 $\mu Em^{-2}s^{-1}$ light, ΔapcE and ΔapcF cells encapsulated in gels from aqueous precursors both produced approximately 25% more hydrogen than *wt* cells under identical conditions, accumulating approximately 1.2% hydrogen compared to 0.9% from *wt* cells (Figure 4-3c). The difference over *wt* cells under these conditions was the result of significantly less hydrogen production from the *wt* cells paired with a slight, statistically insignificant increase in hydrogen accumulation from the two mutants. Under most conditions, the ΔcpcAB strain produced less hydrogen compared to the other three strains examined.

Figure 4-4, shows carbon dioxide accumulations in the head space of the GC vials. The nutrient media contains minimal bicarbonate, so most CO_2 in the headspace resulted from respiration, which may be interpreted as a sign of stress. Both liquid controls and samples in gels from aqueous precursors consistently accumulated approximately 0.4% CO_2 in the headspace. That the samples encapsulated in the gels from aqueous precursors respired approximately the same amount of CO_2 as the liquid controls is a surprising result when compared with the

elevated hydrogen production. By contrast, samples in alkoxide gels typically contained far more CO_2, consistently around 1.2%, which is indicative of greater stress. Similarly elevated CO_2 accumulation in all alkoxide gel samples suggests a similar metabolic response to what is presumably stress induced by ethanol present in the gel precursor.

Figure 4-4(a)

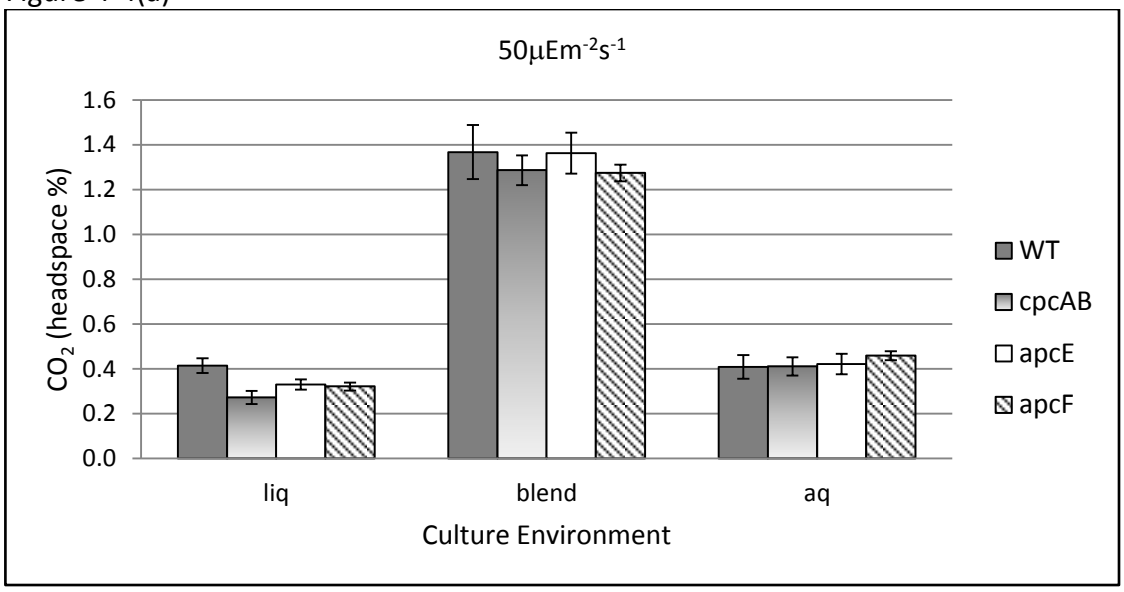

Figure 4-4(b)

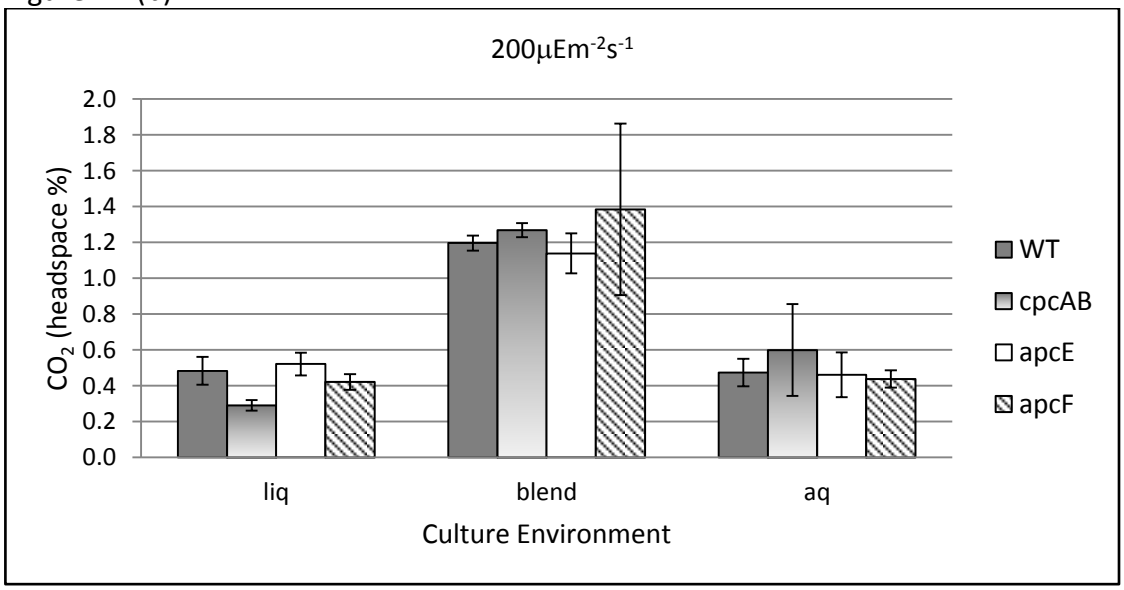

Figure 4-4(c)

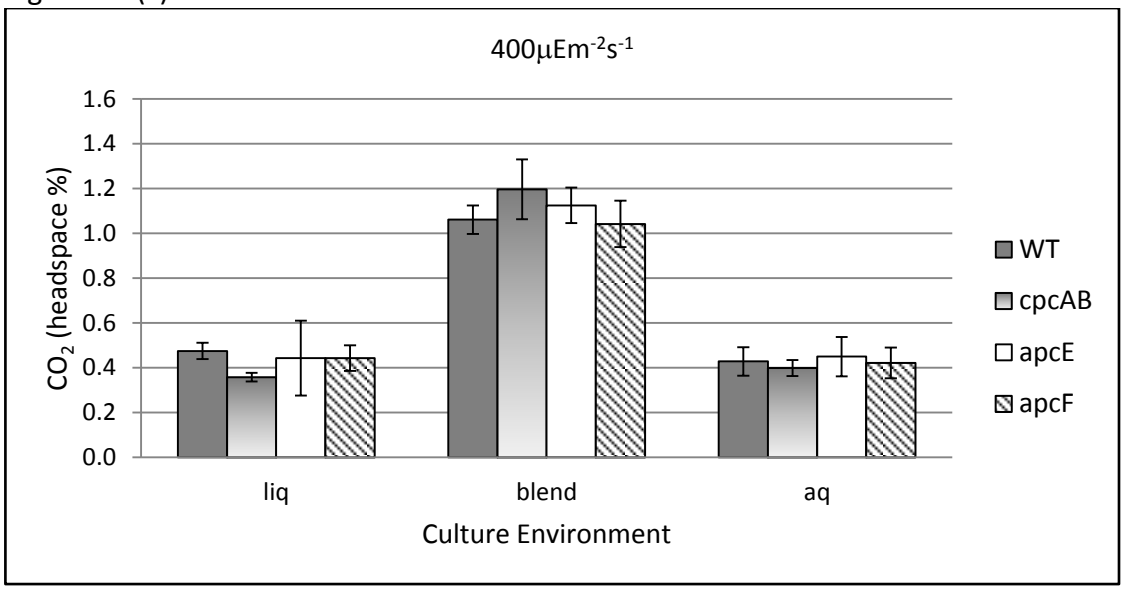

Figure 4-4: Carbon dioxide production from all four strains, encapsulated in two types of silica gels and liquid controls, conditioned under (a) 50 $\mu Em^{-2}s^{-1}$ light, (b) 200 $\mu Em^{-2}s^{-1}$, and (c) 400 $\mu Em^{-2}s^{-1}$. "Liq" = liquid culture; "blend" = an ORMOSIL alkoxide gel composed of 80% TEOS and 20% MTES; "aq" = a gel derived from aqueous precursors. Error bars represent one standard deviation among triplicate samples.

4.4.2 - Glycogen Accumulation

Glycogen content was measured for samples prepared under 200 and 400 $\mu Em^{-2}s^{-1}$, after 48 hours in BG-11 and after 48 hours in EHB-1 (Figure 4-6). In BG-11, although there was variation between strains, all accumulated relatively little glycogen. Under 200 $\mu Em^{-2}s^{-1}$ with 48 hours conditioning in EHB-1, all strains accumulated glycogen at approximately 46 to 53 $\mu g/OD_{730}$-mL, corresponding to approximately a 50-fold increase in stored glycogen over BG-11. Under 400 $\mu Em^{-2}s^{-1}$ with 48 hours conditioning in EHB-1, *wt*, ΔapcE, and ΔapcF cells accumulated approximately 150 $\mu g/OD_{730}$-mL glycogen while ΔcpcAB cells accumulated

approximately 94 μg/OD_{730}-mL. Glycogen accumulation, presumably the energy source for fermentative hydrogen production, approximately tripled for three of the four strains with a doubling in light intensity.

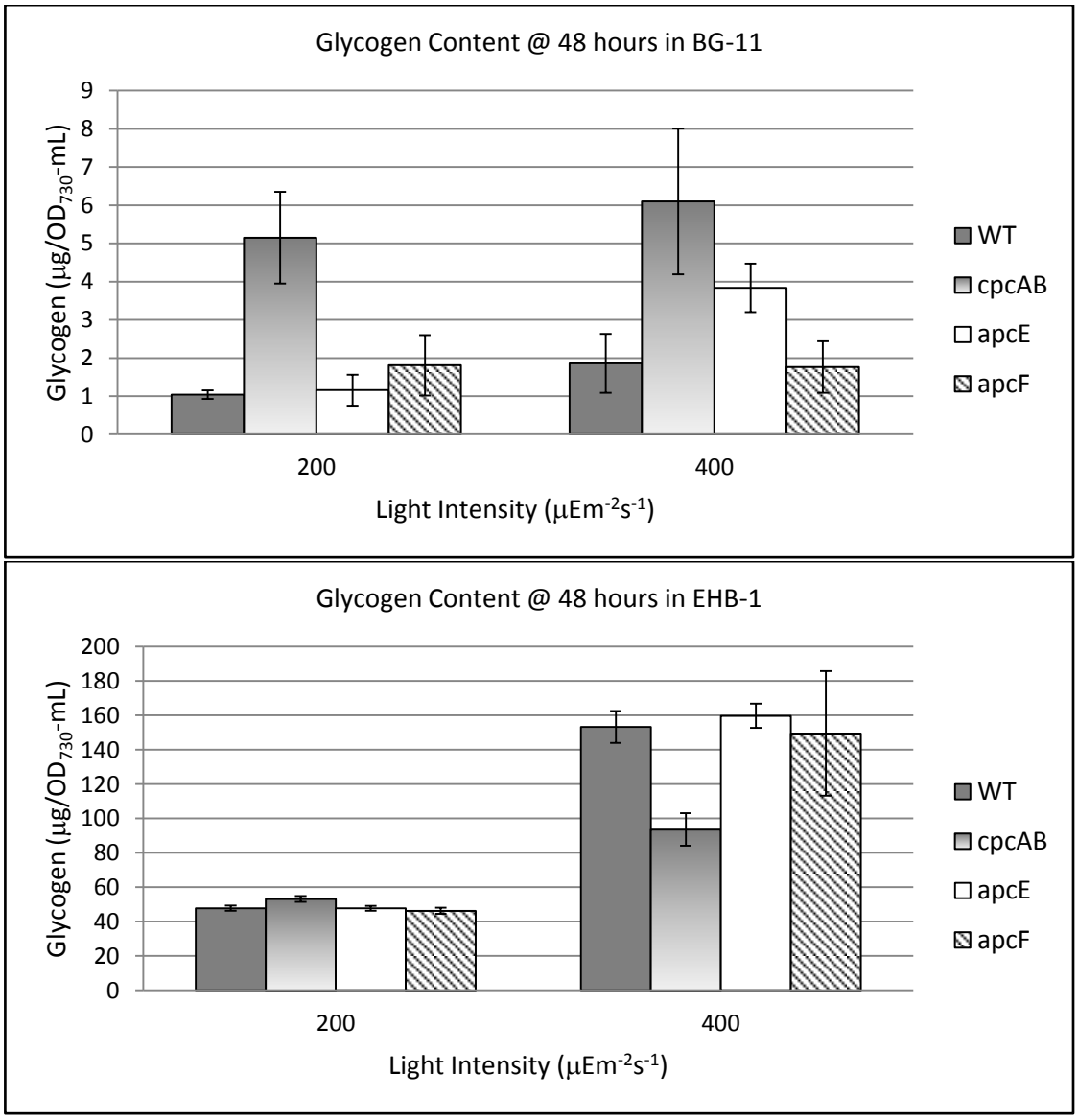

Figure 4-5: Glycogen content from cultures grown under 200 and 400 μ$Em^{-2}s^{-1}$ light, after acclimating in BG-11 for 48 hours (top) and conditioning in EHB-1 for 48 hours (bottom). Glycogen content was normalized to a per unit OD_{730} basis to account for

increases in culture density. Error bars represent one standard deviation among triplicate samples.

4.4.3 - Chlorophyll Fluorescence

Chlorophyll fluorescence was measured for *wt* cells and the three mutant strains, grown under three light intensities (50, 200, and 400 $\mu Em^{-2}s^{-1}$), to determine the influence of the antennae mutations on the quantum efficiency of PSII (F_v/F_m dark acclimated, ϕPSII light acclimated), the efficiency of the photoantennae (F_v'/F_m'), and photochemical (q_P) and nonphotochemical (q_N) quenching parameters. Figure 4-6 illustrates typical fluorescence traces for cultures acclimated for two days in BG-11 at (a) 200 $\mu Em^{-2}s^{-1}$ light and (b) 400 $\mu Em^{-2}s^{-1}$ light (fluorescence from cultures under 50 $\mu Em^{-2}s^{-1}$ light was very similar to those under 200 $\mu Em^{-2}s^{-1}$ light, and is not shown).

Figure 4-6(a)

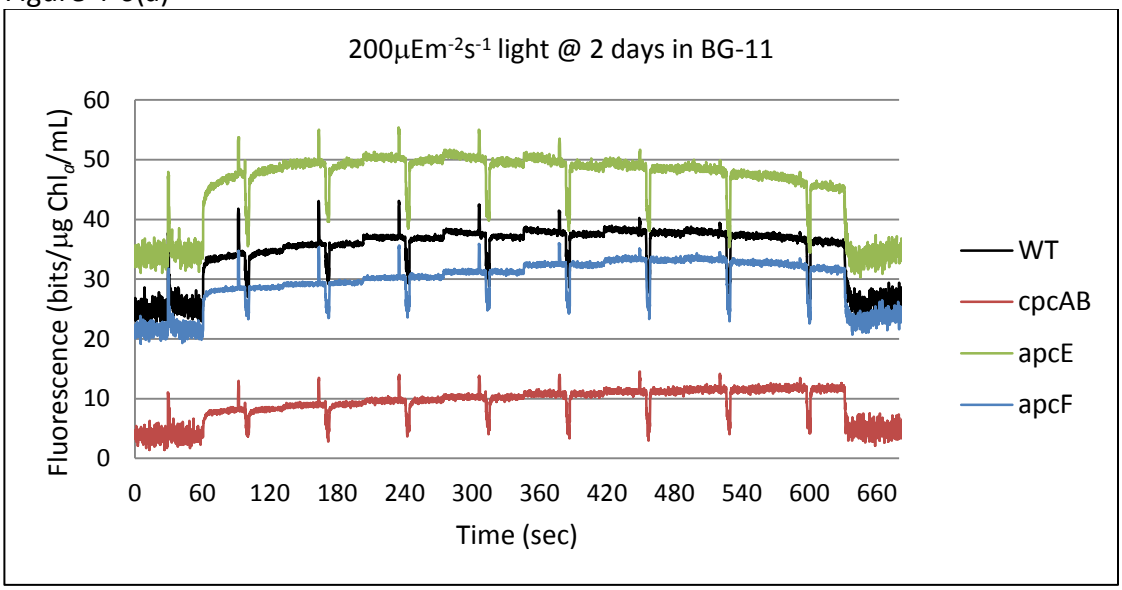

Figure 4-6(b)

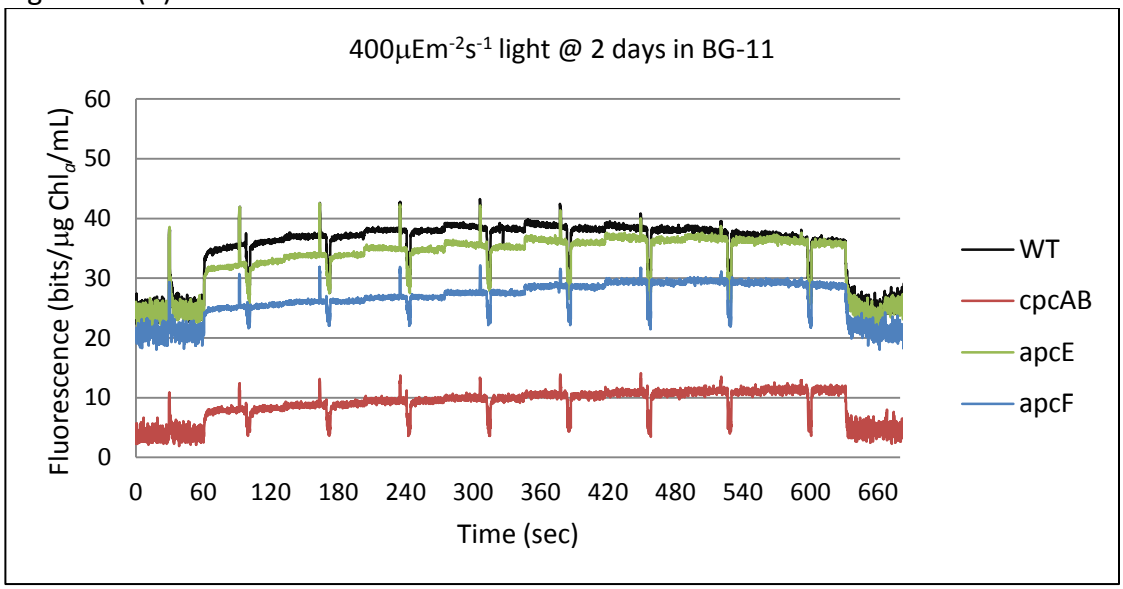

Figure 4-6: Fluorescence trace for *wt* and each antennae mutant, after 2 days in BG-11 at constant 200 or 400 $\mu Em^{-2}s^{-1}$ illumination, normalized per μg chlorophyll.

The ΔcpcAB strain shows a weaker fluorescence signal, indicative of its mutation, lacking rods attached to the PBS. As a result, the strain has difficulty saturating PSII reaction centers and, perhaps more importantly, also has limited ability to direct energy to PSI. Under 200 $\mu Em^{-2}s^{-1}$ light, the ΔapcF strain behaves most like *wt* cells, as expected, while the ΔapcE strain shows a stronger fluorescence signal. Under 400 $\mu Em^{-2}s^{-1}$ light, *wt* and ΔcpcAB cells present fluorescence signals nearly identical to those exhibited under 200 $\mu Em^{-2}s^{-1}$, while in the ΔapcF and ΔapcE strains, fluorescence decreases approximately 10% and 30%, respectively.

The fluorescence traces were used to calculate ϕPSII (Figure 4-7a), F_v'/F_m' (Figure 4-7b), q_P (Figure 4-7c), and q_N (Figure 4-7d). These parameters were calculated over a range of actinic light intensities up to approximately 1,000 $\mu Em^{-2}s^{-1}$. It should be noted that there are varying methods of calculating some of these

parameters. The equations shown in Table 1 were used consistently throughout to provide a qualitative comparison across the strains under the same conditions. The parameters shown in Figure 4-7 were for cells acclimated under 200 $\mu Em^{-2}s^{-1}$ light in BG-11. Cells acclimated with 50 and 400 $\mu Em^{-2}s^{-1}$ light showed slightly different absolute values of the parameters but similar overall trends (data not shown).

Figure 4-7(a)

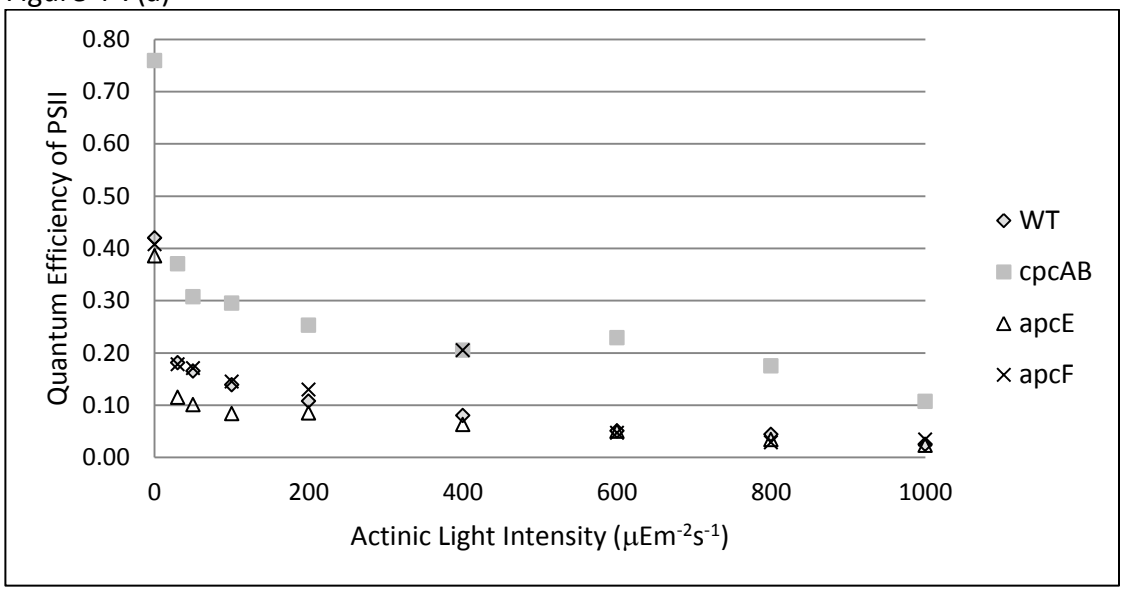

Figure 4-7(b)

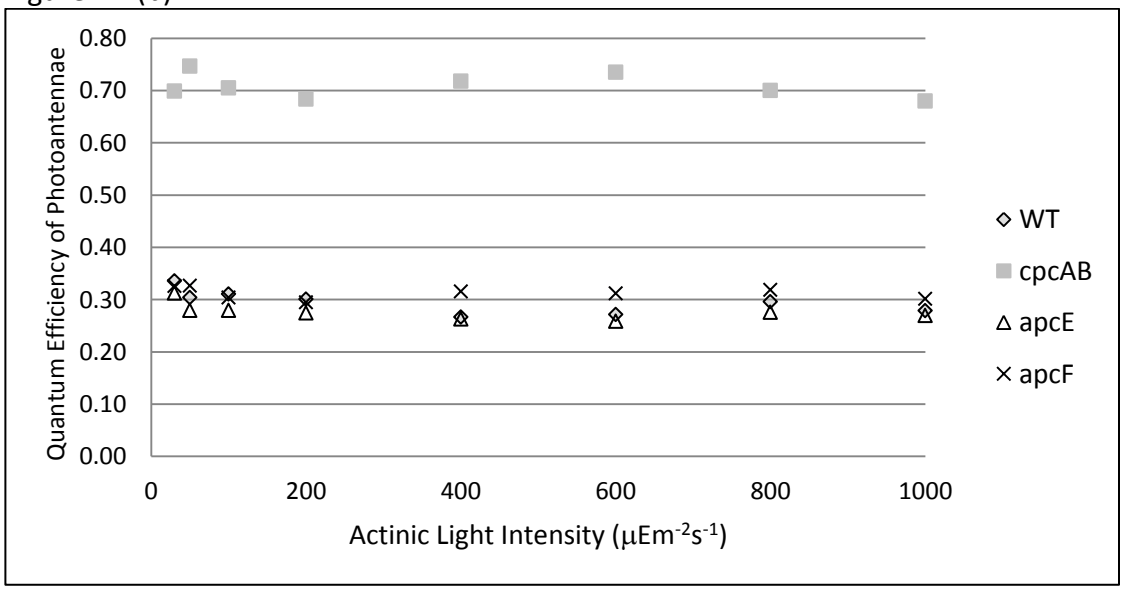

Figure 4-7(c)

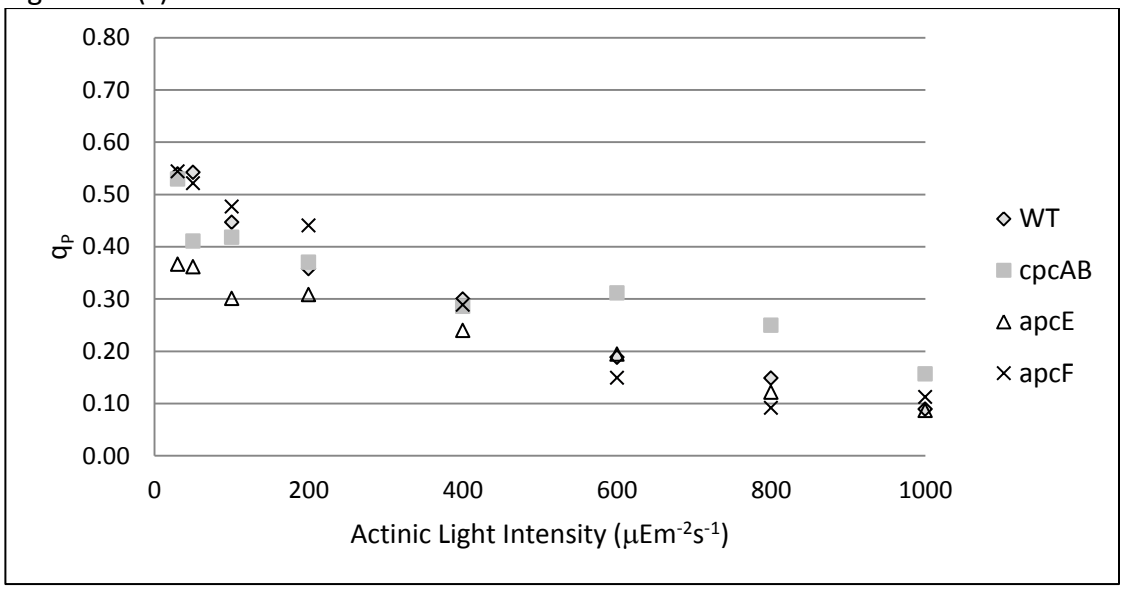

Figure 4-7(d)

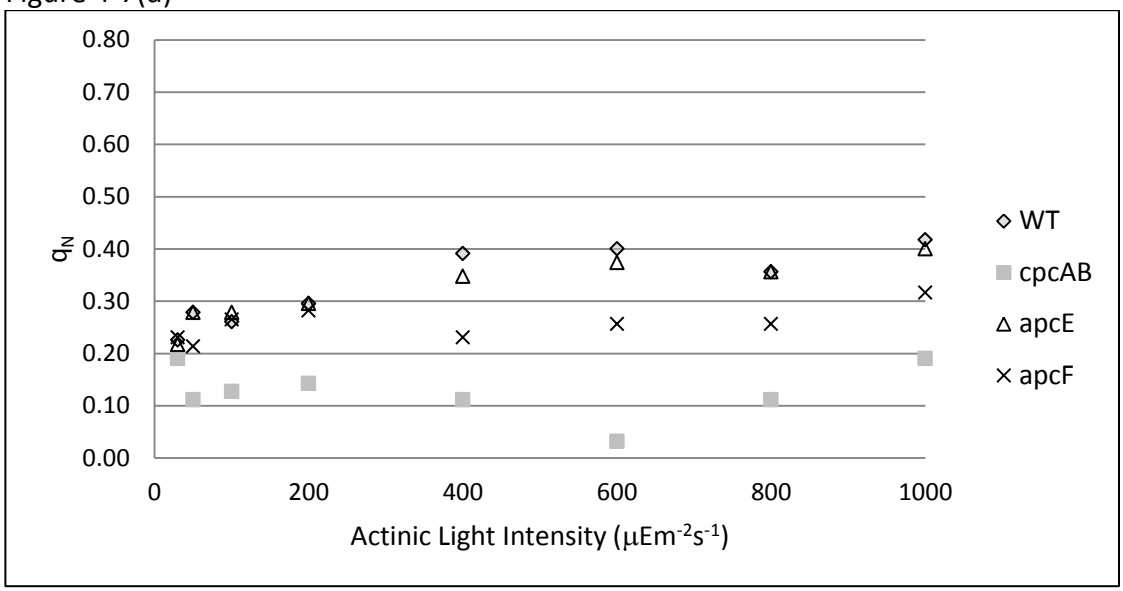

Figure 4-7: (a) The quantum efficiency of PSII (F_v/F_m for dark acclimated cells with actinic light = 0; ϕPSII for all actinic light intensities $\neq$ 0); (b) the quantum efficiency of the PSII photoantennae (F_v'/F_m'); (c) the coefficient of photochemical quenching; and (d) the coefficient of nonphotochemical quenching. All results from cell strains grown under 200 μEm^{-2}s^{-1} light.

The quantum efficiency of PSII gives an estimate of the efficiency at which absorbed photons achieve reduction of the first quinone acceptor, Q_A. Typical values for healthy, dark-acclimated plants may approach 0.8, with lower values indicating some inhibition of PSII activity. However, in cyanobacteria, values are often lower and more variable due to contributions to the fluorescence signal from PSI chlorophyll and changes in excitation energy distribution between the photosystems [57]. As a result, this parameter is more useful for relative comparisons between cultures with similar treatments rather than for drawing conclusions about PSII activity based solely on absolute values [56]. ϕPSII for the ΔcpcAB mutant is significantly higher than in the other three strains (Figure 4-7a). As expected, efficiency decreased for all strains at increasing light intensity. More striking is the high values of F_v'/F_m' for the ΔcpcAB strain (Figure 4-7b), which held steady at approximately 0.7 up to a light intensity of 1,000 $\mu Em^{-2}s^{-1}$. This parameter provides an indication of the efficiency of energy transfer from the PBS to the reaction centers. All four strains had similar q_P values up to 400 $\mu Em^{-2}s^{-1}$, but at light intensities ≥600 $\mu Em^{-2}s^{-1}$, the ΔcpcAB strain had slightly larger q_P values (Figure 4-7c). Although q_P behaves differently for cyanobacteria as compared to plants, it is expected to give a reasonable comparison of the proportion of open PSII reaction centers [57]. Correspondingly, the ΔcpcAB strain also showed q_N values that were consistently lower across all light intensities (Figure 4-7d), suggesting lower losses to nonphotochemical quenching processes.

4.4.4 - Pigment Composition

The primary pigments, chlorophyll *a*, PC, and APC were measured in all four strains after 48 hours in BG-11 under each light intensity, and after 48 hours in EHB-1 at the same light intensities (Figure 4-8). Chlorophyll content (normalized to OD_{730}) did not vary dramatically between *wt* cells and each of the mutant strains, which is consistent with other investigations with similar antennae mutants [31, 61].

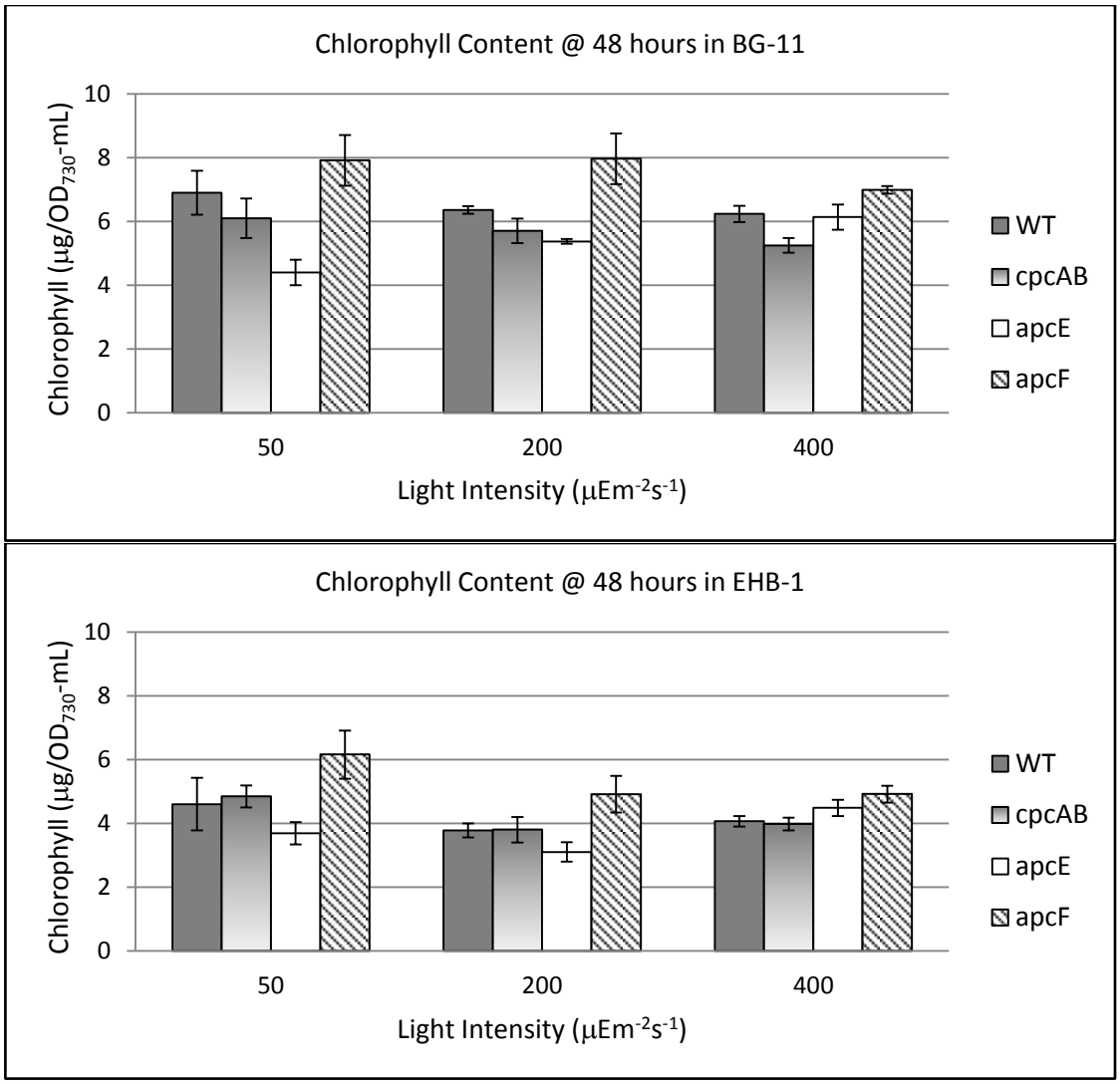

Figure 4-8: Chlorophyll concentrations for all four strains after 48 hours in BG-11 (top) and after another 48 hours in EHB-1 (bottom). Error bars represent one standard deviation among triplicate samples.

The ΔapcE and ΔcpcAB strains contained slightly less or similar amounts of chlorophyll compared to *wt* cells, the difference being most pronounced at the lowest light intensity, while ΔapcF cells contained slightly more. The amount of chlorophyll in each strain also did not vary dramatically across light intensities, and

decreased moderately (≤ ~40%) when the cultures were shifted to EHB-1 media for 2 days of glycogen accumulation under constant illumination. Chlorosis, or the degradation of chlorophyll under nitrogen and sulfur stress, was an expected result.

PC content varied more dramatically as compared to chlorophyll (Figure 4-9). As expected, the ΔcpcAB strain contained very little PC, uniformly in the range of 3 to 5 μg/OD_{730}-mL, compared with approximately 35 μg/OD_{730}-mL for *wt* cells grown at 50 or 200 μ$Em^{-2}s^{-1}$. The ΔcpcAB mutant cannot synthesize α and β phycocyanin, although it still synthesizes phycocyanobilin, the chromophore used in both APC and PC. (The non-zero measurement is believed due to overlap in absorbance spectra of PC and APC at room temperature.) The ΔapcF mutant, which had the most *wt*-like phenotype, also had very similar or slightly lower PC content, while the ΔapcE had 60% to 88% the PC content of *wt* cells. After conditioning in EHB-1, PC content was dramatically reduced in all strains, by as much as 85% in some cases, except in ΔcpcAB. This decrease is likely due to catabolism of the phycobilisomes, which was an expected result of nitrogen and sulfur deprivation stress placed upon the cells by the EHB-1 media. Cyanobacteria are well known to catabolize PBS under sulfur and nitrogen stress, beginning with distal PC rods and continuing to the APC core, in a process mediated by nblA1 [25, 62-65].

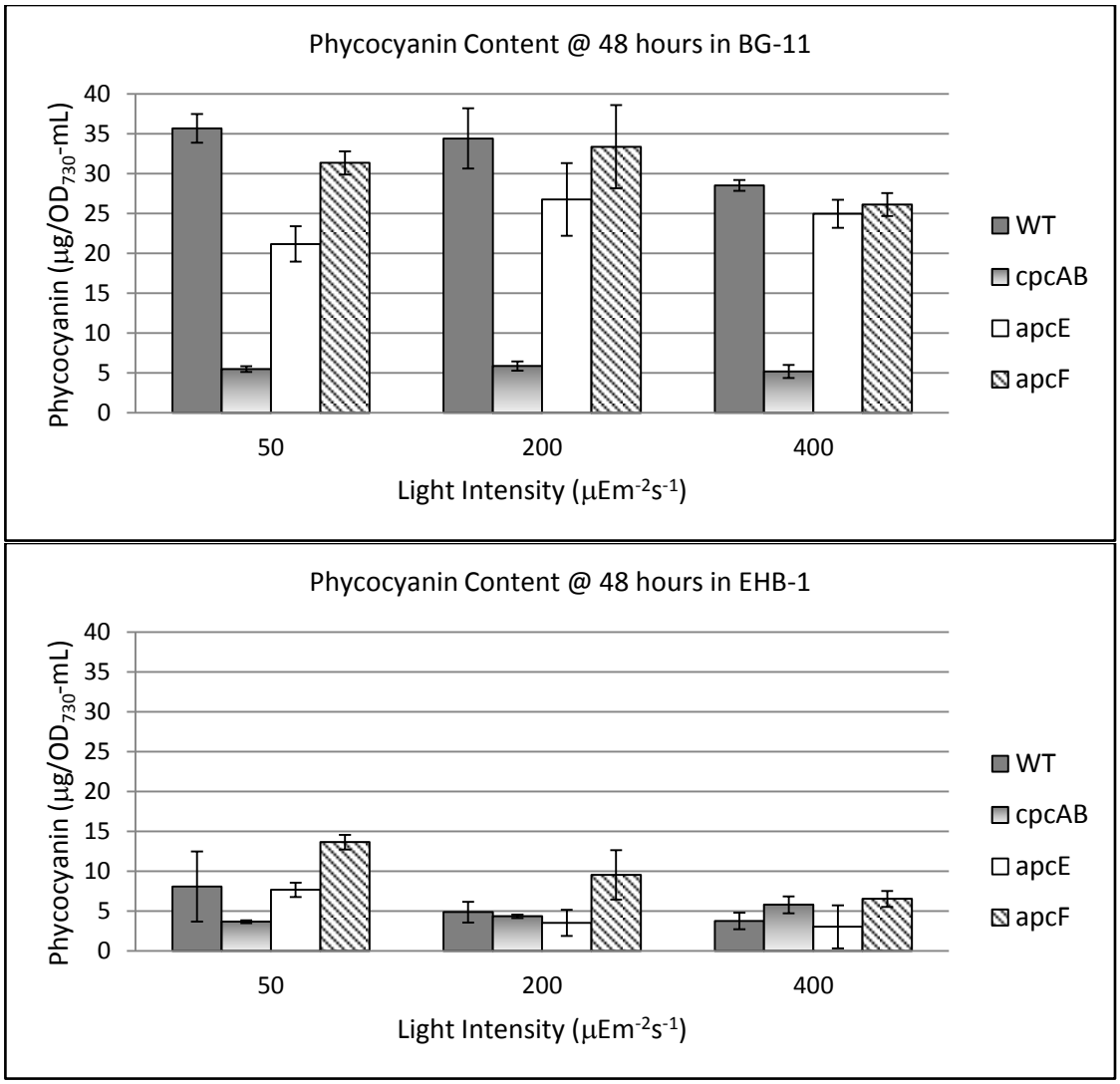

Figure 4-9: PC concentrations for all four strains after 48 hours in BG-11 (top) and after another 48 hours in EHB-1 (bottom). Error bars represent one standard deviation among triplicate samples.

APC content is illustrated in Figure 4-10. In BG-11 media, the three antennae mutants had similar APC contents across all three light intensities, and consistently less than *wt* cells, although the differences were most pronounced at the lowest light

intensity (~40% less under 50 $\mu Em^{-2}s^{-1}$, ~25% less under 200 $\mu Em^{-2}s^{-1}$, and ~35% less for ΔcpcAB and ΔapcF cells and 10% less for ΔapcE cells under 400 $\mu Em^{-2}s^{-1}$ light).

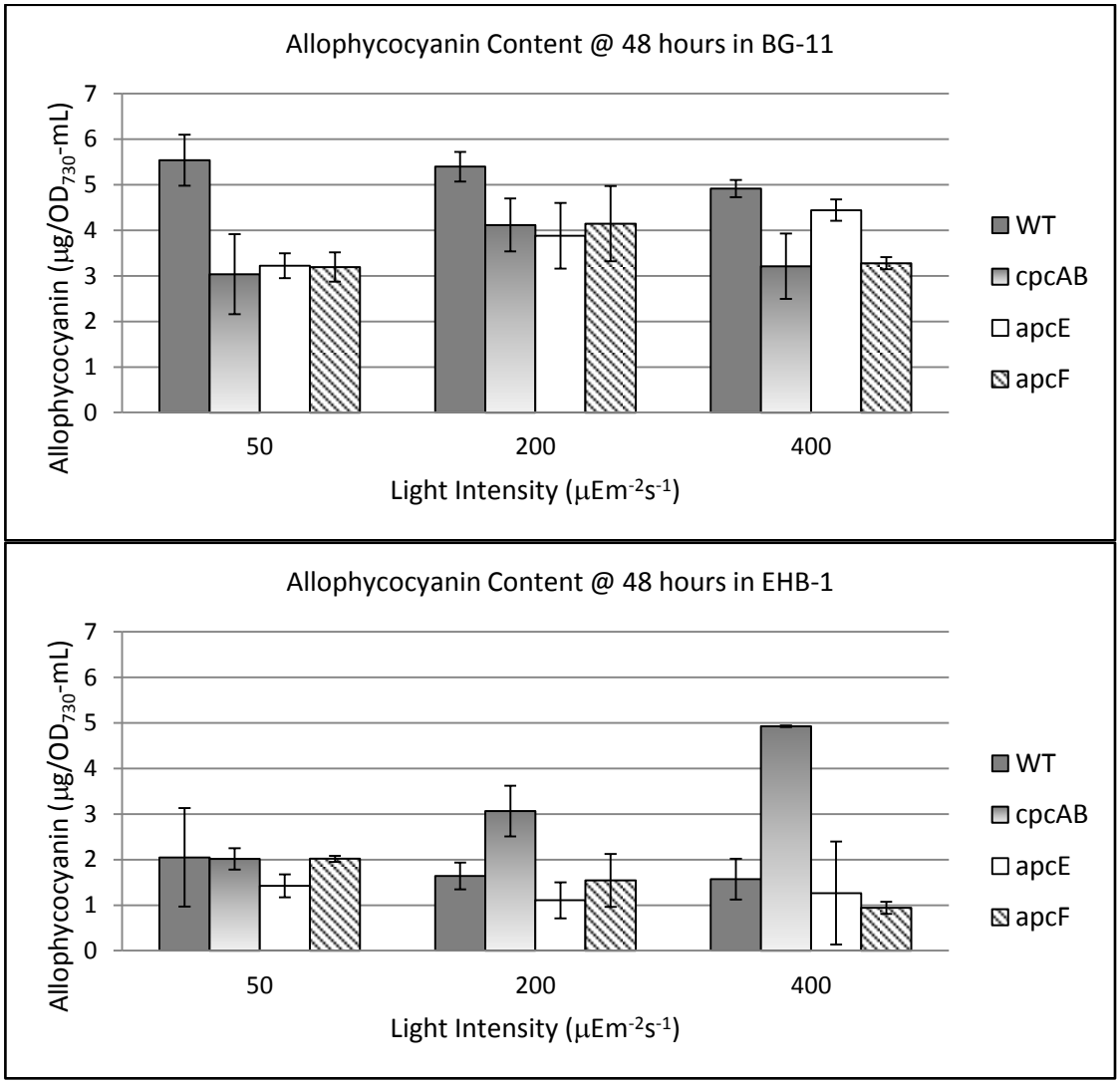

Figure 4-10: APC concentrations for all four strains after 48 hours in BG-11 (top) and after another 48 hours in EHB-1 (bottom). Error bars represent one standard deviation among triplicate samples.

It was somewhat surprising to detect amounts of APC in the ΔapcE mutant comparable to the other mutants considering this strain cannot assemble a

functional PBS core. It is unknown whether this may be due to spectral overlap with PC, as suspected with the detection of PC in the ΔcpcAB mutant, or because the degradation pathways for the APC core, which are comparatively less well understood than the PC degradation pathways, are slower or less efficient. As with PC, APC content is dramatically diminished with conditioning in EHB-1. The one exception is in the ΔcpcAB mutant conditioned under 400 $\mu Em^{-2}s^{-1}$ light, which actually showed an increase in APC content.

4.5 - Discussion

4.5.1 - Hydrogen Production & Glycogen Accumulation

Although fluorescence data suggested that the ΔcpcAB mutant was more efficient at directing absorbed excitation energy through the photoantennae toward the photosystem reaction centers (higher F_v/F_m and F_v'/F_m' values coupled with lower q_N values), this did not manifest in dramatically improved light utilization toward photochemistry (i.e., slightly improved q_P) leading to higher glycogen storage. At 200 $\mu Em^{-2}s^{-1}$, the mutant stored a similar amount of glycogen as did the other three strains, and at 400 $\mu Em^{-2}s^{-1}$ it stored approximately 75% the amount of glycogen as the other strains. Hydrogen production by ΔcpcAB cells under both conditions was also about 75% of that by *wt* cells, initially indicating the mutant was less efficient at fermenting glycogen to hydrogen when acclimated at 200 $\mu Em^{-2}s^{-1}$, and equally efficient as *wt* cells when acclimated at 400 $\mu Em^{-2}s^{-1}$.

However, considering Figures 4-8, 4-9, and 4-10 together, it becomes clear the ΔcpcAB mutant contained less pigment overall, per mL of culture at approximately the same cell density, when compared to the other three strains prior to incubating in EHB-1. If the amount of glycogen accumulated during incubation in EHB-1 is normalized to total pigment content upon the beginning of that incubation, the ΔcpcAB mutant actually appears to store more glycogen per unit of pigment

when compared to the other strains (Figure 4-11a). Furthermore, if hydrogen production is normalized on a similar per unit of pigment basis, this also indicates the ΔcpcAB strain produces more hydrogen per μg of pigment (Figure 4-11b). At similar cell density compared to the other strains, ΔcpcAB cells store less glycogen and produce less hydrogen, net, yet are able to more efficiently leverage the pigment they have toward these two objectives. Although more investigation is warranted, this leads to the conclusion that more light is transmitted through the ΔcpcAB cultures compared to the other strains, meaning it remains a good candidate for hydrogen production, possibly better utilized either at higher cell density or as the top layer in a system including some or all of the other strains. However, due to disruptions to two key nonchemical quenching pathways, as mentioned, the possibility that the ΔcpcAB is more vulnerable to photoinhibition and photodamage at higher light intensities cannot be excluded.

Figure 4-11(a)

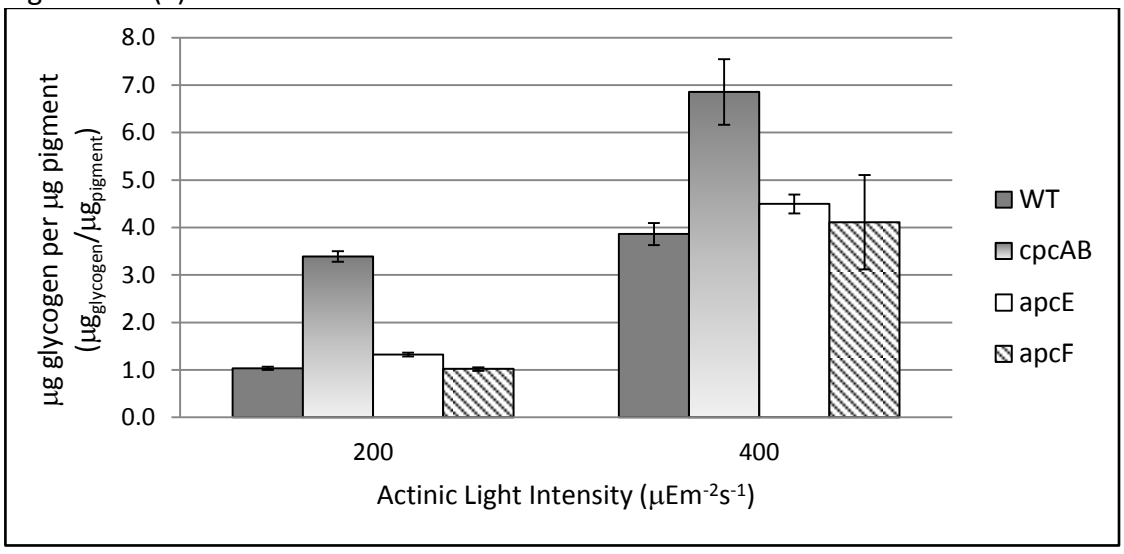

Figure 4-11(b)

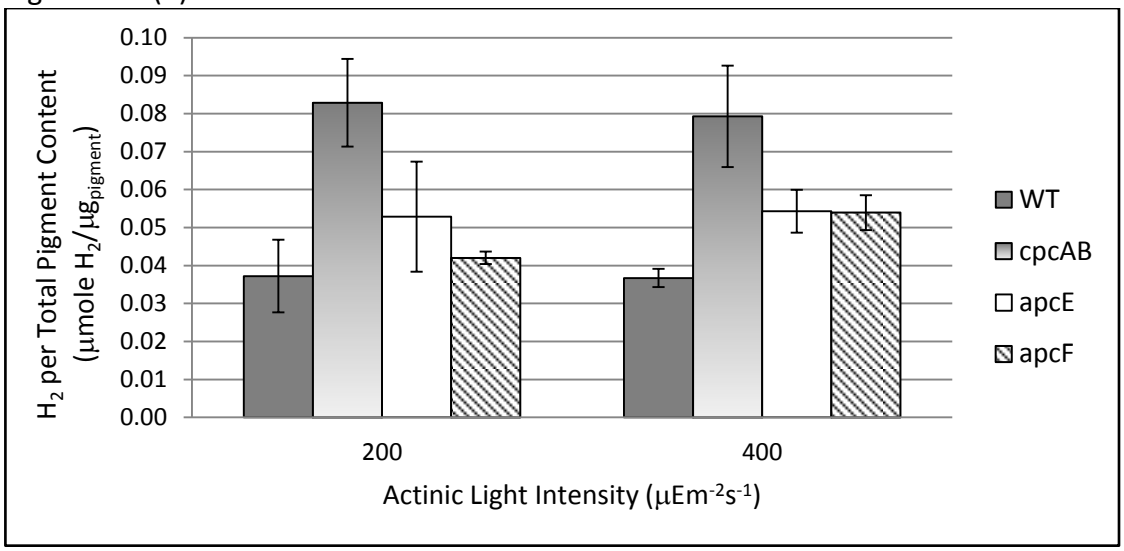

Figure 4-11: (a) glycogen content normalized per unit of total pigment content prior to initializing glycogen accumulation in EHB-1 media. (b) Hydrogen production normalized per unit of total pigment content, prior to glycogen accumulation. Error bars represent one standard deviation among triplicate samples.

The ΔapcE and ΔapcF mutants accumulated amounts of glycogen similar to *wt* cells under both 200 and 400 $\mu Em^{-2}s^{-1}$ light. Hydrogen production from 50 and 200 $\mu Em^{-2}s^{-1}$ conditioning was also similar to that by *wt* cells, although at 400 $\mu Em^{-2}s^{-1}$, hydrogen accumulation from these two mutants was similar and about 25% higher than that by *wt* cells. There was a slight but insignificant increase in hydrogen production with an increase in light intensity during glycogen accumulation for the ΔapcE and ΔapcF, but the primary cause of the difference with *wt* cells was a significant decrease in hydrogen production from the *wt* strain. One possible explanation is that the *wt* cells incubated under higher light intensity were subsequently devoting more energy toward cellular maintenance and repair, although this is not clearly indicated by the data. Slightly elevated q_N values compared to the three mutants (not shown) is the only indication the *wt* cells may

have been experiencing more photoinhibition under 400$\mu Em^{-2}s^{-1}$ light. However, these data do raise the question of whether light intensities above those examined in this investigation could provide still higher levels of hydrogen production from the antennae mutants.

In the indirect, fermentative pathway for hydrogen production used in the current investigation, it was expected that increased glycogen accumulation by antennae mutants under higher light combined with encapsulation would lead to higher hydrogen yields. However, this was not consistently observed. Although glycogen accumulation by the mutants increased substantially with higher light intensities, it was not significantly higher than in *wt* cells, and did not result in a corresponding increase in hydrogen production. The notable exception was at 400 $\mu Em^{-2}s^{-1}$, where the ΔapcE and ΔapcF mutants did show significantly more hydrogen production than *wt* cells (Figure 4-3c), as mentioned.

There are numerous possible explanations for these results. First, because the [Ni-Fe] hydrogenase enzyme is reversible, with hydrogen concentrations in the headspace exceeding 1% in some instances, some uptake activity was likely to have occurred. Without an effective way to draw away hydrogen as it is produced, uptake of hydrogen will complicate the ability to achieve full hydrogen production potential from this pathway. Second, although these mutations only directly affect PBS structure and function, which should have very little direct influence on fermentative hydrogen production, the mutations may have other unpredicted effects on the electron transport chain (ETC). The photosynthetic ETC is interconnected with the respiratory ETC, and although it is not active in the dark, changes in relative protein expression, redox balance, response to photoinhibition, and other metabolic demands that manifest during glycogen accumulation could certainly persist during anaerobic hydrogen production, thereby altering the yield of hydrogen from glycogen. Thirdly, with cells conditioned at higher light intensity, some energy that

might otherwise be available for glycogen accumulation leading to hydrogen production might be required to repair photodamage. Increasing light intensity from 200 to 400 $\mu Em^{-2}s^{-1}$ increased glycogen accumulation approximately three-fold, yet hydrogen production increased only slightly with the ΔapcE and ΔapcF strains, and decreased slightly with the ΔcpcAB and *wt* strains. However, as shown in Figure 4-11b, hydrogen yield per unit pigment was consistent between 200 and 400$\mu Em^{-2}s^{-1}$ for the *wt*, ΔcpcAB, and ΔapcE strains and improved slightly for the ΔapcF strain. Further investigation is required to explain how light intensity, light utilization, glycogen accumulation, and fermentative hydrogen production are related.

Hydrogen production also did not present a strong correlation with fermentative carbon dioxide production. Carbon dioxide production from all four strains was similar under similar conditions. In gels from aqueous precursors, cells produced similar to slightly more CO_2 as compared to liquid controls, yet produced 2.5 to 3.5 times more hydrogen. In contrast, fermentative CO_2 production was approximately three-fold higher from cells in alkoxide-derived gels, while hydrogen yield was comparable to slightly higher than the liquid controls. The one exception in terms of hydrogen production was the ΔapcF, which seemed to favor alkoxide-derived gels and produced nearly as much hydrogen as it did in gels from aqueous precursors. Its production of CO_2 was comparable to the other three strains. It is unclear why this occurred, although one likely explanation may be that the cells had to devote energy toward managing some amount of ethanol stress present in the alkoxide-derived gels. EtOH would be expected to attack membranes, including the thylakoids, necessitating increased metabolic activity for maintenance and repair. There is also some evidence that *Synechocystis* sp. PCC 6803 can use EtOH as a carbon source [66]. These data are unable to decipher which processes are occurring.

It is also unclear why hydrogen production was dramatically increased in cells encapsulated in gels from aqueous precursors. Encapsulated cells are in a confined

environment where they cannot grow or are not expected to be able to grow well, meaning this energy is available for increased production of secondary metabolites [7, 51]. However, the differences observed between hydrogen and carbon dioxide production in the alkoxide-derived gels versus the gels from aqueous precursors suggest that complicated metabolic effects may be taking place.

4.5.2 - Fluorescence, Photosynthetic Efficiency, & Pigment Profile

Fluorescence investigations were conducted to determine whether the mutant strains can utilize absorbed light more efficiently, with the ultimate objective being improved conversion efficiency of incident light energy to hydrogen energy. Fluorescence confirmed that the ΔcpcAB strain was deficient in its ability to harvest incident light, presenting a low fluorescence baseline (Figure 4-6). Because PSI fluorescence contributes significantly to fluorescence in cyanobacteria [57], this suggests that minimal excess excitation energy was reaching PSI chlorophylls. This mutant also presented a yellowish army-green phenotype with slower growth than *wt* cells (data not shown), consistent with other observations in the literature [31, 61]. Although this mutant may absorb less incident radiation, high values of F_v'/F_m' (Figure 4-7b) and low values of q_N (Figure 4-7d) as compared to the other three strains indicate this mutant is capable of efficiently using the light it does absorb. This conclusion is corroborated by the data in Figure 4-11, showing improved glycogen accumulation and hydrogen production per unit of pigment in this mutant.

As expected, the ΔapcF strain appeared most like *wt* cells in both fluorescence and phenotype, although the smaller increase in maximum fluorescence from dark acclimation to the onset of actinic light (first two peaks of the fluorescence trace in Figure 4-6) is indicative of an impaired transition from State 2 to State 1 [41]. Results with the ΔapcE strain were surprising, showing a high fluorescence signal with prolonged acclimation to actinic light of 200 $\mu Em^{-2}s^{-1}$ light (Figure 4-3a). Although the ΔapcE strain lacks a functional PBS, presumably the organism will still

have PC rods which can direct excitation energy to PSI [29, 33], where the majority of chlorophyll resides, contributing to the high fluorescence signal. In terms of photosynthetic efficiency and glycogen accumulation, this mutant was more similar to *wt* cells than expected. It is possible this mutant has increased its PSII/PSI ratio to compensate for the loss in excitation energy being directed toward PSII reaction centers, although further investigation is required to explore this hypothesis.

The analysis of photosynthetic pigments, including chlorophyll, PC, and APC, provided some expected as well as unexpected results. Chlorophyll content varied little between mutants and *wt* cells, although ΔapcF cells had a slight tendency toward more chlorophyll than the other three strains while ΔapcE cells less (Figure 4-8). This lends indirect evidence to the ΔapcE cells containing functional PC rods which preferentially direct excitation energy toward PSI. Chlorophyll content in PSI constitutes the majority of chlorophyll in cyanobacteria [57], so reduced chlorophyll content may indicate fewer PSI complexes, which would be expected if these photosystems were preferentially receiving more excitation energy. However, this cannot be confirmed without protein analysis. The slightly increased chlorophyll content in ΔapcF cells may indicate an increase in the PSI/PSII ratio, which would be an expected result if this strain is inhibited in its ability to transition out of State 1 to State 2. Again, this cannot be verified without protein analysis.

PC content was minimal in the ΔcpcAB cells, as expected, and fairly similar for the other three strains at intermediate and high light intensity (Figure 4-9). At low light, ΔapcE contained about 60% as much PC as *wt* cells. As mentioned, the predominant form of antenna in ΔapcE cells is expected to be PC-containing rods that preferentially direct energy to PSI. At lower light intensity, this mutant did have higher q_P values compared to *wt* cells (data not shown), which may mean it can utilize light more efficiently and therefore requires less pigment. This same phenomenon seems to be more pronounced in the ΔcpcAB strain, which has

significantly less pigment, particularly PC, yet has dramatically higher antennae efficiencies (F_v'/F_m') and can store similar amounts of glycogen compared to the other three strains, at least up to 200 $\mu Em^{-2}s^{-1}$ light. Together, these data support the conclusion that the antennae mutants can more efficiently use absorbed radiation, yet much additional investigation is required to determine the exact mechanisms.

Detecting APC in the ΔapcE mutant was an unexpected result. Spectral overlap with PC likely occurred, but the magnitude of the signal was comparable to the other two antennae mutants and only slightly below that of *wt* cells, whereas the small amount of PC detected in the ΔcpcAB was well below the other three strains. One possible explanation is that free chromophores may have been present [64], or the degradation pathway for unstable APC core subunits may not be as robust or as rapid as the mechanism mediated by NblA1 for the PC rods [63, 65].

Severe degradation of pigments while incubated in EHB-1 for glycogen accumulation, most evident with the degradation of PC, but also APC to some extent, and even a small amount of chlorophyll, is consistent with a well documented catabolic response to sulfur and nitrogen stress [25, 63]. Although it was not specifically explored as part of this investigation, if cycling between glycogen accumulation and hydrogen production is to be pursued as a means of prolonged hydrogen production, this stress must be managed. Placed back in the light with severely degraded antennae will, at the very least, require some time for the organisms to repair damage and/or synthesize new antennae, or, at worst, induce photoinhibition that might be lethal.

4.6 - Conclusion

Three antennae mutants of the cyanobacterium *Synechocystis* sp. PCC 6803 have been examined for photosynthetic efficiency, pigment production, glycogen accumulation, and hydrogen production while grown under three different light intensities. Cells were also encapsulated in silica gel in order to evaluate whether the

strains were amenable to the process and might yield more hydrogen. While the ΔcpcAB mutant, in particular, indicated improved photosynthetic efficiency as determined by fluorescence measurements, this did not result in a net improvement in glycogen accumulation or hydrogen production. However, this mutant also contained less pigment than the other strains, so on a per unit pigment basis, this strain stored significantly more glycogen and produced significantly more hydrogen. Conditioned under 400 $\mu Em^{-2}s^{-1}$ light, the ΔapcE and ΔapcF mutants accumulated glycogen in similar amounts as did *wt* cells, but produced approximately 25% more hydrogen when encapsulated in silica gel derived from aqueous precursors. When encapsulated in gels from aqueous precursors, all strains showed improved hydrogen production, varying from a 2.5 to 3.5 fold increase over liquid controls. Cells encapsulated in alkoxide-derived gels showed small increases in hydrogen production and a dramatic increase in fermentative CO_2 production. Additional work is warranted to determine how these, and possibly other, antennae mutants thrive under increasing light intensity, how they manage nonphotochemical quenching and photodamage, and ultimately, how well they may accumulate glycogen and produce hydrogen.

Acknowledgements

The authors wish to acknowledge the Air Force Office of Scientific Research, Grant # RF0260, for funding this research, and Chevron Energy Corp., Grant # V02640, for providing funding for the purchase of the FMS-1 fluorometer. The authors also thank Dr. Elizabeth Burrows, Dr. Jed Eberly, and Markael Luterra for helpful comments, and Soleil Rowan-Caneer for laboratory assistance.

Chapter 4 References

1 Appel J, Phunpruch S, Steinmüller K, Schulz R. The Bidirectional Hydrogenase of Synechocystis sp. PCC 6803 Works as an Electron Valve during Photosynthesis. Arch Microbiol. 2000; 173: 333-338.

2 Cournac L, Mus F, Bernard L, Guedeney G, Vignais P, Peltier G. Limiting Steps of Hydrogen Production in Chlamydomonas reinhartii and Synechocystis sp. PCC 6803 as Analysed by Light Induced Gas-Exchange Transients. Int J Hydrogen Energy 2002; 27: 1229-1237.

3 Cournac L, Guedeney Gv, Peltier G, Vignais PM. Sustained Photoevolution of Molecular Hydrogen in a Mutant of Synechocystis sp. Strain PCC 6803 Deficient in the Type 1 NADPH-Dehydrogenase Complex. J Bacteriol 2004; 186(6): 1737-1746.

4 Antal TK, Lindblad P. Production of H_2 by sulphur-deprived cells of the unicellular cyanobacteria Gloeocapsa alpicola and Synechocystis sp. PCC 6803 during dark incubation with methane or at various extracellular pH. J Appl Microbiol 2005; 98(1): 114-120.

5 Antal TK, Oliveira P, Lindblad P. The bidirectional hydrogenase in the cyanobacterium Synechocystis sp. strain PCC 6803. Int J Hydrogen Energy 2006; 31(11): 1439-1444.

6 Burrows EH, Chaplen FWR, Ely RL. Optimization of media nutrient composition for increased photofermentative hydrogen production by Synechocystis sp. PCC 6803. Int J Hydrogen Energy 2008; 33(21): 6092-6099.

7 Dickson DJ, Page CJ, Ely RL. Photobiological hydrogen production from Synechocystis sp. PCC 6803 encapsulated in silica sol-gel. Int J Hydrogen Energy 2009; 34(1): 204-215.

8 Navarro E, Montagud A, Córdoba PFd, Urchueguía JF. Metabolic flux analysis of the hydrogen production potential in Synechocystis sp. PCC6803. Int J Hydrogen Energy 2009; 34(21): 8828-8838.

9 Tamagnini P, Costa J-Ls, Almeida Lg, Oliveira M-J, Salema R, Lindblad P. Diversity of Cyanobacterial Hydrogenases, a Molecular Approach. Curr Microbiol 2000; 40(6): 356-361.

10 Tamagnini P, Axelsson R, Lindberg P, Oxelfelt F, Wunschiers R, Lindblad P. Hydrogenases and hydrogen metabolism of cyanobacteria. Microbiol Mol Biol Rev 2002; 66: 1 - 20.

11 Ghirardi ML, Posewitz MC, Maness P-C, Dubini A, Yu J, Seibert M. Hydrogenases and Hydrogen Photoproduction in Oxygenic Photosynthetic Organisms. Annual Review of Plant Biology 2007; 58(1): 71-91.

12 Vignais PM, Billoud B, Meyer J. Classification and phylogeny of hydrogenases. FEMS Microbiology Reviews 2001; 25(4): 455-501.

13 Vignais PM, Colbeau A. Molecular biology of microbial hydrogenases. Current Issues in Molecular Biology 2004; 6: 159-188.

14 Vignais PM, Billoud B. Occurrence, Classification, and Biological Function of Hydrogenases: An Overview. Chemical Reviews 2007; 107(10): 4206-4272.

15 Burrows EH, Chaplen FWR, Ely RL. Effects of selected electron transport chain inhibitors on 24-h hydrogen production by Synechocystis sp. PCC 6803. Bioresour Technol 2010; 102: 3062-3070.

16 Ghirardi ML, Dubini A, Yu J, Maness P-C. Photobiological hydrogen-producing systems. Chem Soc Rev 2009; 38(1): 52-61.

17 Melis A. Solar energy conversion efficiencies in photosynthesis: Minimizing the chlorophyll antennae to maximize efficiency. Plant Science 2009; 177(4): 272-280.

18 Nakajima Y, Ueda R. Improvement of microalgal photosynthetic productivity by reducing the content of light harvesting pigment. Journal of Applied Phycology 1999; 11: 195-201.

19 Polle JEW, Kanakagiri S-D, Melis A. tla1, a DNA insertional transformant of the green alga Chlamydomonas reinhardtii with a truncated light-harvesting chlorophyll antenna size. Planta 2003; 217(1): 49-59.

20 Berberoglu H, Pilon L, Melis A. Radiation characteristics of Chlamydomonas reinhardtii CC125 and its truncated chlorophyll antenna transformants tla1, tlaX and tla1-CW+. Int J Hydrogen Energy 2008; 33(22): 6467-6483.

21 Prince R. The Photobiological Production of Hydrogen: Potential Efficiency and Effectiveness as a Renewable Fuel. Critical Reviews in Microbiology 2005; 31: 19-31.

22 Kruse O, Rupprecht J, Mussgnug JH, Dismukes GC, Hankamer B. Photosynthesis: a blueprint for solar energy capture and biohydrogen production technologies. Photochemical & Photobiological Sciences 2005b; 4(12): 957-970.

23 Benemann JR. Hydrogen production by microalgae. Journal of Applied Phycology 2000; 12(3): 291-300.

24 Carrieri D, Kolling D, Ananyev G, Dismukes C. Prospecting for biohydrogen fuel. Industrial Biotechnology 2006; 2: 133-137.

25 Grossman AR, Schaefer MR, Chiang GG, Collier JL. Environmental effects on the light-harvesting complex of cyanobacteria. J Bacteriol 1993; 175(3): 575-582.

26 Ughy B, Ajlani G. Phycobilisome rod mutants in Synechocystis sp. strain PCC6803. Microbiology 2004; 150(12): 4147-4156.

27 Liu H, Grot S, Logan BE. Electrochemically Assisted Microbial Production of Hydrogen from Acetate. Environmental Science & Technology 2005; 39(11): 4317-4320.

28 Arteni AA, Ajlani G, Boekema EJ. Structural organisation of phycobilisomes from Synechocystis sp. strain PCC6803 and their interaction with the membrane. Biochimica et Biophysica Acta (BBA) - Bioenergetics 2009; 1787(4): 272-279.

29 Kondo K, Ochiai Y, Katayama M, Ikeuchi M. The Membrane-Associated CpcG2-Phycobilisome in Synechocystis: A New Photosystem I Antenna. Plant Physiol 2007; 144(2): 1200-1210.

30 Kondo K, Mullineaux CW, Ikeuchi M. Distinct roles of CpcG1-phycobilisome and CpcG2-phycobilisome in state transitions in a cyanobacterium Synechocystis sp. PCC 6803. Photosynthesis Research 2009; 99: 217-225.

31 Ajlani G, Vernotte C, DiMagno L, Haselkorn R. Phycobilisome core mutants of Synechocystis PCC 6803. Biochimica et Biophysica Acta (BBA) - Bioenergetics 1995; 1231(2): 189-196.

32 Ashby MK, Mullineaux CW. The role of ApcD and ApcF in energy transfer from phycobilisomes to PS I and PS II in a cyanobacterium. Photosynthesis Research 1999; 61: 169-179.

33 Mullineaux CW. Phycobilisome-reaction centre interaction in cyanobacteria. Photosynthesis Research 2008; 95(2): 175-182.

34 Shen G. Synechocystis sp. PCC 6803 Strains lacking Photosystem I and Phycobilisome Function. The Plant Cell 1993; 5: 1853-1863.

35 Rakhimberdieva MG, Vavilin DV, Vermaas WFJ, Elanskaya IV, Karapetyan NV. Phycobilin/chlorophyll excitation equilibration upon carotenoid-induced non-photochemical fluorescence quenching in phycobilisomes of the cyanobacterium Synechocystis sp. PCC 6803. Biochimica et Biophysica Acta (BBA) - Bioenergetics 2007a; 1767(6): 757-765.

36 Rakhimberdieva MG, Bolychevtseva YV, Elanskaya IV, Karapetyan NV. Protein-protein interactions in carotenoid triggered quenching of phycobilisome fluorescence in Synechocystis sp. PCC 6803. FEBS Lett 2007b; 581(13): 2429-2433.

37 Stadnichuk IN, Lukashev EP, Elanskaya IV. Fluorescence changes accompanying short-term light adaptations in photosystem I and photosystem II of the cyanobacterium Synechocystis sp. PCC 6803 and phycobiliprotein-impaired mutants: State 1/State 2 transitions and carotenoid-induced quenching of phycobilisomes. Photosynthesis Research 2009; 99: 227-241.

38 Rakhimberdieva MG, Elanskaya IV, Vermaas WFJ, Karapetyan NV. Carotenoid-triggered energy dissipation in phycobilisomes of Synechocystis sp. PCC 6803 diverts excitation away from reaction centers of both photosystems. Biochimica et Biophysica Acta (BBA) - Bioenergetics 2010; 1797(2): 241-249.

39 Yeremenko N. Supramolecular Organization and Dual Function of the IsiA Chlorophyll-Binding Protein in Cyanobacteria. Biochemistry 2004; 43: 10308-10313.

40 Joshua S, Bailey S, Mann NH, Mullineaux CW. Involvement of Phycobilisome Diffusion in Energy Quenching in Cyanobacteria. Plant Physiol 2005a; 138(3): 1577-1585.

41 Bailey S, Grossman A. Photoprotection in Cyanobacteria: Regulation of Light Harvesting. Photochem Photobiol 2008; 84(6): 1410-1420.

42 Bernát G, Waschewski N, Rögner M. Towards efficient hydrogen production: the impact of antenna size and external factors on electron transport

dynamics in Synechocystis PCC 6803. Photosynthesis Research 2009; 99(3): 205-216.

43 Nassif N, Roux Cc, Coradin T, Rager M-N, Bouvet OMM, Livage J. A Sol-gel Matrix to Preserve the Viability of Encapsulated Bacteria. J Mater Chem 2003; 13: 203-208.

44 Taylor A, Finnie KS, Bartlett JR, Holden PJ. Encapsulation of Viable Aerobic Microorganisms in Silica Gels. J Sol Gel Sci Technol 2004; 32: 223-228.

45 Kuncova G, Podrazky O. Monitoring of the Viability of Cells Immobilized by Sol-Gel Process. J Sol Gel Sci Technol 2004; 31: 335 - 342.

46 Desimone MF, De Marzi MC, Copello GJ, Fernandez MM, Pieckenstain FL, Malchiodi EL, et al. Production of recombinant proteins by sol-gel immobilized Escherichia coli. Enzyme Microb Technol 2006; 40(1): 168-171.

47 Nguyen-Ngoc H, Tran-Minh C. Sol-gel process for vegetal cell encapsulation. Materials Science and Engineering: C 2007a; 27(4): 607-611.

48 Nguyen-Ngoc H, Tran-Minh C. Fluorescent biosensor using whole cells in an inorganic translucent matrix. Anal Chim Acta 2007b; 583(1): 161-165.

49 Fiedler D, Hager U, Franke H, Soltmann U, Bottcher H. Algae biocers: astaxanthin formation in sol-gel immobilised living microalgae. J Mater Chem 2007; 17(3): 261-266.

50 Carturan G, Monte RD, Pressi G, Secondin S, Verza P. Production of Valuable Drugs from Plant Cells Immobilized by Hybrid Sol-Gel SiO_2. J Sol Gel Sci Technol 1998; 13: 273 - 276.

51 Pressi G, Toso RD, Monte RD. Production of Enzymes by Plant Cells Immobilized by Sol-Gel Silica. J Sol Gel Sci Technol 2003; 26: 1189 - 1193.

52 Perullini M, Rivero MM, Jobbágy M, Mentaberry A, Bilmes SA. Plant cell proliferation inside an inorganic host. J Biotechnol 2007; 127(3): 542-548.

53 Boninsegna S, Bosetti P, Carturan G, Dellagiacoma G, Monte RD, Rossi M. Encapsulation of Individual Pancreatic Islets by Sol-Gel SiO_2: A Novel Procedure for Perspective Cellular Grafts. J Biotechnol 2003; 100: 277 - 286.

54 Sakai S, Tsutomu Ono, Hiroyuki Ijima, & Koei Kawakami. Proliferation and Insulin Secretion Function of Mouse Insulinoma Encapsulated in Alginate/Sol-

Gel Synthesized Aminopropyl-Silicate/Alginate Microcapsule. J Sol Gel Sci Technol 2003; 28: 267 - 272.

55 Rooke JC, Leonard A, Su B-L. Targeting photobioreactors: Immobilisation of cyanobacteria within porous silica gel using biocompatible methods. J Mater Chem 2008; 18: 1333-1341.

56 Baker NR. Chlorophyll Fluorescence: A Probe of Photosynthesis In Vivo. Annual Review of Plant Biology 2008; 59: 89-113.

57 Campbell D, Hurry V, Clarke AK, Gustafsson P, Oquist G. Chlorophyll Fluorescence Analysis of Cyanobacterial Photosynthesis and Acclimation. Microbiol. Mol. Biol. Rev. 1998; 62(3): 667-683.

58 Campbell D, Oquist G. Predicting Light Acclimation in Cyanobacteria from Nonphotochemical Quenching of Photosystem II Fluorescence, Which Reflects State Transitions in These Organisms. Plant Physiol 1996; 111(4): 1293-1298.

59 El Bissati K, Delphin E, Murata N, Etienne A-L, Kirilovsky D. Photosystem II fluorescence quenching in the cyanobacterium Synechocystis PCC 6803: involvement of two different mechanisms. Biochimica et Biophysica Acta (BBA) - Bioenergetics 2000; 1457(3): 229-242.

60 Bennett A, Bogorad L. COMPLEMENTARY CHROMATIC ADAPTATION IN A FILAMENTOUS BLUE-GREEN ALGA. The Journal of Cell Biology 1973; 58(2): 419-435.

61 Su X, Fraenkel PG, Bogorad L. Excitation Energy Transfer from Phycocyanin to Chlorophyll in an apcA-defective Mutant of *Synechocystis* sp. PCC 6803. J Biol Chem 1992; 267(32): 22944-22950.

62 Yamanaka G, Glazer AN. Dynamic aspects of phycobilisome structure. Arch Microbiol 1980; 124(1): 39-47.

63 Collier JL, Herbert SK, Fork DC, Grossman AR. Changes in the cyanobacterial photosynthetic apparatus during acclimation to macronutrient deprivation Photosynthesis Research 1994; 42(3): 173-183.

64 Toole CM, Plank TL, Grossman AR, Anderson LK. Bilin deletions and subunit stability in cyanobacterial light-harvesting proteins. Mol Microbiol 1998; 30(3): 475-486.

65 Luque I, Ochoa de Alda JAG, Richaud C, Zabulon G, Thomas J-C, Houmard J. The NblAI protein from the filamentous cyanobacterium Tolypothrix PCC 7601: regulation of its expression and interactions with phycobilisome components. Mol Microbiol 2003; 50(3): 1043-1054.

66 Panda B, Jain P, Sharma L, Mallick N. Optimization of cultural and nutritional conditions for accumulation of poly-β-hydroxybutyrate in Synechocystis sp. PCC 6803. Bioresour Technol 2006; 97(11): 1296-1301.

CHAPTER 5 - CONCLUSIONS & FUTURE WORK

5.1 - Efficacy of Silica Sol-Gel Encapsulation

The initial stages of this research evaluated different protocols for encapsulating *Synechocystis* sp. PCC 6803 in gels derived from silicon alkoxide precursors only. A high throughput screening assay was used to iteratively screen through many formulations until a protocol was developed that enabled successful encapsulation and hydrogen production from encapsulated cultures that was comparable to liquid controls.

Subsequent research sought to explore how encapsulated cells respond to the stress of encapsulation in order to improve encapsulation protocols for enhanced cell viability, activity, and hydrogen production. Surprisingly, *Synechocystis* sp. PCC 6803 was shown to be extremely sensitive to glycerol and PEG, both common additives with documented success in protecting various kinds of non-photosynthetic cells from the stress of encapsulation. Photosynthetic processes were vulnerable to these additives and, to a lesser extent, EtOH generated by alkoxide precursors. Stress induced by these compounds was immediately apparent, observed by a decrease in both the quantum efficiency of PSII and photochemical quenching. However, encapsulated cells recovered well in both alkoxide and aqueous-derived gels, regaining nearly all of their original photosynthetic efficiency, which persisted with only slight degradation over a period of six weeks. While it has also been demonstrated that encapsulation within gels of either type promotes increased hydrogen production compared to liquid controls, cells in gels derived from aqueous precursors produced nearly double the amount of hydrogen as cells in alkoxide gels under otherwise identical conditions. Finally, the most recent investigations showed that when conditioned under 400 $\mu Em^{-2}s^{-1}$ light, antenna mutants ΔapcE and ΔapcF produce approximately 25% more hydrogen than *wt* cells under similar conditions, despite accumulating approximately the same amount of glycogen.

This research demonstrates a clear proof of concept; encapsulation of *Synechocystis* sp. PCC 6803 in silica gel is an effective way to stabilize photosynthetic activity over the course of many weeks and enhance short term hydrogen production. However, the potential of this application is far from fully realized. There are numerous ways to improve our understanding of the encapsulation process which will not only serve the goals of this research but also improve the efficacy of silica sol-gel encapsulation for many other applications. Some avenues of continued research relevant to this project are discussed below in §5.3.

5.2 - Synechocystis *as a Platform for Photobiological Hydrogen Production*

Synechocystis sp. PCC 6803 is one of the primary model organisms for photosynthesis and for photobiological hydrogen production. The organism contains a bidirectional [Ni-Fe] hydrogenase that produces hydrogen predominantly through an indirect pathway resulting from fermentative breakdown in the dark of glycogen that has been accumulated in the light. This research has successfully improved hydrogen production from *Synechocystis* sp. PCC 6803 by encapsulation in silica gel and by manipulating light harvesting photoantennae.

While a conversion efficiency of 1%, light to hydrogen, has been demonstrated here, this was under laboratory conditions with a relatively weak, controlled light source, much weaker than full sunlight. As a result, this remains well below the benchmark conversion efficiency of 10%, widely judged to be technically feasible throughout the peer reviewed literature in the field [1-3]. Yet, even with the indirect pathway, there is no thermodynamic constraint that prohibits achieving 10% efficiency. Considering the significant amount of progress made toward improving hydrogen production, *Synechocystis* sp. PCC 6803 remains a viable model organism for photobiological hydrogen production.

There are a few fundamental constraints which currently slow improvements in light-to-hydrogen conversion efficiencies. The first and most obvious, which was

not addressed explicitly in the current research, is the oxygen sensitivity of the [Ni-Fe] hydrogenase. This demands the temporal separation of oxygenic photosynthesis and hydrogen production. An alternative to requiring an oxygen tolerant hydrogenase, however, is reducing the rate of oxygen evolution at PSII. This is an approach that has been successful in algae, achieved through sulfur deprivation [4, 5], but has received less attention in cyanobacteria, possibly because of the complex overlap of photosynthetic and respiratory electron transport. Nevertheless, manipulations to photoantennae will inevitably affect the activity of PSII, which was only given cursory attention in the current work and warrants additional investigation.

Another limitation is that *Synechocystis* sp. PCC 6803 and many other cyanobacteria have evolved to grow optimally under low light conditions, saturating when light is perhaps 10% to 20% the intensity of direct sunlight. With excess radiation, non-productive and ultimately wasteful degeneration of absorbed energy occurs, reducing photosynthetic efficiency in terms of utilization of absorbed light. The photoantennae mutants characterized during this work have demonstrated higher photosynthetic efficiency than *wt* cells under light intensity beyond saturating (~400 $\mu Em^{-2}s^{-1}$), and showed improved hydrogen production. However, the current investigation of the antenna mutants did not consider transmitted light. The data indicate the mutants more efficiently utilize absorbed photons, reducing unproductive absorption, but it remains unclear how much light actually is being absorbed or how much is transmitted, remaining available to other cells in the culture. These, and other similar types of mutants, should continue to be examined in order to improve the overall efficiency of light utilization for hydrogen production at increasing intensity, approaching full sunlight at approximately 2,000 $\mu Em^{-2}s^{-1}$.

Finally, the current format utilizes intact viable cells encapsulated within silica gel. While this is advantageous in the sense that all co-factors, accessory proteins,

requisite metabolites, and other protein machinery of the intact cell are present, it also creates an efficiency penalty through energy diverted away from hydrogen production toward cell maintenance. Protein expression, metabolic profile, and overall cell activity may not be optimal for hydrogen production at any given moment. Therefore, an improved understanding of the overall system and context of hydrogen production will lead toward the ability to extract and stabilize only the necessary proteins required to carry out the process, at a higher density and efficiency than could otherwise be achieved with whole cells. Encapsulation in silica gel then presents a way to stabilize those extracted proteins to retain structure and activity.

Despite the constraints mentioned, *Synechocystis* sp. PCC 6803 remains an excellent platform organism for photobiological hydrogen production. Incremental improvements are continually being made, building upon dramatic improvements that have already occurred. While some additional work intimated above requires numerous intermediate steps or a drastic change in tack, future work outlined below leads directly from the work contained in this investigation and could be undertaken immediately to further improve hydrogen production from this organism.

5.3 - Future Work

This project has successfully improved hydrogen production from *Synechocystis* sp. PCC 6803 through encapsulation in silica sol-gel and manipulation of its photoantennae. However, many questions remain unanswered and many new questions have arisen. Below are a few avenues for continuing research to further improve our understanding of photobiological hydrogen production, encapsulation in silica gel, and combining the two for maximal hydrogen production efficiency. The multiple paths of inquiry listed below represents an enormous level of effort, yet are certainly not intended to be exhaustive.

- Examining the use of other additives to improve survival and minimize encapsulation stress:
    - While PEG and glycerol were detrimental to *Synechocystis* sp. PCC 6803, many other additives are available, as mentioned in §1.5.8. Other compounds which create osmotic stress, including sugar alcohols, are not likely to be beneficial and may be excluded a priori. Surfactants, while useful for creating a template for the gel structure, also aggressively attack membranes, so would also presumably be detrimental to photosynthetic processes. However, organic polymers, including alginate, collagen, gelatin, agar, and others, allow for the creation of mixed phase or layered structures, taking advantage of the biocompatibility of the organic polymers and the stability of silica. This has been successfully demonstrated in other applications [6, 7], but has not yet been explored with cyanobacteria. In a system that may require cycling between media replete with nutrients and deprived media for the accumulation of glycogen, cells encapsulated in silica-alginate composite beads, for example, could be rapidly transferred between media types. Depending on scale-up format, this approach could certainly have advantages over bulk monoliths.
- Exploration of salt acclimation and the correlation with encapsulation survival, cyclic electron flow, and hydrogen production:
    - Upon exposure to salt, *Synechocystis* sp. PCC 6803 responds with the production of GG, an endogenous osmotic protectant. Early results indicate pretreatment in salt prior to encapsulation may improve encapsulation survival, yet the effects on hydrogen production are unclear. Preliminary experiments have not presented a clear and distinct correlation between salt stress response and hydrogen production (data not shown). Therefore, balancing the benefits of salt pretreatment

protocols requires additional investigation to determine how beneficial the process might be and at what expense or benefit to hydrogen production.

- Exploration of the use of ORMOSILs for improved biocompatibility of the sol-gel matrix:
    - A vast array of ORMOSIL precursors are available to optimize gel characteristics for biological encapsulation. The simplest ORMOSILs contain alky groups covalently bound directly to the silicon atom, and some of these compounds have been used with modest success in the current research. However, changes in the concentration or chemical nature of these side groups could dramatically alter the chemical properties of the gels. It is plausible that increasing the hydrophobicity of the gel matrix may facilitate the formation of pockets around the encapsulated cells, creating a liquid buffer that may reduce encapsulation stress and improve viability.
- Cycling of encapsulated cultures between glycogen accumulation and hydrogen production:
    - Continuing with the same format investigated herein, the next logical progression would be optimizing a repeated cyclic switch between glycogen accumulation in the light followed by hydrogen production in the dark. One pitfall is the fact that this organism will catabolize its photoantennae when deprived of sulfur and nitrogen (Figure 4-4), which is a requisite condition for enhanced glycogen accumulation. So, unless *Synechocystis* sp. PCC 6803 is also given a cycle in the light with nutrient replete media, the cells will degrade their photoantennae to the point of inducing photoinhibition and photodamage, slowing activity and leading eventually to senescence. Therefore, optimization of the competing processes is required in order to provide adequate recovery while also

enabling sufficient glycogen accumulation for appreciable hydrogen production.

- Examination of other storage compounds, particularly PHB, and its relation to hydrogen production:
    - Synechocystis sp. PCC 6803 has received recent attention as a candidate species for the production of PHB, a compound of value in the development of bioplastics. Under normal conditions, the organism tends not to accumulate more than 6% dry cell weight PHB [8, 9]. However, under conditions that often resemble conditions exerted for increased glycogen accumulation, particularly nitrogen deprivation, *Synechocystis* sp. PCC 6803 has been observed to accumulate a significant amount of PHB, on a dry cell weight basis [8-10]. While the cited studies begin to suggest how carbon storage is allocated between glycogen and PHB, this process is not fully understood. Furthermore, how PHB storage interacts with fermentative hydrogen production is completely unexplored.
- Characterization of gene response after encapsulation:
    - Transcriptomics, or micro-array analysis, with mRNA extracted from encapsulated cells would allow a look at gene expression profiles within those cells. It is unknown exactly what genes are being up regulated or down regulated in response to encapsulation. Further information in this area will improve our understanding of the exact response to encapsulation stress, providing a basis for rational improvements to encapsulation protocols.
- Continued characterization of the photoantennae mutants:
    - These mutants are robust under higher light intensities than *wt* cells, and have been shown to produce more hydrogen when conditioned under 400 $\mu Em^{-2}s^{-1}$ light and encapsulated. However, it is not known why. Additional investigation is warranted into photosynthetic efficiency at

higher light intensities (approaching sunlight, or ~2,000 $\mu Em^{-2}s^{-1}$), gene expression and protein management, and the activity of PSII with specific regard to oxygen evolution.

- Improved systems for optimal use of incident radiation for hydrogen production:
  - The photoantennae mutants have structural changes to their photosynthetic apparatus of varying severity. This research has demonstrated that each uses light at different efficiencies, and while the ultimate goal has always been creating a system of encapsulated strains to most efficiently use incident radiation, the feasibility of this approach has not yet been explored. Multiple parameters would need to be optimized, including the order in which selected strains are exposed to incident light, whether the strains should be mixed or segregated, which strains to include, cell density, pigment density, gel thickness, and light cycling, among many other design parameters. If such a system is ever going to be an economically feasible means of renewable hydrogen production, a thorough engineering analysis to optimize the design will be critical.

These additional areas of inquiry could substantially improve the efficiency of photobiological hydrogen production from *Synechocystis* sp. PCC 6803 and generate valuable information for enhancing the process in other organisms. Although the above suggestions are generally aimed at improving indirect photobiological hydrogen production, these lines of inquiry will naturally lead toward direct photobiological hydrogen production pathways as oxygen evolution is better controlled and more electron flux is directed away from non-essential pathways toward hydrogen production. In conclusion, this body of research has simply demonstrated the validity of the approach and confirmed it warrants a great deal of additional investigation.

Chapter 5 References

1 Prince R. The Photobiological Production of Hydrogen: Potential Efficiency and Effectiveness as a Renewable Fuel. Critical Reviews in Microbiology 2005; 31: 19-31.

2 Kruse O, Rupprecht J, Mussgnug JH, Dismukes GC, Hankamer B. Photosynthesis: a blueprint for solar energy capture and biohydrogen production technologies. Photochemical & Photobiological Sciences 2005b; 4(12): 957-970.

3 Ghirardi ML, Dubini A, Yu J, Maness P-C. Photobiological hydrogen-producing systems. Chem Soc Rev 2009; 38(1): 52-61.

4 Kosourov S, Patrusheva E, Ghirardi ML, Seibert M, Tsygankov A. A comparison of hydrogen photoproduction by sulfur-deprived Chlamydomonas reinhardtii under different growth conditions. J Biotechnol 2007; 128(4): 776-787.

5 Melis A, Zhang L, Forestier M, Ghirardi ML, Seibert M. Sustained Photobiological Hydrogen Gas Production upon Reversible Inactivation of Oxygen Evolution in the Green Alga Chlamydomonas reinhardtii. Plant Physiol 2000; 122(1): 127-136.

6 Boninsegna S, Bosetti P, Carturan G, Dellagiacoma G, Monte RD, Rossi M. Encapsulation of Individual Pancreatic Islets by Sol-Gel SiO_2: A Novel Procedure for Perspective Cellular Grafts. J Biotechnol 2003; 100: 277 - 286.

7 Callone E, Campostrini R, Carturan G, Cavazza A, Guzzon R. Immobilization of yeast and bacteria cells in alginate microbeads coated with silica membranes: procedure, physico-chemical features and bioactivity. J Mater Chem 2008; 18: 4839-4848.

8 Wu GF, Wu QY, Shen ZY. Accumulation of poly-b-hydroxybutyrate in cyanobacterium *Synechocystis* sp. PCC6803. Bioresour Technol 2001; 76: 85-90.

9 Panda B, Mallick N. Enhanced poly-β-hydroxybutyrate accumulation in a unicellular cyanobacterium, *Synechocystis* sp. PCC 6803. Letters in Applied Microbiology 2007; 44: 194-198.

10 Panda B, Jain P, Sharma L, Mallick N. Optimization of cultural and nutritional conditions for accumulation of poly-β-hydroxybutyrate in Synechocystis sp. PCC 6803. Bioresour Technol 2006; 97(11): 1296-1301.

CHAPTER 6 - BROADER ENVIRONMENTAL & SOCIETAL IMPACTS

Reliable, available, and affordable energy is arguably *the* key defining feature of developed, modern civilization. It enables every subsequent activity required for maintaining the health and well-being of that civilization. The United Kingdom initiated this modern energy revolution in the 19th century with coal. The United States took the next step and became a world super power in the 20th century, rising on a tide of domestic oil. This trajectory ushered in a modern era that relies upon fossil fuels as the energy behind water treatment, locomotion, electricity production, and petrochemicals, enabling modern agriculture, pharmaceuticals, and plastics. In short, the modern world as we know it simply would not exist without fossil fuels. At this point, premature exhaustion of fossil fuels, prior to a dramatic and complete shift toward alternative forms of energy, has the potential to be profoundly disruptive, if not incredibly disastrous. Yet, fossil fuels are a finite resource; they will not be abundant or cheap forever. The detrimental effects to human health and the environment as a consequence of prolonged and continued fossil fuel use, combined with increasing prices due to tightening supplies and intense competition for scarce energy resources, provides the perfect scenario for two possible outcomes: we either rise to the occasion, and immediately transition to a sustainable energy economy; or we continue with business as usual and risk economic and environmental catastrophe on a global scale.

6.1 - The Urgency of Renewable Energy

This energy intensive modernity is threatened by two forces: geopolitical instability, manifest in terrorist threats, volatile markets, and imminent supply disruptions; and climate change, fueled by decades of unencumbered greenhouse gas (GHG) emissions, mostly in the form of carbon dioxide. The United States recently concluded a war in Iraq and continues a conflict in Afghanistan, both campaigns initiated under the guise of defending national security. However, as long as the

American economy and American citizens continue to consume vast amounts of foreign oil, the export of American wealth toward hostile producer nations will continue, providing revenue to the very enemies we are trying to defeat. Motives aside, the cost of military engagements in the Middle East, estimated at more than $50 billion per year, already exceeds the value of oil imported from this region [1]. Therefore, from the perspectives of national security and economic interest, the merit, indeed the necessity, of developing renewable and domestic energy sources is self-evident.

Unfortunately, the existing energy system has deep roots, enjoying the support of powerful financial and political interests and a consuming public comfortable and familiar with the product. The continued off-shore drilling in the Gulf of Mexico despite the recent Deepwater Horizon disaster, coupled with our collective indifference to this shocking incident, is just one example of how entrenched the existing energy system has become. Considering the billions of dollars invested in creating and maintaining the energy infrastructure, it comes as no surprise to find the system quite recalcitrant to change. With diminishing supplies of fossil fuel, particularly petroleum, the price of maintaining such a system will soon exceed the value derived from the energy moving through it [2], which, by definition, will render the system obsolete. A more appropriate solution would be investing the vast revenue generated by the existing system into a new, more flexible and diversified system, facilitating the transition before the capital and resources are no longer available, irrecoverably sunk into antiquated infrastructure.

In addition to obvious economic and security benefits in developing domestic renewable energy, there is a clear need to mitigate GHG emissions and slow climate change. In its latest report, representing the consensus of the global scientific community, the Intergovernmental Panel on Climate Change (IPCC) concluded that not only is climate change absolutely occurring, but that human activity is “very

likely" responsible [3]. Since accurate records began around a century ago, the decade just concluded was the hottest on record, and 2010 the hottest year on record. Since pre-industrial times (~1750), average global temperatures have risen 0.76°C, atmospheric carbon dioxide concentration has climbed from 280 ppm to 390 ppm, and the rate of sea level rise has been accelerating [3]. By the end of this century, global temperatures are expected to climb approximately 3°C, carbon dioxide may exceed 500 ppm or more, and sea level may rise 0.2 meters by thermal expansion alone. Should the ice sheets of Greenland or Antarctica collapse, sea level could rise significantly more, on the order of many meters.

Cumulatively, this poses a variety of serious environmental risks to many regions of the globe. Drought and desertification will become more intense in mid-latitude regions, like the American West, reducing agricultural yields and placing severe water stress on large urban centers, while other areas, like the American Northeast, could experience increased rainfall with a corresponding increase in flood events. Intense weather events, like tropical cyclones, are expected to increase in both intensity and frequency, and low lying coastal areas will be inundated, displacing millions of "climate refugees." This is already occurring in countries like Tuvalu and The Maldives, island nations situated on low profile atolls that may be completely submerged within a few decades due to climate change. In short, life for millions, likely billions of people around the globe will be disturbed on an unprecedented scale.

6.2 - A Moral Obligation for Individual Action

Climate change is a challenge faced by the entire global community, posing threats in scale and magnitude never seen in all of human history. Unfortunately for the poorer developing nations of the world, they stand to bear the brunt of a problem created by a minority of wealthy developed nations [4]. The scope of negotiations occurring within and between nation states to achieve coordinated

action on climate change, as well as related economic, political, and ideological motivations, is an enormous area of inquiry which will not be discussed here. Of interest is the rationale behind individual action, or inaction, on climate change. As citizens of the wealthiest nation on earth, responsible for the largest cumulative share of greenhouse gas emissions, we are each morally obligated to take decisive, unambiguous action toward mitigating the effects of climate change, and we have the financial and technical means to do so.

There are numerous excuses invoked for individual *in*action to reduce GHG emissions, although four core arguments seem to be most prevalent, encompassing most variations in the breadth of excuses. The first is an excuse of scale, based on the assumption that the choices of an individual are negligible when compared to the choices of a state, nation, corporation, or some other nebulous large entity. One can easily blame America, or Exxon-Mobil, or the regional power utility for exorbitant emissions, while simultaneously taking excessively long road trips, enjoying long flights to distant holiday destinations, turning up the air conditioning in a poorly insulated home, or making countless other choices that needlessly waste energy. The fact is, and it would seem obvious, that the aggregate emissions of all these various entities result from the choices of the individuals interacting with those entities. Without customers buying and using electricity, a power utility, for example, would generate very little GHG emissions. So, this is a weak excuse, resulting from a failure to see how individual choices contribute to the community as a whole.

Second, the detached temporal and spatial scales of the problem often lead people to believe there is no problem, especially in developed nations that are largely insulated from the emerging impacts of climate change. When there is no evident problem, there is little incentive to take individual action to change habit or diminish standard of living [5, 6]. The looming threats of climate change remain abstract to many. Flooding in some distant corner of the globe, drought that might

occur 20 years from now, or the displacement of coastal populations a century from now are all too impersonal to compel many individuals to act. Yet, the cumulative impact of the choices made by individuals today is precisely what will bring these adverse impacts to pass, and this does nothing to absolve the current generation of responsibility. Therefore, spatial or temporal separation do not reduce moral obligation to take action.

Thirdly, an argument favored by developed nations, especially the United States, is the position that inaction by others justifies inaction at home. Why should the United States act to reduce GHG emissions when China or India are not acting as aggressively? Arguments of historical responsibility or economic and technical wherewithal aside, the moral transgressions of one actor never justify moral transgressions of another. If stealing is wrong, then it remains wrong even if my neighbor still commits the act. Similarly, if reckless and excessive emission of GHG is wrong because of the harm it causes, or will cause to others, whether next door or around the globe, then it is wrong no matter who does it. This argument is often invoked as a form of projection, criticizing in others what we least like to acknowledge in ourselves [5], and as an appeal to fairness, since we are unlikely to sacrifice when others are not doing the same [6]. Either way, it amounts to an attempt to justify personal moral transgressions through the actions of others. Although is it common human nature, it is unequivocally wrong, and we must rise above such petty arguments.

Fourth, perhaps the simplest argument of all, is the suggestion that reducing GHG emissions will simply cost too much. The one small kernel of truth here is that reducing GHG emissions and adapting to climate change will, no doubt, be expensive, estimated at approximately 1% of global GDP for many years to come [7]. (Global GDP was $58 trillion in 2009 (Source: World Bank), so 1% would be approximately $580 billion. By comparison, the United States military budget in 2009 was $515

billion (Source: US Dept. of Defense), with an additional $70 billion allocated for the wars in Iraq and Afghanistan.) Furthermore, if actions are too aggressive and financial ruin results, then we may very well lack the capital to make a smooth transition away from fossil fuels. However, this seems highly unlikely, as the projected cost of doing nothing far exceeds the cost of adapting, even aggressively adapting [7].

What is dishonest about this argument is its appeal to the ambiguities and uncertainties surrounding the projected impacts of climate change. While the IPCC states that climate change is "very likely" occurring as a result of human actions, a statement with more than 90% confidence [3], nearly a certainty in scientific circles, this is not compelling enough for many economists and policy makers to support action. Furthermore, the estimates about the impacts and costs of climate change are far less certain and more ambiguous. There is little doubt that the global climate is changing and that negative impacts will result, but because we cannot accurately predict or quantify those impacts, many leverage this uncertainty as an excuse for inaction. Framed in the context of a personal choice, if one knew with 90% certainty that something bad was going to happen, most of us would take preventative measures to prevent such a thing from happening, or would, at the very least, take precautions to deal with the impacts, like purchasing insurance. The unwillingness of most governments to take action in the face of similar odds is nothing short of irresponsible and outrageous. Many individuals in the developed nations of the world share the same culpability.

Finally, this argument is morally reprehensible because it justifies the status quo at the expense of less fortunate people currently living elsewhere and future generations everywhere. We know, with reasonable certainty, that climate change will result in the displacement of millions, with adverse impacts on agricultural production and water availability, threatening not just economic livelihood, but the very lives of affected people. Our inability to calculate accurate estimates of the

number of people or dollars lost is irrelevant; that fact that both are greater than zero should be enough. In short, ignoring climate change because it costs too much to do something about it is the moral equivalent of “harming other people for money” [5]. Indeed, a truly shocking position to defend.

Taken together, all arguments for inaction are weak and some are even morally outrageous. There is a great deal of vigorous debate about what should be done to mitigate and adapt to climate change, and this is warranted, but doing nothing clearly is not. What is also clear is that individual action, in addition to government action, is critical. Individual choices about consumption and life style define cumulative GHG emissions of a society, and the government of that society reflects the values of its members. If government is not doing enough, then a more compelling call to action must come from within.

6.3 - Transitioning Toward a Sustainable Energy Economy

Action is required, and it is required in numerous arenas. We must first reduce the energy we use by dramatically improving energy efficiency and conservation. We must also accelerate the development and adoption of renewable energy technologies, including, but certainly not limited to, hydrogen and fuel cells. If renewable energy is to become a major portion of our energy portfolio, it will require more than simply the appropriate technologies. It will require a confluence of successful technology, political will, and public demand. Renewable energy cannot be developed without concerted research efforts and it cannot be effectively deployed into the market without intelligent government policy, savvy entrepreneurs, and willing consumers. This is a major shift in paradigm, but one that must occur if humanity is to meet the energy demands of providing, at the very least, clean water, food, shelter, modest mobility, and adequate health care for a growing population.

A first and immediate step toward a meaningful reduction in GHG emissions and a sustainable energy economy is improvements in energy efficiency and energy

conservation. This means achieving the same result with less energy and doing less to waste energy. This can be done now, with existing technology, by changing use patterns and purchasing habits. A change in habit is the critical factor in significant change. People are often willing to make minor adjustments when convenient, such as recycling and using compact fluorescent light bulbs, but these actions have relatively minor impact compared with choices like driving less, using public transit, and weatherizing homes, all choices people have demonstrated much less willingness to undertake [6].

Another particularly vicious and counterintuitive trend is the tendency for people to consume *more* energy despite improvements in the efficiency of each individual device or appliance used. This is known as the Khazzoom-Brookes postulate, and it states that any reduction in resource use in one area will be more than offset by an increase elsewhere [8]. In the United States, for example, the efficiency of appliances and electronics have steadily improved over recent decades, yet the average household energy consumption has increased because homes are larger, appliances and electronics are larger, faster, and increasing in number of units per home, and the sheer number and variety of devices contributing to energy load have increased, many requiring a steady parasitic load to maintain device memory and settings. Short of Draconian government policy, improved public awareness, fostered by education and intelligent policy, may be the most promising option for altering this behavioral trend in the developed world [6].

The other major arena is the development of renewable energy technologies and improved management of the energy produced. In terms of energy utilization, especially electrical energy, the prevailing model is of large, centralized production facilities distributing energy by a wire grid to customers. The flow of energy is one way, from producer to user, and the management of production and demand is reactionary, not proactive. Producers can only control supply, they have no ability or

authority to responsively alter demand without cutting off customers. This system has evolved into an enormous web of infrastructure that is increasingly clumsy, fragile, overloaded, and unable to meet the dynamic demands of a modern economy. Improving the system to meet future demand with the same model, that is, more large production facilities and thousands of miles of transmission lines, is likely more expensive than fundamentally transforming the grid into a responsive and dynamic entity capable of matching demand and production in real time [9].

Updating the grid with so-called “smart technology” and Non-Transmission Alternatives (NTA)(i.e., distributed generation facilities) is already underway with utilities around the country, under encouragement from DOE and EPA [10]. What is meant by a “smart” grid is a system that achieves two things the current grid cannot. First, it enables managers of the grid to control both production *and* demand. Externally altering building thermostats, for example, is one way to manage load rather than supply. Second, the transfer of energy is two-way, between consumers and distributed small generation facilities, sometimes at the same site, that can be summoned quickly and shut down just as quickly. This allows for a more reliable, dynamic, and efficient system that has the potential to dramatically reduce GHG emissions, especially when heat is included as part of the energy distribution scheme (combined heat and power) [9, 11].

This is where hydrogen has an important role to play. Since hydrogen can readily buffer between demand and any form of electricity (preferably renewable), it is perfectly suited to play a key role in the future of “smart” grid technologies. Household or neighborhood-scale fuel cells can be used for heat and power production, on demand, while renewable sources of hydrogen, like photobiological production, can be used to support production in parallel with renewable forms of electricity.

The introduction of hydrogen into the transportation sector with fuel cell vehicles presents a feasible option to further significantly reduce GHG emissions, as well as emissions of particulates and oxides of sulfur and nitrogen [12]. Fuel cell vehicles could even be used to provide household heat and power or provide power back to the grid since much of a vehicle's lifetime is spent idle in the owner's driveway or in a parking lot. Such an energy system, characterized by thousands of entities that fluctuate between consumer and producer, connected by a sophisticated network that can match demand and supply, is the energy system of the future. While this will require a fundamental shift in the way society operates, and perhaps some reductions in the most luxurious expenditures of energy, it should maintain the current standard of living enjoyed by millions in the developed world and hopefully enable millions more in the developing world to follow.

Transitioning toward a sustainable energy economy will require a vast number of technologies, working in parallel, deployed appropriately in the context of local and regional needs and resources. No technology will be a panacea, hydrogen included, and the work contained here does not take such an optimistic view of hydrogen technology. Indeed, the idea that hydrogen can provide "abundant, cheap, and pollution-free" energy for the entire world has been described as "fantasy" [13]. This is an appropriately strong and pessimistic criticism of an equally inappropriate expectation for hydrogen energy, especially given the existing energy infrastructure and state of the technology. However, numerous analyses have shown that hydrogen provides economic and environmental benefits when deployed in suitable circumstances [14-17], suggesting the technology, as a whole, warrants further development and will provide an important contribution in weaning humanity off its insatiable diet of fossil fuels.

Chapter 6 References

1 Pascual C, Elkind J, ed. Energy Security: Economics, Politics, Strategies, and Implications. Brookings Institution Press, Washington DC, 2010.

2 Rifkin J. The Hydrogen Economy. New York: J.T. Tarcher/Putnam, 2002.

3 IPCC. Climate Change 2007: The Physical Science Basis, Summary for Policy Makers. Intergovernmental Panel on Climate Change. 2007.

4 Grasso M. A normative ethical framework in climate change. Climatic Change 2007; 81(3): 223-246.

5 Garvey J. The Ethics of Climate Change. New York: Continuum International Publishing Group, 2008.

6 Whitmarsh L. Behavioural responses to climate change: Asymmetry of intentions and impacts. Journal of Environmental Psychology 2009; 29(1): 13-23.

7 Stern N. The Economics of Climate Change. Cambridge: Cambridge University Press, 2007.

8 Saunders HD. The Khazzoom-Brookes Postulate and Neoclassical Growth. Energy Journal 1992; 13(4): 131-148.

9 Achenbach J. The 21st Centrury Grid. National Gegraphic. July, 2010.

10 NCEP. Updating the Electric Grid: An Introduction to Non-Transmission Alternatives for Policymakers. 2009.

11 Strachan N, Farrell A. Emissions from distributed vs. centralized generation: The importance of system performance. Energy Policy 2006; 34(17): 2677-2689.

12 Doll C, Wietschel M. Externalities of the transport sector and the role of hydrogen in a sustainable transport vision. Energy Policy 2008; 36(11): 4069-4078.

13 Sovacool BK, Brossmann B. Symbolic convergence and the hydrogen economy. Energy Policy 2010; 38(4): 1999-2012.

14 Schultz MG, Diehl T, Brasseur GP, Zittel W. Air Pollution and Climate-Forcing Impacts of a Global Hydrogen Economy. Science 2003; 302: 624-627.

15 Crabtree GW, Dresselhaus MS, Buchanan MV. The Hydrogen Economy. Physics Today 2004; December 2004: 39-44.

16 Marban G, Valdes-Solis T. Towards the hydrogen economy? Int J Hydrogen Energy 2007; 32(12): 1625-1637.

17 National Hydrogen Energy Roadmap. United States Department of Energy, 2002.